

A Prototype Transformer Partial Discharge Detection System

Stewart R. Hardie, B.E. (Hons)

A thesis presented for the degree of
Doctor of Philosophy
in
Electrical and Computer Engineering
at the
University of Canterbury,
Christchurch, New Zealand.

January 2006

ABSTRACT

Increased pressure on high voltage power distribution components has been created in recent years by a demand to lower costs and extend equipment lifetimes. This has led to a need for condition based maintenance, which requires a continuous knowledge of equipment health. Power transformers are a vital component in a power distribution network. However, there are currently no established techniques to accurately monitor and diagnose faults in real-time while the transformer is on-line.

A major factor in the degradation of power transformer insulation is partial discharging. Left unattended, partial discharges (PDs) will eventually cause complete insulation failure. PDs generate a variety of signals, including electrical pulses that travel through the windings of the transformer to the terminals. A difficulty with detecting these pulses in an on-line environment is that they can be masked by external electrical interference.

This thesis develops a method for identifying PD pulses and determining the number of PD sources while the transformer is on-line and subject to external interference. The partial discharge detection system (PDDS) acquires electrical signals with current and voltage transducers that are placed on the transformer bushings, making it unnecessary to disconnect or open the transformer. These signals are filtered to prevent aliasing and to attenuate the power frequency, and then digitised and analysed in Matlab, a numerical processing software package. Arbitrary narrowband interference is removed with an automated Fourier domain threshold filter. Internal PD pulses are separated from stochastic wideband pulse interference using directional coupling, which is a technique that simultaneously analyses the current and voltage signals from a bushing. To improve performance of this stage, the continuous wavelet transform is used to discriminate time and frequency information. This provides the additional advantage of preserving the waveshapes of the PD pulses for later analysis.

PD pulses originating within the transformer have their waveshapes distorted when travelling through the windings. The differentiation of waveshape distortion of pulses from multiple physical sources is used as an input to a neural network to group pulses from the same source. This allows phase resolved PD analysis to be presented for each PD source, for instance, as phase/magnitude/count plots. The neural network requires no prior knowledge of the transformer or pulse waveshapes.

The thesis begins with a review of current techniques and trends for power transformer monitoring and diagnosis. The description of transducers and filters is followed by an explanation of each of the signal processing steps. Two transformers were used to conduct testing of the PDDS. The first transformer was opened and modified so that internal PDs could be simulated by injecting artificial pulses. Two test scenarios were created and the performance of the PDDS was recorded. The PDDS identified and extracted a high rate of simulated PDs and correctly allocated the pulses into PD source groups. A second identically constructed transformer was energised and analysed for any natural PDs while external interference was present. It was found to have a significant natural PD source.

ACKNOWLEDGMENTS

I would like to thank the many people who have contributed to this thesis, directly and indirectly. Many thanks go to my supervisor Professor Pat Bodger, who has provided me with guidance during the important latter stages of the project. Thanks also to the staff and students of the Department of Electrical and Computer Engineering for the friendly research environment and providing help when needed, especially Phil Bones, Mike Cusdin, Ken Smart and Jac Woudberg.

The financial support of Meridian Energy during the earlier stages of this thesis was highly appreciated. It shows that they have an active interest in research, in working with the University to encourage the study of power engineering and to support the education of power engineers.

Cheers to the lads of R9 and the endless stream of visitors for entertaining discussions about a pretty wide variety of topics. They provided a very useful service for bouncing ideas off and providing some experience. Thanks to Phil Barclay, Ed Pilbrow, Steve Fortune, Al Hunter and Hayden Callow.

Some big thanks go to family and friends for supporting me for the duration of my study. My parents have always been interested in what I was doing and were willing to let me figure out things my way. Friends and flatmates have distracted, hassled and encouraged, which provided some impetus to make progress. A special thanks to Julianne who is particularly fond of penguins, as shown in Figure 1. She has provided extra support, encouragement and patience. It has helped me and meant a lot.

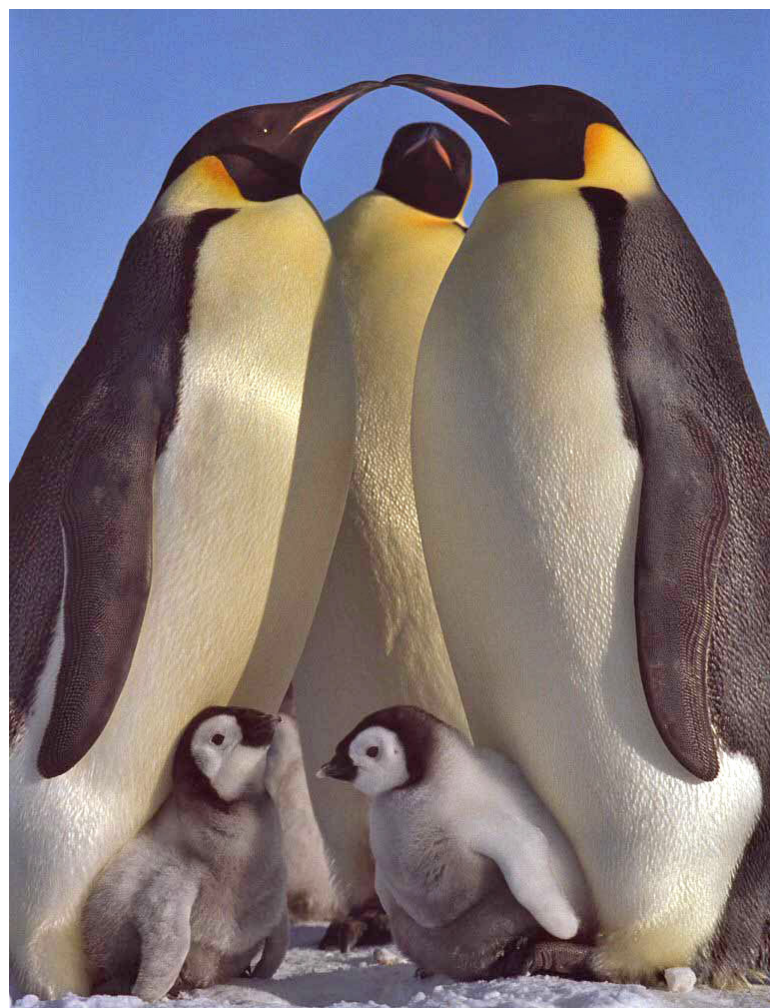


Figure 1 Emperor penguins with chicks.

CONTENTS

ABSTRACT	iii
ACKNOWLEDGMENTS	v
ABBREVIATIONS	xi
CHAPTER 1 INTRODUCTION	1
1.1 Motivation	1
1.2 Condition based maintenance (CBM)	2
1.3 Existing techniques	4
1.4 Partial discharge detection	5
1.5 The partial discharge detection system (PDDS)	6
1.6 Thesis overview	7
1.7 Aim of the project	8
CHAPTER 2 INSULATION MONITORING AND DIAGNOSTIC TECHNIQUES	11
2.1 Transformer insulation	12
2.1.1 Insulation aging	13
2.2 Transformer life assessment	15
2.2.1 Thermal measurements	16
2.3 Existing maintenance procedures	17
2.4 Diagnostic techniques	18
2.4.1 Oil dielectric strength test	19
2.4.2 Oil analysis	19
2.4.2.1 Dissolved gas analysis (DGA)	20
2.4.2.2 Total combustible gas (TCG) analysis	21
2.4.2.3 Furanic compound analysis	22
2.4.2.4 Expert systems and fuzzy logic	22
2.4.3 Degree of polymerisation (DP)	23
2.4.4 Oil pressure monitoring	24
2.4.5 Dielectric response	24
2.4.6 Transformer impulse testing	25
2.4.7 Low voltage impulse (LVI) testing	27
2.4.8 Leakage inductance	28

2.4.9	Frequency response analysis (FRA)	28
2.4.10	Partial discharge detection	29
2.4.11	Integrating fault diagnosis methods	33
2.5	Monitoring systems	33
2.5.1	Buchholz relay	34
2.5.2	Differential relay protection	35
2.5.3	Model-based monitoring	36
2.5.4	Hydrogen monitoring	36
2.5.5	Monitoring other gases in oil	37
2.5.6	On-line transfer function monitoring	38
2.5.7	On-line partial discharge detection	39
2.5.8	Other monitoring systems	44
2.5.9	On-line diagnosis	45
2.6	Conclusions	47
CHAPTER 3 HARDWARE		49
3.1	Overview	49
3.2	Calibration pulse, artificial pulse and narrowband signal generation	50
3.3	Power cycle synchronisation module (PCSM)	52
3.4	Transducers	53
3.4.1	Analog filter specifications	54
3.4.2	Current transducer and filter	55
3.4.3	Voltage transducer and filter	58
3.4.4	Transducer and filter responses	62
3.4.5	Oscilloscopes	63
3.5	Conclusions	63
CHAPTER 4 SIGNAL PROCESSING		65
4.1	Overview	65
4.2	Fourier domain threshold filter (FDTF)	67
4.2.1	Fourier domain threshold level	70
4.2.2	Notch filter beat effect	75
4.3	Wavelet transform	78
4.3.1	Why not the discrete wavelet transform (DWT)?	80
4.4	Continuous wavelet directional coupling filter (CWDCF)	81
4.5	Cluster neural network (CNN)	88
4.6	Pulse source grouping	94
4.7	Conclusions	96
CHAPTER 5 RESULTS		99
5.1	Test transformer construction and modification	99
5.2	Artificial PD detection results	103
5.2.1	Calibration	106
5.2.2	Narrowband interference rejection using the FDTF	107

5.2.3	PD identification using the CWDCF	121
5.2.4	Identification of separate PD sources	125
5.3	On-line PD detection results	142
5.3.1	Calibration	142
5.3.2	Narrowband interference rejection using the FDTF	142
5.3.3	PD identification using the CWDCF	146
5.3.4	Identification of separate PD sources	151
5.4	Conclusions	154
CHAPTER 6 CONCLUSIONS		161
6.1	Future research and developments	163
APPENDIX A PDDS EQUIPMENT AND TEST PHOTOS		167

ABBREVIATIONS

- AC** - alternating current
ADC - analog to digital converter
AM - amplitude modulation
ANN - artificial neural network
BIL - basic insulation level
BITE - built-in test equipment
CBM - condition based maintenance
CNN - cluster neural network
CT - current transformer
CWDCF - continuous wavelet directional coupling filter
CWT - continuous wavelet transform
DC - direct current
DFT - discrete Fourier transform
DGA - dissolved gas analysis
DP - degree of polymerisation
DWPT - discrete wavelet packet transform
DWT - discrete wavelet transform
EOL - end-of-life
FDTF - Fourier domain threshold filter
FFA - furfuraldehydes
FFT - fast Fourier transform
FRA - frequency response analysis
FRSL - frequency response of stray losses
GPIB - general purpose interface bus
HF - high frequency
HP - Hewlett-Packard
HPLC - high performance liquid chromatography

- HV** - high voltage
ICWT - inverse continuous wavelet transform
IDFT - inverse discrete Fourier transform
IFFT - inverse fast Fourier transform
IEC - International Electrotechnical Commission
IEEE - Institute of Electrical and Electronics Engineers
ISODATA - iterative self-organisation data analysis
LMS - least mean squares
LV - low voltage
LVI - low voltage impulse
MIT - Massachusetts Institute of Technology
OIR - output to input signal power ratio
pC - pico-coulomb
PC - personal computer
PCSM - power cycle synchronisation module
PD - partial discharge
PDDS - partial discharge detection system
PRPDA - phase resolved partial discharge analysis
RMS - root mean square
RF - radio frequency
RTD - resistance temperature device
RVM - return voltage measurement
SN - source number
SNR - signal to noise ratio
STFT - short time Fourier transform
TCG - total combustible gas
TDDS - time domain dielectric spectroscopy
Tx1 - transformer 1
Tx2 - transformer 2
USB - Universal Serial Bus
UV - ultra-violet

Chapter 1

INTRODUCTION

The purpose of this chapter is to provide an overview of and a justification for the research reported in this thesis. The first section gives a motivation for the research, both in terms of a world electrical power setting and with regard to power transformers in particular, which is followed by a description of condition based maintenance (CBM) and its benefits. The third and fourth sections introduce some of the techniques for transformer fault monitoring and diagnosis, especially partial discharge (PD) detection. The final sections provide a brief description of the partial discharge detection system (PDDS), a guide to the following chapters and a statement of the aim of the project.

1.1 MOTIVATION

Demands for electrical power and its distribution have been continuing to increase worldwide during the past few years. Naturally, this leads to the requirement for more power generation and for networks to transport it. Also, an increasing variety of electrical and electronic consumer loads use the power in ways that create pressures on the existing electrical network infrastructure, through unwanted generation of harmonics and transient signals. Typical network faults along with lightning impulses add stress to the networks. The combination of these effects places a burden on the insulation of sometimes aging high voltage (HV) equipment.

Power transformers are central and often critical components of any power distribution network and their continued reliability is necessary for the integrity of that network. Some reasons why failures of power transformers are problematic are:

- The location of transformers is often at junctions of distribution systems and, hence, any problems have a natural flow-on effect to a wide area further down the system.
- Unless redundancy is built into the network, there is an immediate loss of revenue not only to the utility company but also to the downstream consumers.

- Besides loss of service, other negative effects such as destructive surging can damage other equipment near the transformer.
- Most power transformers are physically hazardous items containing flammable oil. Fire or spillage of oil present problems of extensive damage not only to the transformer but also to surrounding equipment. Catastrophic failure can cause explosions that can potentially injure nearby personnel.
- More resources are required to replace failed transformers than would be needed to repair them.
- Power transformers typically have a high capital cost, and larger models can have long manufacturing lead times.

The privatisation and deregulation of power utilities along with legislation creating a more open-market based system have changed the focus of companies. Electricity has become a bulk commodity that is traded and sold under free competition. In turn, more severe stress is being applied to cut costs in order to be more competitive.

This trend of cost consciousness is a result of wanting to maximise the return on investment. To achieve this, preventing outages and their consequential issues has the effect of reducing total maintenance costs. Optimisation of electrical equipment lowers the amount of wasted resources invested in a system. This brings into force a system called CBM. Repairing or replacing electrical equipment is done as needed rather than on an emergency or periodical basis. This allows operation of existing equipment to be optimised, working it harder and longer based on what it is truly capable of.

1.2 CONDITION BASED MAINTENANCE (CBM)

To fulfil the requirements of CBM, an accurate knowledge is needed of the current state of the electrical equipment, which includes the insulation of power transformers. This information has to be gathered in a timely fashion and while the transformer is operating on-line. Some reasons that increase the need for a CBM regime based on the knowledge of the actual state of the transformer include:

- Some of the stresses placed on the insulation are related to the loading of a transformer, such as increased thermal degradation of insulation with increased currents that generate heat. Normally, transformers are designed and built to perform to defined levels satisfactorily and are operated in such a way. However, increasing power system expansion and change is putting pressure on operators to increase the loads of power transformers above their nameplate rating. This means a corresponding increase in electrical and thermal stress resulting in an earlier transformer end-of-life (EOL).

- To lower manufacturing costs in a competitive market, power transformers are being designed and produced with tighter design tolerances and safety margins. This allows less room for error and increases the chance of faults.
- The typical load presented by consumers is changing. There is an increase in the amount of fast solid state switching equipment used, resulting in higher levels of harmonic stress on transformers.
- Power transformers often have high repair or replacement costs. Instead, timely repair or refurbishment would extend the life of the transformer beyond recommended manufacturer limits if the transformer is otherwise known to be in a satisfactory condition.
- Gradual deterioration due to normal operation is not easily apparent. While deterioration may be observed during periodic maintenance, extensive checking and possibly unneeded repairs could be carried out requiring extended downtime. Prior knowledge of insulation issues helps to prevent this.
- The majority of the power transformer population is old, and it is within this group that most of the emerging faults will be detected. This leads to the need for monitoring equipment to be designed that is able to be installed on transformers already in operation in the field.

Implementation of CBM requires that [1]:

- Mechanisms of component failure and deterioration are known, and their criticality.
- Suitable indicators are available for the status of failure and degradation.
- There are appropriate diagnostic tools to measure these indicators.
- There are appropriate assessment tools to reliably interpret measurements and assess the transformer condition and maintenance need.

Different types of diagnostic and monitoring techniques may be employed to provide the necessary information for CBM [1]:

- On-line monitoring is used to continuously observe relevant parameters and provide an early warning.
- On-line diagnosis is used to provide a quick in-service diagnosis, either periodically (maintenance) or in case possible failure or degradation is expected (intensive care).

- Off-line diagnosis may be used periodically for strategic or expensive transformers, or to determine the exact cause, location or action required once failure or degradation is observed.

The benefits of condition monitoring can be summarised as follows [2]:

- Reduced maintenance costs.
- The results provide a quality control feature.
- It limits the probability of destructive failure, and thus leads to improvements in operator safety and quality of supply.
- It limits the severity of any damage incurred, thus minimising consequential repairs, and it helps identify the root cause of failures.
- Information is provided on the transformer operating life, enabling business decisions to be made either on transformer refurbishment or replacement.

1.3 EXISTING TECHNIQUES

The insulation in power transformers slowly degrades over several decades, due to factors such as thermal, dielectric and mechanical related stress [3]. One of the most common methods for analysing the condition of insulation is to take oil samples from the tank [3]. These are studied to determine what dissolved chemicals are present, and the amount and relative ratio they are in, which gives an indication of what processes or reactions are occurring inside the transformer. However, the sampling interval can be in the order of several months to a year or more [4]. This does not provide timely information and can even be misleading if the sampling conditions change, for example, if the transformer has just been in operation as opposed to having been off-line for an extended period of time.

Other techniques have gradually been developed to complement and add information to the study of transformer insulation. These provide warnings and help with the diagnosis of problems. Besides considering the base data of loading and temperature, techniques include dissolved gas analysis (DGA), total combustible gas (TCG), furanic compound analysis, degree of polymerisation (DP), tank pressure, dielectric response, low voltage impulse (LVI) testing, leakage inductance measurements, internal winding temperature profiling, thermography, static charge monitoring, frequency response analysis (FRA) and PD detection [3, 5, 6, 7, 8, 9, 10]. While combinations of techniques provide useful information, the problem of knowing the condition of a transformer and when a problem is going to occur is not yet solved. Transformers still experience problems and catastrophic failures.

Failure rates of transformers in western networks are low, normally 0.2-2% per transformer year [3]. This means high cost monitoring and diagnostic systems cannot be justified on economic terms, especially if there is redundancy [3]. Trade-offs are required to balance the value of information gathered against the cost of gathering that information. However, a factor that has changed in recent years is the availability of powerful and cheap digital systems. New sensors for measurements are becoming available, although their cost is still not cheap. However, increased digital processing power is becoming ever more obtainable at relatively low costs compared with the cost of the transformer and fixing its problems. Linking of these digital systems can provide the means for presenting timely information, so that a human operator can make informed decisions on what course of action to take. Automation of information processing, analysis and decision making can be incorporated, allowing automatic disconnection of suspect units before failure [11]. As base technology progresses, new methods of transformer insulation monitoring should be investigated.

1.4 PARTIAL DISCHARGE DETECTION

PDs within power transformers cause gradual degradation of the insulation and eventually catastrophic breakdown. It has long been recognised that PDs are a primary cause of the failure of transformers. Knowledge, recommendations and eventually standards have been achieved to incorporate the best practices into transformer design, construction, monitoring and repair in order to minimise PDs. Some new methods for monitoring PDs have been able to be implemented on transformers previously constructed. This is important as a large population of transformers has already been installed around the world.

A common method for detection of PDs is DGA. Some diagnosis of the type of fault can be provided by analysing quantities and ratios of molecules. The Buchholz relay collects and monitors hydrogen gas produced by PD sources, but is limited in its effectiveness to determine the condition of the transformer. The primary established techniques for electrical PD detection by measuring current or radio frequency (RF) pulses when the transformer is energised, as detailed in standards [12], are performed when the transformer is off-line and preferably within a shielded enclosure to eliminate electrical interference. These methods, being non-continuous in nature, have implications for testing regimes in terms of cost and time. Only snapshots in time of part of the transformer's condition can be gained. Even when transformers are off-line, interference from surrounding on-line transformers can disrupt PD tests. Acoustic waves travelling within the insulating oil can be detected at the tank walls, but they are also subject to interference.

Suppression of interference is one of the main challenges in detecting PDs, either while the transformer is off-line or on-line in a noisy environment. No standards have

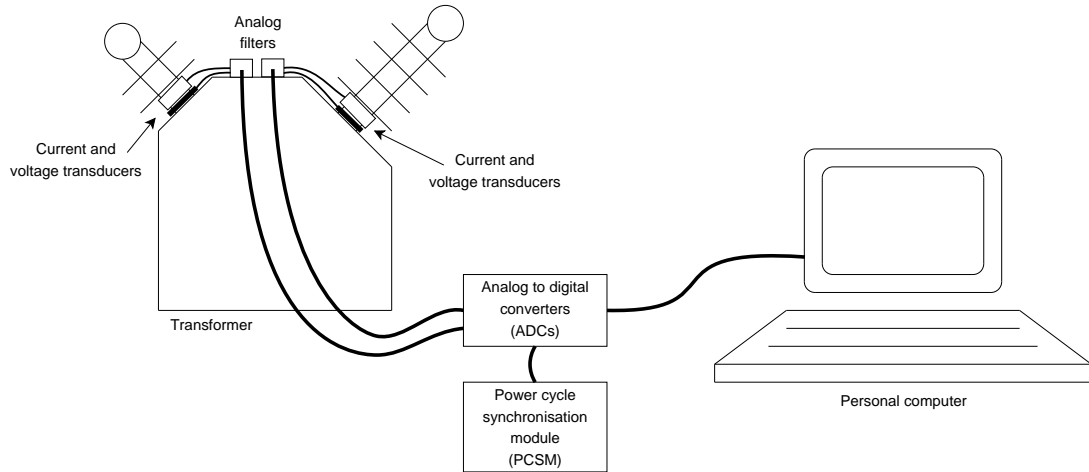


Figure 1.1 Simplified description of the partial discharge detection system.

yet been developed for on-line electrical monitoring of PDs, although several areas of research have focused on this challenge. The main sources of interference are narrowband signals, such as radio stations, and other pulse generators, such as external corona sources. The digitisation of signals allows complex signal processing in computers. Signal processing techniques under research include Fourier domain analysis and adaptive filtering, gating of pulses, directional coupling, PD-free reference signals, wavelet analysis, pattern recognition and the use of neural networks.

This thesis presents the development of a system that captures current and voltage signals at external taps of a transformer while it is operating on-line. It is designed to be able to be fitted to transformers already in use and will not require HV components that typically have a high cost. New variations of signal processing techniques are used to identify PD pulses that may be buried in external narrowband and pulse interference.

1.5 THE PARTIAL DISCHARGE DETECTION SYSTEM (PDDS)

The main components of the PDDS are shown in Figure 1.1. Each section is described briefly as follows, with details provided in Chapters 3 and 4:

- **Transducers:** A current transducer and a voltage transducer are attached to the base of each bushing of the transformer. The current transducer is in the form of a Rogowski coil and the voltage transducer consists of two parallel metal sheets forming a capacitive voltage divider with the bushing central HV conductor. The bushing ceramic is used as the HV dielectric medium. Each pair of current and voltage signals acquired from a single bushing is termed a ‘channel’.
- **Analog filters:** A highpass filter for each current and voltage transducer prevents aliasing effects when signals are digitised. A lowpass filter attenuates power

frequency signals to improve the digital vertical resolution of captured signals.

- **Signal digitisation:** An analog to digital converter (ADC) for each channel captures the signals for use in a personal computer.
- **Power cycle synchronisation module (PCSM):** In order to reference PD pulses to the phase of the power cycle, the PCSM provides a trigger signal for ADC timing and synchronisation purposes.
- **Personal computer (PC):** Digitised signals are analysed by the PC through several sequential processing stages to identify any transformer PDs and the number of internal PD sources.
- **Software stages:**
 - **Fourier domain threshold filter (FDTF):** Each signal is transformed to the Fourier domain, and any significant narrowband signals are attenuated.
 - **Continuous wavelet directional coupling filter (CWDCF):** The current and voltage signals from a bushing are transformed using the continuous wavelet transform (CWT) and then combined to search for pulses travelling from the transformer. This is repeated for each bushing to confirm that a pulse has not originated from an external source and traversed the transformer winding.
 - **Cluster neural network (CNN):** A neural network that does not require any prior knowledge is provided with the waveshapes of all identified internal PD pulses. The network groups the pulses to determine the number of PD sources and to provide information for phase resolved partial discharge analysis (PRPDA) for each source.

1.6 THESIS OVERVIEW

The contents of this thesis consist of the following main components:

- A review of existing transformer monitoring and diagnostic techniques, both on-line and off-line.
- A description of the PDDS hardware components and signal processing stages.
- Results from three tests of the PDDS on two 11kV/240V, 7.5kVA single phase distribution transformers.

These components are discussed in the following chapters:

- **Chapter 2:** This chapter reviews background information on existing power transformer fault detection and diagnostic techniques. Also included are recent trends and developments in a variety of research areas. Identification of some of the limitations of each technique is provided. Included are reviews of temperature based measurements, oil analysis, dielectric response, differential relays, model based monitoring, impulse testing, transfer function profiling and PD detection. An indication of the success rates of these methods is also provided. A section on the life assessment of transformers is also included, which is one of the top goals of power transformer research.
- **Chapter 3:** The chapter describes the hardware components of the PDDS. The current and voltage transducer specifications are detailed, as are analog filters for anti-aliasing and power frequency attenuation. The PCSM is described. Relevant specifications are provided for the oscilloscopes used for signal digitisation and the arbitrary waveform generators used for artificial signal generation.
- **Chapter 4:** The purpose of this chapter is to describe the signal processing principles that identify, extract and group internal PD pulses from any external interference. After an overview of the signal processing stages and how they interconnect, details of the FDTF, CWDCF and CNN are provided. More general information about wavelets and neural networks is also included.
- **Chapter 5:** Results from three tests are presented. Two off-line tests, simple and complex, were designed to measure the effectiveness of the PDDS. Here, artificial PD pulses were injected into a modified transformer Tx1. Artificial external electrical interference was also added. Knowledge of when PD pulses were injected allowed a comparison with the PDDS output. A third test on an identically constructed transformer Tx2 was performed when the transformer was energised and subject to external narrowband and corona interference. In this case, it was unknown whether the transformer had a PD problem.
- **Chapter 6:** A discussion of the PDDS test results is provided, including the strengths and weaknesses of the system. An outline of future improvements is suggested, along with comments about the PDDS being suitable as a subset of a complete transformer monitoring and diagnostic solution.

1.7 AIM OF THE PROJECT

The aim of this project is to initiate a transformer insulation condition monitoring program based on the electrical detection of PDs generated within a power transformer in an on-line real-time situation. Two identically constructed 11kV/240V, 7.5kVA

single phase distribution transformers are to be used to develop and evaluate different detection systems.

Chapter 2

INSULATION MONITORING AND DIAGNOSTIC TECHNIQUES

The purpose of this chapter is to present background information on existing and developing power transformer insulation fault monitoring and diagnostic techniques and systems. Capabilities and limitations of each technique are identified where appropriate. The detection and recognition of insulation faults allow preventive maintenance and asset management that extend the life of the transformer. Sections on insulation and transformer life assessment are included to provide an understanding of the situation for which monitoring and diagnostic systems are being developed.

In the present context, it is useful to differentiate between ‘monitoring’ and ‘diagnostics’. ‘Monitoring’ is here defined as the collection of data, and it mostly involves sensor development and measurement techniques for on-line applications and data acquisition. ‘Diagnostics’ includes the interpretation of data collected from monitoring sensors. It has historically been mostly involved with off-line measurements on transformers, due to a lack of suitable techniques to study a power transformer in depth while on-line. Some natural overlap is found between monitoring and diagnostics. For example, a specific on-line gas monitor provides fault detection along with information about the type of fault.

Monitoring equipment, which is often on-line and permanently mounted on the transformer, must primarily be reliable and low cost. It should also be designed for field installation on transformers already in operation. The main reason for installing monitoring equipment is that developing faults can be detected before they lead to catastrophic failure. Diagnostics are normally used either for determining the actual condition of a transformer or as a response to a received warning signal. Since it is typically not a permanent installation, the use of high-tech, sophisticated and costly equipment combined with skilled personnel can be economically justified. The use of on-line monitoring with some diagnostics allows a change from periodic maintenance to CBM.

Since failure rates of transformers in western power networks are low, normally 0.2-2% per transformer year [3], high cost monitoring systems for failure prevention cannot

be justified on economic terms. However, in many European countries, essential power system components were renewed after the Second World War and as a result, there are a lot of power transformers that are over 30 years of age [13]. Therefore, many transformers may reach the end of their lifetime in the next few years, possibly leading to cascade failures. This may justify increased allocation of resources for selective installation of more costly monitoring systems.

Monitoring is the basis for diagnostics, but without diagnostics, measured data is of limited value. However, the distinction is blurring because cheap computer hardware that is permanently mounted is providing more analytical information than just a warning signal, and is leading to more in-depth on-line diagnosis. An IEEE task force [5] has reviewed key parameters for monitoring power transformers. A system that monitors these parameters and interprets the data will provide a more thorough understanding of the status of the transformer than just the monitoring of a single signal.

In this chapter, general diagnostic techniques are discussed first as they have been historically developed first, mostly in an off-line environment. Many monitoring systems are more recent and on-line, and they have been built on the knowledge gained from off-line diagnostics. Where relevant, references are made to the newer field of on-line diagnostic techniques that use data collected from on-line monitoring systems.

2.1 TRANSFORMER INSULATION

Insulation is recognised as one of the most important constructional elements of a transformer. Its chief function is to confine the load current to useful paths, preventing its flow into harmful channels. Any weakness of insulation may result in failure of the transformer. Since the invention of the power transformer, conventional conductor insulation has been some form of paper or cloth. The main constituent of these fibrous materials is cellulose, an organic compound whose molecule is made up of a long chain of glucose rings or monomers, typically numbering in the range from 1000 to 1400 [14]. The chemical structure of a portion of a cellulose molecule is shown in Figure 2.1.

In solid insulation systems, it is essential to eliminate air or gas from within insulation layers. It is thus necessary to impregnate solid insulation systems, such as paper, for transformers with suitable oil of adequate dielectric constant to prevent the voltage stresses in the air voids from causing PDs and subsequent breakdown. The most commonly used insulating liquid is mineral oil. This is due to its low cost and ready availability. The alternatives are usually synthetic oils which are used when special properties are required. These properties are high temperature stability, fire resistance, high permittivity and gas absorbing characteristics. In general though, the combination of mineral oil and cellulose has remained the standard transformer insulation system up to the present time.

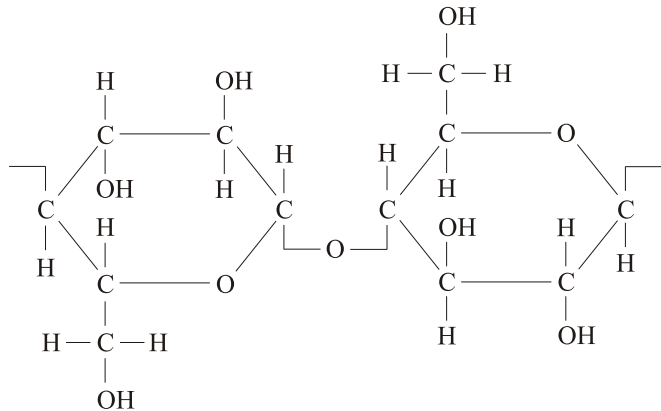


Figure 2.1 Cellulose molecule structure.

The oil serves the dual purpose of providing insulation and being a cooling medium. To serve as a dielectric medium, the oil must be free from water and suspended matter. Additionally, the oil must have good oxidation stability. Oxidation will produce oil decay products which cause transformer overheating and premature failure. As a cooling medium, oil conducts away the losses that are produced in the transformer in the form of heat. This requires low viscosity and volatility plus good specific heat capacity and thermal conductivity.

The electrical quality of the cellulosic material is highly dependent on its moisture content. When exposed to air, cellulose absorbs moisture from the air quite rapidly. If the cellulose is not impregnated with oil, equilibrium with the moisture content of air is reached in a relatively short time. Thus, cellulosic material has to be processed under heat and vacuum to remove the moisture before oil impregnation, in order to obtain maximum dielectric strength. For most applications, a maximum initial moisture content of 0.5% moisture per dry weight cellulose is considered acceptable. For modern extra high voltage (EHV) and ultra high voltage (UHV) transformers, a maximum initial moisture content of 0.3% or less is recommended [15].

Cellulosic material shrinks when moisture is removed [15]. It also compresses when subjected to pressure. Therefore, it is necessary to dry and dimensionally stabilise windings before adjusting them to the desired size during the transformer assembly process. Ideally, the prestabilising pressure should be equal to or larger than the anticipated loading that the winding will experience during fault conditions, so that further compression of insulation and loosening of windings in service is minimised.

2.1.1 Insulation aging

Electrical, thermal, mechanical and environmental stresses are factors attributed to insulation aging. They can act simultaneously. On a molecular level, the DP is the

average number of glucose rings in the cellulose molecule. A single cellulose fibre is made up of many of these long chains of glucose rings. Since the mechanical strength of the cellulose material depends on the length and condition of the fibres, the DP gives a good measure of retained functionality as the transformer insulation ages in service. Three mechanisms contribute to cellulose degradation in an operating transformer, principally hydrolysis (water), oxidation (air) and pyrolysis (heat) [14]. All of these factors break cellulose molecules down in size, lowering the mechanical and electrical strength of the paper insulation. Chemical by-products of breakdown include carbon monoxide, carbon dioxide, water and hydrogen.

Electrical aging takes place when the electrical stresses in an insulation system cause ionisation and PDs to occur at operating voltages. PDs should not occur at operating voltages, but overvoltages can produce PDs which do not disappear at the normal voltage.

Although transformer insulation is affected by many factors, temperature is probably the most severe of the aging factors. The rate of thermal aging of cellulose accelerates rapidly at temperatures not far above the accepted normal operating temperature of transformer conductors. As a result, there is an inter-relationship between the life expectancy and the operating temperature of a transformer.

A law describing this relationship was put forward by Montsinger in 1930. It states in general terms that an increase or decrease of 5-10 °C in the operating temperature, depending on the insulation material, will result in a doubling or halving of the aging rate of the insulation [16]. In 1948, Dakin proposed a theory for the interpretation of thermal aging based on the Arrhenius chemical reaction rate relationship [17]. Still used today, it is given by:

$$L = Ae^{B/T} \quad (2.1)$$

where L is the life, T is the temperature and A , B are constants determined by the activation energy of the reaction. Normal transformer insulation life expectancy is based on a continuous hot spot temperature of 110 °C. However, hot spot temperatures of 130 °C to 140 °C are commonly accepted under emergency loading conditions. Relative to 110 °C, the aging rate at 130 °C accelerates by a factor of 8 and at 140 °C by a factor of 21 [15], according to the Arrhenius relationship.

The insulation system of a transformer is invariably stressed to some extent by mechanical forces occurring during the operation of the equipment, for example, forces resulting from short circuit currents. Mechanical stresses can also be a major consideration during the manufacturing and processing stages of production. Loss of insulation mechanical properties and increased brittleness may lead to rupture of the insulation during a short circuit.

Environmental effects such as humidity, pressure changes, dust and chemical fumes will contribute to the early onset of PD activity.

2.2 TRANSFORMER LIFE ASSESSMENT

The assessment of the remaining life of a transformer is one of the most important issues related to monitoring and diagnostics. The ultimate question to be asked is how many years a unit has before it fails, that is, when has its EOL been reached, where EOL is taken to mean that the transformer is no longer able to fulfil its required function economically.

Distinctions can be made between economical, technical and strategical EOL [3]. It is seldom that transformers are replaced for technical reasons only. The main reasons for taking transformers out of service are cost related since the total operating cost should be minimised. Strategic reasons arise, for example, from changes in load patterns and changes in voltage level. It is important to distinguish between the technical EOL of the insulation materials and the EOL of the transformer itself. The technical EOL of a transformer is a function of many factors including design, historical events, previous operating conditions, its present state and future service conditions. Most methods proposed for estimating technical EOL focus on only one of these aspects, the present state of the insulating material. Furthermore, load and temperature are not the only factors that should be taken into consideration for estimating the technical EOL of a transformer. The number of short circuits and overvoltages experienced, design weaknesses, repairs and transportations between sites will influence a transformer's ability to perform its function and therefore should be taken into account. It is important that utilities keep historical records concerning the operating conditions if accurate technical EOL predictions are to be made.

The projected equipment life is a subject of major concern to the utility industry. For transformers, utilities apply industry loading guides [18] to assist in establishing load practices that will not unduly jeopardise life. Loading guides provide equations to enable estimation of insulation hottest spot temperature as a function of load, leading to a temperature/time relationship that can be used to compute consumption of life [14]. Transformer loading guides define the life of the material in the insulation system as it is influenced by temperature, not the functional life of the transformer, which may also be affected by mechanical and dielectric stresses.

If an end point for insulation life is to be defined, it must be done in terms of a measurable physical characteristic of the material. In the past, 50% deterioration of the tensile strength of the paper has been used as an EOL indicator [14]. An alternative EOL definition has been suggested by some investigators, namely the DP discussed in Section 2.4.3. This approach seems to have merit as reduction in the DP corresponds with a deterioration of mechanical properties. Bozzini [19] suggests that a DP value of 100-150 be used to indicate the EOL of the insulation.

The work of Allan [20, 21] on the distinction between nameplate age and insulation age is significant in assessing the remaining life of transformers. His papers show how

micro-samples of paper insulation from transformers in service can be used to yield information on the aging of the insulation. In addition, Allan makes the point that there is no definite time at which a transformer can be predicted to fail, only an increasing probability that the unit will fail.

2.2.1 Thermal measurements

As increased temperature is a critical factor in rapid insulation aging, much research has focused on determining the internal transformer temperature profile with a view to estimating the insulation life and, indirectly, the EOL. It is essential to know the maximum temperature reached by the winding insulation if a transformer is to be loaded efficiently and its insulation life expectancy calculated. In the past, thermocouples and resistance temperature devices (RTDs) have been used for winding temperature measurements [22]. However, a major difficulty encountered in the practice is that the temperature is generally not uniform throughout the winding due to localised variations in the effectiveness of the coolant. Furthermore, the locations of the highest temperatures, the hot spots, are often within the winding and inaccessible to external probes.

Techniques for estimating the points of highest temperatures in windings based on temperature measurements at other locations have therefore been developed. The thermal image temperature indicator, which produces a hot spot estimate based on oil temperature and load current, is one of the most widely used instruments [4, 23]. Other instruments and techniques use factors such as average winding temperature, bottom oil temperature and top oil temperature to estimate hot spot temperature [23]. Improved thermal modelling of the transformer heat flow enhances the estimated temperature distribution accuracy [24]. However, these methods are mostly still inaccurate, and because allowing hot spots to exceed certain temperatures dramatically increases the risk of breakdown, conservative loading policies have been applied. Accurate knowledge of the true hot spot temperature would lead to more improved transformer utilisation and better life expectancy estimates.

The above limitations can be overcome by measuring the winding temperature directly. However, a measuring unit must be produced that is rugged and small enough to be embedded in the winding without causing too much disturbance. Most importantly, such a device must in no way weaken the electrical insulation of the transformer. Recently, implanted temperature measurement devices fitting these criteria have been developed and used to directly measure winding insulation hot spot temperatures. The main techniques that have been employed include:

- **A vapotherm capsule:** This method uses the vapour pressure of acetone contained in a capsule embedded in the winding. Temperature is measured by trans-

mitting the vapour pressure to a pressure transducer via a capillary tube filled with oil [25].

- **Fibre optics:** Devices based on temperature dependent light phenomena using optical fibres for light transmission are being refined. Two main types of sensors have been used [3]. Firstly, in fibres which measure the temperature at one point [22, 25], laser light is temperature dependently altered in the angle of polarisation or wavelength by a quartz block placed in the winding. Secondly, distributed fibres measure the temperature along the length of the fibre [26]. A drawback is that fibre systems are expensive.

In addition, thermography and infra-red scanning systems [3] indicate the position of thermal problems and can be used on-line.

It is well known that voltages and currents with frequencies above 50Hz result in additional heating in iron-cored devices like transformers [27]. Because the increasing use of harmonic loads on power systems has resulted in transformers running at rated or higher temperatures at less than full load current [28], monitoring hot spot temperatures can be valuable if loss of life is to be avoided [29].

2.3 EXISTING MAINTENANCE PROCEDURES

Preventative maintenance techniques play an important role in maintaining the health of transformers. The objectives in maintaining any item of plant are [30]:

- To obtain the maximum practicable operating efficiency.
- To obtain optimum life.
- To minimise the risk of premature and unexpected failure.

Currently practised preventative maintenance procedures used to increase transformer insulation reliability include [4]:

- **Visual inspections:** Defects, abnormalities and the general condition of the transformer are noted together with information on parameters such as oil levels, temperatures, pressures and loadings. Visual inspections are often performed on a scheduled basis.
- **Insulation resistance measurements:** Insulation resistance measurements are often made with a Megger during transformer overhauls and repair work, and are therefore done on an irregular basis.
- **Dielectric loss measurement:** Insulation dielectric loss is determined through dielectric loss angle measurements. A change in the $\tan\delta$ during the life of a transformer is a good indication of insulation deterioration.

- **Scheduled examination:** Transformers are taken out of service and undergo detailed examination. However, often transformers that are in good order may be dismantled just because they are due. Alternatives to time based schedules have been proposed [4].
- **Oil analysis:** Oil samples are taken from the tank at periodic intervals (six monthly or annually) for use in gas chromatography tests in a laboratory, and its information added to a database of results for each individual transformer. Standards are available regarding oil tests and evaluation procedures [31].

2.4 DIAGNOSTIC TECHNIQUES

As diagnostics is normally used either for determining the actual condition of a transformer or as a response to a received warning signal, it covers the subject of interpreting various signals to understand what stresses have been applied and the results of those stresses. It is important that diagnostic techniques are used that match the sensor systems that are already installed, or those sensors that can be easily attached to the transformers. In general, as the diagnostic methods become more advanced, the importance of a deep knowledge of transformer design increases. In many cases, it is not possible to make a reliable diagnosis without knowing the transformer design in detail.

The major stresses acting on the windings of a power transformer, either in combination or individually, are [32]:

- Mechanical stresses between conductors, leads and windings due to overcurrents and fault currents caused by system short circuits.
- Thermal stresses due to local overheating, cooling system malfunctions and over-load currents and leakage flux when loading above the nameplate rating.
- Dielectric stresses due to system overvoltages, transient impulse conditions and internal winding resonance.

Most of the monitoring and diagnostic techniques presented in this chapter are generally sensitive to all three fundamental stresses, and therefore interpretation of the outputs for fault diagnosis can be problematic. Hence, decisions made on the basis of the results of only one diagnostic technique can be misleading. For this reason, the final decision regarding insulation failure mechanisms is best made by evaluating and interpreting the results of more than one technique, and it must take into account the construction characteristics specific to the transformer being tested.

Faults in the HV insulation of power transformers in service can generally be divided into the following three categories, according to the time of evolution [33]:

- An internal discharge caused by a winding displacement following a short circuit current, or a discharge due to a large steep-fronted transient overvoltage may lead to instantaneous and complete breakdown.
- Local faults that develop into a complete breakdown over a few days, weeks or even months are common, and their early detection is the main task of automatic diagnostic devices continuously monitoring transformers in service.
- Long term deterioration of HV insulation (which can be perceived as accelerated aging) over a period of a few years can be detected by analysing oil samples, usually taken at six or twelve month intervals.

2.4.1 Oil dielectric strength test

The dielectric strength test is performed according to the IEC-156 standard [34]. The dielectric strength of oil, which is effectively a measure of the oil's ability to withstand electrical stress without failure, is exceptionally sensitive to contaminants such as water, sediment and conducting particles [4].

The IEC-156 basic test consists of applying to the test electrodes immersed in the oil sample an increasing alternating current (AC) voltage at mains frequency, starting from 0V and increasing at a steady rate of 2kV/s until the value producing breakdown is reached. Breakdown is defined as the voltage when the first spark-over occurs, whether transient or established. The test is repeated six times on the same sample. Maximum and minimum times among the six tests are specified for each test sample. The final result is the arithmetic mean of all six tests. By determining the dielectric strength along with other parameters, such as moisture content, loss angle and resistivity, an overall assessment of the status of the insulation oil can be made.

2.4.2 Oil analysis

Oil analysis is one of the primary means used to monitor the insulation condition of power transformers. A regime for taking oil samples is typically done as follows [4]:

- Once a month for the first six months of service.
- Once or twice annually after the first six months.
- Within 24 hours of a fault as a matter of procedure.
- Up to once a week for a troublesome transformer.

Gases that have not dissolved into the oil can be collected from fitted Buchholz relays and analysed with the results of oil testing. Buchholz relays are discussed in Section 2.5.1.

2.4.2.1 Dissolved gas analysis (DGA)

The presence of faults such as arcing, local overheating and PDs in transformers always results in chemical decomposition of the insulating materials, that is, mineral oil and cellulose. The gases formed tend to dissolve, either entirely or partially, into the mineral oil. By monitoring the concentration of these gases, it is possible to detect incipient faults at an early stage and take corrective actions before the faults lead to unexpected failure.

The laboratory technique used to separate and analyse fault gases is called DGA. The analytical instrument used is a gas chromatograph. The process requires the careful collection of an oil sample which is usually sent to a third-party laboratory specialising in transformer oil analysis. The gases are extracted under a vacuum and analysed individually for gas concentration in parts per million and percentage.

DGA is often performed in the following situations:

- During a heat run test in a factory.
- A few days after a new transformer goes into service.
- For routine annual testing as part of a maintenance program.
- After a Buchholz relay alarm or trip during normal operation.
- After a protection trip due to a system fault close to the transformer.
- After a short circuit condition due to failure of other equipment.
- When overheating is suspected due to overloaded operating conditions.

The nature and the amount of the individual component gases extracted from the oil are indicative of the type and degree of the abnormality present. Investigations performed over the years have associated the presence of the following gases with the given fault conditions [35]:

- **Hydrogen (H_2):** Large quantities are associated with PD conditions.
- **Hydrogen, methane (CH_4) and ethene (or ethylene) (C_2H_4):** Result from thermal decomposition of the oil.
- **Carbon monoxide (CO):** Produced by thermal aging of the paper.
- **Acetylene (C_2H_2):** Associated with an electric arc in the oil.

The above gases are the ones usually identified in gas chromatography and are generally referred to as the ‘key gases’ for diagnostic purposes. The above research results allow the following fault diagnosis to be made in practice based on the presence of the indicated gases [35, 36]:

- Overheated cellulose ($> 150^{\circ}\text{C}$) will lead to carbon monoxide, carbon dioxide and water being formed.
- Excessively heated cellulose ($> 1000^{\circ}\text{C}$) results in the formation of carbon oxides, water and carbonaceous materials such as tar. This leads to destruction.
- Overheated transformer oil leads to the liberation of hydrocarbon gases, most notably ethylene, ethane and methane.
- Under electrical stress conditions (PDs and arcing), oil decomposes into large quantities of hydrogen and lesser amounts of acetylene along with small volumes of light hydrocarbons.

The DGA results can be interpreted by using different methods, the guidelines of which are set out and listed in international standards [37]. In addition to making a diagnosis based on the concentration of key fault gases, fault diagnosis can also be performed based on the relative concentration ratios of the individual gases dissolved in the oil, which Rogers [38] comprehensively established in 1974. These have become known as Rogers ratios and are still widely used as a means of attempting to identify fault conditions from DGA. The gas ratio methods are useful because they eliminate the effect of oil volume.

In order to get a reliable interpretation, it is necessary to take into account not only the absolute values but also the production rates of the different gases, as the rate of gas formation can be indicative of the severity of the fault. Moreover, the type of transformer under investigation should be considered when making the analysis. For example, a generator step-up transformer shows a different pattern than a system transformer, and a transformer with more solid insulation differs from a furnace transformer [3].

The procedure of oil sampling, gas extraction, chromatographic analysis and data interpretation is typically performed annually by most owners of large power transformers. However, this sampling only reflects the present condition and does not provide any guarantee of the status quo remaining until the next DGA test takes place. Dilution of gases, DGA instrument complexity, diagnosis time delays and lack of fault location information are some of the disadvantages of DGA.

2.4.2.2 Total combustible gas (TCG) analysis

Heat and PDs can lead to the generation of combustible gases. The concentration of these gases, especially hydrogen, dissolved in the oil gives a good indication of the extent of insulation degradation. TCG analysis is used to detect the thermal decomposition of the oil and paper insulation into these gaseous components. The first portable TCG devices measured the presence of combustible gases in the transformer gas space

by their heat of combustion using samples periodically removed from the gas space. Continuous TCG monitoring employs a thermal conductivity cell that measures the percent combustibles in a continuously circulating sample of the transformer gas space. The detection of 0.5% TCG initiates surveillance procedures [39]. When a portable TCG detector is used, a sampling interval of 4 to 6 months is customary.

2.4.2.3 Furanic compound analysis

When cellulose materials age as a result of thermal stress, liquid furanic compounds are generated as a degradation product. The monitoring of furanic compounds by annual sampling of the oil and its analysis using high performance liquid chromatography (HPLC) has been used for condition monitoring on a routine basis for some years [32]. Generally, furfuraldehydes (FFAs) are extracted from the oil either by solvent extraction or solid phase extraction and measured by HPLC using an ultra violet (UV) detector [40].

It has been shown that there exists a relationship between DP and the concentration of furanic compounds [3], which allows for an indirect measurement of the degree of aging of the cellulose. However, the situation is complicated by the fact that different types of paper show different production rates of furanes and that the concentration is dependent on the mass ratio between oil and cellulose. As a result, the relationship between the generation of these by-products and the condition of the in-service paper has not been well established [40]. However, furanic compound analysis may be a method for determining the EOL of transformer insulation [3].

Recent developments include fluorescence based measurement methods for assessment of FFA in transformer oil [41] and an optoelectronic sensor for the determination of FFA in transformer oil to concentrations as low as 0.1 parts per million [42]. This sensor could form part of a compact, portable instrument that could be used by a non-specialist operator on-site, rather than having to rely on skilled laboratory based analysis.

2.4.2.4 Expert systems and fuzzy logic

Transformer fault diagnoses based on DGA (see Section 2.4.2.1) results do not have a firm mathematical description, and as a result, are still in the heuristic stage. Since the conditions under which fault gases dissolve in transformer oil are related to manufacturers, construction processes, loading history, volume of oil and oil in the sampling container, imprecision and incompleteness are characteristic of the fault diagnostic problem. As a result, the effectiveness of existing DGA diagnostic methods is still unsatisfactory. Knowledge based programming is a suitable approach for implementing a diagnostic solution, and is currently an intense research topic around the world [6].

The use of knowledge contained within prior transformer DGA records has allowed complex expert systems based on neural networks, fuzzy logic and similar techniques to be developed. An adaptive fuzzy diagnosis system developed by Yang et al. [43] uses various rules to pick trends out of data based on historical records and applies them to new situations automatically, modifying the fuzzy if-then rules as needed. Schemes were included to prune out insignificant or redundant rules. The capabilities have also been extensively tested through practical test data. Combinations of fuzzy set theory, expert systems and neural networks are suggested by Xu et al. [44]; they can help to improve the correctness of the diagnosis and ensure the accuracy of the knowledge base. Neural networks can reveal complex mechanisms that may be unknown to a human expert.

2.4.3 Degree of polymerisation (DP)

In the past, the rate of degradation of paper insulation was measured by mechanical strength tests such as tensile, bursting and tearing tests. This has generally been replaced by chemical measurements of the DP. Determination of the DP value of cellulose is a standard method for quantifying the degradation of cellulose. It is a measure of the average number of glucose rings in the cellulose molecules (see Figure 2.1). When cellulose ages thermally, the molecular chains are broken and when aging is far progressed, the paper becomes brittle and loses its mechanical stability. The method is good for a quantitative measurement of thermal aging. The DP of paper varies from about 1100-1200 for new material but drops rapidly during the drying and processing stage of the transformer to around 850-900, which might be taken as a typical starting point for a new transformer [30]. The end of paper life is reached when the DP has dropped to about 250 and the paper starts to lose its ability to withstand mechanical forces. Standards are available for the measurement of DP [45].

The DP is used to detect the following three mechanisms, each of which contributes to cellulose degradation in an operating transformer [14]:

- **Hydrolysis (water):** The oxygen bridge between the glucose rings (see Figure 2.1) is affected by water, causing a rupture of the chain and leading to a reduction in the DP.
- **Oxidation (air):** Oxygen attacks the carbon atoms in the cellulose molecule to form aldehydes and acids, and thereby releases water, carbon monoxide and carbon dioxide. The bonds between the rings are weakened, leading to a lower DP. Water released contributes to hydrolysis.
- **Pyrolysis (heat):** Heat contributes to the breakdown of the monomers in the cellulose chain, thereby liberating gases, which also leads to a reduction in the DP.

The main drawback associated with DP tests is that a paper sample taken from the transformer is required. This is an intrusive action which requires qualified service personnel and the transformer to be taken out of service which tends to be labour intensive. An additional problem is that any insulation which is sufficiently accessible to sample will not be representative of the more critical insulation in the vicinity of any hot spots.

2.4.4 Oil pressure monitoring

Oil pressure can be used as another indicator of insulation deterioration. Pressure behaviour can be divided into the following three categories, depending on the condition of the transformer's insulation [46]:

- **For a good transformer whose insulation has a low power factor:** The pressure fluctuates with temperature, increasing in hot weather due to the expansion of the confined oil.
- **For a transformer with moderate gassing and an insulation power factor that is increasing:** The pressure increases with the power factor due to the self-heating of the transformer.
- **For a transformer with excessive gassing:** Once the oil becomes saturated with gases, they have nowhere to go except to form a blanket above the oil. As a result, pressure increases proportionately, sometimes to several times the original value. Thus, excessive pressure can indicate excessive gassing.

Although pressure can be used as an indicator of a bad transformer, ambient temperature effects need to be compensated for during the middle stages of failure. Temperature compensation is not needed during the final stages of failure, but because leaving a transformer in service until it has reached such an advanced state of deterioration is not advisable due to the possibility of premature failure, pressure monitoring often cannot be applied practically. In some applications, pressure sensors can take several months to detect any significant pressure change [5].

2.4.5 Dielectric response

Dielectric response testing consists of analysing the relaxation of the insulation after the application of a low frequency sinusoid or direct current (DC). This method is used to determine the moisture content, but has also been applied to determine aging. Measurements can be made in either the time domain or in the frequency domain, and it has been shown that the two methods reflect the same physical quantities [47]. The newer diagnostic measurement techniques recognise that insulation systems are electrically complex in nature, being a wide ladder of capacitances, inductances and

resistances [10]. Various techniques include dielectric spectroscopy, time domain dielectric spectroscopy (TDDS), dielectric discharge method and return voltage measurement (RVM). These methods are all based around the monitoring of the polarisation and depolarisation of insulation material. Disadvantages of dielectric response testing include:

- The transformer must be disconnected from the power system.
- It is not possible to make a quantitative statement concerning the moisture content of the transformer if no reference measurements for the transformer are available.
- The transformer design needs to be taken into consideration since the dielectric response also depends on the geometry of the active part and on volume ratios between solid and liquid insulation.
- A lack of historical data severely limits the interpretation of results for more modern methods and so far prevents the description of the physical mechanisms associated with each of the various responses [10].

The dielectric loss angle procedure ($\tan\delta$ measurement) is a special case of dielectric response testing, that is, the response at 50Hz or 60Hz is measured.

2.4.6 Transformer impulse testing

Voltage surges have always occurred on transmission systems, and these surges, whether arising from lightning or switching, are liable to be propagated along transmission lines and into the windings of a transformer. To prevent breakdown of the transformer and interruption of the supply, transformer insulation systems must be designed to withstand surges with peak values that are many times the normal working voltage of the system.

For many years, voltage impulse testing has played an important role in the development of the modern power transformer. Voltage impulses produced in a laboratory to simulate lightning and switching surges are used to obtain the surge withstand characteristics of power transformer insulation systems. Standard tests are now common practice on new power transformers [48]. These typically include the following:

- **Standard impulse test:** This standard test includes the application of one calibration impulse at between 50% and 75% of the basic insulation level (BIL), followed by three impulses at the BIL. Here, the BIL refers to the peak voltage of the test impulse, which is related to the highest expected system overvoltage.
- **Chopped impulse test:** This test is applied according to the following test sequence:

- Application of one full wave at between 50% and 75% of the BIL.
- One full wave at the BIL.
- One or more chopped waves at between 50% and 75% of the BIL.
- Two chopped waves at the BIL.
- Two full waves at the BIL.

Both tests employ a $1.2/50\mu\text{s}$ wave shape, where the chopped impulse is obtained from the $1.2/50\mu\text{s}$ wave shape by chopping the voltage after $2-6\mu\text{s}$, thereby simulating an incoming surge chopped by a flashover of the coordination gaps close to the transformer. Voltage waveforms are recorded for all tests.

Detection of a breakdown in the major insulation of a transformer is usually made by comparing the voltage waveform recorded at the BIL with that obtained during the calibration test at the reduced level. Faults can be detected through any change in the wave shape observed by comparing the full wave voltage waveforms taken before and after a chopped impulse test. Also, any difference between the full wave voltage waveforms and the chopped wave voltage waveforms up to the time of chopping can indicate a fault.

Current waveforms may give an indication of the position of a fault by a burst of high frequency (HF) oscillations or a divergence from the no-fault wave shape. Since the speed of propagation of the wave through a winding is about $150\text{m}/\mu\text{s}$, the time interval between the entry of the wave into the winding and the fault indication can be used to obtain the approximate position of the fault, provided the breakdown has occurred before a reflection from the end of the winding has taken place. Distortion of the voltage waveforms may also help in the localisation of a fault, but it generally requires a large fault current to distort the voltage wave and breakdown is then usually obvious.

Disadvantages of impulse testing as detailed above are that:

- Any differences in the shape of the applied voltage impulse due to the impulse generator producing a slightly different impulse at full and reduced levels will cause a difference between the neutral current waveforms which, according to the above testing procedure, may be incorrectly interpreted as a winding fault.
- Due to the difficulty in accurately controlling the chopping time, recorded neutral current waveforms cannot be compared for the chopped impulse test.
- The differences between observed waveforms are interpreted subjectively which can lead to controversy as there are no generally recognised evaluation criteria.

2.4.7 Low voltage impulse (LVI) testing

Mechanical stresses produced by short circuit forces can distort and displace transformer windings. The distorting effects of short circuit forces may lead to catastrophic failure immediately in which case, diagnosis is trivial. However, if the windings merely displace, the transformer may continue to function but in a much weakened state. The windings may subsequently fail due to insulation abrasion or during another short circuit on the connected system. Inadequate clamping arrangements may also lead to winding movement under service conditions. Clamping may become inadequate due to insulation shrinkage and results in a weakened winding, making the transformer vulnerable to failure due to winding abrasion or winding forces developed during service, for example, at switch-on or upon external short circuit. The test techniques most widely used for assessing the degree of winding movement in power transformers are applied off-line, and include the leakage inductance method described in Section 2.4.8. This section addresses the low voltage impulse (LVI) test technique, which is a predecessor to the FRA described in Section 2.4.9.

Winding deformation that is caused by lightning, switching faults or system faults can be determined by LVI testing. The transformer consists of a complex array of capacitances, inductances and resistances that change slightly when the winding physically distorts. The technique involves exciting the resonant modes of the winding by applying a steep-fronted impulse, typically $1.2/50\mu s$. The time domain response at the remote end of the winding is then recorded and compared with prior recordings. Experience has shown that changes in the winding structure can be detected by comparing ‘as new’ responses with responses taken later. Interpretation of the changes in response is largely a matter of experience, aided by knowledge of the winding arrangement of the transformer. This knowledge of the transformer winding being tested is desirable for the most effective use of the LVI method, and should be allowed for when selecting the measurements to be made [49].

Instead of one winding being impaled and the induced current flowing to earth in the other winding being measured by a shunt, greater sensitivity can be obtained with a circuit in which the difference is measured between the currents flowing to earth from two phase windings that are simultaneously being impaled, that is, two primary windings. This is more suitable for measurements on three phase transformers, but has limited application to single phase units, where instead the induced current approach is used. When measurements are made on a transformer using the LVI method, the service connections to the terminals must be disconnected so that the measurements are not affected by any changes in the layout or earthing of these connections. However, trials have been conducted to test the LVI method on-line using switching transients as the signal excitation [50].

Although LVI is recognised as being exceptionally sensitive, its application has

been limited due to the difficulty in relating response alterations to the physical changes causing them. Because the waveshape and amplitude of the applied impulse affect the response, the application of LVI has also been limited by the practical difficulties of achieving noise free and repeatable results under on-site conditions [51].

2.4.8 Leakage inductance

Leakage inductance measurements have traditionally been used to detect mechanical deformations and changes in winding geometry. As a result of a short circuit, the inner winding has a tendency to decrease in diameter whereas the outer winding increases in diameter. This leads to a higher leakage flux between the windings and thus a higher measured leakage reactance [3]. The relationship between winding displacement and changes in leakage inductance is recognised in [52], which sets a criterion of a 2% change as being significant. However, the test, though useful, can be insensitive to winding displacement [51].

A related technique has been developed by Hydro Quebec [53] that involves the measurement of stray load loss across a range of frequencies. The technique, referred to as frequency response of stray losses (FRSL), is based on the observation that axial winding displacement causes an increase in stray losses. For the FRSL test, the transformer is short circuited on the secondary winding, while the primary winding is supplied with a low voltage over a frequency range of 20-400Hz. The technique is considered to be sensitive down to axial displacement of the order equivalent to winding separation, although it is considered insensitive to radial displacement [53].

2.4.9 Frequency response analysis (FRA)

As discussed in Section 2.4.7, the LVI method is used to detect mechanical deformations of windings caused by short circuit fault currents and other mechanical stresses. An alternative method, FRA [54], is based on the fact that the alteration of the spatial disposition of a winding alters its distributed parameters and consequently its frequency response. Therefore, the frequency response of a winding directly reflects its spatial disposition.

The FRA method uses a sweep frequency generator to apply low voltage sinusoids at different frequencies to one terminal of a transformer winding. Typically, the frequency sweep is performed up to a few MHz. Amplitude and phase signals from selected terminals of the transformer are recorded and used to determine voltage ratio and impedance transfer functions at each discrete frequency included in the sweep. Comparisons are then made between transfer functions determined before and after winding damage. The FRA is typically performed using a network analyser [54], and it is employed for large power transformers to provide fingerprint information at man-

ufacture and when commissioned on-site. This data is then used as a future reference for comparisons with results obtained after winding deformation.

In applying FRA, the transformer must be physically disconnected at all bushing terminals in order to prevent external components from affecting the FRA results [54]. As a result, preparation time can be considerably longer than the test itself. Furthermore, the resources required to carry out FRA testing may limit its application to one-off problem solving and as a preliminary measure to justify more expensive detanking.

The transfer function determined by FRA provides a highly stable transformer model and is sensitive to factors that affect the impedance of the transformer. This includes the insulating oil where there is a change in dielectric constant, the condition of the core where there is a change in the total reluctance or total losses in the iron, and the winding insulation if there are changes in the winding capacitance or shorts between turns [55].

Advantages of the FRA method include improved signal to noise ratio (SNR) through the use of effective narrowband filters and the ability to determine the integrity of the winding insulation. It does not require the extensive calibration of the LVI method. Disadvantages of the FRA method include the problem that the instrumentation used can have a large effect on the transfer function [54], the lengthy time consumed to thoroughly test all the various transfer function combinations on a three phase transformer, parasitic capacitance effects, bushing capacitance having a dominating effect, availability of reference transfer functions and that the transformer under test must be removed from service.

A closely related technique is the transfer function method. It applies low voltage impulses similar to the LVI method, and voltage and current time domain recordings are digitised at relevant terminals. The transfer function can be calculated as the quotient of the spectra of the voltage and current. The transfer function method and other similar impulse testing methods, such as LVI and FRA, only differ in the processing of the recorded data. The transfer function may be regarded as a ‘signature’ of the transformer and is independent of the applied waveform [56].

2.4.10 Partial discharge detection

A PD is an electron avalanche that only partially bridges the insulation between electrodes in a HV apparatus. These discharges occur in gas, usually air bubbles embedded in solid insulation, when the voltage exceeds some limiting value and discharges the capacitance of the gas bubble or other material in which the PD crosses. Solid insulation may be damaged where either or both ends of the discharge are rooted to a surface. The very high dielectric stresses associated with the electron avalanche cause a local breakdown and conduction in the solid insulation. A succession of these avalanches can

ultimately cause complete breakdown of the solid, rendering the complete insulation ineffective. Abnormal levels of PDs may indicate any of the following conditions [10]:

- Voids in the insulation.
- Delamination at insulation surfaces.
- Cracking or fissures in brittle insulation.
- Contamination in the insulation.
- ‘Electrical trees’ in the insulation.
- Abnormal electrical stress areas due to improper manufacture or application.

Discharges are generally considered to take place as a precursor to total insulation failure, but may exist for a long period of time, possibly years, before total breakdown occurs [30]. In some circumstances, the existence of the discharge will modify the stress distribution so as to initially reduce the tendency to total breakdown. In time, however, total breakdown will always result, often because the discharge itself leads to chemical breakdown of the insulation which reduces its electrical strength. Ideally, the level of acceptable PDs is nil in a healthy transformer under normal operating conditions, which includes overvoltages of up to 10% [30].

The early detection and location of PDs within power transformers is important if degradation or incipient breakdown of insulation is to be avoided. PD erosion of the insulation of power transformers is one of the main deteriorative mechanisms leading to early failure [57]. The detection and localisation of PDs in transformers during factory manufacture tests is well established and dealt with by current standards [52, 58].

It is known that a PD produces a number of signals at different locations within a large transformer. These signals can be categorised as follows [57]:

- Discharge current in the transformer’s neutral terminal.
- Displacement current through the capacitive tapping of a bushing.
- Ultrasonic/acoustic signals that emanate from the source of the PD activity.
- Radiated RF signals.
- Degradation products produced by the PD that can be detected indirectly using chemical measuring techniques.

Historically, reliance has been placed on DGA for the initial detection of excessive PD activity [59], as DGA has been extensively established as a tool in this field. Only after excessive PD activity was detected was the localisation of the PDs attempted.

Table 2.1 Classification of insulation condition in terms of several PD parameters.

Insulation condition	Magnitude of max pulse (pC)	Repetition rate (pulses/cycle)	PD power (mW)
Clean	<30	25-30	<0.2
Fairly clean (after repair)	250-380	1-2	0.5-0.9
Contaminated	300-400	120-150	50-90
Severely contaminated	220-250	1000-1800	470-800

The preferred measure of intensity of a PD is the apparent charge q as defined by the standard IEC-60270 [12]. This standard provides a uniform method of electrical off-line measurement of PD. This measurement of PD relies on the fact that, in a transformer, PDs cause transient changes of voltage to earth at every available winding terminal [30]. A PD free source is used to energise the transformer, and measuring equipment is connected to the terminals, via the bushing taps if necessary. Calibration of the measuring circuit is carried out by injecting a series of known charges at the calibration terminals from a calibration generator. The generator typically consists of a square pulse generator connected in series with a known capacitance. Precautions must be taken to eliminate interference from radio broadcast stations, spurious PD from other sources in the surrounding area, the power supply source and the terminal bushings. To help with repairs of PD damage, attempts should be made to locate the source of any PD before the transformer is removed from its tank [30]. Recommendations for determining PD location include the comparison of magnitude of PD charge from simultaneous indications at different terminals and the acoustic detection of the physical PD source location.

The acceptable PD limits for new transformers depend on the voltage and size of the transformers and range from less than 100pC to 500pC [8]. Sokolov et al. [60] present a classification of insulation conditions in terms of PD parameters over a range of power transformers, as shown in Table 2.1.

On the practical side, noise suppression in a substation environment poses the largest challenge [61]. For in-situ measurements, sometimes the electrical signal is too weak compared to the level of interference and therefore cannot be detected. However, because the signals are repetitive, averaging can be used to improve the SNR. This allows the detection of very weak PD signals that are buried in noise. IEC-60270 [12] suggests various methods for disturbance reduction such as phase signal gating, pulse polarity discrimination and tuned filters.

Multichannel pulse height analysers have been used for PD analysis since the 1970s, mainly for the measurement and sorting of discrete pulse heights and corresponding discharge rates. The current trend in digital recording is the substitution of much of the pulse height analyser hardware with personal computer oriented software. Many hardware and software systems have been described in the literature

[4, 22, 25, 26, 27, 28, 29, 31, 32, 33]. Basically, all of these systems use some method to record pulse heights along with the corresponding applied voltage magnitude and phase. The sophistication of the hardware determines the accuracy and resolution of the measurement of these parameters. Software enables further parameters to be determined and the results to be displayed in various ways.

PDs occurring within the insulation inside a transformer initiate acoustic waves which travel in all directions and reach the tank walls. Acoustic and/or ultrasonic transducers installed on the tank walls to both detect and locate PDs have been used in off-line and on-line applications. PDs are localised using different triangulation techniques. This requires deep knowledge of wave propagation in different types of solid materials and liquids [62] and is a task for highly qualified experts. This technique makes use of the time interval between the appearance of a PD, possibly detected using a discharge current, and the sensing by a detector fitted on the tank wall, which allows the source to detector distance to be measured. Through the use of multiple sensors, several of these distances can be determined, and triangulation is applied to geometrically locate the source within the transformer. Because the transformer is not a homogenous medium, the speeds of propagation of the transmitted wave are dependent on the materials through which the wave propagates.

Another technique that has been used for locating the source of PD activity within a transformer is the profile comparison method [61]. This method is used to electrically locate a fault, independent of its geometrical position. The profile comparison method consists of injecting a known signal across two accessible points of a transformer and collecting the responses at selected points, so that a profile representing the transmission coefficients may be obtained. After a number of profiles have been determined, the transformer is energised and PD levels are measured at the locations used to determine the profiles. By comparing the new profiles with the former ones, it is possible to locate the source of the PDs.

Knowledge of the presence of a PD source and its location offers the following advantages:

- Repairs can be made immediately before more extensive damage is incurred, which often requires more expense in costs and time.
- When a PD location is determined during factory testing by a manufacturer, it is possible to open the transformer and repair the fault. Location information allows the manufacturer to assess the extent of the necessary repair work and perform the work after minimum dismantling.
- The operator of a transformer with PDs may make the decision to continue operating the unit under regular supervision based on this information in order to wait for the most favourable strategic time to carry out the repair work. Alterna-

tively, the user may use PD level and location information to estimate when the unit should be taken out of operation before a discharge threshold is exceeded which may be destructive. In these cases, repairs can be made at a lower cost.

2.4.11 Integrating fault diagnosis methods

The methods presented in this chapter are used to identify transformer fault conditions before they deteriorate to a severe state. All of the methods presented require some experience in order to correctly interpret the observations. Researchers have applied artificial intelligence concepts in order to encode these diagnostic techniques. Many of these attempts have concentrated on only a single diagnostic technique and have failed to fully manage the inherent uncertainty in the various methods [63]. A better analysis would result from aggregating information from more than one of these techniques.

The inherent uncertainty in transformer fault diagnosis techniques has led several researchers to apply various combinations of fuzzy logic, artificial neural networks (ANN) and knowledge based expert systems to the results of many techniques. In [64] and [65], a combined ANN and expert system tool has been developed for fault diagnosis using DGA. The knowledge base of its expert system is derived from IEEE and IEC DGA standards and expert experiences to include as many known diagnostic rules as possible. In [66], a diagnostic method considering the information of DGA and electrical items is presented. An ANN using the DGA results is applied to achieve the initial conclusion. Then several fuzzy equations including electrical and relevant DGA data are established to realise the detailed diagnosis. Tomsovic et al. [63] describe an approach that integrates different diagnostic techniques and systematically manages uncertainties that arise from the different diagnostic techniques. In the developed expert system, each diagnostic method is represented by a rule base. Within each rule base, conflicts arising between rules are resolved to find the most consistent solution. Finally, the diagnoses are combined into a single analysis where more weight is attached to more certain diagnoses. The system is robust to missing or inaccurate data and can easily be expanded to accommodate new diagnostic techniques.

2.5 MONITORING SYSTEMS

To detect abnormalities in transformer insulation systems, various diagnostic techniques such as DGA and FRA are used, as discussed previously. The problem with these conventional off-line techniques is that they are periodic, labour intensive and they require the transformer to be taken out of service for some time. Furthermore, it has not always been possible to perform these tests at sufficiently regular intervals due to resource and operational constraints. As a result, emphasis has recently been placed on the development of on-line systems to reduce the number of transformer

failures that have been experienced in power systems around the world. In the past, it has not been possible or practical to use conventional analog instruments in many of these systems, but the advent of digital data acquisition and processing equipment has enabled the development of on-line measuring and diagnostic systems suitable for use in power systems.

The primary advantage of on-line systems is that they give immediate indication if something is wrong, perhaps in time to remove a transformer from service and prevent a catastrophic system failure. However, as the cost of removing and replacing a large power transformer increases with its capacity and remoteness, the decision to remove a power transformer from service can imply an expense of several tens of thousands of dollars and is justified only by a high degree of confidence in the predicted imminent insulation failure given by such systems.

Assessment of the condition of the HV insulation of transformers in service has long been of major concern of public utilities, and many attempts have been made to predict incipient insulation faults and extend transformer life. This section gives an overview of recent advances made in the development of on-line condition monitoring equipment used to detect faults and to monitor insulation condition in power, distribution and instrument transformers. Monitoring systems tend to fall between the following two extremes:

- Expensive, complex systems that can automatically monitor several parameters, process the acquired data, determine rates of change of parameters, establish correlations between parameters and transmit the results to a control centre.
- Simple automatic systems that record a single parameter, and signal exceeded levels to the substation operator.

Systems of the latter type that monitor hydrogen, for example, have an inherent limitation in that they cannot answer the basic question of whether the transformer should be removed from service immediately to avoid insulation breakdown. Rapid assessment of multiple parameters is required, and advancements in this area have been made. This is because the more complex systems have become cheaper and simpler to implement in the past few years, due to the increased availability of more advanced digital acquisition and processing hardware and a better understanding of transformer fault and aging processes.

2.5.1 Buchholz relay

Power transformers are often protected by gas accumulation devices commonly called Buchholz relays. Gas generated in the transformer oil rises to the highest point in the oil where it is trapped in the accumulation chamber of the device. When a predetermined

amount of gas has been accumulated, this information is transmitted via electrical signals to the device's protection relay.

The service record over many years shows clearly that the relay is extremely sensitive in operation and that it is possible to detect faults in their incipient stages. Gas within the device can be collected from a small valve at the top of the relay for analysis so as to provide an approximate diagnosis. Some of the faults against which the relay will give protection are [30]:

- Core-bolt insulation failure.
- Short circuited core laminations.
- Bad electrical contacts.
- Local overheating.
- Loss of oil due to leakage.
- Ingress of air into the oil system.

2.5.2 Differential relay protection

Relays that use over-current, over-flux and over-heating principles protect transformers against overloads and externally applied conditions. Differential relays are used to protect transformers against internal faults. These relays convert the primary and secondary currents to a common base and compare them. During normal operating conditions, the differences between the currents are small and are due to magnetising and core loss currents. The differences are also small during external faults, although they are larger than the differences during normal operating conditions. When either an internal fault or magnetising inrush (a transient signal that occurs during energisation) occurs, the differences are large. Conventional relays use the second and/or fourth harmonic components of the difference currents, which are larger for magnetising inrush, to distinguish between the two conditions. This prevents the relays from operating during magnetising inrush.

During the last few years, progress has been made in the design of microprocessor based differential relays [67]. These systems use digital acquisition of the power waveform and control the protection relays using the same theoretical techniques as analog circuits by implementing signal processing algorithms. For typical fault situations, the systems trip the transformer in less than 20ms. More recently, more advanced signal processing techniques such as wavelets, fuzzy logic [68] and ANNs [69] have been applied to differential relay protection systems in order to improve the reliability of the prevention of tripping the transformer during magnetising inrush. In [70] and [71], the wavelet transform is used to extract the transient components from the captured

transformer currents. Unlike the Fourier transform, the wavelet transform is a powerful tool in analysing non-static signals typical of transformer fault waveforms. In the system tested, high selectivity is achieved with the new relay possessing the advantages of high speed response, immunity to current transformer (CT) saturation and an ability to detect low level internal faults against inrush currents. A disadvantage with differential relay protection is that preventative techniques to avoid outages based on early detection of faults cannot be applied.

2.5.3 Model-based monitoring

The Massachusetts Institute of Technology (MIT) has developed an adaptive, intelligent monitoring system for large power transformers [11]. The system consists of a collection of data acquisition modules that monitor temperature, gas content and PD activity. A connection to the system can be made through a modem, which allows MIT personnel to operate the system and examine the data independently of the host utility. Each acquisition module uses model-based monitoring which compares measured data with that predicted from a model and generates a residual signal that is the difference between the measurement and the prediction. When a residual signal exceeds a predefined range or changes faster than a given rate, messages are generated to appropriate personnel via a paging system to indicate that a problem has developed.

An adaptive transformer model based on parameter estimation is used. This facilitates transformer condition monitoring on multiple time scales and allows for differences between individual transformers. When testing the system in the field, the following problems were experienced:

- The IEEE temperature model used does not properly account for variations in ambient temperature.
- When a transformer cooling pump was activated, the gas module predicted a drop in gas content (a model based on temperature is used). The resulting increase in the residual caused the system to generate a message when no fault had developed.

2.5.4 Hydrogen monitoring

Hydrogen is a key gas for several types of active problems within transformer insulation, and an increase in the output signal of a hydrogen sensor is an indication that irregularities exist, such as PDs or thermal overload [72]. On-line hydrogen monitors have been developed that measure hydrogen content in oil in parts per million [73]. The devices work best when they are mounted close to the windings so that oil circulation to them is maximised. If this ideal mounting cannot be attained, devices will not be very accurate but they will still give an indication within a few days of a large increase in hydrogen, that is, more than a few hundred parts per million. The devices can usually

be easily interfaced to microprocessor or computer-based protection systems. On-line hydrogen gas detectors are generally based on one of the following extraction systems [64]:

- **Vacuum suction system:** Gas is extracted by reducing the pressure of the space above the oil surface using a piston arrangement. High vacuum and long extraction times are an essential requirement.
- **Permeable membrane system:** These systems employ polymeric membranes which in general have the property of letting only gases pass through them while stopping liquids. A problem with these systems is that it takes several tens of hours for the hydrogen gas concentration in the gas chamber to reach equilibrium, which makes it unsuitable for use in quick field measurements.
- **Air blow system:** Air blow systems take advantage of the fact that the extraction efficiency increases with increasing amounts of residual air in the oil. Either air is blown into the oil and the air passed through the oil is collected, or a given amount of air is repeatedly circulated through the oil until equilibrium is reached between the hydrogen gas concentration in the oil and in the air space of the device. Advantages of the air blow system include an extraction time of a few minutes at most and an extraction efficiency independent of oil temperature. A SnO₂ sensor can be used to measure hydrogen gas concentration through gas absorption which changes the electrical resistance of the sensor [74].

2.5.5 Monitoring other gases in oil

For a number of years, on-line sensors for detecting hydrogen (mainly indicative of PDs, but also arcing) have been available on the market, for example, the Hydran sensor from General Electric. These sensors are most sensitive to hydrogen, but also measure other combustible gases to a certain extent. The readings are to be regarded as warning signals, and a conventional DGA should be performed after an alarm. The risk of missing a beginning fault due to long sampling intervals is reduced considerably by continuous monitoring [3].

The Hydran sensor uses a selectively permeable membrane and a miniature electrochemical gas detector. Hydrogen dissolved in the transformer oil permeates through the membrane and reacts with oxygen from the ambient air. This reaction generates an electrical current that is measured as a voltage drop across a load resistor. A thermistor is embedded in the sensor for temperature compensation. Recent sensor developments have enabled the detection of carbon monoxide, making it possible to monitor degradation of the solid insulation [75]. The advantages of the Hydran sensor are that it has no moving parts and that the gases under analysis are the fuel required to energise the sensor, thus eliminating the need to replenish an internal agent.

Originally only a hydrogen on-line monitor was available, but now instruments detecting several gases are commercially available with a total oil monitor recently launched [76]. Efforts have also been made to develop on-line sensors that measure individual concentrations of several gases. Such sensors are also warning systems that give a better indication of the type of the fault. In addition, these sensors give warning for heating of cellulose that present sensors do not.

To improve the detection capabilities of oil analysis techniques, the use of on-line DGA equipment has been investigated. However, the cost of such equipment can be prohibitive and therefore may only be justified on very high MVA rating transformers or as a semi-permanent installation on a problem transformer. Portable field DGA test sets can be used, but do not have the precision of laboratory based equipment. These field sets can detect the presence of the primary gases (namely H₂ and CH₄) and identify the need for more detailed analysis.

2.5.6 On-line transfer function monitoring

The transfer function method (see Section 2.4.9) can also be used for on-line monitoring of transformers in power systems. Recently, Leibfried and Feser [13, 77] have been looking at the prospect of using system generated transients and disturbances as the source of excitation for determining the transfer function. However, these signals must have adequate spectral characteristics if the transfer function is to be determined to a high enough frequency to ensure reliable fault detection.

The use of system generated and natural transients and disturbances poses the following difficulties:

- Surge arrestors are used in power systems to divert potentially harmful transients. Using these transients as an excitation source exposes the transformer's insulation to additional stresses that may affect the service life of the transformer.
- The frequency of occurrence of transients with adequate spectral characteristics may mean that the required transfer function is determined on an infrequent basis.
- Complex data acquisition hardware needs to be designed due to the unknown parameters of the signals to be digitised, such as the peak voltage and time duration.
- A large amount of data is generated that requires powerful hardware for processing in real-time.
- Transfer function calculations can have errors introduced if long oscillations are truncated.

- The power system components surrounding a transformer can have an effect on the transfer function calculated across a transformer. This is because the signal measured at one winding may have a load reflection component superimposed.
- The influence of the position of transformer tap changers also needs to be studied.

2.5.7 On-line partial discharge detection

Many experiences have shown that the insulation damage caused by internal PD activity is a main detrimental factor influencing the continued reliable operation of a power transformer. In particular, the erosion of the insulation is one of the main deteriorative mechanisms leading to early failure. As it is suspected that PDs of high magnitude develop shortly before a major failure, continuous monitoring of large or critically located transformers for such PDs is very desirable [57]. However, no internationally recognised standards currently exist for the measurement of PDs in on-line power transformers. PDs produce a number of signals at different locations within a large transformer as detailed in Section 2.4.10. More indirect PD detection methods such as DGA, the Buchholz relay and hydrogen monitoring have already been reviewed in this chapter.

Choice of detection techniques is limited to what can be applied to a transformer in an on-line operational mode. There are two commonly used PD detection methods: detection of the acoustic signals and measurement of the electrical signals produced by the PDs [8]. However, the main challenge of on-line PD detection is interference suppression. A wide range of noise generating phenomena interferes with on-line PD measurements. Acoustic noise sources include [57]:

- Mechanical vibration of the transformer tank.
- Magnetostriction noise of the transformer core and other nearby equipment.
- Synchronous mechanical noise from sources such as rotating machinery.
- Environmental noise, such as rain and sandstorms, in certain situations.

External electromagnetic noise sources include [7]:

- PDs and corona from the power system which can be coupled directly or radiatively to the apparatus under test.
- Arcing between adjacent metallic components in an electric field where some of the components are poorly bonded to ground or HV.
- Arcing from poor metallic contacts which are carrying high currents.
- Arcing from slip ring and shaft grounding brushes in rotating machinery.

- Arc welding.
- Power line carrier communication systems.
- Thyristor switching.
- Radio transmissions.

These interferences can be categorised into two types [78]:

- **Continuous periodic interferences:** All of the signals in this group are sinusoidal, such as carrier communication, HF protection signals and radio broadcast. They can be considered narrowband interference in the frequency domain.
- **Pulse interference:**
 - Periodic pulse interference that occurs at fixed positions within the AC cycle, for instance, thyristor switching.
 - Non-periodic pulse interference. Signals appear more or less at random, such as corona, external partial discharging and arcing between adjacent metallic components or from rotating machinery.

Many of the PD detection systems under research attempt to tackle each of these types of interference separately with different methods, because a single algorithm has not been shown to effectively remove all interference signals that have all of these individual characteristics. This is due to the very different temporal and frequency characteristics of narrowband signals and various types of interfering pulses.

Due to these systems being required to operate under severe noise and interference conditions within a substation environment, one method uses transducers that detect two or more of the resultant PD signals [57]. As a result, systems are able to apply noise-rejection algorithms to differentiate PD activity from noise and interference when signals are only present at the output of one transducer type. A brief summary of some of the recent techniques and progress in the development of on-line PD detection systems is now presented.

PDs occurring in oil produce pressure waves (in the range of 100kHz to 300kHz [8]) that are transmitted throughout the transformer via the oil medium [10]. Piezoelectric sensors can be connected to the outside of the tank to measure the acoustic waves impinging on the tank either directly or via wave guides. These systems can become ineffective in high noise environments unless steps are taken to enhance the SNR by, for example, signal processing techniques. If multiple sensors are used, the PDs can be located based on the arrival time of the pressure waves at the sensors. The sensitivity of the test is dependent on the location of the PDs, since the signal is attenuated by the oil and winding structure [8]. The use of optical fibre sensors in which ultrasonic PD

pulses phase modulate the propagating optical beam has been attempted with some success [79]. An advantage of this method is that it is immune to electromagnetic interference.

Unsworth et al. [57] have designed an on-line PD monitor that consists of ultrasonic and RF transducers, signal conditioning electronics, a digital signal processor and a display monitor. Location information is determined by using the RF signal as a time reference and measuring the delay to the ultrasonic signals. As the transducers are mounted inside the tank of the transformer, they have been designed to operate:

- In the corrosive medium of mineral oil.
- At temperatures up to 120 °C.
- In the presence of strong 50Hz electric and magnetic fields.
- Reliably for a long period of time as removal is difficult.

PDs cause high frequency, low amplitude disturbances on the applied voltage and current waveforms that can be detected electrically. Electrical PD signals can be measured and analysed at a number of different locations, including bushing tap current or voltage, and neutral current [8, 78, 80, 81, 82, 83, 84, 85, 86, 87, 88]. Digitisation of signals for subsequent analysis is commonly undertaken.

Most types of PD are manifested by positive and negative current pulses of at most a few nanoseconds in duration [7]. PDs in oil-paper insulation or gas bubbles normally occur in the ranges of 0° to 90° and 180° to 270° of the AC voltage waveform, and have variable pulse repetition rates [7, 89, 90]. The pulses are typically attenuated and distorted while travelling through the windings of the transformer. PD pulse shapes can be very different on various transformers, having a duration of 10ns to 10 μ s when measured at an external tap [80]. The frequency spectra of PD pulses and continuous noise signals are completely different. While PD pulses show a constant value spectrum greater than 10MHz, continuous interference signals are characterised by narrowbanded spectral lines in the frequency domain [80].

Hardware methods for narrowband interference elimination include the use of a band pass, band rejection or combination filter [78, 83]. Differential balance systems that can suppress common-mode narrowband interferences, and pulse polarity discrimination systems that can suppress common-mode pulse interference have been built with only moderate success [78, 83, 86].

A variety of digital filtering techniques for narrowband interference have been used. A least mean squares (LMS) adaptive filter can be effective [78]. A reference signal containing interference signals is required and is obtained by using a delayed input signal which contains a PD signal plus interference signals. In practice, it is found that choosing key filter parameters is a problem and requires user experience. The

training convergence process can be deteriorated or convergence not achieved when non-narrowband interference, such as white noise, is large.

Variations of digital fast Fourier transform (FFT) domain filtering have been tested [78, 88]. A PD pulse has a wide, uniform spectrum, whereas continuous, periodic interference appears as a narrowband peak in the frequency domain. Elimination of these peaks can be performed according to a predetermined threshold. After elimination, the signal can be transformed back into the time domain by application of the inverse FFT. A disadvantage of this filtering method is uncertainty in the choice of band rejection because its filtration effect will change with the threshold. Also, a PD pulse is often recorded as a decaying oscillation and may be filtered if it coincides with one of the filtered bands. Using a multi-bandpass filter has been shown to allow for a choice of which bands are chosen for monitoring, typically those with the best SNR [78]. For semi-narrowband oscillating PD pulses, selection of this band has been shown to allow good rejection of interference, including white noise inside the rejected bands. However, manual selection of suitable bands to reject and keep is needed. Pulse waveshapes can be distorted due to the rejection of pulse information contained in the frequencies of the rejected bands. However, the suppression of sinusoidal interferences should generally preserve the shapes of the pulses within the measured signal [80]. Another method for Fourier domain based narrowband filtering is to search for the highest spectral amplitudes and reduce these interference frequencies to the amplitude spectrum of the adjoining frequencies [80]. These Fourier domain based filters were found to have the best characteristics in all comparisons to other digital filters studied, except in computer calculation time [80].

There are several techniques under study for the removal of pulse interference. Pulses that occur at fixed positions of the power cycle can be deleted by time domain filtering or gating [7]. Stochastic noise pulses can cause significant problems for PD detection since they have many characteristics in common with the PDs being measured because they involve brief bursts of current flow across short gas gaps, just as PDs do in a cavity within a transformer dielectric [7].

Because the PD pulse has to pass through several windings, the signal is strongly modified on its way from the PD source to the external sensors and, as a result, the PD pulse may have many oscillations [80]. Pattern recognition methods use the characteristic features of different sources of pulses as classes that have to be separated. For these signals, the sampled values can be used as characteristic features, as well as amplitude spectra, the phase angle of the pulses relative to the main power cycle or features extracted by various transforms [91, 92]. Study of signals from more than one phase can be advantageous [80].

Many pattern recognition algorithms require reference pulses for training, which may not be available for an on-line transformer. It is therefore advantageous to use

algorithms that get suitable results without any prior knowledge [80]. Cluster methods detect common features in the data and divide the objects into groups, with those in each group almost similar, while the groups are as different as possible [80, 93, 94]. Various methods have been investigated, such as iterative self-organisation data analysis (ISODATA), fuzzy ISODATA and hybrids. The determination of the number of clusters and learning rates are challenges for using these methods. Error rates of less than 2% have been achieved for the separation of noise and PD pulses in laboratory testing [80].

The use of a reference signal that includes pulse interference without PD pulses in the signal has been used in a laboratory setup [84]. The reference signal was detected from the power line of the transformer's cooling fan. Then, oscillatory pulses were compared by timing the polarity and amplitude of the half-waves that make up the oscillation.

Wavelet analysis has been used in various studies. It has been shown that the use of the discrete wavelet transform (DWT) can remove some narrowband interference and random noise with better SNRs and less PD pulse distortion than FFT filtering [85, 88, 95, 96, 97]. Threshold levels of wavelet coefficients are chosen to remove low level noise. Wavelet levels can even be removed altogether if they are determined to have no PD pulse energy, before the inverse DWT is applied. Hard or soft thresholding can be used to adjust DWT coefficients. Methods exist to automate threshold levels [98]. The discrete wavelet packet transform (DWPT) has been employed to try to provide an automated method for narrowband interference removal [99]. This method uses a thresholding information cost function to determine if wavelet packets should become more localised in frequency, which naturally separates them from pulse information. The choice of the mother wavelet has been shown to be a consideration because pulses can be exponentially decaying or oscillatory in nature [96, 100].

Directional coupling methods for PD pulse and interference separation are not digital filtering methods. They determine the energy flux of the signal by measuring its voltage and current components at the same time [80, 81, 86, 87]. By comparing the polarities of the measured components, a differentiation of the pulse direction is possible. Thus, noise pulses, which result from outside the examined transformer, can be well distinguished from PD pulses, which have an internal origin [80]. However, for an unambiguous analysis, the voltage and current components at all outer taps of the transformer must be measured. This is because pulses that enter the transformer at one tap from the outside will be detected at all other taps as coming from the inside, caused by an overcoupling between the windings [80]. If PD pulses are oscillating with increasing amplitude, the determination of their polarity is difficult [86].

Borsi [80] used two sensors to measure the voltage and current pulses generated by the PDs. The sensor for the voltage pulse was a capacitive voltage divider, which is usually integrated into the bushings. Where no measuring tap is available, an external

divider can be used. A high pass filter served to attenuate the power frequency and its harmonics, thereby improving sensitivity. An air cored Rogowski coil was used to measure the current pulse. The advantage of an air core is a linear and higher frequency response. The analog signals were passed through an anti-aliasing filter and digitised. Analog narrowband rejection filters were used where necessary to remove known interference signals such as local radio stations before digitisation.

Internal transformer PDs are caused by defects in the insulation. It is of interest to know the location of the defects for efficiency of repair work. Electrical PD detection methods can provide some PD source location information. Borsi [80, 92] has injected artificial pulses into the internal windings of an off-line transformer using a needle plane arrangement, and recorded the signals at the external taps. The resulting PD signals are variously distorted due to travelling through the windings of the transformer. Pattern recognition algorithms have had moderate success in grouping the pulses, although this does not actually provide a specific location within the transformer.

The majority of approaches presented here assume that only one PD source is active at a given instance. However, the situation encountered during practical PD measurements is that several sources may be active simultaneously, both internal and external. When more than one PD source is active, the resultant PD pattern obtained will in a broad sense be the sum of the patterns due to the individual sources [101]. Low frequency external pulses may be overlapped with small, high frequency internal PD pulses. Overlapping internal PD phase patterns can be difficult to separate when patterns are similar in phase and amplitude distribution or when one source is relatively minor compared to the others. Lalitha et al. [101] attempted to use a wavelet analysis to extract features from PD phase patterns so as to differentiate sources with a neural network. Success rates of >88% were achieved.

2.5.8 Other monitoring systems

Other types of on-line sensors have also been investigated. Examples of such systems are on-line measurements of the moisture content of the oil, static charge in oil and pump monitoring. On-line measurements of the moisture in the cellulose by optical fibre techniques are also being studied. In general, these systems do not have a strong coupling to important and frequent failure modes [3].

A continuous transformer oil processing system was developed by Lampe and Spicar [102] to restore the dielectric strength of HV insulation showing signs of deterioration. This processing unit effectively removes oxygen dissolved in the oil and also metallic and dielectric impurities, thus preventing the evolution of an internal fault.

The power factor of electrical insulation is recognised as a good indicator of its quality and future serviceability. Cummings et al. [46] have developed an on-line microprocessor-based system that detects insulation deterioration within a substation

current transformer (CT) by continuously monitoring the insulation power factor and capacitance. The system also measures temperature and applies a correction to estimate the internal temperature of the insulation. The estimated temperature is then used in power factor calculations to make temperature corrections [103]. The authors claim that the temperature corrected power factor gives the best indication of long term changes in the CT, but that the uncorrected power factor is the best forecaster of imminent failure. Data supplied to the microprocessor from a commercially available hydrogen monitor and an oil pressure transducer was additionally used to detect insulation deterioration.

Checking for winding looseness can be performed through vibration monitoring [104]. Vibration data can be taken from both the core and windings of the monitored transformer via accelerometers and are used with current and thermal data to ascertain the on-line condition of the transformer [105]. Changes in the physical structure of the winding can also be analysed through FRA, as discussed in Section 2.4.9.

Other methods which have been tried and show some promise for detecting destructive trends or imminent failure include pressure monitoring and an extremely sensitive relay which looks at the insulation current.

2.5.9 On-line diagnosis

In a multi-sensor environment, a step toward a fully automated on-line diagnostic system would be to appropriately process the information received from all sensors, in order to provide the power system engineer with information-rich diagnostic messages. Diagnosis would be most effective if several levels of analysis were performed. A potential system would need both a fast response, to avoid catastrophic failure of the transformer, as well as detailed, time-intensive levels of analysis of the health of the transformer. A possible system may include the following analysis steps [11]:

- **System check:** When a severe or rapidly developing anomaly or problem occurs, the fastest response will be required. A decision will have to be made as to whether the transformer needs to be shut down or can be left on-line. Because of the costs involved with transformer shutdown, fast checks based on built-in test equipment (BITE) tests may first be done to verify that there is not a sensor problem. Some anomalies may not be determinable, indicating the need to invoke human intervention.
- **Correlation check:** When a problem develops more slowly, more analysis will take place over a longer period of time. The correlation check will be concerned with correlating results from different sensors, in order to make a more accurate diagnosis. To give even more accuracy, this level of diagnosis will have access to off-line and periodic test results for the transformer, such as DGA test data.

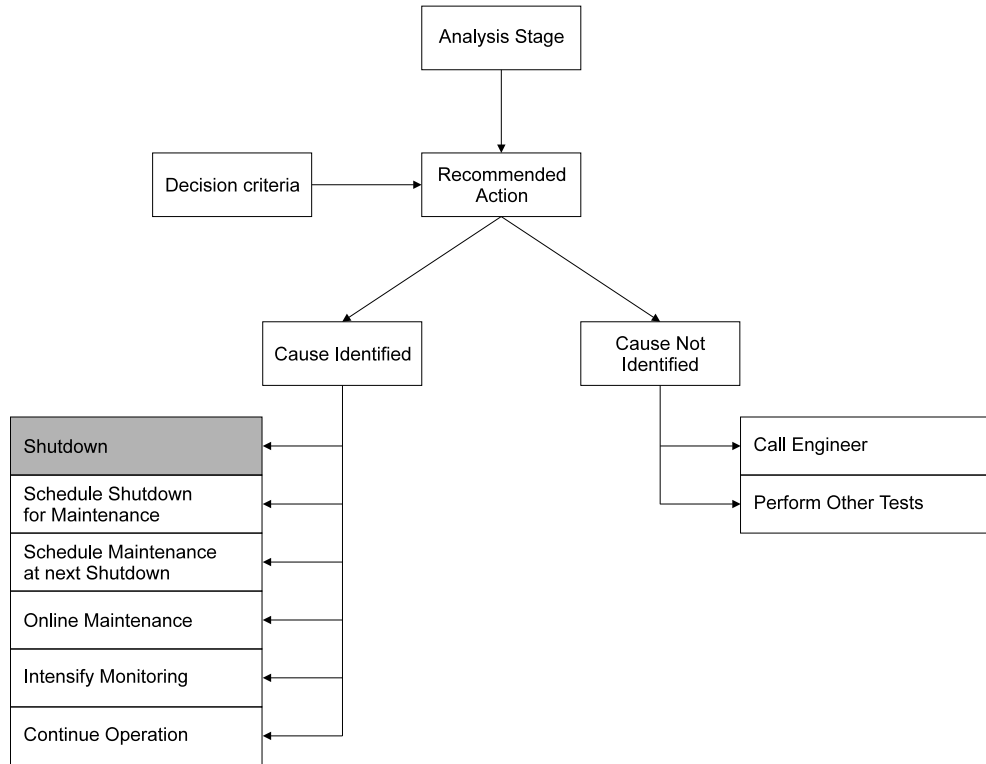


Figure 2.2 Decision making following each analysis stage.

- **Statistical trending and database comparison:** The most slowly developing anomaly or problem may require the previously mentioned analysis stages, and in addition, statistical trending and database comparison. This will allow a more detailed analysis of all the information available including that residing in external databases, such as parameter trending information for the class of transformer.

If the system can identify the cause of the anomaly or problem with some certainty, a recommended action based on some set decision criteria can be made to the power system engineer. The decision making illustrated in Figure 2.2 may follow each analysis stage [11].

In support of the ideas presented in this section, recent publications indicate the following technical trends [3]:

- A shift from sensor development towards diagnostics that involve the application of more powerful digital and artificial intelligence systems for interpreting sensor outputs. The use of information technology and artificial intelligence will gradually increase as the interpretation skills grow.
- Development of diagnostic methods which can be applied without taking the transformer out of service.

- The utilisation of transformers is expected to increase, and new types of diagnostic methods will thus become necessary.
- System aspects will become more important. The transformer will not be looked upon as a separate apparatus, but rather as a part in a system. This will put demands both on the monitoring systems as well as on the relative importance of different diagnostic methods.
- A shift from on-line monitoring and off-line diagnostics to on-line diagnostics.

2.6 CONCLUSIONS

Transformers are complicated structures, physically and electrically, and thus a large number of failure mechanisms can occur. This explains partially why there is a wide variety of power transformer fault detection and diagnostic techniques which have been reviewed in this chapter. Insulation is possibly the most important component for effective transformer operation. Hence, there is a focus on understanding cellulose and oil degradation in terms of transformer functionality and future operation. A number of methods observe and interpret results of chemical analysis, such as DGA, TCG, DP and hydrogen monitoring.

Another focus of research is the electrical characteristics and responses of transformers, such as the dielectric response, impulse testing, FRA and PD detection. A key indicator to a transformer's health is the condition of its insulation, and direct chemical analysis of the insulation can provide a fair insight into that condition. However, some electrical characteristic and response techniques need additional information, often only gained through experience, to be converted or interpreted in terms of transformer insulation health and operating future. For instance, FRA results by themselves do not necessarily provide answers to the question of whether the transformer insulation is physically healthy enough for the transformer to be left on-line.

Partial discharging is a common effect that degrades transformer insulation. Successful detection of PDs still needs to be interpreted in terms of transformer insulation health. However, a body of experience has been built up world-wide providing insulation condition information for varying characteristics of PD. Standards exist describing methods to detect PDs' electrical signals, but electrical interference can obscure the PD pulses. Various signal processing techniques have been trialled to eliminate interference, focusing on narrowband and pulse signals. Techniques researched include adaptive filters, Fourier domain filters, power cycle gating, basic directional coupling, wavelet transform level selection and thresholding, and neural network recognition of PD patterns.

The PDDS presented in this thesis uses easily attachable low cost current and voltage transducers that do not require opening or modifying the transformer under test.

It implements an automated FDTF for removal of narrowband interference sources. To determine which observed pulses are internal or external to the transformer, directional coupling is used. The CWT helps separating PD pulses from simultaneous interfering signals. Finally, once PD pulses have been isolated, a neural network that does not require prior knowledge can recognise and group pulses according to their source, if multiple PD sources are active. This allows clear and decisive separation of PD sources in PRPDA. The hardware used to implement the PDDS is described in Chapter 3 and the signal processing algorithms are detailed in Chapter 4.

Chapter 3

HARDWARE

The purpose of this chapter is to describe the hardware components of the PDDS developed by the author. The first section gives an overview of the hardware aspects of the PDDS and their interconnections. The second section describes how calibration pulses, simulated PDs and external interference pulses are created for signal processing testing purposes. Section three details the PCSM that provides a universal timing signal related to the phase of the power cycle. The last section discusses the current and voltage transducers, including the digitisation of the signals.

3.1 OVERVIEW

The PDDS broadly consists of current and voltage transducers attached to a 2.8GHz PC as shown in Figure 3.1. More specifically, current signals are acquired using current probes and voltage signals are acquired using capacitors that use the transformer bushings as a dielectric medium.

The signals are passed to analog filters and amplifiers before being digitised. PRPDA is a common technique of displaying PD timing patterns against the power frequency cycle [3]. The PCSM allows signals to be presented in this format by providing a universal trigger for the artificial pulse signal generation and signal acquisition equipment at a specified power frequency phase point.

Oscilloscopes are used to digitise the signals, and the data is passed to the PC via General Purpose Interface Bus (GPIB/IEEE 488) cables. The PC is a standard device, although it is preferable to have a clock speed as fast as possible to increase software processing speed. Data is analysed on the PC using Matlab, a numerical processing software package. Matlab also controls functions of the arbitrary waveform generators, PCSM and oscilloscopes by sending commands through the GPIB interface. At the end of analysis, Matlab functions provide results graphically for user interpretation.

Pulse generators are used for PDDS calibration and testing purposes. They essentially consist of voltage step generators connected in series to a capacitor. The use of multiple pulse generators for artificial PD sources and external interference provides

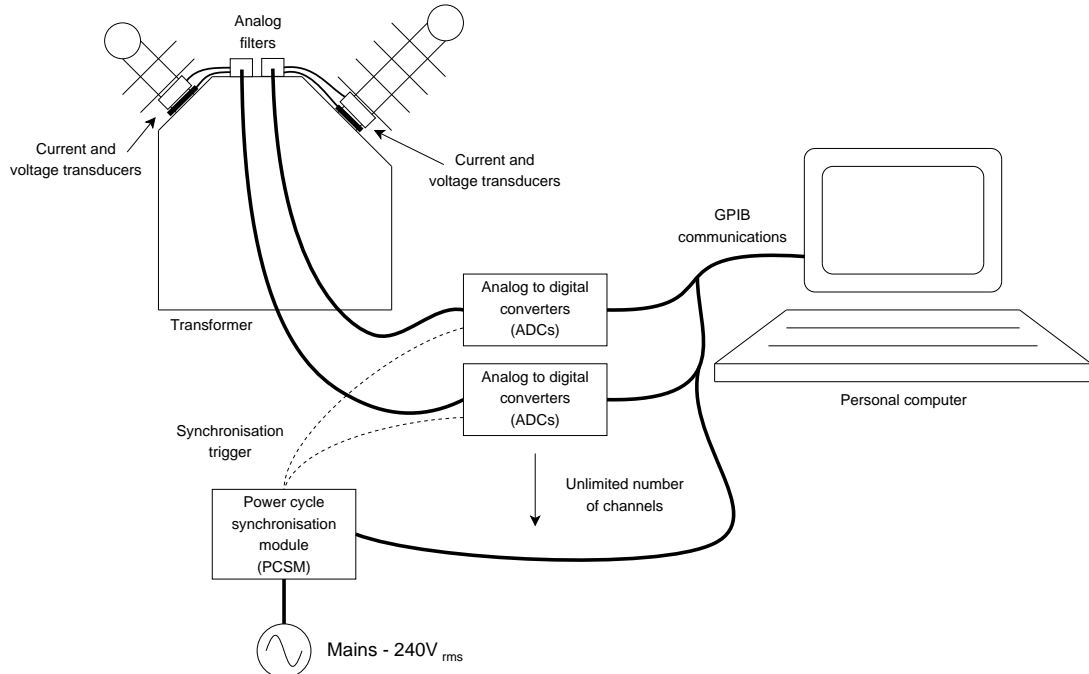


Figure 3.1 The partial discharge detection system.

accurate information used to gauge the effectiveness of the PDDS. The pulse generators are connected to the PC and controlled by Matlab through the GPIB interface. In addition, sine wave generators are used to provide artificial narrowband interference.

The hardware transducer components described in this chapter are customised to the power transformers used for testing the PDDS. Details of these transformers, including construction information, and the tests performed on them are provided in Chapter 5. Adaption of the PDDS to other power transformers would involve modification of the transducers and analog filters. Three phase transformers would require extra transducers, filters and ADCs for the additional transformer bushings. However, the digitisation and software signal processing components are generic in nature and could easily process signals from a different transformer. Photos of some hardware components of the PDDS are included in Appendix A.

3.2 CALIBRATION PULSE, ARTIFICIAL PULSE AND NARROWBAND SIGNAL GENERATION

A series of off-line tests of the PDDS is described in Chapter 5 in which PD pulses must be separated by the PDDS from other interfering pulse and narrowband signals. To provide a controlled environment for tests to determine the effectiveness of the PDDS, artificial narrowband signals and PD and interference pulses are generated with known timings and magnitudes.

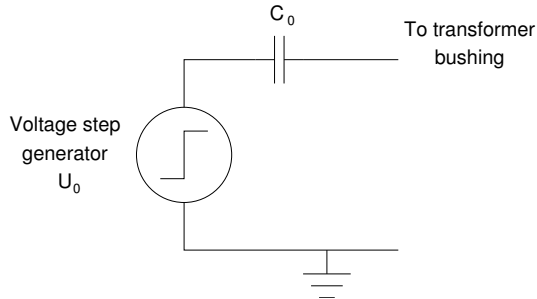


Figure 3.2 Artificial pulse generation.

For the creation of each source of artificial calibration pulses, PD pulses or interference pulses, a square wave generator connected in series to a capacitor of known value was used, as shown in Figure 3.2. This provided a pulse of known charge, as detailed in Chapter 5.

Individual natural PD pulses in a transformer occur stochastically in time, although PD sources have been shown to have varying pulse count densities in time with respect to the power frequency phase [90]. Pulse magnitudes are also stochastic within a range. To simulate this random timing and magnitude, Agilent 33250A 80MHz arbitrary waveform generators were programmed with a series of voltage steps that occur randomly during a section of the power frequency cycle, and with random magnitudes within a specified range. Each waveform generator was connected by GPIB cable to the control PC. Matlab scripts were used to create arbitrary voltage step waveforms which were then uploaded to each waveform generator.

Calibration pulses serve to determine scaling factors z_i and z_v that relate actual transformer bushing current and voltage pulse peak amplitudes to the digitised signals. This allows the reporting of PD magnitude results in milliamps (mA), millivolts (mV) or, more commonly in PD measurements, in pico-coulombs (pC). However, the magnitude of an internal PD pulse at a transformer bushing does not equal the magnitude of the pulse at its source because the pulses are deformed and attenuated as they propagate through the transformer windings. The pulses' waveshapes are also affected by the electrical circuit external to the transformer. The common technique in PD measurement is to measure the 'apparent' magnitude. This is the magnitude that, if injected at the terminals of the test object, would give the same reading as the PD pulse itself [12]. To generate the calibration pulses, a series of voltage steps of known amplitude were generated using a script in Matlab and uploaded to an arbitrary waveform generator that was connected to a capacitor of known value. For further information on this, see Section 5.2.1.

The Agilent 33250A 80MHz arbitrary waveform generators used in the testing of the PDDS have the following relevant specifications [106]:

- Generation of an arbitrary waveform of up to 65536 points with an amplitude resolution of 12 bits.
- Arbitrary waveform repetition rate of $1\mu\text{Hz}$ to 25MHz.
- Output amplitude of 10mV_{pp} to 10V_{pp} (into 50Ω).
- Edge time of less than 10ns.
- Ability to be triggered from an external source.

Narrowband interference was generated using sinusoidal waveform generators. To simulate the characteristics of radio stations or similar narrowband communications, the interference waveform was modified with amplitude modulation (AM) using built-in functions in the generators. Each sinusoidal generator's output channel was connected in series with a resistor to a bushing of the tested transformer. The resistor was used to prevent a low impedance path to ground for other signals.

3.3 POWER CYCLE SYNCHRONISATION MODULE (PCSM)

To perform PRDPA, the timings of PD pulses have to be noted with respect to the power cycle phase. The PCSM provides a synchronisation trigger for all of the oscilloscopes at a consistent power cycle phase point, in this case, the voltage positive-going zero crossing [107]. The PCSM trigger output on/off status is controllable from the PC, so that the recording of a new set of data is only initiated once the previous set has been analysed.

The PCSM is needed for on-line transformer testing. However, for off-line testing of the modified transformer Tx1, the PCSM output trigger was still used to synchronise the oscilloscopes with each other. In this case, the PCSM was also connected to the trigger inputs of the arbitrary waveform generators that provided artificial PD pulses. This allowed the timing of the artificial PD patterns to have a known reference starting point.

The PCSM is shown in Figure 3.3 and consists of the following components [107]:

- **Transformer and comparator:** The comparator produces a positive edge every time the mains supply voltage exceeds an adjustable DC level. The DC level is controlled by a multi-turn pot. The peak-to-peak value of the PCSM transformer's secondary voltage is equal to 5V.
- **Flip-flop:** The flip-flop output provides the PDDS's universal trigger. After the flip-flop has been reset, the next positive edge from the comparator sets it and outputs the trigger. The flip-flop remains set until the next test request is made.

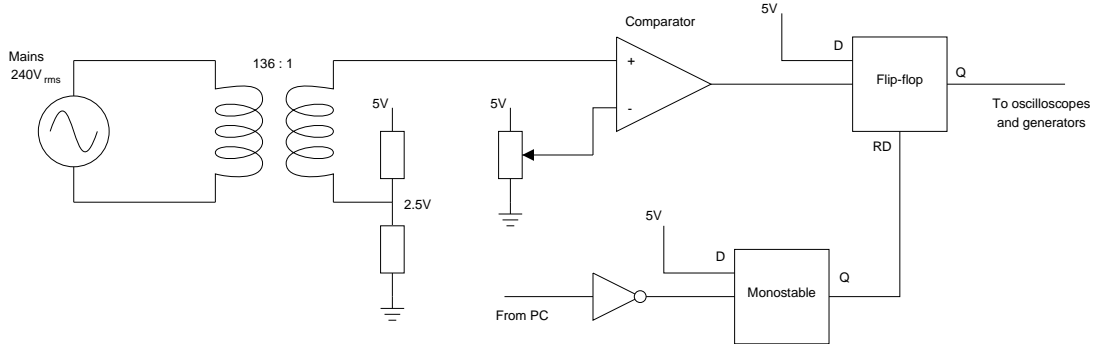


Figure 3.3 Power cycle synchronisation module.

3.4 TRANSDUCERS

Two different types of transducers are used to acquire current and voltage signals from the transformer bushings for digitisation by the oscilloscopes. Amplification and filtering are performed before digitisation to remove unwanted frequency bands and to extend the effective dynamic range of the oscilloscope ADCs.

The choice of digitisation sample rate for the PDDS is broad. However, some factors provide guidance. It has been shown that winding inter-turn faults can create oscillations of up to 2.5MHz [56]. Preliminary testing of transformer Tx1 with artificial PD pulses has shown that transmitted frequencies of up to several tens of MHz are present at the bushing terminal. On the other hand, high sample rates have disadvantages, such as the cost of high speed ADCs and the increased computer processing time for the extra data gathered.

A digitisation sample rate of 10MSa/s is chosen for the PDDS. This allows adequate bandwidth, as observed in preliminary ad-hoc tests, to detect PD pulses. Also, due to the limited sample memory in the oscilloscopes, the sample rate has to be within the oscilloscope's capabilities if at least one complete power cycle of data (20ms) is to be captured.

This sample rate is not sufficient to observe subtle variations in waveshape contained in higher frequencies which can distinguish PD pulses coming from different sources. A sample rate of 50MSa/s was found in preliminary tests to be needed to capture the required higher frequencies. A single sub-channel is dedicated to recording pulses at this higher sample rate. This sub-channel is placed on the bushing which is physically and electrically closest to any likely sources of PD, typically a HV bushing. However, it can easily be switched to another transformer bushing if PD pulses are more strongly detected there by another transducer. Multiple high sample rate channels are possible, but are relatively expensive in terms of hardware costs.

3.4.1 Analog filter specifications

The Nyquist sampling theorem states that to prevent aliasing, the signal to be sampled must be band-limited to f_a such that

$$f_s \geq 2f_a \quad (3.1)$$

where f_s is the sampling frequency [108].

In practice, aliasing is often avoided by lowpass filtering a signal prior to sampling and then sampling at a rate such that aliasing is negligible. The level below which aliasing is negligible is the signal noise floor, whose minimum value is equal to the level of the quantisation noise floor.

Quantisation occurs in the digitisation process when the continuous sample amplitudes are represented by a discrete set of amplitudes for use in a finite word length machine. The root mean square (RMS) SNR for N -bit quantisation with a full scale sinusoidal input is

$$\text{SNR} = 6.02N + 1.76 \quad \text{dB} \quad (3.2)$$

The oscilloscopes used for digitisation use 8 bit ADCs, which give a minimum SNR of 49.9dB. This places the quantisation noise floor at -49.9dB where 0dB represents a full-scale ADC input. However, to ensure signals do not exceed the maximum range of the ADCs, which is known as ‘clipping’, the quantisation steps are set via the oscilloscope volts-per-division setting, to let the maximum ADC values exceed the signal by a significant margin. This is important where the maximum magnitude of the input signal is unknown, for example, for random pulses with occasionally high magnitudes. This setting means that the input signals often do not span the full dynamic range of the ADCs, and the SNR will be smaller. Other sources of noise such as inherent current probe noise lower the SNR further.

The quantisation noise floor represents a base level below which aliased signals will not be resolved by the ADCs, and it allows a lowpass anti-aliasing filter response to be derived, as in Figure 3.4, where f_c is the filter cut-off or corner frequency. The order of the filter must be selected so that at least AdB of attenuation takes place from f_c to f_a .

In the PDDS, a filter cut-off frequency of 2MHz is chosen. This allows the use of a fairly low order filter, minimising magnitude and phase distortion of the filtered signal in the vicinity of the cut-off frequency. Also, a high order filter would have disadvantages, such as large frequency response sensitivity to component variations and being difficult to design.

The PDDS does not require a cut-off frequency of exactly 2MHz. However, it is important that the frequency responses of the current and voltage transducer/filter

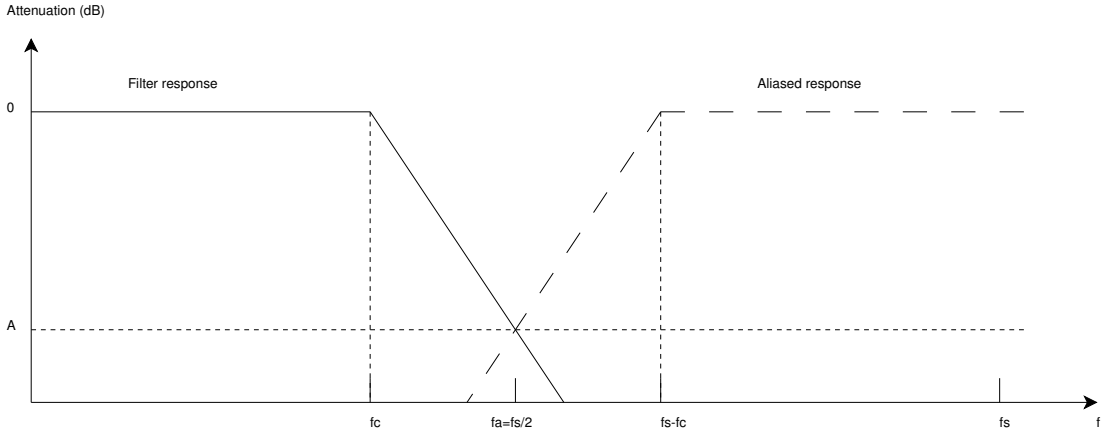


Figure 3.4 Anti-aliasing filter frequency response.

combinations match, so that any pulse oscillations are synchronised in the time domain. This allows directional coupling techniques, described in Chapter 4, to perform effectively.

Highpass filtering is also performed in the PDDS in order to remove the power frequency and its high magnitude harmonics, which improves the dynamic range of the ADCs. The method to achieve this differs between the current and voltage transducers. Each transducer is described later in this chapter. However, the frequency responses of the current and voltage channels still match. It is not necessary to completely remove the power frequency in the PDDS. It is instead sufficient to achieve an attenuation where the power frequency magnitude is reduced to several millamps or millivolts. This results in the magnitude of the attenuated signal frequently being much smaller than the PD pulse peak magnitudes. Remaining 50Hz components are filtered by the FDTF, as described in Section 4.2.

3.4.2 Current transducer and filter

The current transducer used is a Tektronix A6302 current probe connected to its matching Tektronix AM503 current probe amplifier. The current probe aperture is approximately 5mm, which is unsuitable for clipping around the bushing itself but it can be clipped around a wire connected to a transformer bushing. The probe and amplifier do not have any power frequency filtering, and therefore they are not suitable for on-line transformer testing where a large magnitude power frequency current is present that would saturate the probe. However, current probes are commercially available that are suitable for the on-line environment [109]. In the form of air-cored Rogowski coils, these consist of flexible tubes that can be clipped around a ceramic bushing. There are models available that also attenuate the power frequency for better dynamic range, have high frequency responses in the MHz range and are sensitive to below 1mA.

The Tektronix A6302 current probe used in the PDDS has the following relevant specifications [110]:

- Bandwidth from DC to at least 50MHz.
- Risetime of less than 7ns.
- Noise levels less than 0.3mA.
- Maximum input current of 20A.

The corresponding Tektronix AM503 current probe amplifier has the following relevant specifications [111]:

- Bandwidth from DC to at least 50MHz.
- Selectable bandwidth of 5MHz.
- With oscilloscope vertical screen scaling set at 10mV/div, selectable amplifier signal deflection settings are available from 1mA/div to 5A/div.
- Output impedance of 50Ω .

A 5-pole Butterworth normalised prototype filter network is used for the design of a passive lowpass filter [112]. The passive filter has the advantage of not requiring a power supply, which can be problematic when the PDDS is testing in the field. The prototype circuit is shown in Figure 3.5. The filter transformation requirements are that the high frequency -3dB cut-off is designed to 2MHz, and the input and output impedances are 50Ω . This gives the following filter transformation equations [112]:

$$L' = \left(\frac{R'}{R} \right) \left(\frac{\omega}{\omega'} \right) L = \frac{50}{1} \times \frac{1}{2\pi \times 10^6} L = 7.96 \times 10^{-6} L \quad (3.3)$$

$$L'_2 = L'_4 = 7.96 \times 10^{-6} L_2 = 12.9 \mu H \quad (3.4)$$

$$C' = \left(\frac{R}{R'} \right) \left(\frac{\omega}{\omega'} \right) C = \frac{1}{50} \times \frac{1}{2\pi \times 10^6} C = 3.18 \times 10^{-9} C \quad (3.5)$$

$$C'_1 = C'_5 = 3.18 \times 10^{-9} C_1 = 1.96 nF \quad (3.6)$$

$$C'_3 = 3.18 \times 10^{-9} C_3 = 6.36 nF \quad (3.7)$$

where L' and C' are the transformed values.

A 3-pole Butterworth normalised prototype filter network is used for design of a passive highpass filter [112]. The prototype circuit is shown in Figure 3.6. The filter transformation requirements are that the low frequency -3dB cut-off is designed to

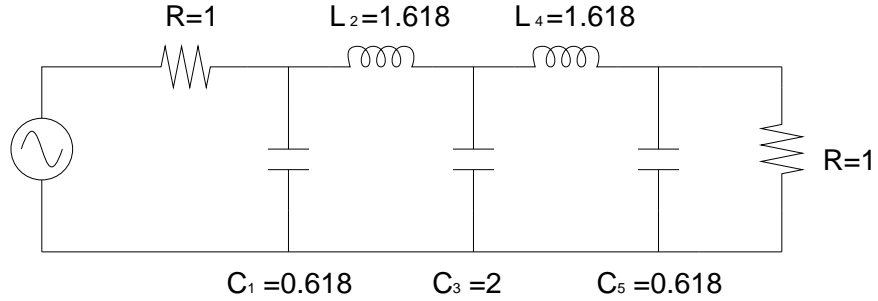


Figure 3.5 Prototype 5-pole Butterworth lowpass filter.

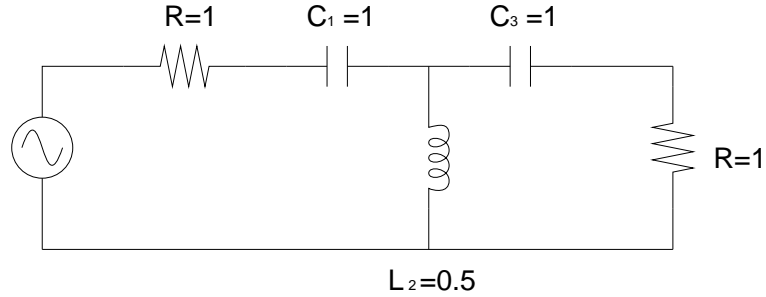


Figure 3.6 Prototype 3-pole Butterworth highpass filter.

30kHz, and the input and output impedances are 50Ω . This gives the following filter transformation equations [112]:

$$L' = \left(\frac{R'}{R} \right) \left(\frac{\omega}{\omega'} \right) L = \frac{50}{1} \times \frac{1}{2\pi \times 30 \times 10^3} L = 265 \times 10^{-6} L \quad (3.8)$$

$$L'_2 = 265 \times 10^{-6} L_2 = 133 \mu H \quad (3.9)$$

$$C' = \left(\frac{R}{R'} \right) \left(\frac{\omega}{\omega'} \right) C = \frac{1}{50} \times \frac{1}{2\pi \times 30 \times 10^3} C = 106 \times 10^{-9} C \quad (3.10)$$

$$C'_1 = C'_3 = 106 \times 10^{-9} C_1 = 106 nF \quad (3.11)$$

where L' and C' are the transformed values.

The final circuit of the bandpass filter which follows the current transducer is shown in Figure 3.7. It is placed in a grounded metal enclosure for shielding purposes. BNC connectors and coaxial cables connect the current probe amplifier, filter and oscilloscope. The output impedance of the filter in Figure 3.7 is 50Ω . However, the input impedance of the oscilloscopes is $1M\Omega$. To present the correct impedances to the filter and oscilloscope, an in-line passive 50Ω to $1M\Omega$ connector is used.

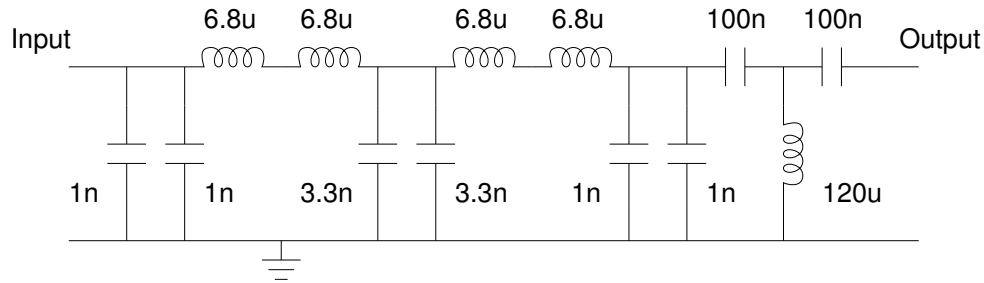


Figure 3.7 Bandpass filter following current transducer.

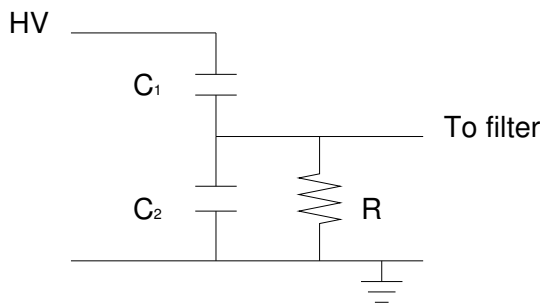


Figure 3.8 Capacitive voltage divider.

3.4.3 Voltage transducer and filter

The voltage transducer consists of a capacitive voltage divider circuit, using the bushing of the transformer as a HV insulator, as shown in Figure 3.8. A resistor is placed across C_2 to form a highpass filter for power frequency voltage attenuation purposes. This brings the magnitude of the signal to within the input voltage range specifications of the following anti-aliasing active filter and oscilloscope, and also increases the dynamic range of the ADC. This design of the transducer also removes the need for an expensive HV measuring capacitor to be connected to the bushing.

A capacitive voltage divider circuit could be implemented using a capacitive bushing tap on a transformer that was designed and constructed with such a feature. However, the transformers used for PDDS testing do not have a bushing tap. Instead, the transducer consists of two layers of metal foil wrapped around the bushing near the tank wall. The foil layers are each 14cm by 5cm in area and are separated by layers of paper. The bushing ceramic is used for the dielectric of C_1 . A cross section of the bushing and capacitors is shown in Figure 3.9. The capacitance values were determined as follows.

Larger values for C_2 reduce the power cycle magnitude, but also reduce the magnitude of high frequency signals, making them more difficult to acquire. However, smaller values of C_2 (in combination with R) may allow the power cycle magnitude to exceed the maximum input voltage range of the following active filter. Ten layers of paper

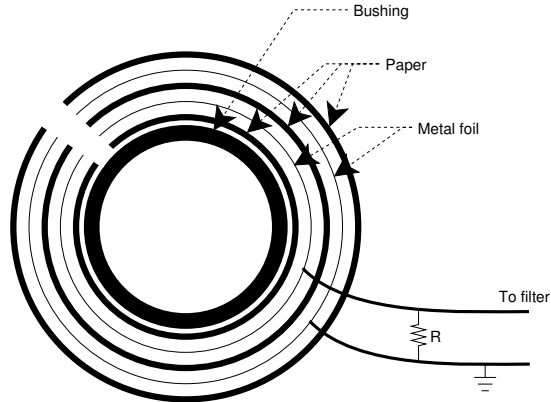


Figure 3.9 Physical cross section of the capacitive voltage divider.

were chosen to separate the two layers of foil that form C_2 . The capacitance of C_2 can be calculated by considering it to be a parallel plate capacitor. However, this method of calculation is unreliable as it is difficult to measure the separation, and the variation of separation, of the foil layers. Also, the dielectric constant is not precisely known. Instead, a Philips PM6304 RCL meter is used and gives a capacitance of 42pF for C_2 .

For determining the capacitance of C_1 , it can be considered a cylindrical capacitor with a ceramic dielectric. For a cylindrical capacitor, the capacitance is:

$$C = \frac{2\pi\kappa\epsilon_0 L}{\ln\left(\frac{b}{a}\right)} \quad (3.12)$$

where κ is the dielectric constant, ϵ_0 is the permittivity constant ($8.85 \times 10^{-12} \text{ F/m}$), L is the length in the axial direction and a and b are the radii of the internal and external surfaces respectively. From Equation 3.12, C_1 is calculated as 11pF. However, measurement error of variables in the calculation make this value only approximate to within several pF.

Another method to calculate C_1 is to apply a sinusoidal waveform of known voltage magnitude at the bushing terminal and to measure the voltage magnitude across C_2 . From Figure 3.8, the capacitance of C_1 can be calculated as follows:

$$\frac{V_{\text{out}}}{V_{\text{in}}} = \frac{C_1}{C_1 + C_2} \quad (3.13)$$

$$C_2 = \frac{C_1 V_{\text{in}} \left(1 - \frac{V_{\text{out}}}{V_{\text{in}}}\right)}{V_{\text{out}}} \quad (3.14)$$

The $V_{\text{out}}/V_{\text{in}}$ ratio is frequency dependent. At 50Hz, $V_{\text{out}}/V_{\text{in}}=1/83$. However, the ratio is reasonably consistent at 1/20 from 1kHz to 5MHz, which is the frequency region of interest for the PDDS. Therefore, the value of C_1 is calculated as 2.2pF.

When testing the energised transformer Tx2 (see Section 5.3), the power frequency

voltage is 11kV_{rms} at the HV bushing and is reduced to approximately 132V_{rms} across C_2 without R , using the measured $V_{\text{out}}/V_{\text{in}}$ ratio at 50Hz. R is chosen as $100\text{k}\Omega$. The output is then attenuated at 50Hz to a ratio of 1/6650, which reduces the power frequency voltage from 11kV_{rms} to approximately 1.6V_{rms} . This is a suitable magnitude for the input specifications of the following active filter.

It is not necessary to precisely know the various attenuation ratios. Once the capacitive voltage divider has been placed on the bushing of the transformer under test, calibration is performed. An artificial pulse of known magnitude is applied to the bushing, and the oscilloscopes record the output magnitude.

An anti-aliasing filter is connected to the output of the voltage transducer. An active filter, rather than a passive filter, is used for the following reasons:

- The input impedance of the filter must be significantly higher than R , so that it does not affect the transducer frequency response. For a filter with responses in the MHz range and high input impedances, a passive filter would require discrete capacitor component values in the low pC range and is therefore difficult to construct. On the other hand, active filters built with operational amplifiers (op-amps) can have very high input impedances.
- PD pulses are often in the μV or mV range. An active filter can provide amplification of the analog signal before digitisation.

The active filter attached to the output of the voltage transducer is not only used for anti-aliasing but also for further power frequency magnitude reduction. The circuit of the active bandpass filter is shown in Figure 3.10. The filter is housed in a small grounded metal box for shielding purposes and connected to the voltage transducer by a coaxial cable approximately 10cm in length, which is significantly short compared to the wavelength of the highest frequency recorded.

The filter consists of 5 op-amps connected in series. The EL2445CN quad op-amp chip is used for the first four stages, and is suitable due to its specified high bandwidth and voltage slew rates. The first op-amp is configured as a non-inverting buffer. The high input impedance of the EL2445CN op-amp chip meets the requirements of the voltage transducer. High speed Schottky diodes prevent the input signal from exceeding the input voltage range specifications of the EL2445CN chip. If overvoltage momentarily occurs, a $6.8\text{k}\Omega$ resistor prevents excessive current flow through the diodes.

To further reduce the power frequency magnitude, a non-inverting second order highpass filter follows the input buffer and has a gain of 1. The -3dB cut-off frequency f_L can be calculated by:

$$f_L = \frac{1}{2\pi RC} \quad (3.15)$$

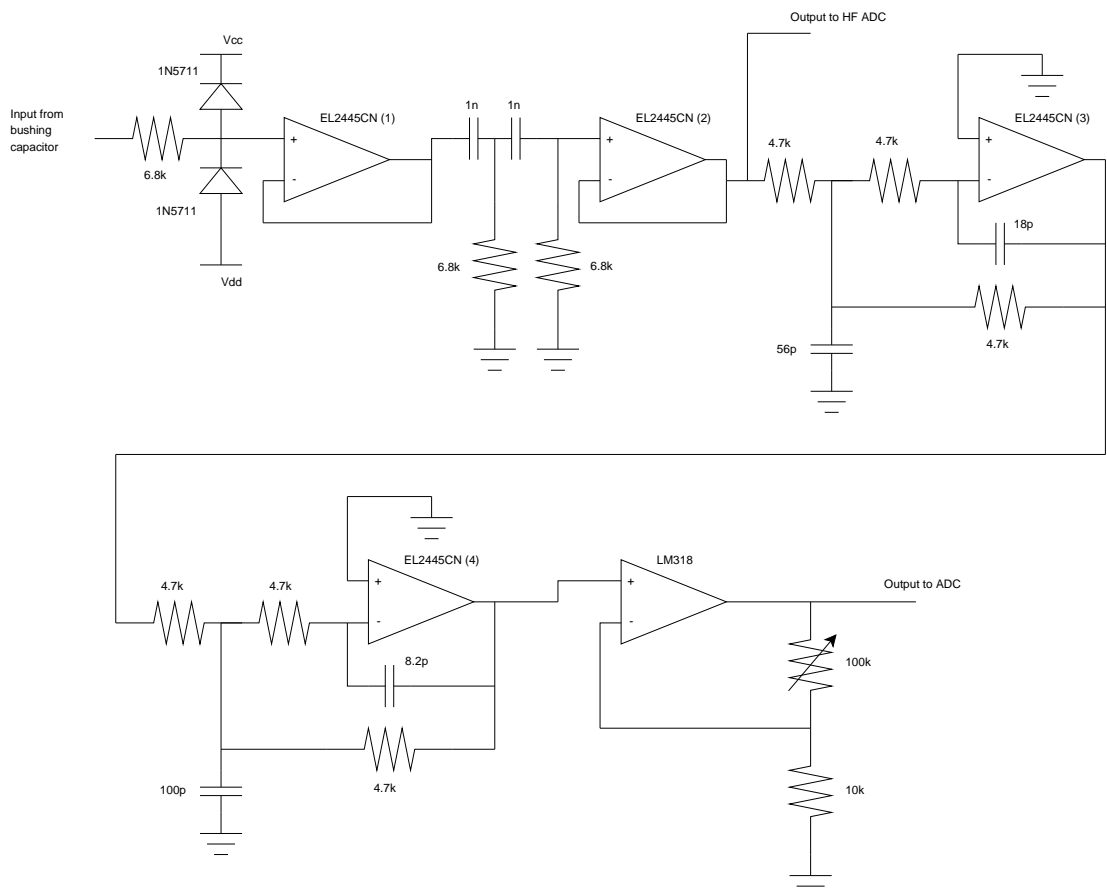


Figure 3.10 Active bandpass filter following voltage transducer.

where R and C are the values of the resistors and capacitors preceding the op-amp. The cut-off frequency is 23.4kHz.

A two stage, fourth order, lowpass Butterworth filter follows the highpass filter. Each stage inverts the signal. It is designed with a -3dB cut-off frequency of approximately 1MHz. This allows the entire frequency response of the voltage transducer and active filter to match the current transducer and filter, as detailed in Section 3.4.4.

The fifth op-amp is configured as a non-inverting amplifier based around a LM318 chip. This chip has lower bandwidth specifications than the EL2445CN chip, but is suitable for the signal parameters at this point in the signal path. This stage provides a gain from 1 to 11.

The high sample rate channel is routed from the point before the two stage lowpass filter. Anti-alias filtering is provided here by the oscilloscopes with the ‘Bandwidth Limit’ function enabled. This provides lowpass filtering with a -3dB cut-off frequency of approximately 20MHz.

3.4.4 Transducer and filter responses

The frequency responses of the current and voltage signal channels is a combination of the frequency responses of the transducers, filters and amplifiers. It is impractical to calculate the frequency responses of all of the individual components that make up each channel, especially the voltage channels. For example, the voltage dividers wrapped around the HV bushings vary their frequency response depending on construction and placement. Inter-component loading effects will also affect individual component frequency responses. However, it is important that the frequency responses of current and voltage signal paths within each channel match before digitisation. In this way, the recorded current and voltage waveshapes in response to pulses will be consistent and time domain oscillations will match when signals are processed in the directional coupling signal processing stage, as described in Section 4.4.

To determine the complete frequency responses of each current and voltage channel before digitisation when all of the hardware components are in place on the transformer, a variable frequency sinusoidal signal was injected at the HV bushing terminal and the output response on the oscilloscopes was recorded.

The frequency responses of each of the transducers, including the respective analog filters, is shown in Figure 3.11. The low frequency response roll-offs is not an exact match between the current and voltage transducers and analog filters, but is sufficient for suppression of power frequencies and its harmonics. The high frequency response roll-offs of the current and voltage channels matches satisfactorily. Some peaks in the response above 2MHz do not present a significant problem to the PDDS as they do not significantly distort the waveshape of any pulses, and any aliased narrowband signals are removed in the software based FDTF, as detailed in Section 4.2.1.

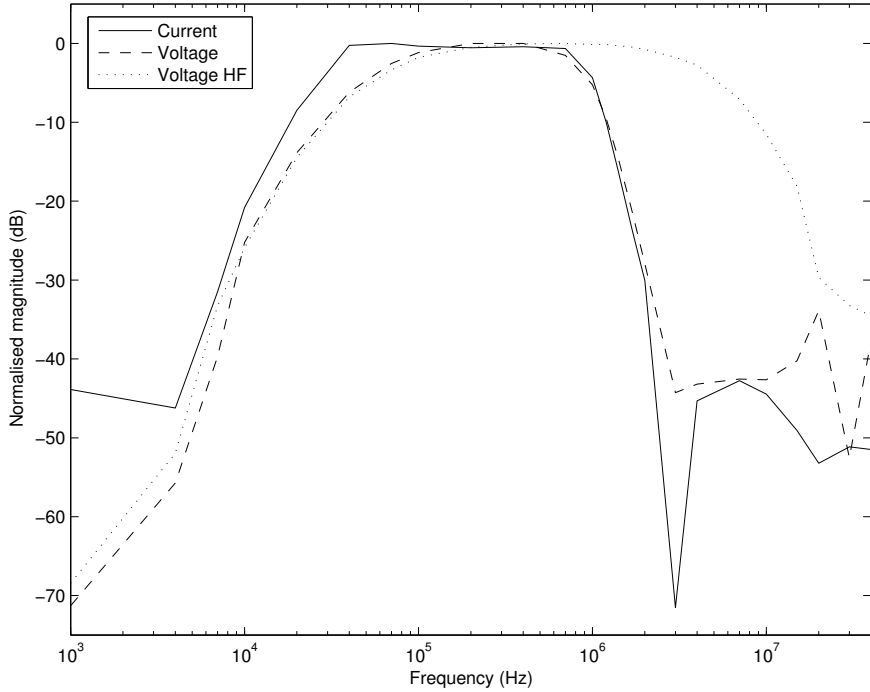


Figure 3.11 Frequency responses of current, voltage and HF voltage transducers and analog filters on transformer Tx1.

3.4.5 Oscilloscopes

Digitisation of signals is performed using Hewlett Packard (HP) 54645A oscilloscopes. Each oscilloscope has a HP54650A HP-IB Interface Module that provides a GPIB port and is connected to the PC GPIB add-in card.

The specifications of the HP54645A oscilloscope include [113]:

- 2 analog channels with an input impedance of $1M\Omega$ and input capacitance of approximately $13pF$.
- Single shot bandwidth of 50MHz.
- Vertical resolution of 8 bits with a range of 1mV/div to 5V/div.
- Sample rate of up to 200MSa/s with a range of 2ns/div to 50s/div.
- Memory depth of up to 1MSa per channel.
- External trigger socket.

3.5 CONCLUSIONS

The hardware components of the PDDS have been described in this chapter, including the PD pulse and interference generators, PCSM and current and voltage transducers

with their respective analog filters and digitisers. Also provided is a description of how the various components are connected together. By design, the PDDS components are readily available, have low cost and are easily constructed and installed. There is flexibility for individual item upgrades or interchanges.

Once signals recorded on the oscilloscopes have been transferred to the PC, the digital signal processing algorithms described in Chapter 4 are applied.

Chapter 4

SIGNAL PROCESSING

The purpose of this chapter is to describe the software based signal processing algorithms used in the PDDS that detect and display transformer PDs. The inputs for these algorithms are acquired from the oscilloscopes that digitise the current and voltage waveforms produced by the transducers. The first section provides an overview of the sequential signal processing stages. The second section details the FDTF which serves to remove arbitrary narrowband interference. The third section describes the CWT and its inverse. A short explanation is included as to why the DWT is not used in the PDDS. The fourth section discusses directional coupling using CWT coefficients. The fifth and sixth sections provide information about clustering techniques with neural networks and their application to PD source identification.

4.1 OVERVIEW

The objective of the digital signal processing stages in the PDDS is to identify and display any PD that may be present within a transformer and to determine if multiple sources are simultaneously active. The signal processing is performed using Matlab, a PC software package that provides an environment for numerical processing. Matlab also provides features for communicating with external instruments and thus controls the oscilloscopes, the PCSM and also the arbitrary waveform generators used for PDDS off-line testing described in Chapter 5.

Signals from each current and voltage transducer, except for the high sample rate sub-channel, are digitised at a sample rate of 10MSa/s and passed to the PC for processing. The high sample rate sub-channel signal is sampled at 50MSa/s. Power frequency attenuation and anti-alias filtering are the only signal shaping techniques prior to digitisation, as described in Chapter 3. It typically requires several seconds for transferring data from the oscilloscopes to the PC, and approximately 2 to 3 minutes for the PC to process the data, as described in this chapter. If needed, further optimisation of the algorithms could significantly decrease this time.

The speed of the digital signal processing in the PDDS is not fast enough for

continuous real-time analysis. As the sample rate of the PDDS is in the order of millions of samples per second, the GPIB connection is not capable of transferring data fast enough. Also, after the captured signals have been transferred to the PC, it will currently take even a fast PC at least several minutes to perform the signal processing operations, detailed in this chapter, on the digitised data covering one power cycle. Only then is the PDDS able to capture and process new data. As a result, the PDDS is currently only capable of analysing a small percentage of power cycles. However, only processing a small percentage of power cycles is still representative of the actual transformer PD condition. PD sources will typically generate at least several pulses every power cycle. Also, a PD source normally changes its magnitude and phase timing characteristics over a much longer time frame than seconds or minutes, rather over days, months or years. Therefore, tracking a gradual increase in PDs is easily possible with the PDDS.

The power transformer on-line environment typically involves interference that has been categorised into two types [78], as already described in Section 2.5.7:

- **Continuous periodic interference:** All of the signals in this group are sinusoidal, such as carrier communication, high frequency protection signals and radio broadcast. They can be considered narrowband interference in the frequency domain.
- **Pulse interference:**
 - Periodic pulse interference that occurs at fixed positions within the AC cycle, for instance, thyristor switching.
 - Non-periodic pulse interference. Signals appear more or less at random, such as corona, external partial discharging and arcing between adjacent metallic components or from rotating machinery.

The temporal and frequency characteristics of narrowband interference and various types of interference pulses have little in common. The PDDS uses two distinct stages for removal of interference. Firstly, the FDTF removes any narrowband interference of arbitrary frequency and significant magnitude. Secondly, the current and voltage waveforms from each transformer bushing are analysed with directional coupling and wavelet techniques to determine if pulses have originated from within the transformer. Any such detected pulses show that the transformer under study has a PD problem.

After PDs have been identified, a neural network implementing clustering techniques identifies if multiple internal PD sources are active. The exclusion of external pulse sources from the neural network stage prevents possible confusion and additional load of the neural network during training and classification.

Figure 4.1 presents the series of steps used by the PDDS to identify and group internal PD sources. The transducers and analog filters used prior to digitisation are

included as well. The FDTF is applied to each captured signal, before current and voltage signals are transformed with the CWT and multiplied together to distinguish internal PD pulses from external ones. Comparison to other channels is made to ensure a recognised internal pulse is not actually an external pulse that has traversed the transformer winding. Sections of a high sample frequency channel CWT are used to provide features for a CNN which determines the number of PD pulse sources. Further details of each of these signal processing stages are provided later in this chapter.

By design, the PDDS can theoretically accept any number of input channels, allowing it to be used on three phase transformers and other transformers with additional taps. To ensure that a PD pulse originates from within the transformer, all external taps must be monitored. However, bushings and taps may be known to be free of external pulse interference and do not require monitoring. If limited PDDS hardware channels are available, swapping channels amongst transformer bushings and taps can identify whether an apparently internal PD source is actually external. This may happen when the external pulse interference passes through the windings of the transformer and appears at another bushing or tap.

4.2 FOURIER DOMAIN THRESHOLD FILTER (FDTF)

One source of interference to PD signal detection is narrowband signals. In order to minimise this type of interference, it is necessary to develop methods that also minimise distortion or removal of PD pulse signals. Transforming the raw digitised signal into the Fourier domain enables strong separation of narrowband and stochastic pulse signal energies. Here, the narrowband signal has a highly localised energy at a particular frequency, whereas a time domain pulse is characterised by a wide frequency spectrum.

The transducers and analog filters remove narrowband sources above the anti-aliasing frequency. The power frequency and its harmonics are also attenuated, but not completely removed. When the PDDS is attached to an arbitrary transformer, an unknown number of narrowband sources within the analog filters' passband can be present. The frequencies and magnitudes of all of these sources will possibly also be unknown. This requires either a human operator to manually select interference free bands, or an automatic method that is capable of filtering narrowband sources with unknown characteristics. Automated filter algorithms are preferable because ultimately human interaction is a financial and time cost if this system is to be deployed to many transformers.

The PDDS uses a FDTF to automatically remove narrowband signals. The algorithm is a form of multi-band rejection filter and consists of the following steps:

- The discrete time domain signal is transformed to the discrete Fourier domain

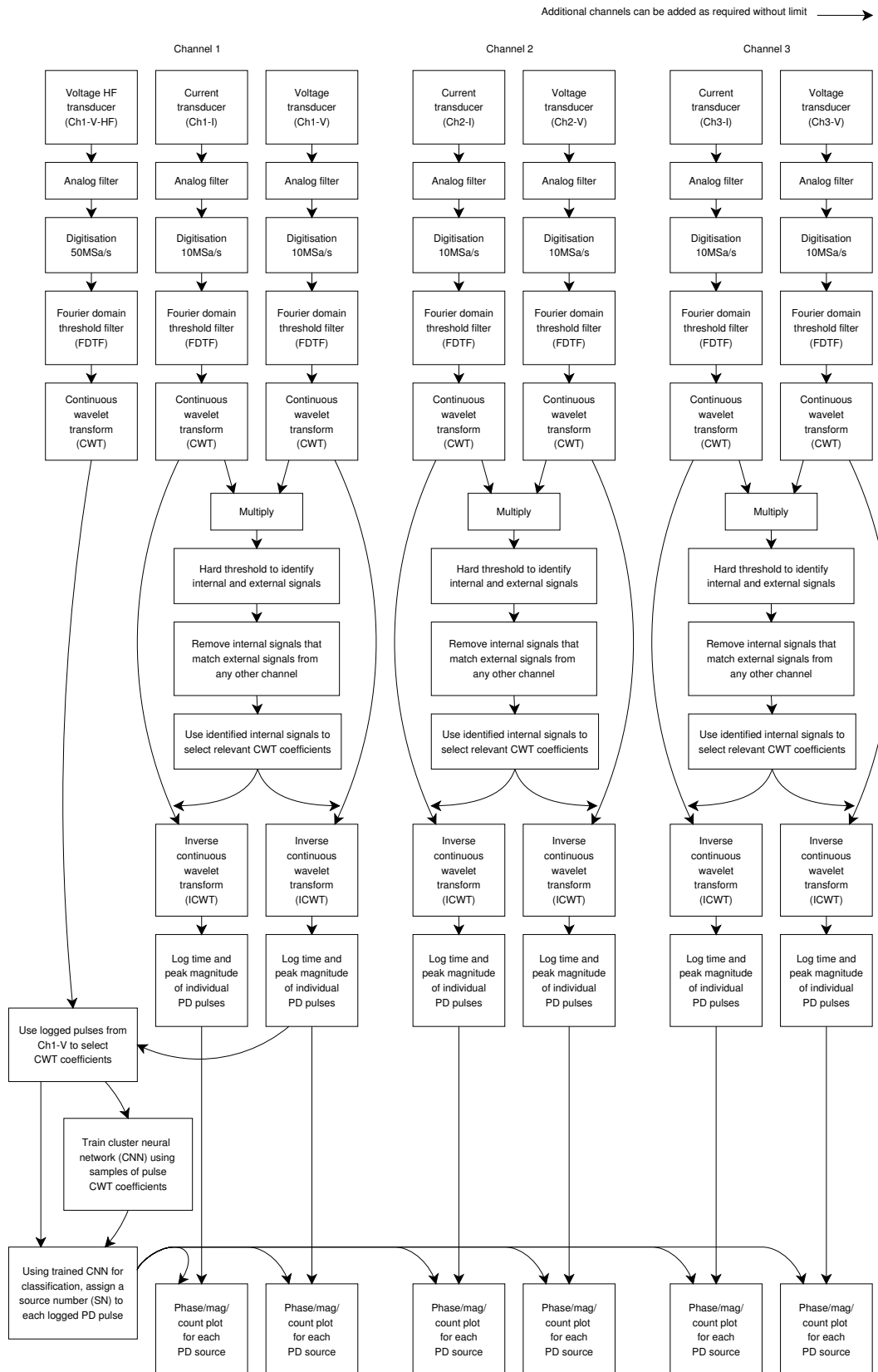


Figure 4.1 Overview of the structure of the signal processing stages in the PDSS.

using the discrete Fourier transform (DFT). The implementation in the PDDS uses the FFT.

- The Fourier domain sequence is divided into an arbitrary number of small, equal sized bins. The median of the absolute magnitude of the Fourier domain samples is calculated for each bin. Over the complete Fourier domain signal, these medians form a varying magnitude indicator that approximately matches the magnitude of the Fourier domain noise floor.
- A threshold level is calculated by multiplying the medians of each bin with a constant u .
- Any Fourier domain samples that have an absolute magnitude greater than the threshold are attenuated to the threshold, keeping phase information unchanged.
- The resulting thresholded signal is transformed back to the time domain using the inverse discrete Fourier transform (IDFT) or the inverse fast Fourier transform (IFFT).

The DFT and IDFT are given by

$$F_m = \sum_{n=0}^{N-1} f_n e^{-i2\pi mn/N} \quad m = 0, 1, \dots, N - 1 \quad (4.1)$$

$$f_n = \frac{1}{N} \sum_{m=0}^{N-1} F_m e^{i2\pi mn/N} \quad n = 0, 1, \dots, N - 1 \quad (4.2)$$

where N is the number of time domain samples and f_n and F_m represent the discrete time and Fourier domain descriptions respectively [108].

In real world signals, the average magnitude of the noise floor can vary with frequency. For example, this may occur where a wide band signal has dominant frequencies. The median function is used to determine approximately where the noise floor is located within a bin in the Fourier domain. By calculating the median of the Fourier domain samples over only a short sequence or bin, an indicator can be created that allows for broad changes in the magnitude of the noise floor with frequency. The median is chosen as this measure most closely represents the majority of values within the bin. If the mean was used as an indicator of noise floor level, it could be skewed by high magnitude samples that represent an unwanted narrowband interference source. It is important to choose a bin length that is significantly wider than any strong narrowband interference sources, yet narrow enough to generally indicate the trend of the level of the noise floor. Some prior knowledge of the bandwidth of any interfering narrowband sources is therefore needed.

The thresholded Fourier domain signal G_m is calculated as follows:

$$G_m = \begin{cases} \frac{F_m uv(m)}{|F_m|} & \text{if } |F_m| > uv(m) \\ F_m & \text{if } |F_m| \leq uv(m) \end{cases} \quad (4.3)$$

where u is the median multiplier constant and $v(m)$ is the median value of the samples of the bin that contains sample m . The filtered time domain signal can be obtained from Equation 4.2 with F_m replaced by the thresholded G_m .

4.2.1 Fourier domain threshold level

When a Fourier domain sample exceeds the calculated threshold, the magnitude of that sample is reduced to the threshold level while keeping its phase information unchanged. This reduction serves to remove narrowband interference, whereby the level of reduction is arbitrary. For example, the magnitude of the sample could be changed to zero, the calculated median of the relevant bin or another value. Reasons for changing Fourier domain samples to the threshold level include:

- Due to spectral leakage and some ‘real world’ significant bandwidth, narrowband signals form ‘triangular peaks’ in the Fourier domain rather than a single sample peak. As a result, samples that exceed the threshold will often have neighbouring samples that almost exceed the threshold. Changing threshold exceeding samples to the threshold maintains similarity to neighbouring samples, preventing radical step changes in the Fourier domain sequence.
- Time domain pulses can have dominant frequency components that may just exceed the threshold. Radically clipping Fourier domain threshold exceeding samples to, for example, zero, unnecessarily removes possibly useful pulse signal energy.

When removing narrowband signals, it is preferred that the shapes of wideband pulse signals experience as little waveshape deformation as possible. This allows better signal analysis at later processing stages. It also allows more accurate magnitude determination, and therefore PD assessment, of any transformer PD pulse sources.

The key variable when applying the threshold filter is the multiplier u in Equation 4.3, which is used with the median of each bin to determine the threshold level. When the median multiplier is small, many Fourier domain sample points may be unnecessarily truncated across the spectrum. Conversely, when the median multiplier is large, narrowband signal energy remains after thresholding and may continue to obscure time domain pulses.

To determine the effect that varying the median multiplier has on narrowband source removal and pulse waveshape distortion, an artificial test signal that consists of

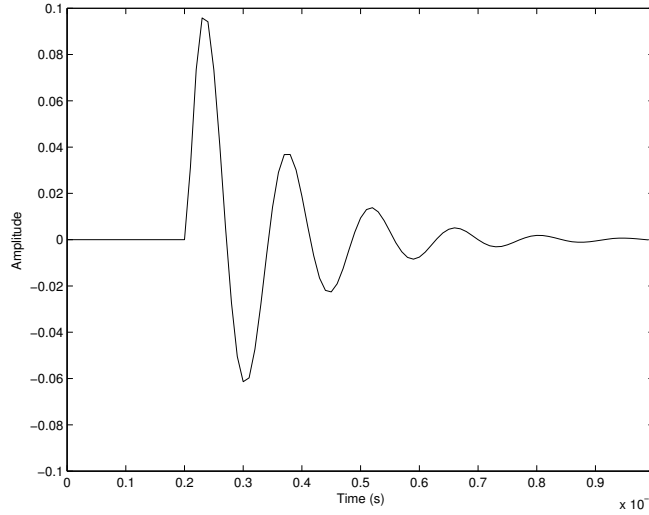


Figure 4.2 A single mathematically created pulse.

several narrowband sources is used. The signal is sampled at an equivalent of 10MSa/s and has a length of 2×10^5 samples. A series of mathematically created pulses are generated and added to the signal. The pulses are calculated as follows:

$$\text{Pulse} = (e^{-0.7t/10^{-6}} - e^{-10t/10^6}) \sin(1.4 \times 10^6 \pi t) \quad (4.4)$$

A sample pulse is shown in Figure 4.2. This pulse is similar in waveshape to a PD pulse that has been distorted by transformer windings. The summation of artificial narrowband signal and artificial pulses is shown in Figure 4.3, which also shows the artificial pulses separately. Figure 4.4 shows the signal after transformation to the Fourier domain, with the median level calculated for 100 bins. An example threshold is shown where the multiplier u has the value 10.

The filtered time domain signal was calculated for a range of median multipliers. In order to quantitatively indicate how much narrowband signal removal and pulse distortion is occurring, the following measurements are used:

- The output signal $g(n)$ to input signal $f(n)$ power ratio.
- The pulse amplitude change, measured for each pulse.
- The pulse waveshape distortion using the cross correlation between each pulse before and after filtering.
- The pulse waveshape distortion using an absolute sample difference algorithm between the pulses before and after filtering.

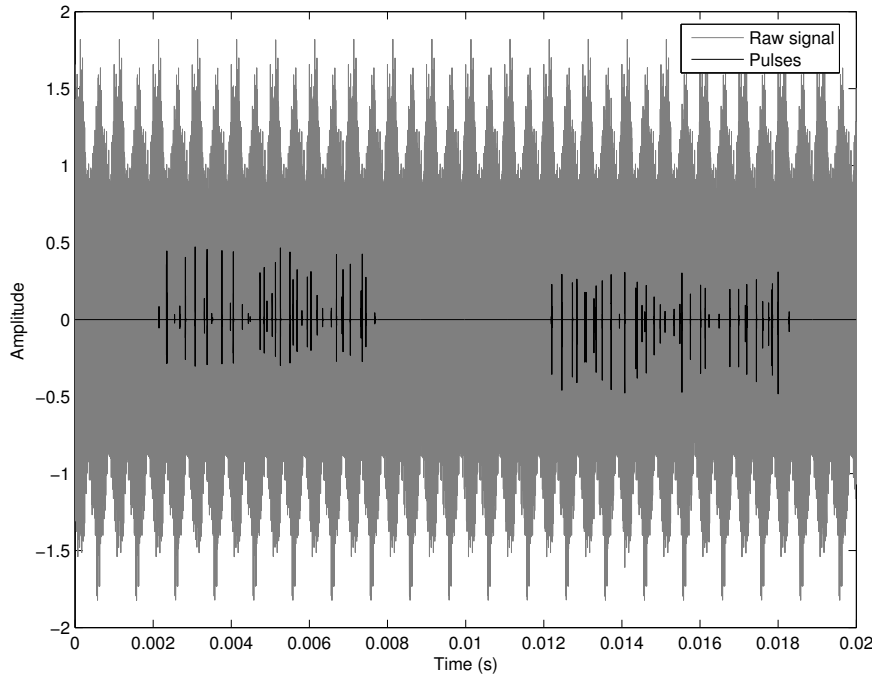


Figure 4.3 Artificial raw signal composed of multiple narrowband waveforms and added pulses used to determine a suitable median multiplier value. The pulses are also shown separately.

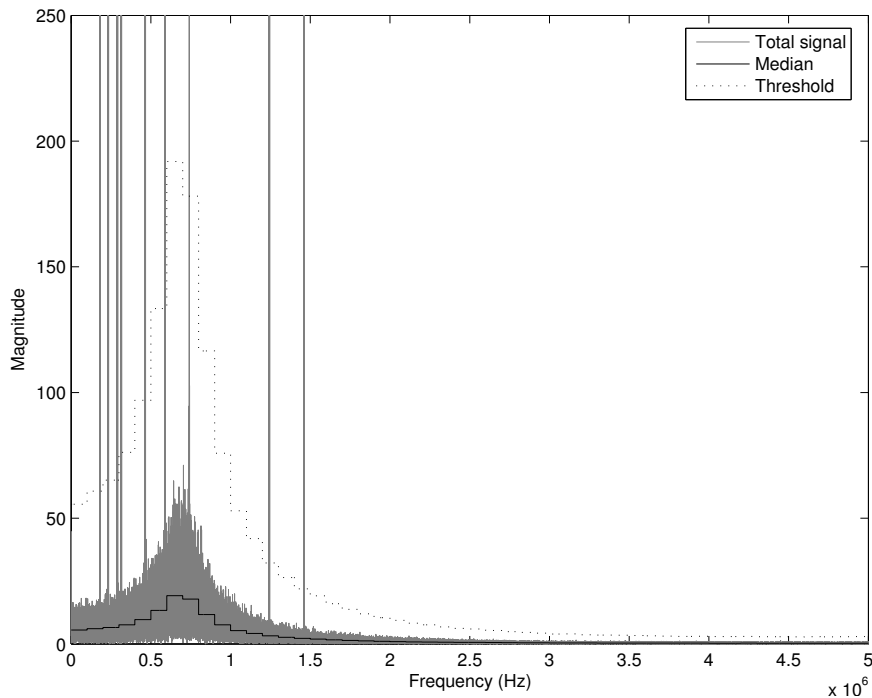


Figure 4.4 Fourier domain signal with calculated bin medians and threshold where $u = 10$.

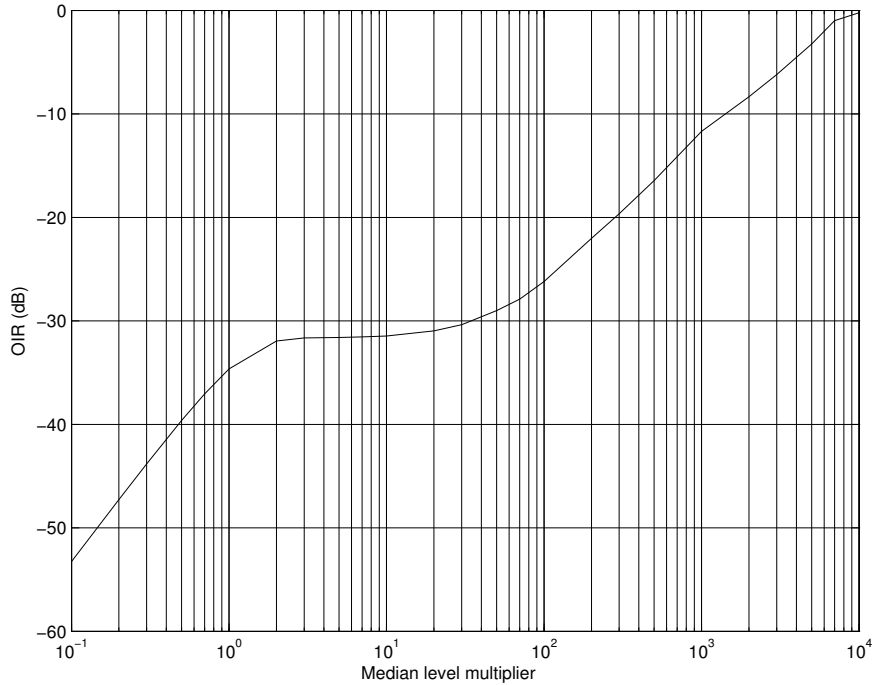


Figure 4.5 Reduction in raw signal power after threshold filtering.

The output signal to input signal power ratio (OIR) is

$$\text{OIR} = 10 \log \frac{\sum g^2(n)}{\sum f^2(n)} \quad n = 1, 2, \dots, 2 \times 10^5 \quad (4.5)$$

where f and g are the input and output signals and n is the sample number. Figure 4.5 shows the OIR for a range of values of u . High u values provide little reduction in the narrowband signal, as little spectral energy has been attenuated. Low values of u attenuate many of the samples that reside in the noise floor, probably also losing pulse signal information. Multiplier values from 2 to 100 have a similar OIR. This indicates that u could be chosen from within this range and narrowband source filtering would be consistent and effective.

As the pulses are mathematically created and added to the narrowband signal, an exact comparison can be made with the filtered response as follows:

$$\text{Pulse peak amplitude change} = \frac{|\max(g(a))|}{|\max(f(a))|} \quad a = 1, 2, \dots, P \quad (4.6)$$

where $f(a)$ and $g(a)$ are short sequences of the input $f(n)$ and output $g(n)$ signals that contain the mathematically generated pulses, and P is the length of the mathematically generated pulse sequence.

For each pulse, the relative change in peak amplitude between each original artificial pulse and the filtered response is shown in Figure 4.6. For the large majority of pulses,

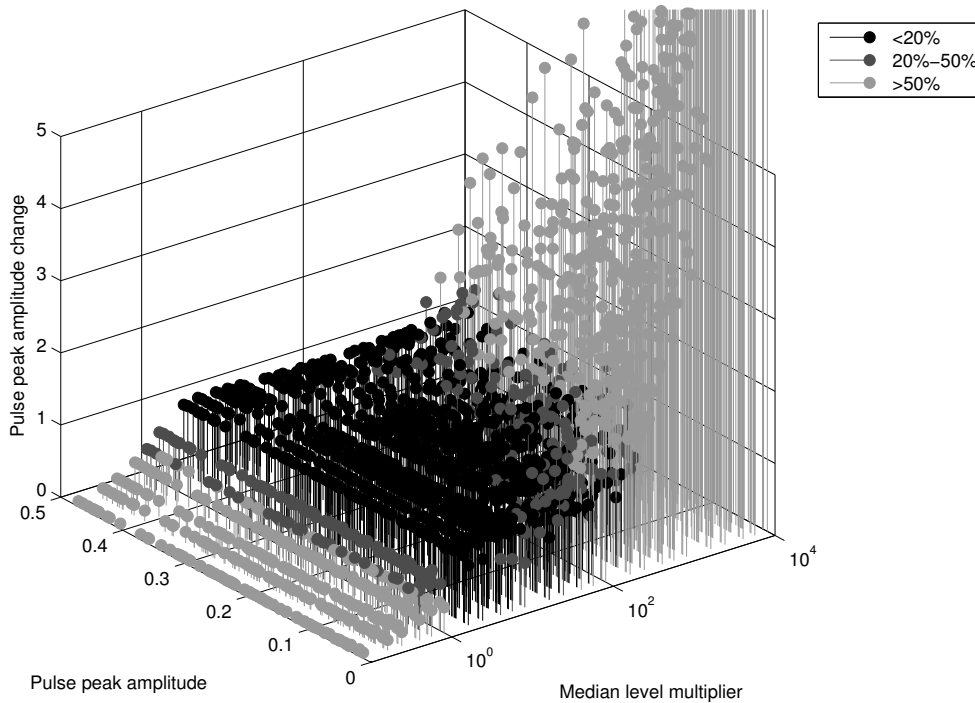


Figure 4.6 Change in each pulse peak amplitude after threshold filtering.

there is little change in peak amplitude when u is between 2 and 100. Smaller values of u tend to clip the pulse height as well as reduce the sinusoidal narrowband waveform. Larger multipliers do not remove enough of the narrowband sinusoid, and pulses are therefore distorted by it when compared to the original. Overall, smaller amplitude pulses are more sensitive to the amount of narrowband sinusoid removal.

Figure 4.7 shows the normalised zero-lag cross correlation factors for each pulse, that is, the correlations between the waveshapes of the mathematically created pulses and the waveshapes of their filtered outputs. It is calculated as follows:

$$\text{Pulse zero-lag cross correlation} = \sum_{a=1}^P f(a)g(a) \quad (4.7)$$

The results are normalised so that a factor of 1 is an identical match, and hence indicates that there is no pulse waveshape distortion, whereas lower values show less correlation. Again, an acceptable range for u is present between 2 and 100. Pulses with a small amplitude are again more sensitive and can be more readily changed even when only a small level of narrowband signal energy remains after filtering.

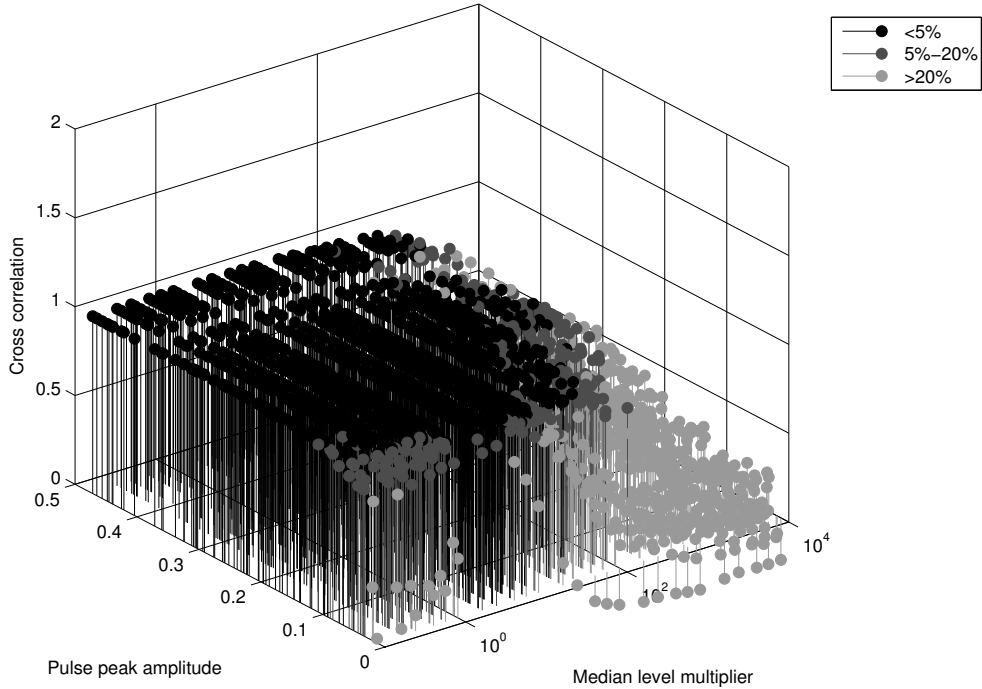


Figure 4.7 Cross correlation for each pulse before and after threshold filtering.

Figure 4.8 shows the sum of the absolute differences between samples that make up each pulse before and after threshold filtering, and is calculated as follows:

$$\text{Pulse difference change} = \sum_{a=1}^P \frac{|f(a) - g(a)|}{P} \quad (4.8)$$

Again, the minimum change is observed where u is in the range of 2 to 100, including small amplitude pulses. This region indicates minimum pulse waveshape distortion.

From this series of quantitative measurements on the effectiveness of the FDTF, values of u below 2 tend to threshold too much of the Fourier domain samples thus removing wanted pulse information. Also, values above 100 leave too much narrowband signal energy when the spectrum is transformed to the time domain. A median multiplier of 10 is chosen for the PDSS. This provides a balance between removing as much narrowband signal energy as possible without thresholding too many Fourier domain samples.

4.2.2 Notch filter beat effect

The FDTF frequency response is not predetermined, but it is automatically created dependent upon any significant narrowband signals which may be present in the spectrum and which exceed the threshold. The filter length is equal to the length of the Fourier transform of the signal. The filter consists of mostly 1s, with values between 0 and 1

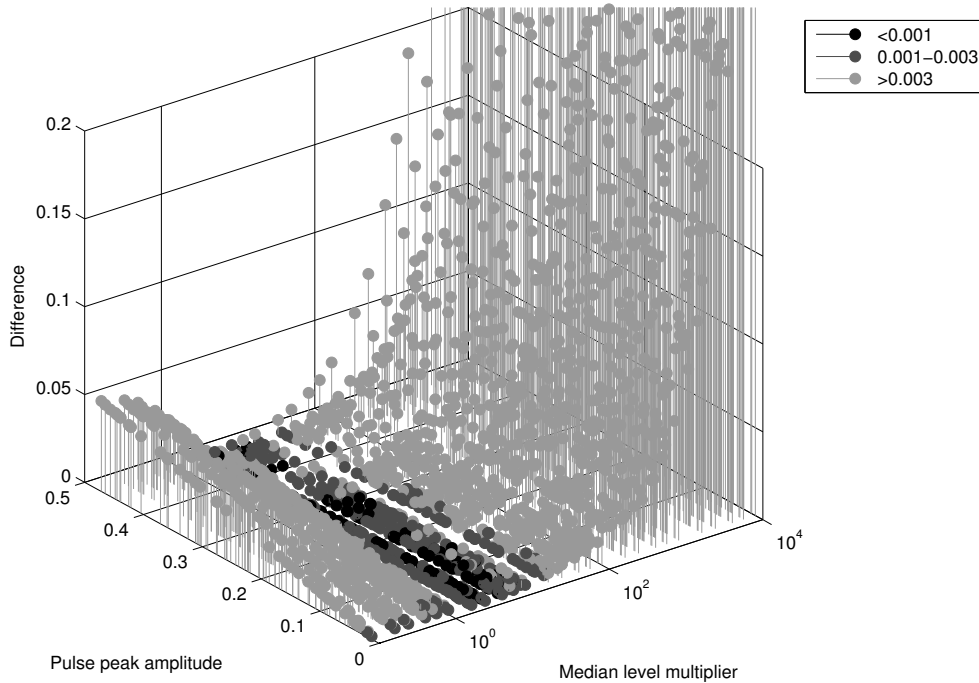


Figure 4.8 Sum of absolute differences for each pulse resulting from threshold filtering.

where the Fourier domain signal exceeds the threshold. The filter is then multiplied with the Fourier transform of the signal.

An effect of multiplying two or more signals in the Fourier domain together is beat patterns in the time domain of the filtered signal. In general, a beat frequency is equal to the absolute value of the difference in frequency of two arbitrary sine waves. In the case of the FDTF, each notch in the filter response is creating a beat frequency in combination with each other notch and low magnitude narrowband sources remaining in the signal. The result is a complex beat pattern that cannot be predetermined due to a lack of prior knowledge of any narrowband interference sources unless artificially created.

The common situation for the FDTF to operate in is to potentially threshold several narrowband sources whose total bandwidth exceeding the threshold is a significantly small proportion of the entire bandwidth. Figure 4.9(a) shows an example of the Fourier transform of five narrowband sources and, in (b), a section of the Fourier domain. Threshold multipliers of 10 and 100 are used, and the resultant time responses of the filtered signal are shown in (c).

The beat effect is observable in Figure 4.9(c) at the start and the end of the time signal. This effect is unwanted as the SNR in these areas is lower, making the identification of PD pulses difficult. To counter this effect, extra data is sampled by the oscilloscopes at the start and the end of the time period of interest, and then discarded

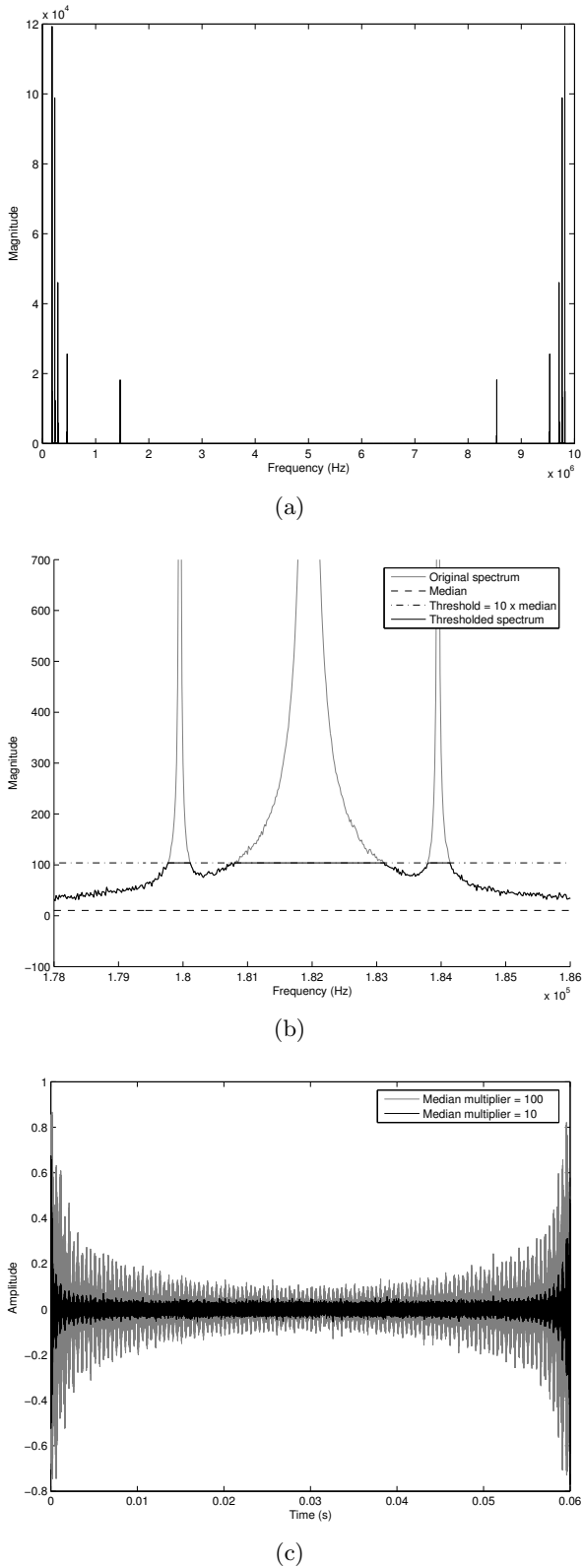


Figure 4.9 Time domain responses from two levels of Fourier domain thresholding of a signal that consists of five narrowband sources: (a) the Fourier transform, (b) selection of the Fourier domain signal when $u = 10$ and (c) superimposed time domain responses for $u = 10$ and $u = 100$.

after the FDTF. In the PDDS, this involves sampling at least three power cycles of data, passing the entire signal through the FDTF and keeping only the power cycle of interest for further PD analysis. A benefit is higher Fourier domain resolution for filtering which allows better selectivity when thresholding. The disadvantage of extra computer processing time is not significant on a fast computer.

4.3 WAVELET TRANSFORM

Fourier analysis breaks a signal down into constituent sinusoids of various frequencies. It is a technique for transforming the view of a signal from time-based to frequency-based. However, when transforming to the frequency domain, time information is lost. That is, when looking at the Fourier transform of a signal, it is difficult to tell when a particular event took place. This is suitable for stationary signals, but is not useful for analysing short events such as PD pulses. The time domain may also not be suitable for distinguishing non-stationary signals because these signals may consist of different frequencies, yet overlap in the time domain. An example would be a small, fast pulse appearing at the same time as a larger and longer pulse.

The short time Fourier transform (STFT) maps a signal into a two dimensional function of time and frequency. For a time signal $f(t)$

$$\text{STFT}(t, \omega) = \int f(\tau) \gamma(\tau - t) e^{-i\omega\tau} d\tau \quad (4.9)$$

where ω is the frequency and $\gamma(t)$ has a short time duration and can be considered a window function [108]. This transform provides a representation of signals in time and frequency. However, an increase in time resolution has a corresponding decrease in frequency resolution and vice versa. Also, once a time resolution has been chosen, the frequency resolution is fixed across all frequencies. Many real-world signals consist of long duration, low frequency signals and short duration, high frequency signals. Such a signal could be better described by a transform which has a high frequency and low time resolution at low frequencies, and a low frequency and high time resolution at high frequencies. Here, the STFT is not the most useful tool and the wavelet transform can provide a better description.

The CWT of a signal $f(t)$ is given by

$$\text{CWT}(s, \tau) = \int f(t) \Psi_{s,\tau}^*(t) dt \quad (4.10)$$

where $*$ denotes complex conjugation [108]. Equation 4.10 decomposes $f(t)$ into a set of basis functions using a single basic wavelet $\Psi(t)$, the mother wavelet, by scaling and translation:

$$\Psi_{s,\tau}(t) = \frac{1}{\sqrt{s}} \Psi\left(\frac{t-\tau}{s}\right) dt \quad (4.11)$$

where τ and s are the translation and scale parameters respectively, and the factor $1/\sqrt{s}$ normalises the energy across all scales.

The ICWT is given by

$$f(t) = \iint \text{CWT}(s, \tau) \Psi_{s,\tau}(t) d\tau ds \quad (4.12)$$

A wavelet must satisfy the admissibility condition to be considered a wavelet. A function $\Psi(t)$ satisfying the admissibility condition

$$\int \frac{|\Psi(\omega)|^2}{|\omega|} d\omega < +\infty \quad (4.13)$$

allows the analysis and reconstruction of a signal without loss of information [114]. $\Psi(\omega)$ is the Fourier transform of $\Psi(t)$. Also, the admissibility condition implies that the Fourier transform of $\Psi(t)$ vanishes at the zero frequency, that is

$$|\Psi(\omega)|^2 \Big|_{\omega=0} = 0 \quad (4.14)$$

This means that wavelets must have a bandpass like spectrum. A magnitude of zero at the zero frequency means that the average value of the wavelet in the time domain must be zero, and therefore it must be oscillatory in nature.

The choice of wavelet depends on the application. For the PDDS, recognition of PD pulses is the relevant application. For a given signal, the optimum wavelet maximises the coefficient values of the signal within the time-scale domain [95]. Unfortunately, the waveshape of any PD pulse is unknown in advance. In general, PD pulses have been shown to have a damped, exponentially decaying shape. Some pulses have a limited oscillation due to the distortions that a PD pulse undergoes while travelling through a transformer winding. The optimum wavelet should maximise the correlation between the relevant PD pulse signal and the wavelet [95]. This can be considered a form of pattern detection. The second order Daubechies wavelet (db2) has been found suitable for damped exponential pulses [95], and is used in the PDDS. The db2 wavelet is shown in Figure 4.10.

Theoretically, the CWT is calculated at all scales and translations, generating much redundant information. In order to perform the CWT on a digital computer and to remove much of the redundancy, Equation 4.11 must be discretised as follows [115]:

$$\Psi_{j,k}(t) = \frac{1}{\sqrt{s_0^j}} \Psi \left(\frac{t - k\tau_0 s_0^j}{s_0^j} \right) \quad (4.15)$$

In general, j and k are integers and $s_0 > 1$. The effect of discretising the wavelet is that the time-scale space is now sampled at discrete intervals. Here, $s_0=2$ is chosen so

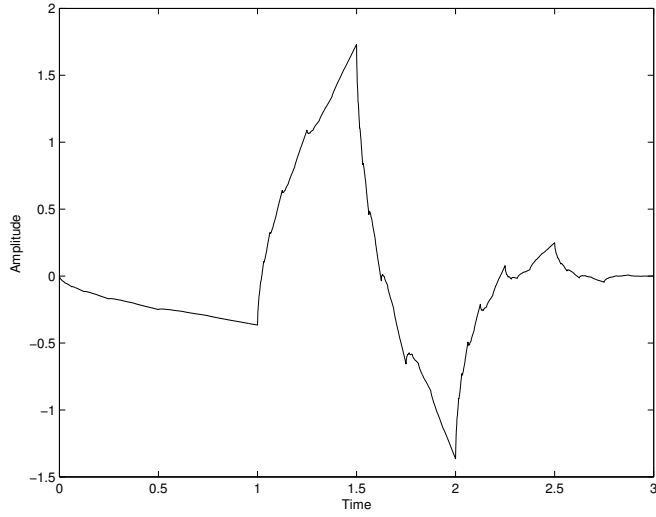


Figure 4.10 Daubechies 2 wavelet (db2).

that the sampling of the scale axis corresponds to dyadic sampling. τ_0 is chosen to be 1.

For signal reconstruction or synthesis from CWT coefficients, the necessary and sufficient condition for stable reconstruction is that the energy of the wavelet coefficients must lie between two positive bounds, that is:

$$A\|f\|^2 \leq \sum_{j,k} |\langle f, \Psi_{j,k} \rangle|^2 \leq B\|f\|^2 \quad (4.16)$$

where $\|f\|^2$ is the energy of $f(t)$, $A > 0$, $B < \infty$ and A and B are independent of $f(t)$ [115].

An arbitrary signal can be reconstructed by summing the orthogonal wavelet basis functions, weighted by the wavelet transform coefficients [114]:

$$f(t) = \sum_{j,k} CWT(j, k)\Psi_{j,k}(t) \quad (4.17)$$

The db2 wavelet is orthogonal and therefore suitable for use in signal reconstruction.

4.3.1 Why not the discrete wavelet transform (DWT)?

Another common form of wavelet analysis is known as the discrete wavelet transform (DWT). This is not the same as the discretised CWT. The DWT decomposes a signal into orthogonal approximation and detail coefficients. DWT analysis ensures space-saving coding and is sufficient for exact reconstruction. However, perfect reconstruction of signals is not required for the PDDS, especially as wavelet coefficients are being

modified to reduce noise, as detailed in the next section.

The CWT, even when not calculated at all scales as in the discretised CWT, is often easier to interpret than the DWT since its redundancy tends to reinforce subtle traits and makes all information more visible. The analysis gains in ‘readability’ and in ease of interpretation but loses in terms of saving data space. PD pulses are often hidden by a range of noise signals, and identification of the pulses is of primary importance. Therefore, the compromise of extra computer processing time when using the CWT is reasonable in exchange for better detection of PD pulses.

4.4 CONTINUOUS WAVELET DIRECTIONAL COUPLING FILTER (CWDCF)

To determine whether a pulse is travelling to or from the transformer when passing electrically through a bushing or tap, analysis of the current and voltage pulse waveforms is performed. By comparing the polarities of the measured components, a differentiation of the pulse direction is possible (see Section 2.5.7). Thus, interference pulses, which result from outside the examined transformer, can be well distinguished from PD pulses, which have their origin inside the transformer [80].

A simple method for determining the direction of a pulse is the multiplication of discrete samples of the current waveform $i(t)$ and voltage waveform $v(t)$:

$$c(t) = i(t)v(t) \quad (4.18)$$

The way the PDDS is configured, this results in a function $c(t)$ where positive values represent internal transformer signals and negative values represent external signals, as shown in Figure 4.11. In this situation, the current transducer is connected so as to produce a positive amplitude pulse when a pulse travelling from the direction of the transformer produces a positive amplitude pulse at the voltage transducer.

In an on-line environment, pulses from sources such as machinery can have longer time constants, that is, longer rise and fall times. Such pulses can also occur when a signal has travelled a long distance from an external source and the high frequency components of the travelling wave have been attenuated. Because these signals are non-stationary, they may pass through the FDTF with insignificant change. If these pulses have a significant magnitude and occur at the same time as an internal PD pulse, then the current and voltage waveform multiplication technique can fail, as shown in Figure 4.12. In (c), the first pulse which is the internal pulse to be detected no longer registers as positive.

To improve the discrimination of PD and external pulses, the CWT of the current waveform $i(s, t)$ and voltage waveform $v(s, t)$ is calculated, and then the discrete

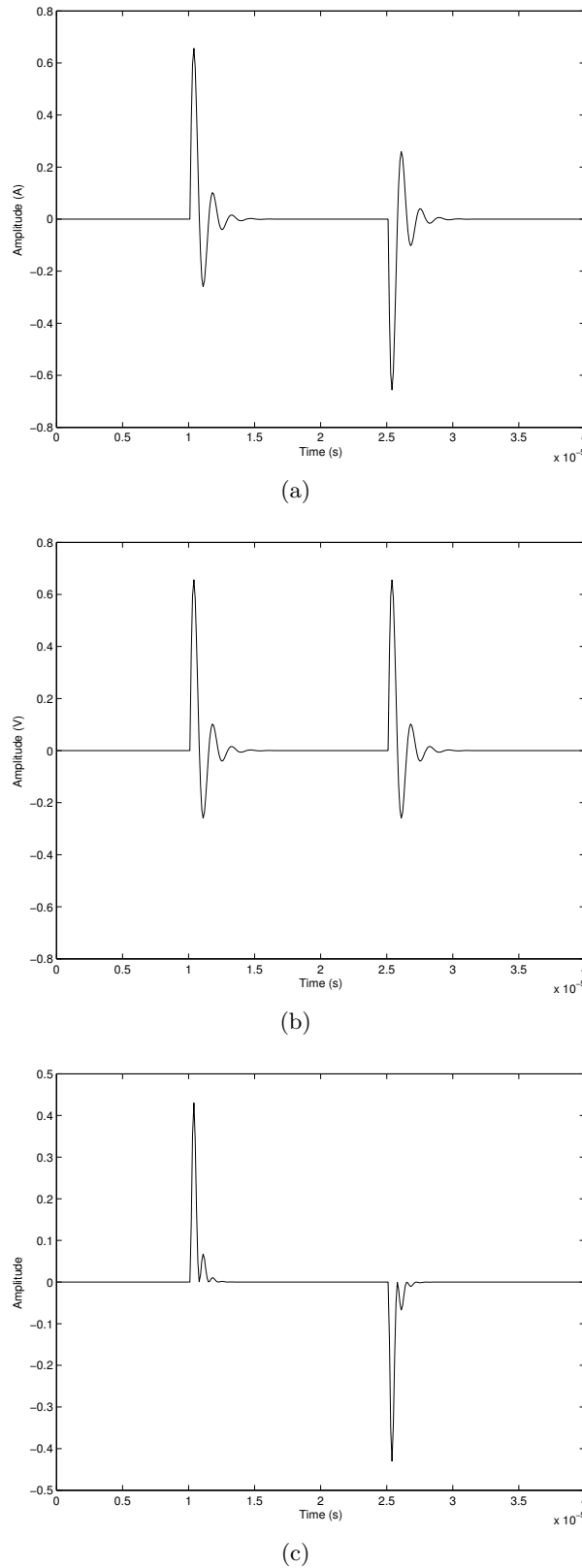


Figure 4.11 Simulated internal pulse followed by an external pulse: (a) current, (b) voltage and (c) multiplication.

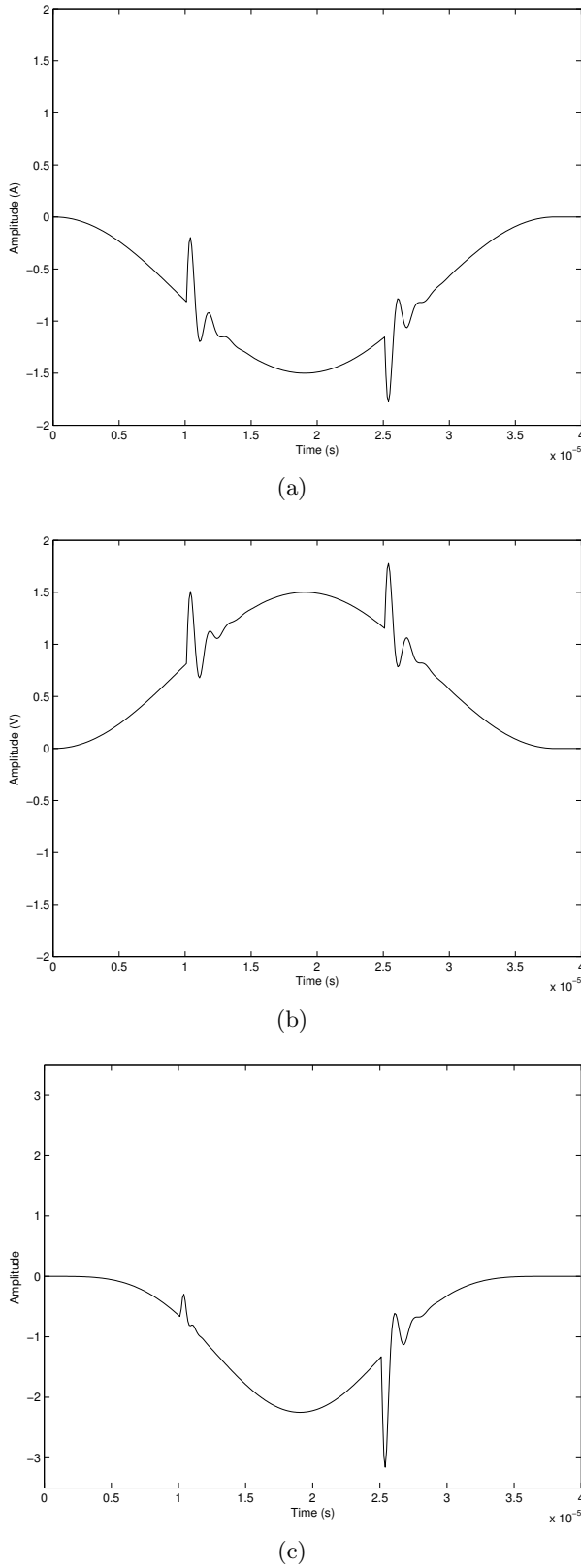


Figure 4.12 Simulated internal pulse followed by an external pulse with an overlapping lower frequency external pulse: (a) current, (b) voltage and (c) multiplication.

samples of the two transforms are multiplied together as follows:

$$d(s, t) = i(s, t)v(s, t) \quad (4.19)$$

The non-stationary signals with lower frequency content are now separated from PD pulses on the scale axis, as shown in Figure 4.13. Moreover, a PD pulse consists of a mix of frequencies that also get separated. In the $d(s, t)$ form, each frequency or scale band of the pulse can be analysed separately when determining pulse direction.

Overall, the CWT only needs to be computed for a limited range of scales that contain PD pulse signal energy. Further, when looking for internal pulse signals in $d(s, t)$, only a subset of computed values needs to be searched for obvious internal signals, as PD pulses often have a dominant component frequency after passing through the transducers and analog filters.

To make a decision about whether a signal is internal to the transformer, that is, whether the coefficients of $d(s, t)$ are positive, a hard threshold k_{int} is applied to all coefficients in $d(s, t)$. The default value of the threshold is chosen manually. A suitable value can be found when calibration pulses are being injected, as detailed in Section 5.2. A threshold that is too high will miss small internal signals, whereas a low threshold will allow spurious interference in $d(s, t)$ to register as confirmed internal signals. The use of calibration pulses before a test transformer is energised provides a source of known pulses for determining a value of k_{int} that is large enough to avoid interference, as only the calibration pulses should be present in the output. For identifying external signals, a second threshold k_{ext} is created, where $k_{\text{ext}} = -k_{\text{int}}$.

A problem that occurs when thresholding $d(s, t)$ for internal pulses is that pulse oscillations in the current and voltage waveforms may be slightly out of phase. The result of this is that a pulse may cause localised peaks on the positive and negative side of $d(s, t)$, as shown in Figure 4.14. Peaks on both sides, if sufficiently large, would lead to the signal being classified as both internal and external.

To prevent the possibility that a single pulse is classified as both internal and external, each hard threshold becomes a function of scale and time, $l_{\text{int}}(s, t)$ and $l_{\text{ext}}(s, t)$, set at k_{int} and k_{ext} and then varied according to coefficient magnitudes on the opposite side of $d(s, t)$. The ‘false’ peak in $d(s, t)$ due to current and voltage waveforms being out of phase will be smaller in general than the peak on the opposite side, and therefore will not exceed the modified threshold coefficients. The internal threshold function $l_{\text{int}}(s, t)$ is set as follows:

$$l_{\text{int}}(s, t) = \begin{cases} k_{\text{int}} & \text{if } d(s, t) \geq k_{\text{ext}} \\ -d(s, t) & \text{if } d(s, t) < k_{\text{ext}} \end{cases} \quad (4.20)$$

A small ‘buffer’ region of several coefficients in both the scale and time directions

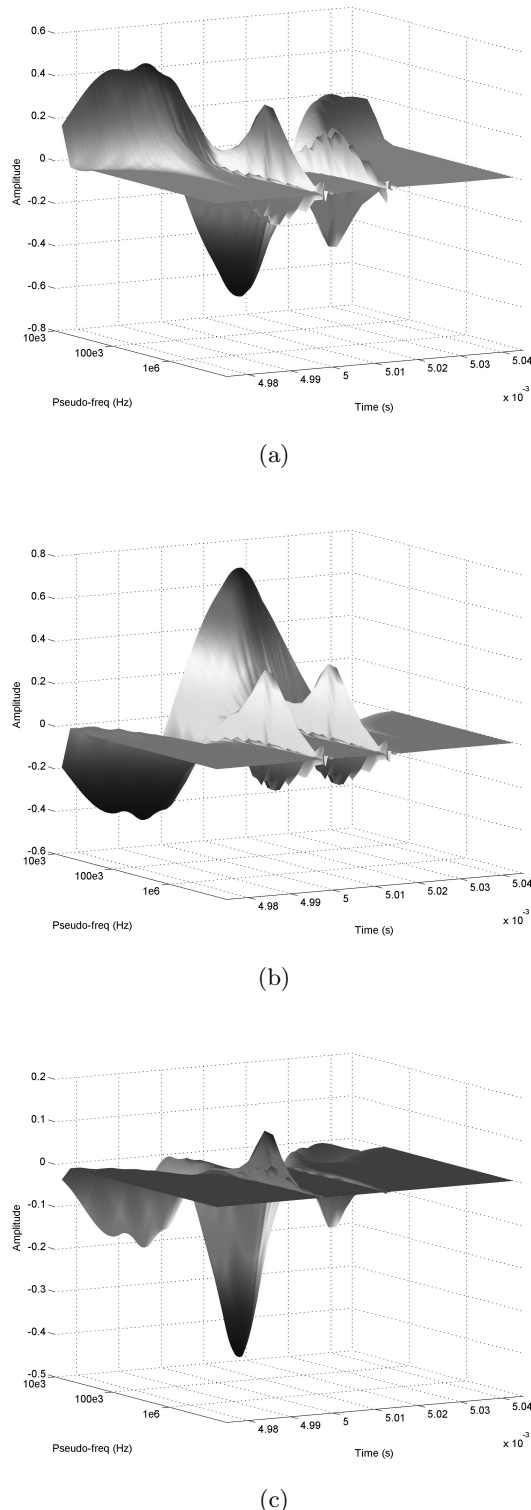


Figure 4.13 Simulated internal pulse followed by an external pulse with an overlapping lower frequency external pulse: (a) CWT of current, (b) CWT of voltage, and (c) multiplication of (a) and (b).

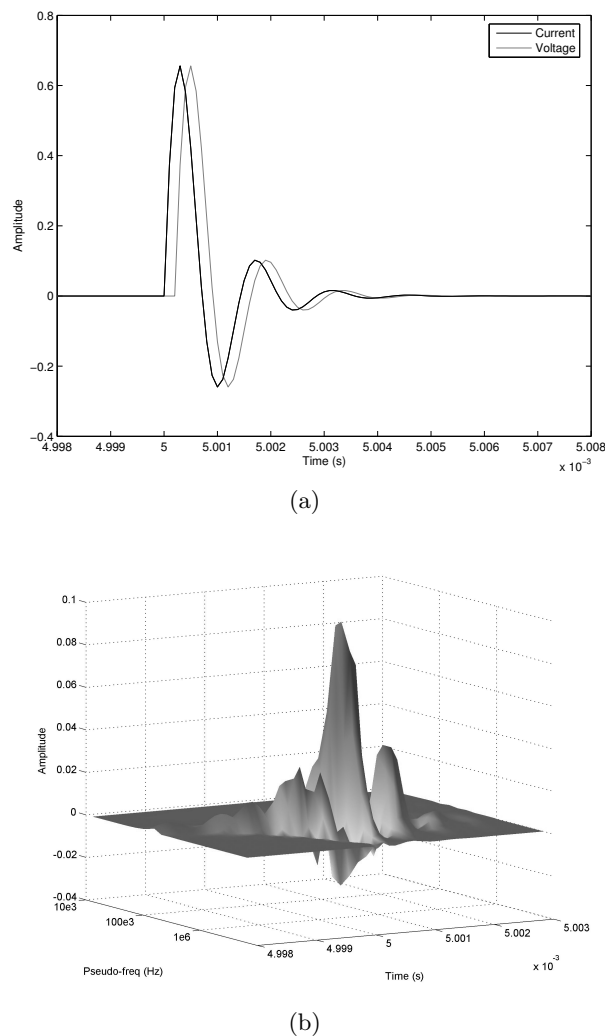


Figure 4.14 Simulated internal pulse where the current and voltage waveforms are slightly out of phase: (a) current and voltage and (b) multiplication of CWT of current and CWT of voltage.

is created around each $l_{\text{int}}(s, t)$ coefficient that is modified to $-d(s, t)$. If one of these surrounding coefficients has a lower value, it is raised to the value of the modified coefficient. This has been found to prevent errors in recognition by including some neighbour coefficients that are often just beneath the threshold.

After the internal threshold function $l_{\text{int}}(s, t)$ is created, a binary decision is made for each coefficient in $d(s, t)$ determining whether it is an internal signal:

$$b_{\text{int}}(s, t) = \begin{cases} 1 & \text{if } d(s, t) \geq l_{\text{int}}(s, t) \\ 0 & \text{if } d(s, t) < l_{\text{int}}(s, t) \end{cases} \quad (4.21)$$

A pulse that is detected as being internal by exceeding $l_{\text{int}}(s, t)$ may actually be a pulse that is generated external to the transformer, but has passed through the transformer from another bushing. Detected internal signals that have actually passed through the transformer will have been larger when entering externally, and therefore will be detected and classified as external at that channel. Therefore, all external signals also have to be identified as follows to provide a reference for comparisons with other channels:

$$l_{\text{ext}}(s, t) = \begin{cases} k_{\text{ext}} & \text{if } d(s, t) \leq k_{\text{int}} \\ -d(s, t) & \text{if } d(s, t) > k_{\text{int}} \end{cases} \quad (4.22)$$

$$b_{\text{ext}}(s, t) = \begin{cases} 1 & \text{if } d(s, t) \leq l_{\text{ext}}(s, t) \\ 0 & \text{if } d(s, t) > l_{\text{ext}}(s, t) \end{cases} \quad (4.23)$$

Again, a small ‘buffer’ region is created around changed threshold values by extending the changed value to surrounding coefficients.

To determine whether a signal that has been classified as internal, represented as $b_{\text{int}}(s, t) = 1$, has external signals that are at a similar time and scale on other channels, represented as $b_{\text{ext}}(s, t) = 1$ for that channel, the following comparison is made:

$$h(s, t)_z = b_{\text{int}}(s, t)_z - \sum_y b_{\text{ext}}(s, t)_y \quad (4.24)$$

where $z = 1..N$, $y = 1..N$ excluding z , and N is the number of channels. Any coefficients in $h(s, t)$ of each channel that equal 1 have now been shown to have no equivalent external signal at any other transformer tap. All other coefficients in $h(s, t)$ that are equal to 0 or less are set to 0.

The information contained in $h(s, t)$ is used to select coefficients in $i(s, t)$ and $v(s, t)$ for each channel for time domain signal reconstruction purposes. However, internal signals have nearby coefficients in $i(s, t)$ and $v(s, t)$ that are part of the internal signal, but are just beneath the threshold and are therefore not included. This is typically at the start and the end of the internal signal where it rises and falls. To recreate the original pulse signal as closely as possible, extra coefficients in $h(s, t)$ of each channel

are classified as internal by creating a ‘buffer’ region of several coefficients around each coefficient that already equals 1. However, if the value of the equivalent coefficient in $d(s, t)$ is a significantly large negative value, for instance, part of a nearby large external pulse, unwanted signals may be present in the CWDCF output. Therefore, only $d(s, t)$ coefficients that have values greater than an arbitrary value, chosen to be $-k_{\text{int}}$, are included in the buffer region. Figure 4.15(a) shows a section of Figure 4.13(c). Here, the coefficients that have been determined to be part of an internal signal are a lighter colour and represent the region where $h(s, t) = 1$.

The coefficients identified as being internal signals are selected in $i(s, t)$ and $v(s, t)$ as follows:

$$i_{\text{PD}}(s, t) = b_{\text{int}}(s, t)i(s, t) \quad (4.25)$$

$$v_{\text{PD}}(s, t) = b_{\text{int}}(s, t)v(s, t) \quad (4.26)$$

where $i_{\text{PD}}(s, t)$ and $v_{\text{PD}}(s, t)$ are current and voltage time domain signals containing only pulses that have originated from within the transformer. Figure 4.15(b,c) shows sections of Figure 4.13(a,b). Here, the coefficients that have been determined to be part of an internal signal are a lighter colour and represent the region where $h(s, t) = 1$.

The ICWT, as detailed in Section 4.3, is applied to $i_{\text{PD}}(s, t)$ and $v_{\text{PD}}(s, t)$ to achieve a time domain current and voltage signal for each channel that consists of only internal PD pulses with intact waveshapes. Figure 4.16 shows the current and voltage outputs of the CWDCF with a comparison to the original signals in Figure 4.12.

4.5 CLUSTER NEURAL NETWORK (CNN)

In order to differentiate PD pulses travelling from potentially multiple source locations within the transformer, a CNN is used. A CNN can separate inputs into logical groups without prior knowledge about the criteria for grouping [116]. In the case of the PDDS, the waveshapes of all identified PD pulses are used as inputs for the CNN.

Neural networks consist of simple elements working together in parallel. Parts of the human brain are examples of biological neural networks. The connections between the elements of a neural network create the functions of the network. The network can be trained to perform a certain function by modifying the values, or weights, of connections. A typical example of training a network is altering the weights of connections so that a certain input will result in a certain output. A common method of training such a network, known as supervised training, is shown in Figure 4.17. The initial output of the network is compared with a target and the weights are adjusted accordingly. Often many pairs of known inputs and outputs are presented to the network. Eventually, the network’s weights will be adjusted so that new inputs will be correctly classified to an output.

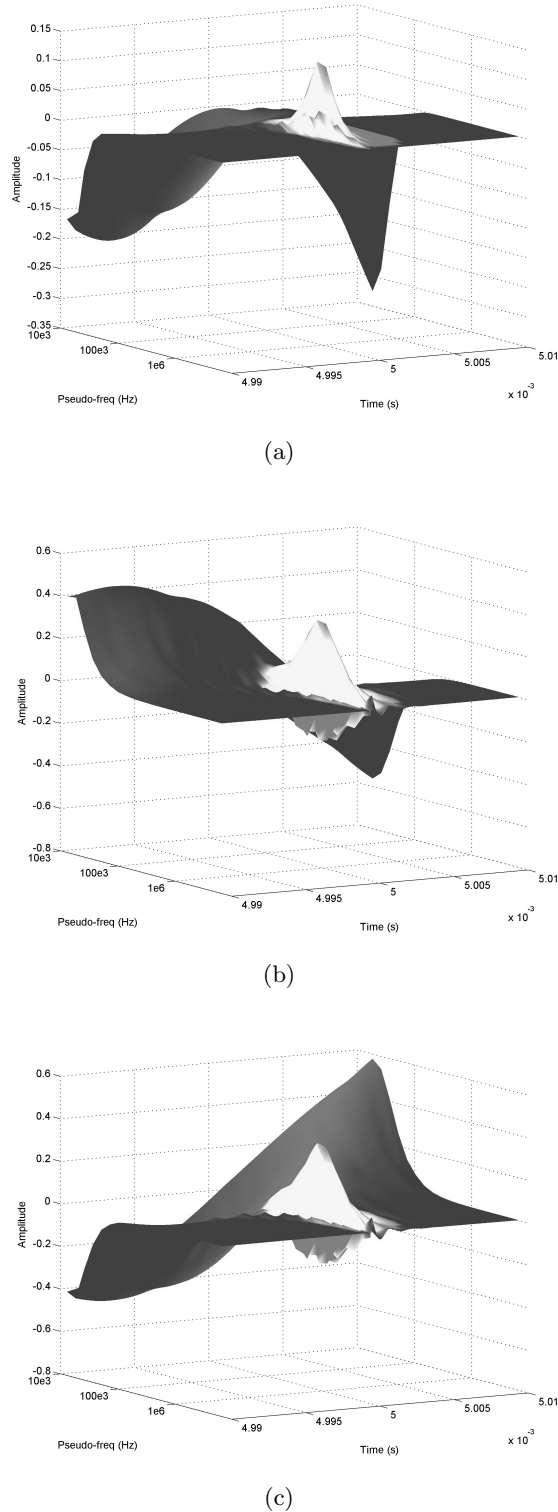


Figure 4.15 Simulated internal pulse with an overlapping lower frequency external pulse: (a) section of Figure 4.13(c) showing the multiplication of CWT of current and CWT of voltage where light coloured coefficients represent where $h(s, t) = 1$, (b) section of Figure 4.13(a) showing the CWT of current $i(s, t)$ where light coloured coefficients represent where $h(s, t) = 1$, and (c) section of Figure 4.13(b) showing the CWT of voltage $v(s, t)$ where light coloured coefficients represent where $h(s, t) = 1$.

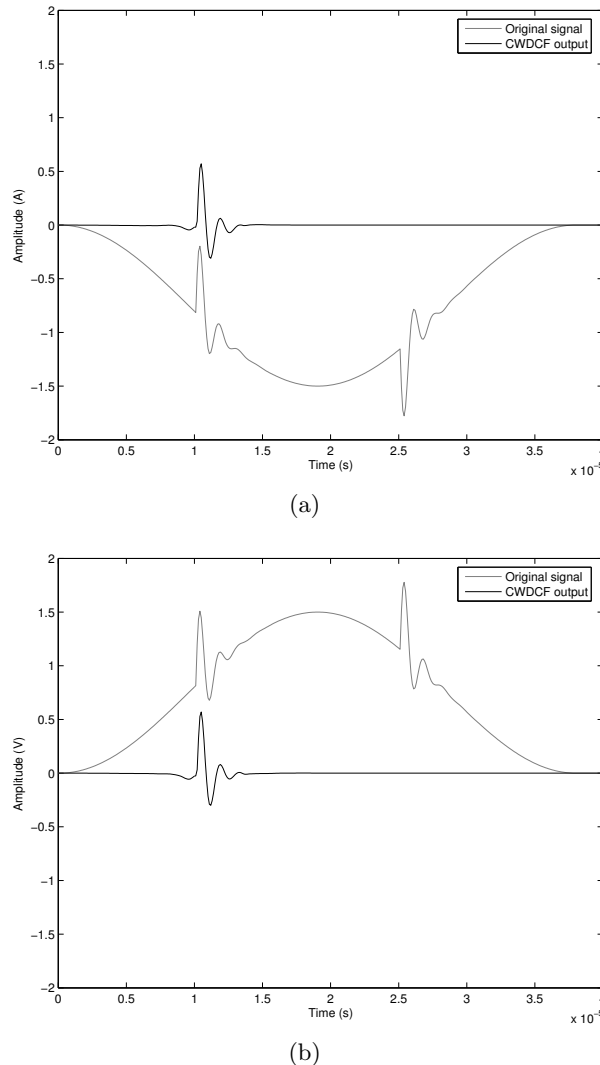


Figure 4.16 Simulated internal pulse followed by an external pulse with an overlapping lower frequency external pulse: (a) original current signal and CWDCF output signal, and (b) original voltage signal and CWDCF output signal.

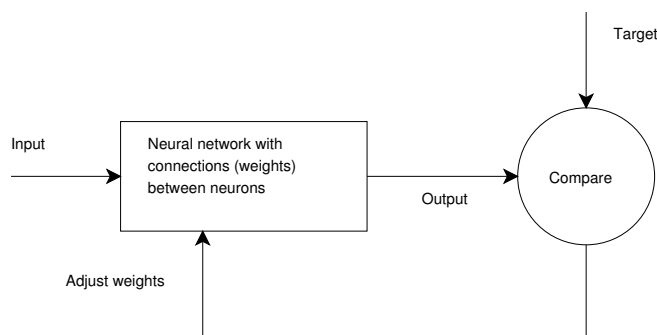


Figure 4.17 Supervised training of a neural network.

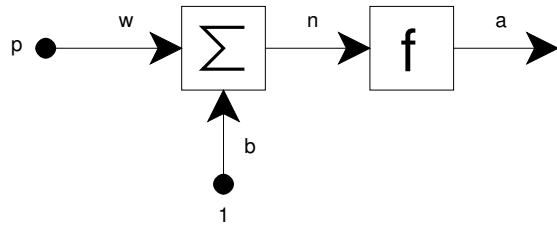


Figure 4.18 Neuron with a single scalar input.

The basic element of the neural network is the neuron, which is shown in Figure 4.18. A scalar input p is multiplied by a scalar weight w and is modified by a bias b . The result is the argument n of a function f that produces a scalar output a . Examples of common functions are a linear, sigmoid or step function. The weights and biases can be adjusted according to rules, in order to make the neuron exhibit a desired behaviour. The generalised expression for this basic single neuron is:

$$a = f(wp + b) \quad (4.27)$$

Multiple neurons in parallel, as shown in Figure 4.19, in multiple layers and with different functions can mimic complex systems. The expression for the network in Figure 4.19 is:

$$\mathbf{a} = \mathbf{f}(\mathbf{w}\mathbf{p} + \mathbf{b}) \quad (4.28)$$

where bold-type variables represent vectors.

In the case of the PDDS, the inputs of the CNN are the waveshape samples of the PD pulses from Ch1-V-HF and the outputs are the source location group to which a PD pulse belongs. However, in the situation where the PDDS is monitoring an operating and unopened transformer, the outputs are not known in advance.

In this case, another type of neural network, the self-organising network, can be used. This family of neural networks can learn and detect patterns and correlations in presented inputs and adjust their weights so that future outputs will be similar to future similar inputs. A basic form of the self-organising network is the competitive network whose neurons learn to recognise groups of similar input vectors, such as the waveshape of a pulse.

A competitive network has an architecture shown in Figure 4.20. The number of neurons is equal to the number of groups that the input data is to be collected into, and each weight vector is equal in length to the input vector. The ‘distance’ box calculates a vector that is the negative of the distance between the input vector and weight vector. Biases are added to the result and form the input to the competitive transfer function. Therefore, the maximum value of n is 0. This occurs when, for any neuron, the input

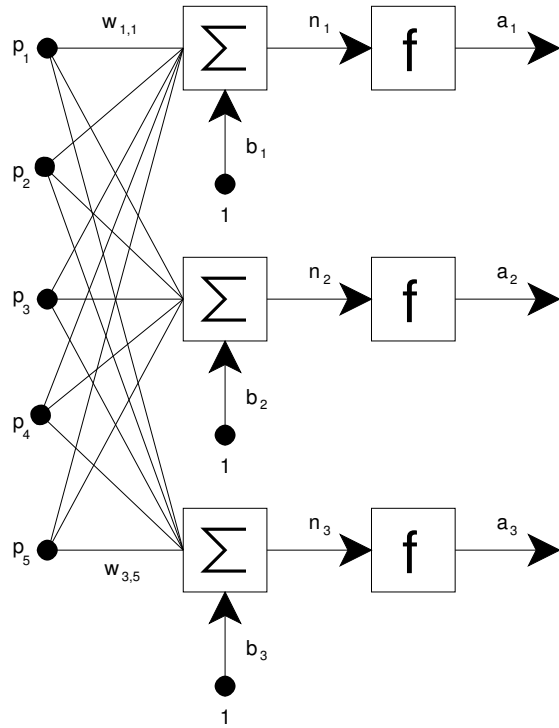


Figure 4.19 A network of three neurons with five scalar inputs.

vector is equal to the weight vector and the bias vector is also zero.

The competitive transfer function accepts multiple inputs from the summation nodes in each neuron and outputs a 0 for all neurons except one winning neuron, for which the function outputs a 1. The winner is decided by which value of n is the closest to 0. If the biases are all vectors consisting of zeros, then the neuron whose weight vector is closest to the input vector has the least negative net input and will win the competition in the transfer function to output a 1.

To make it more likely that the winning neuron will win again when the same or similar input is given, the weights of the winning neuron are adjusted using the Kohonen learning rule:

$$\mathbf{w}_{\text{new}} = \mathbf{w}_{\text{old}} + \alpha(\mathbf{p}_{\text{new}} - \mathbf{w}_{\text{old}}) \quad (4.29)$$

where α is a constant that adjusts the learning rate. This learning rule allows the winning neuron to update its weights so that its results are closer to the input vector. Hence, this neuron is more likely to win again next time the same or a similar input is made, and it is less likely to win if a radically different input vector is made.

After many inputs are given, each group of similar inputs will have at least one neuron centred in the group. Therefore, when a previously unseen input is presented, the neuron whose weights are most similar to the group the input belongs in will output a 1 and all other neurons will output a 0.

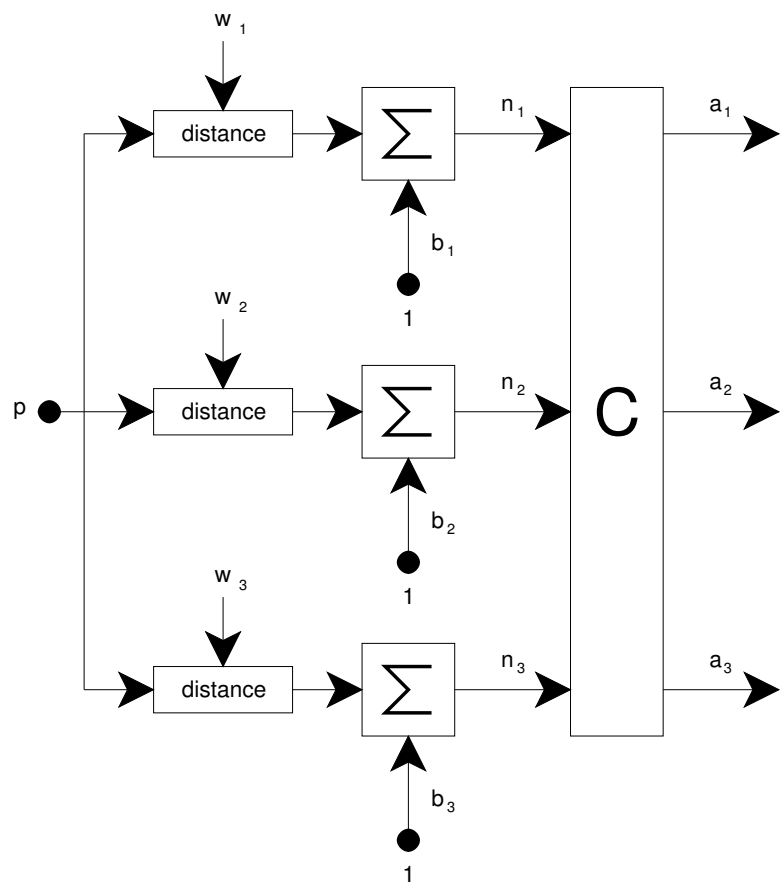


Figure 4.20 A competitive network of three neurons with a vector input consisting of multiple scalars.

Some neurons may not ever win the competition while training of the network is performed. As a result, they do not learn any input vectors and are considered to be dead neurons. To allow them to learn about a group of inputs, the bias that feeds into each losing neuron is positively adjusted so that they are more likely to win the competition next time an input is presented. The bias values are adjusted with the Conscience Bias learning rule:

$$\mathbf{b}_{\text{new}} = e^{(1-\log(\mathbf{d}))} - \mathbf{b}_{\text{old}} \quad (4.30)$$

$$\mathbf{d} = (1 - r)\mathbf{c} + r\mathbf{a} \quad (4.31)$$

$$\mathbf{c} = e^{(1-\log(\mathbf{b}_{\text{old}}))} \quad (4.32)$$

where \mathbf{b} is the bias vector and r is the bias vector adjustment rate constant. The bias tends to decrease to 0 once a neuron is winning consistently when centred in a group of inputs. Equations 4.32 to 4.30 force each neuron to classify approximately the same number of input vectors. This allows areas of input space that have a dense number of input vectors to attract more neurons for better classifying and subdividing of this area.

4.6 PULSE SOURCE GROUPING

Once pulses have been recognised and confirmed as originating from within the transformer using the previous signal processing stages, CNN analysis can be performed to determine if the pulses are being generated by one, two or even more source locations. This can be done without any prior knowledge of the internal construction or electrical response of the transformer. By identifying from which source each individual PD pulse came, further analysis of source characteristics can be performed, such as the production of a plot that shows average pulse height, power cycle phase timing and total number of pulses for each source, known as PRPDA.

The transformer winding can be modelled as a complicated series of distributed inductances, capacitances and resistances [51]. Pulses generated at different sources within the transformer will travel through different combinations of distributed inductances, capacitances and resistances, and hence will be modified in a unique way when viewed at an external transformer tap. The PDDS determines the source group of each pulse by the waveshape of the individual pulse.

It is unknown what the waveshape of a transformer PD pulse will be in advance. However, as the location of the pulse source does not change significantly over time, the unique waveshape will be consistent for each pulse normalised in magnitude. The waveshapes of PD pulses are submitted to the CNN for separation into logical groups.

Differences in the waveshape of pulses from different locations has been found to be

most significant at higher frequencies [107]. The bandwidth of the main PDDS channels is not wide enough to significantly capture these higher frequencies. Therefore, a single high frequency sub-channel Ch1-V-HF is used to capture the relevant frequencies at a sample rate of 50MSa/s. The voltage channel on one of the HV bushings is used, as the voltage signal has a better transducer SNR and it is expected that any internal PDs that occur will be generated within the HV winding. Additional high frequency channels could be used, but this would increase the cost and complexity of the PDDS.

The signal captured from the Ch1-V-HF channel is passed through the FDTF as shown in Figure 4.1. The CWT of the channel is then computed because it provides additional information about the waveshape of any internal PD pulses present. These additional scale and time details provide the CNN with more information for the differentiation of pulses that travel from different sources. The sections of the Ch1-V-HF CWT that show a PD pulse are presented as inputs to the CNN.

The following steps are performed with the CNN in order to create suitable input vectors, train the network and classify the source of each PD pulse:

- A single PD pulse is identified in the output of the CWDCF by looking in Ch1-V for non-zero values that have multiple zeros on its border, which represents a PD pulse. The time and maximum amplitude of this pulse is logged.
- In the CWT of the Ch1-V-HF channel, the coefficient with the maximum amplitude is identified that is within the same time frame as the previously found PD pulse in Ch1-V. Pulses presented to the CNN must be consistent in time. That is, waveshape features of pulses from a single group must be in an identical location in the presented input vector. The CWT coefficient in Ch1-V-HF with the maximum amplitude is used to synchronise or align input vectors. Pulse waveshapes in the CWT waveform will be different when they are generated at different locations within the transformer, but with the maximum coefficient value centred in the input vector, surrounding coefficients will also align with the coefficients of similar input vectors. This process is repeated for all logged pulses from the previous step.
- A CNN is set up with an excessive number of neurons, that is, more neurons than expected internal PD sources. Training of the network using pulses from multiple power cycles is performed. The use of pulses from several power cycles ensures that pulses from all source locations are likely to be presented.
- At the final stage, pulses that were used to train the network and additional pulses from further power cycles are presented to the CNN. The neuron in the CNN that is trained to recognise a particular pulse outputs a 1. This information is logged so that all pulses that have a similar result can be grouped.

The Matlab Neural Network Toolbox provides functions for creating, training and running a CNN. Functions for the Kohonen learning rule and Conscience Bias learning rule are also provided in Matlab.

While input vectors are being presented, each neuron's weights are gradually moving towards a group of similar pulses. It is useful to know when the network is satisfactorily trained, that is, when the weights of all neurons have changed from their initial values and have settled to a final set of values that represent the shape of PD pulses from a common source. After this point, insignificant minor adjustments in the weights will continue while the network is being trained because pulses from the same location will still have slight variations in waveshape that cause the weights to shift slightly.

In order to monitor the training of a neuron's weights, the sum of the differences in weight values is calculated every epoch or at a fixed rate of epochs as follows:

$$w_{\text{change}}(n) = \sum_{i=1}^I (w_i(n) - w_i(n-1)) \quad n = 2, 3, \dots, N \quad (4.33)$$

where i is the index of the weight vector, I is the length of the weight vector, n is the epoch and N is an arbitrary total number of training epochs. When the neuron has settled to represent a group of input vectors, $w_{\text{change}}(n)$ will remain relatively constant.

If there is more than one group of input vectors, at least one neuron will represent each group as long as there are more neurons than input vector groups. To provide an indication if two neurons represent the same group or different groups, the sum of the difference of the weights between the two neurons is calculated as follows:

$$w_{\text{diff}} = \sum_{i=1}^I (w_i(1) - w_i(2)) \quad (4.34)$$

This is a relative measurement that can only be compared to the difference of weights between other pairs of neurons. If each group of input vectors has several neurons, then lower values of w_{diff} will be observed for pairs of neurons in the same group compared to a pair of neurons in different groups. The CNN results for similar neurons can then be combined.

4.7 CONCLUSIONS

The signal processing algorithms used in the PDDS have been described in this chapter, including an overview of the steps for detecting PD pulses and the number of PD sources, the FDTF that removes narrowband interference, the CWDCF that distinguishes PD pulses from other pulses, and the CNN which determines the number of

active PD sources. The ability to assign a recorded PD pulse to a particular PD source allows PRPDA for each PD source.

As the signal processing algorithms and testing software have been implemented in Matlab, there is flexibility in modification and upgrades to the ability of the PDDS to detect PDs. The algorithms could also be implemented in other software platforms.

The performance of the algorithms is described in Chapter 5 in a series of three tests on pole distribution transformers in which the algorithms try to distinguish PD pulses from amongst heavy electrical interference signals.

Chapter 5

RESULTS

The purpose of this chapter is to present results from tests that were designed to determine the accuracy of the PDDS in detecting internal transformer PDs while subject to external electrical interference, and to also present results from an on-line test. Two identically constructed transformers were used. The first transformer Tx1 was used for off-line testing and has been internally modified as described in the first section. In the second section, results are presented from two sets of artificial interference and internal PD conditions that form tests 1 and 2. The third section illustrates the PDDS in test 3 where it was monitoring the second transformer Tx2. This transformer was energised and was subject to external coronal interferences generated by spark gap instruments and other sources. Lastly, a summary of the results is presented.

5.1 TEST TRANSFORMER CONSTRUCTION AND MODIFICATION

The PDDS considers any transformer to be a ‘black box’ when under observation, both off-line and on-line. This has the twin advantages of not requiring knowledge of the internal construction or repair state of the transformer, and not requiring the transformer to be opened for placement of transducers. However, knowledge of the internal construction of the transformer Tx1, including where the artificial PD pulses are injected in a physical and electrical sense, provides insights as to the performance of the PDDS.

Two identically constructed transformers were used for testing the PDDS. The first transformer Tx1 has been modified in order to allow artificial PD signals to be injected into the windings of the transformer coil. As this modification compromised the integrity of the insulation, transformer Tx1 is not able to be energised. In addition, dangerously high currents would pass through the relatively low resistance of the artificial PD signal generators. However, to simulate an on-line external environment, artificial narrowband and pulse interference was generated and conducted to Tx1 at the bushings. The second transformer Tx2 is unmodified and was used for on-line tests.

Table 5.1 Nameplate information of transformers Tx1 and Tx2.

KVA	7.5
Volts HV	11000
Volts LV	240
Amps HV	0.682
Amps LV	31.2
Phase	1
Periods	50

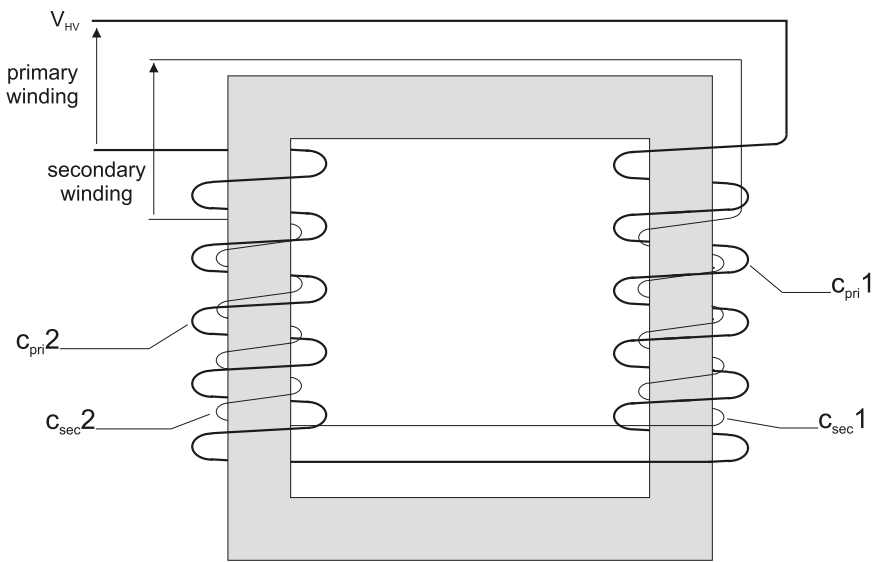
**Figure 5.1** Coil winding arrangement of transformers Tx1 and Tx2.

Table 5.1 presents the information stamped on both of the transformers' nameplates.

Both transformers use a core-type construction with the primary HV winding wound over the top of the secondary winding. Both the primary and secondary windings are divided into two coils that are wound on opposite sides of a square core and connected in series, as shown in Figure 5.1.

A winding construction method consisting of alternate layers of copper winding and paper was used for the primary winding coils, c_{pri1} and c_{pri2} . The layered winding arrangement for the beginning of c_{pri1} is shown in Figure 5.2. Connections were made into the primary winding of Tx1 by tapping off of c_{pri1} at a number of strategic locations. Tapping was performed by cutting away the paper insulation and stripping back the wire insulation from points such as A, B, and C in Figure 5.2 and soldering a length of transformer winding wire to the exposed winding point [107]. The placement of each tap point along with the number of layers of paper insulation between the tap points is illustrated in Figure 5.3. Tap points are labelled T, M, and B to indicate that they have been taken from the top, middle and bottom of c_{pri1} respectively.

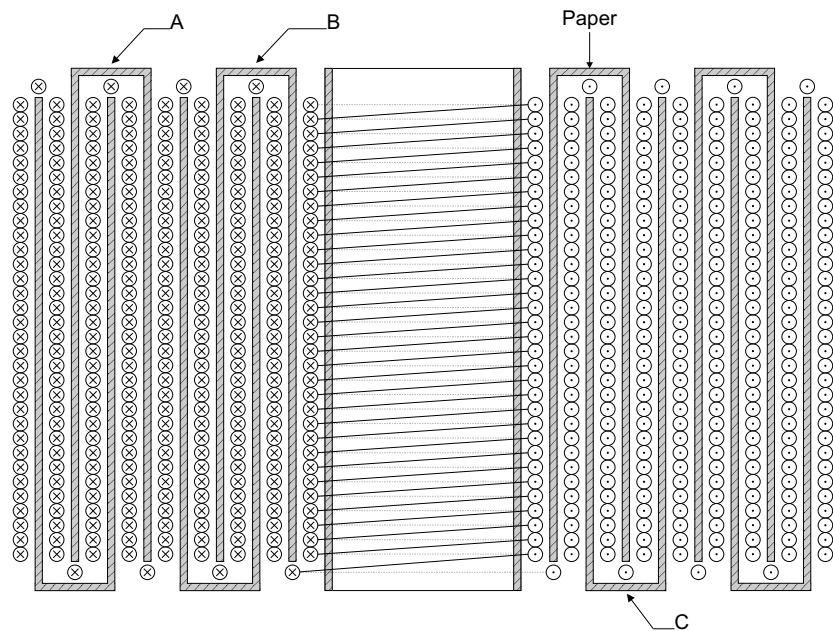


Figure 5.2 Layered winding of c_{pri1} .

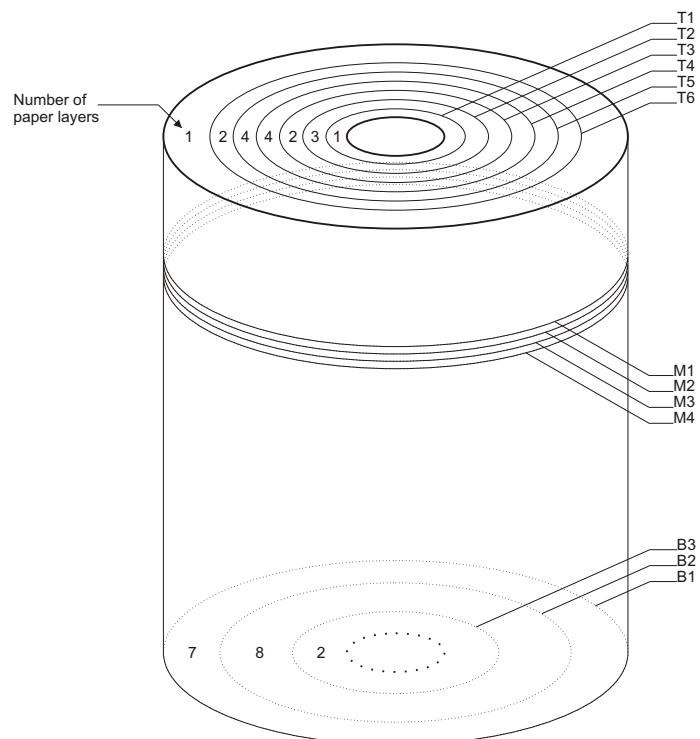


Figure 5.3 Placement of winding taps for introduction of artificial PDs.

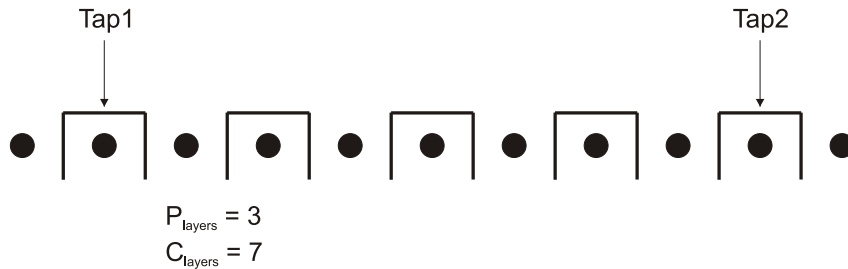


Figure 5.4 Copper and paper layers.

Table 5.2 DC resistances from tap point to HV terminal of $c_{\text{pri}1}$.

Tap point	Resistance to V_{HV} (Ω)	Tap point	Resistance to V_{HV} (Ω)
T1	96.8	M4	2.4
T2	84.9	B1	6.6
T3	73.1	B2	42.2
T4	48.5	B3	90.7
T5	22.8	Tap 1	5.6
T6	13.3	Tap 2	11.1
M1	2.3	Tap 3	193.1
M2	2.3	Tap 4	198.6
M3	2.4	Tap 5	204.3

The number of copper layers is calculated from the number of paper layers as follows:

$$C_{\text{layers}} = P_{\text{layers}} + (P_{\text{layers}} + 1) \quad (5.1)$$

where C_{layers} and P_{layers} represent the number of copper layers and paper layers respectively. Equation 5.1 is readily verified with reference to Figure 5.4, showing the number of copper layers between two sample tap points.

From Figure 5.3, the total number of paper layers for $c_{\text{pri}1}$ is 17. Therefore, from Equation 5.1, the total number of layers of copper is 35. The number of turns on the outer layer is 205, allowing the total number of turns for the primary winding to be calculated as follows:

$$205(\text{turns}/\text{layer}) \times 35(\text{layers}/\text{coil}) \times 2(\text{coils}/\text{winding}) = 14350(\text{turns}/\text{winding}) \quad (5.2)$$

The proximity of each tap point to the HV end of coil $c_{\text{pri}1}$ was determined by measuring the DC resistance between the two points. These resistances have been measured using a Wheatstone bridge and are presented in Table 5.2 [107]. The total winding resistance is 204.4Ω . The tap points labelled 'Tap 1' to 'Tap 5' were placed in by the transformer manufacturer.

5.2 ARTIFICIAL PD DETECTION RESULTS

To effectively provide useful information about any PD sources within an arbitrary transformer, confidence in PDDS results is required. Reporting PD where there is none, or failing to recognise obvious internal PDs renders the PDDS untrustworthy. However, there are potentially many scenarios in which the PDDS could be used, with large variations in internal PD and interference levels and quantities. It would not be practical to test the PDDS for all of these possibilities within this project. Also, the PDDS has multiple stages of processing which creates further variations of potential scenarios.

For initial practical reliability testing of the PDDS, two artificial scenarios were created in the attempt to simulate typical real-world situations. This involved a simple scenario and a second more complex scenario. Each of these scenarios had differing levels of internal transformer PDs and external interference. Rather than generating real PDs, it was acceptable for tests to use pulse generators described in Section 3.2 to simulate PDs, as the PDDS detects internal transformer pulses irrespective of wave-shape and source type. The effectiveness of the PDDS was determined by how well it recognised internal PDs and rejected external interference, after all signal processing stages were completed.

Figure 5.5 shows the arrangement for the PDDS reliability testing and Figure A.3 in Appendix A shows a photo of the setup. Only two channels were placed on the transformer, on the HV winding bushings, as only two current probes were available for research with the PDDS project. This testing setup allowed the introduction of controlled artificial PDs and interference into the transformer at known amplitudes and times, and was independent of the PDDS acquisition and signal processing. A comparison of PDDS results could then be made to the known internal PD pulses in order to determine PDDS reliability.

Table 5.3 presents the signal parameters for each module of the PDDS and its test equipment. In the first scenario which was the less complex one, some internal PD and interference sources were not used and their outputs were set to zero.

In addition to the artificial interference sources set up in Figure 5.5, lower levels of narrowband and wideband interference were present. These were introduced into the test circuit from local radio stations, electrical machinery and electronic equipment nearby. These interference sources were thought to be coupled conductively through test equipment and radiatively to various exposed wires connected to the transformer. No attempt was made to suppress these interference sources as they contributed to a more rigorous test of the PDDS for successfully detecting PDs. The various interference sources are seen in the time and frequency domains of the acquired signals.

For each of the calibration and test results, the vertical resolution (V/div) of the oscilloscopes was adjusted to ensure maximum dynamic range as follows:

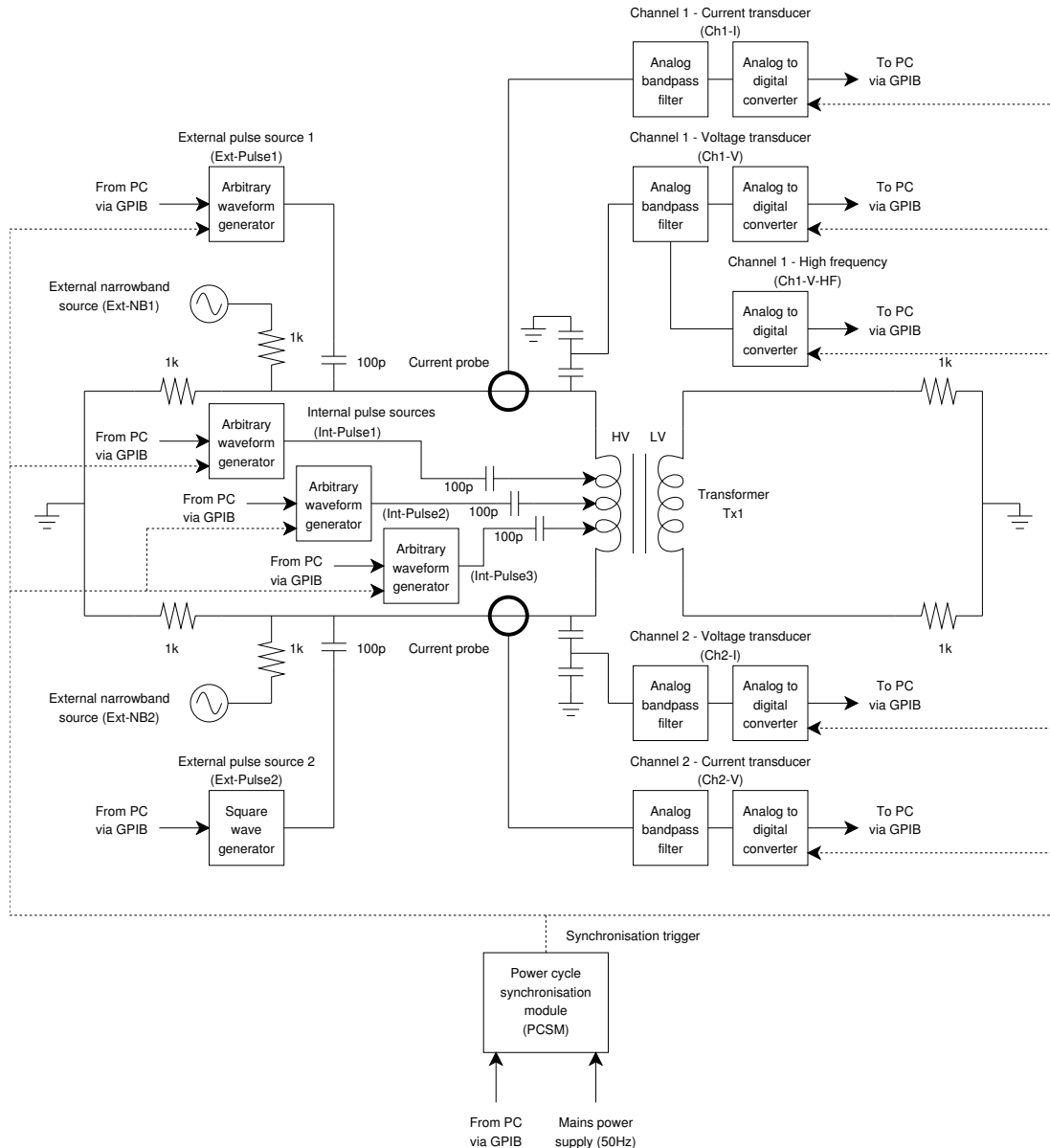


Figure 5.5 Tests 1 and 2 - Artificial PD and interference test setup on transformer Tx1.

Table 5.3 Parameters for artificial PD and interference tests 1 and 2.

Equipment	Test 1	Test 2
Int-Pulse1	10 pulses per power cycle in two groups (1-5ms and 11-15ms), step amplitude 14-20V (1400-2000pC), into tap T3.	50 pulses per power cycle in two groups (1-5ms and 11-15ms), step amplitude 4-20V (400-2000pC), into tap T1.
Int-Pulse2	10 pulses per power cycle in two groups (3-5ms and 13-15ms), step amplitude 16-18V (1600-1800pC), into tap M1.	50 pulses per power cycle in two groups (1-5ms and 11-15ms), step amplitude 4-20V (400-2000pC), into tap M1.
Int-Pulse3	Not used.	20 pulses per power cycle in two groups (3-5ms and 13-15ms), step amplitude 4-10V (400-1000pC), into tap T6.
Ext-Pulse1	20 pulses per power cycle in two groups (0-6ms and 10-16ms), step amplitude 8-20V (800-2000pC).	80 pulses per power cycle in two groups (0.5-8ms and 10.5-18ms), step amplitude 1-10V (100-1000pC).
Ext-Pulse2	Not used.	32.4 pulses per power cycle, step amplitude 10V (1000pC).
Ext-NB1	Sine wave at 113kHz, 300mV _{p-p} .	Sine wave at 113kHz, 1V _{p-p} , with 50% amplitude modulation of 5kHz triangular wave.
Ext-NB2	Not used.	Sine wave at 430kHz, 500mV _{p-p} .
Oscilloscope settings	Ch1-I, Ch1-V, Ch2-I and Ch2-V at 10MSa/s. Ch1-V-HF at 50MSa/s.	Ch1-I, Ch1-V, Ch2-I and Ch2-V at 10MSa/s. Ch1-V-HF at 50MSa/s.

- ‘Peak detect’ and ‘Screen storage’ modes were selected on the oscilloscopes to capture and display the highest amplitude values of the input signals.
- The oscilloscope screen was watched for a period of time, typically 2 minutes (6000 power cycles) to observe any signal that went beyond the top or bottom of the screen, and was therefore ‘clipped’ by the oscilloscope ADC.
- The vertical resolution was set when the input signal maximised the dynamic range of the oscilloscope screen without being ‘clipped’.

5.2.1 Calibration

Imprecision in the transducers’ measured electrical characteristics, especially the voltage transducers, makes it difficult to determine actual amplitudes of PD pulses from acquired signals. Scaling factors z_i and z_v that relate transformer bushing current and voltage pulse amplitudes to the digitised signals is needed to calculate PD amplitude results in millamps (mA), millivolts (mV) or, more commonly in PD measurements, in pico-coulombs (pC). However, the amplitude at the transformer bushings does not equal the amplitude of the internal PD at its source because the pulses are deformed as they propagate through the transformer windings and they are also affected by the external electrical circuit. As explained in Section 3.2, the common technique in PD measurement is to measure the ‘apparent’ amplitude. This is the amplitude that, when injected at the terminals of the test object, would give the same reading as the PD pulse itself [12].

Current standards [12, 89] provide relevant recommendations for the calibration of PD detection instruments. The suggested method is to inject a known charge at the transformer bushings, created by a generator producing step voltage pulses of amplitude U_0 connected in series with a capacitor C_0 . The calibration pulses q_0 are repetitive charges, measured in coulombs, each of the magnitude

$$q_0 = U_0 C_0 \quad (5.3)$$

Other recommendations from the standards for calibration include [12, 89]:

- Where the calibration capacitor C_0 is to be removed after calibration, C_0 should not be larger than $0.1C_t$, where C_t is the equivalent terminal capacitance of the transformer under test. A method for determining C_t is provided in the standards [89].
- The generated voltage steps should have a frequency spectrum whose upper limit is higher than any apparent PD pulses measured and also higher than the upper frequency limit of the transducer and analog filter. A rise-time (10% to 90%) less

than $0.03/f_h$ is suggested, where f_h is the upper frequency response limit of the transducer and analog filter.

- The external electrical circuit connected to the transformer under test should not be altered between calibration and testing.

Using the method for determining C_t provided in the standards [89], the equivalent terminal capacitance C_t at the HV bushings of Tx1 was found to be approximately 300pF. From this, the calibration capacitor C_0 is chosen to be 27pF. An Agilent 33250A arbitrary waveform generator is used to provide a voltage step and is sufficiently fast to satisfy the previous requirement, having a specified risetime of less than 8ns. A series of step pulses, as shown in Figure 5.6, was programmed into the calibration signal generator. The 20 levels of step pulses are 20V, 19V, ..., 1V, which, from Equation 5.3, corresponds to 540pC, 513pC, ..., 27pC. The calibration signal is injected so as to simulate internal pulses.

Figures 5.7 and 5.8 show the current and voltage signals from each monitored transformer bushing, after the FDTF and CWDCF were applied. These are the stages that were later also applied to the test data for internal PD pulse signal processing, as described in the following sections. The goal of performing the FDTF and the CWDCF on the recorded calibration signal was to remove any extraneous interference coupled into the transformer electrical circuit from sources such as radio stations, so that internal pulse amplitudes were notable after the FDTF and CWDCF stages. This maintains consistency so that pulse peak amplitudes in calibrations and tests are comparable, that is, so that the magnitudes of detected pulses in a test can be inferred from the ‘apparent’ magnitudes in the calibration.

The CWDCF threshold k_{int} was set to a very low relative level to ensure all calibration pulses were passed through. A few random pulses also shown as internal pulses are a result of the low threshold not being discriminatory enough. In Section 5.2.3, the threshold value was varied to determine which threshold value best shows internal PD pulses correctly and removes external interference pulses, given that the calibration pulses should be the only pulses present at the output of the CWDCF stage. The threshold value also indicates the sensitivity level of the PDDS, where calibration pulses that are present without false positives confirm that internal pulse discrimination to that level is achievable.

5.2.2 Narrowband interference rejection using the FDTF

The effect of applying the FDTF to signals covering a single power cycle (20ms) is presented for tests 1 and 2 in this section. Key parameters in the application of the FDTF to the signals are given in Table 5.4. The signal parameters used for the generation of the artificial PD pulses and interference are presented in Table 5.3.

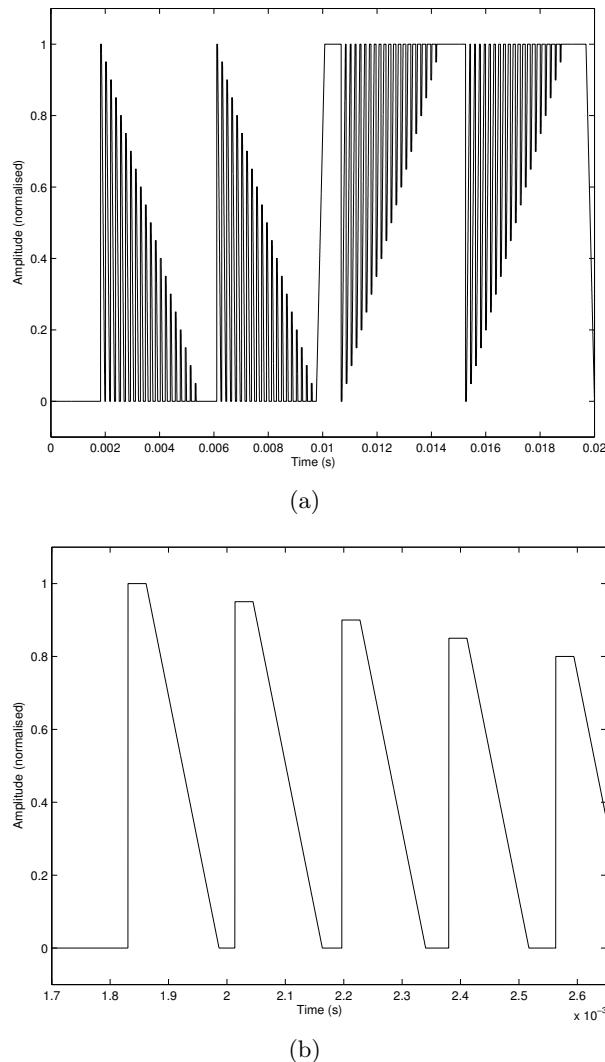


Figure 5.6 (a) Waveform programmed into an arbitrary waveform generator that generates a series of calibration pulses of known charge when connected in series with C_0 , and (b) selective zoom of (a).

Table 5.4 Parameters for the application of the FDTF to signals in tests 1, 2 and 3.

Parameter	Ch1-I, Ch1-V Ch2-I, Ch2-V	Ch1-V-HF
Number of bins	500	500
Data points per bin	2000	2000
Frequency range per bin	20kHz	100kHz
Bin median multiplier	10	10

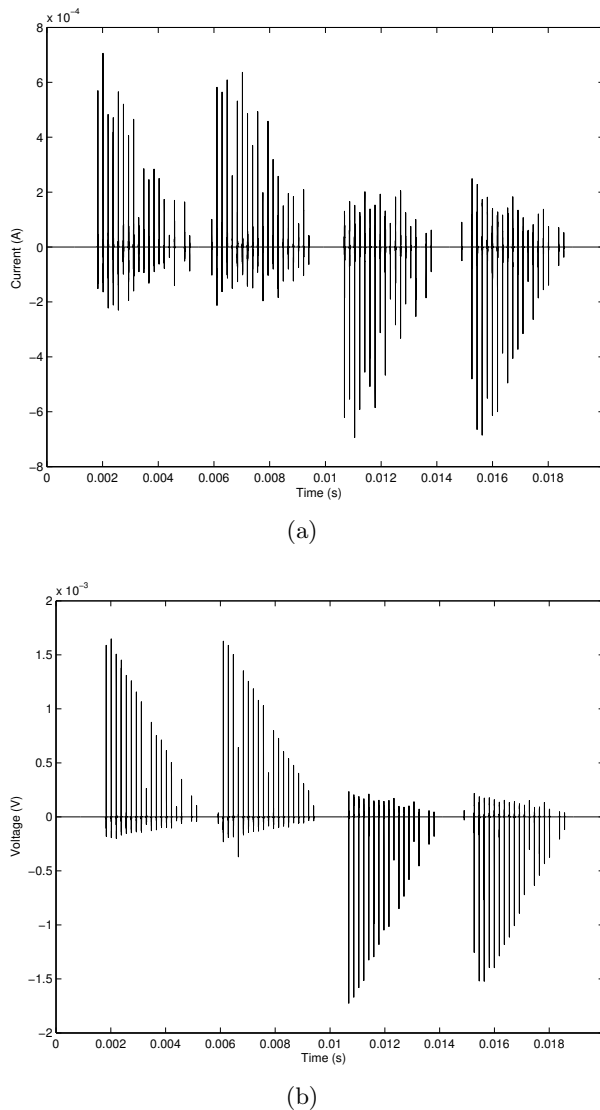


Figure 5.7 Calibration pulses for (a) Ch1-I and (b) Ch1-V after processing through the FDTF and CWDCF stages ($k_{\text{int}} = 2 \times 10^{-8}$). Calibration pulses were applied at the Channel 1 transformer bushing of Tx1.

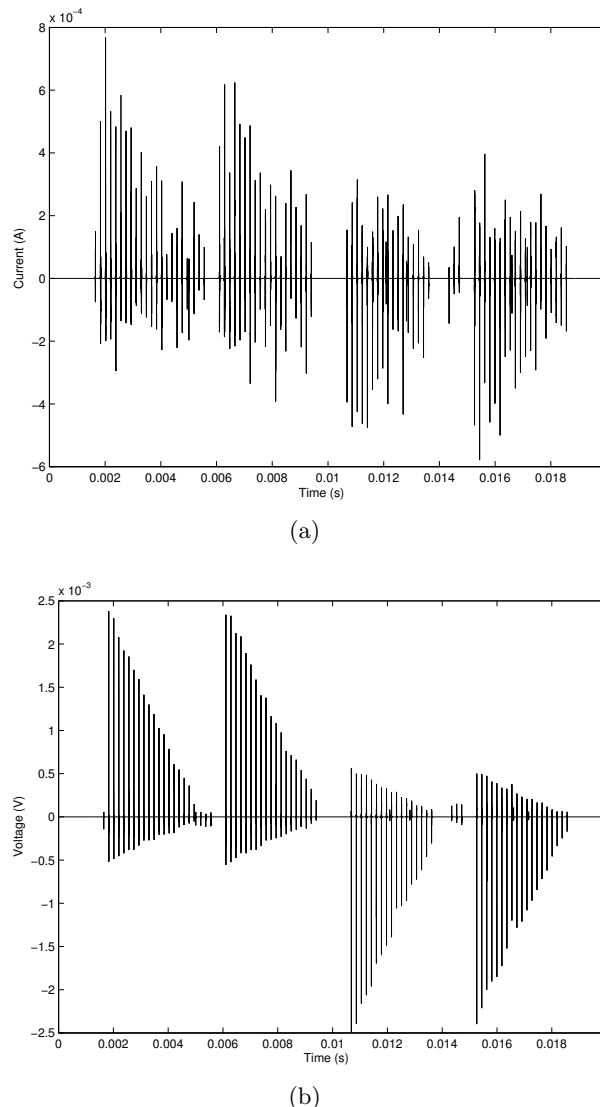


Figure 5.8 Calibration pulses for (a) Ch2-I and (b) Ch2-V after processing through the FDTF and CWDCF stages ($k_{\text{int}} = 4 \times 10^{-8}$). Calibration pulses were applied at the Channel 2 transformer bushing of Tx1.

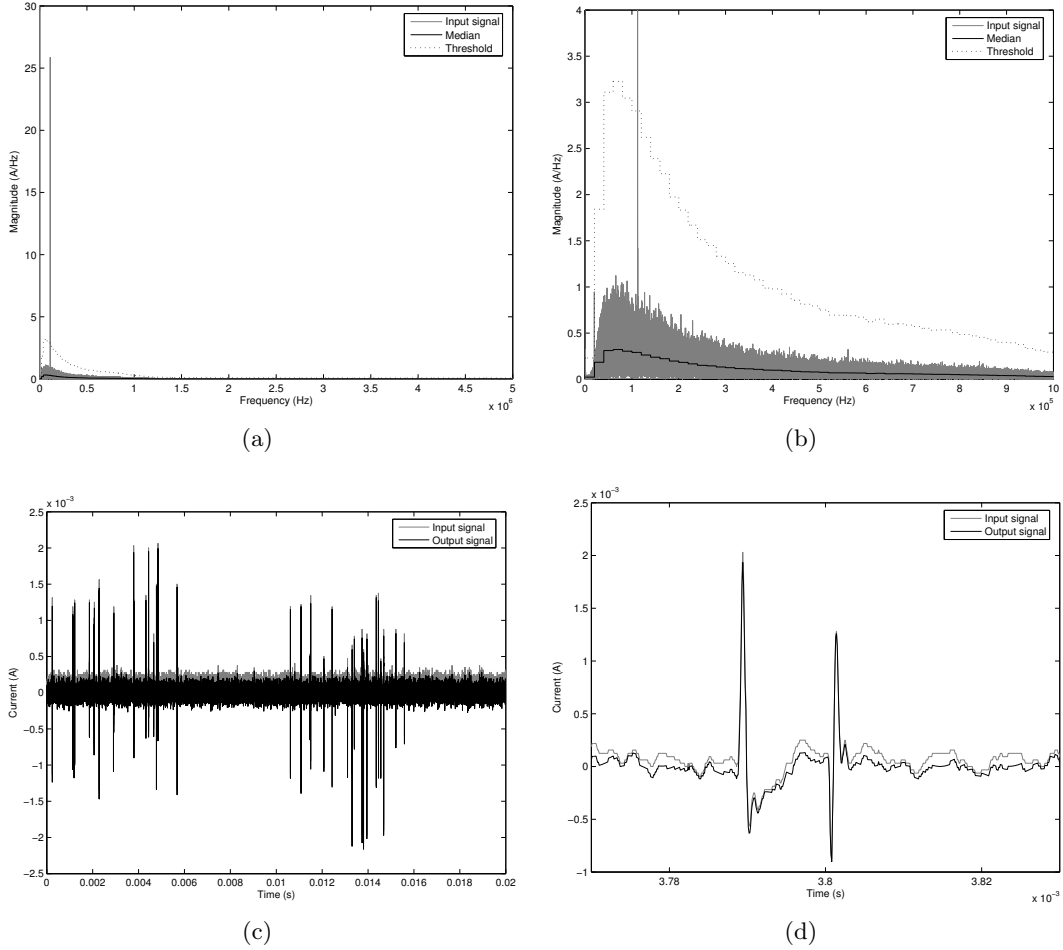


Figure 5.9 Test 1 - Effect of the FDTF for Ch1-I: (a) Frequency spectrum with bin medians and bin thresholds, (b) selective zoom of (a), (c) time domain input and output signals, and (d) selective zoom of (c).

Figures 5.9 to 5.13 show the frequency domain with bin medians and bin thresholds, and time domain input and output signals of test 1 for each of the current and voltage signals. Table 5.5 presents the OIR for each signal, as detailed in Section 4.2.1. Clearly visible in the frequency domain plots of each figure is the injected 113kHz sine wave. In addition, lower magnitude narrowband signals are present in the voltage signals, some of which are known to be local radio stations. These signals are relatively weak and do not produce any significant amplitude in the current signals. However, the narrowband voltage signals cause higher signal power reduction in the OIR results for each of the voltage signals compared to the current signals. Correspondingly, the voltage time domain signals are cleaner. Little visual pulse distortion is observed in sample pulses.

Figures 5.14 to 5.18 show the frequency domain with bin medians and bin thresholds, and time domain input and output signals of test 2 for each of the current and voltage signals. Table 5.6 presents the OIR for each signal. The more complex injected

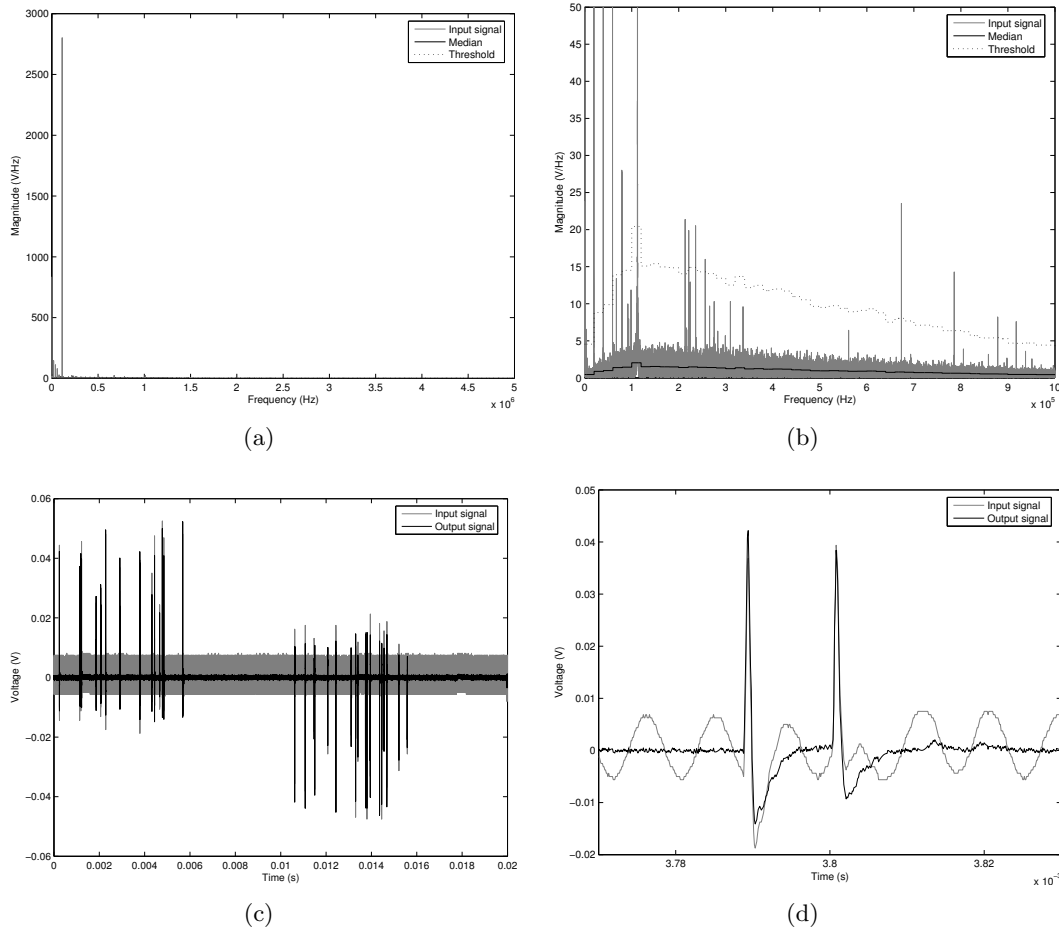


Figure 5.10 Test 1 - Effect of the FDTF for Ch1-V: (a) Frequency spectrum with bin medians and bin thresholds, (b) selective zoom of (a), (c) time domain input and output signals, and (d) selective zoom of (c).

Table 5.5 Test 1 - FDTF output to input signal power ratios (OIRs).

Signal	OIR (dB)
Ch1-I	-3.42
Ch1-V	-16.1
Ch2-I	-0.169
Ch2-V	-8.67
Ch1-V-HF	-8.76

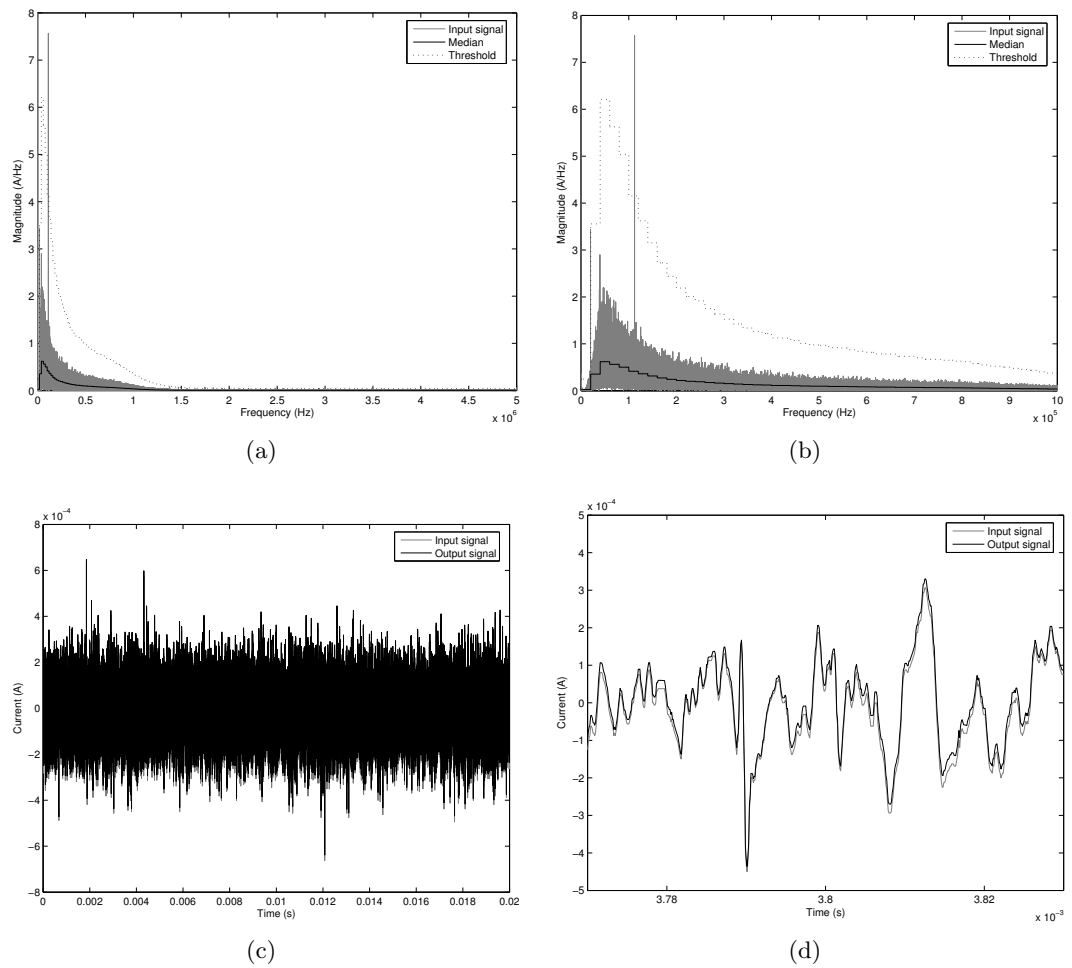


Figure 5.11 Test 1 - Effect of the FDTF for Ch2-I: (a) Frequency spectrum with bin medians and bin thresholds, (b) selective zoom of (a), (c) time domain input and output signals, and (d) selective zoom of (c).

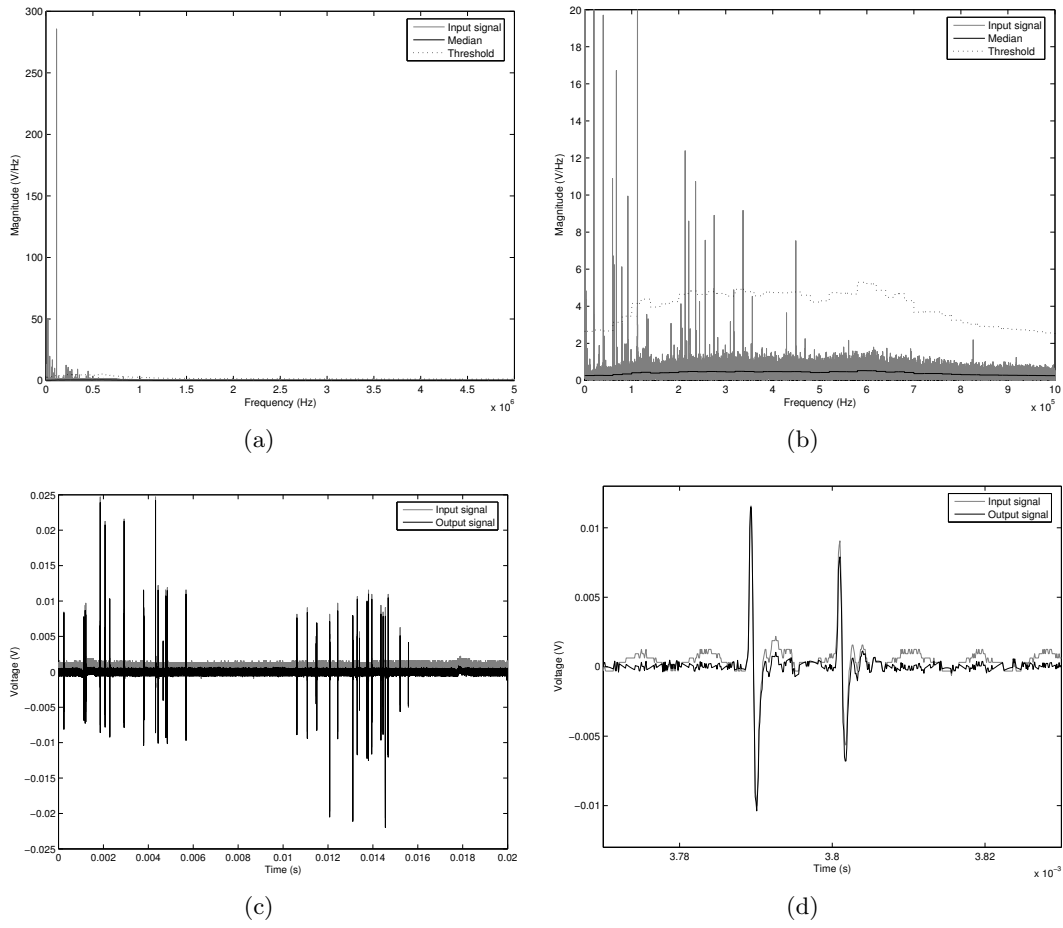


Figure 5.12 Test 1 - Effect of the FDTF for Ch2-V: (a) Frequency spectrum with bin medians and bin thresholds, (b) selective zoom of (a), (c) time domain input and output signals, and (d) selective zoom of (c).

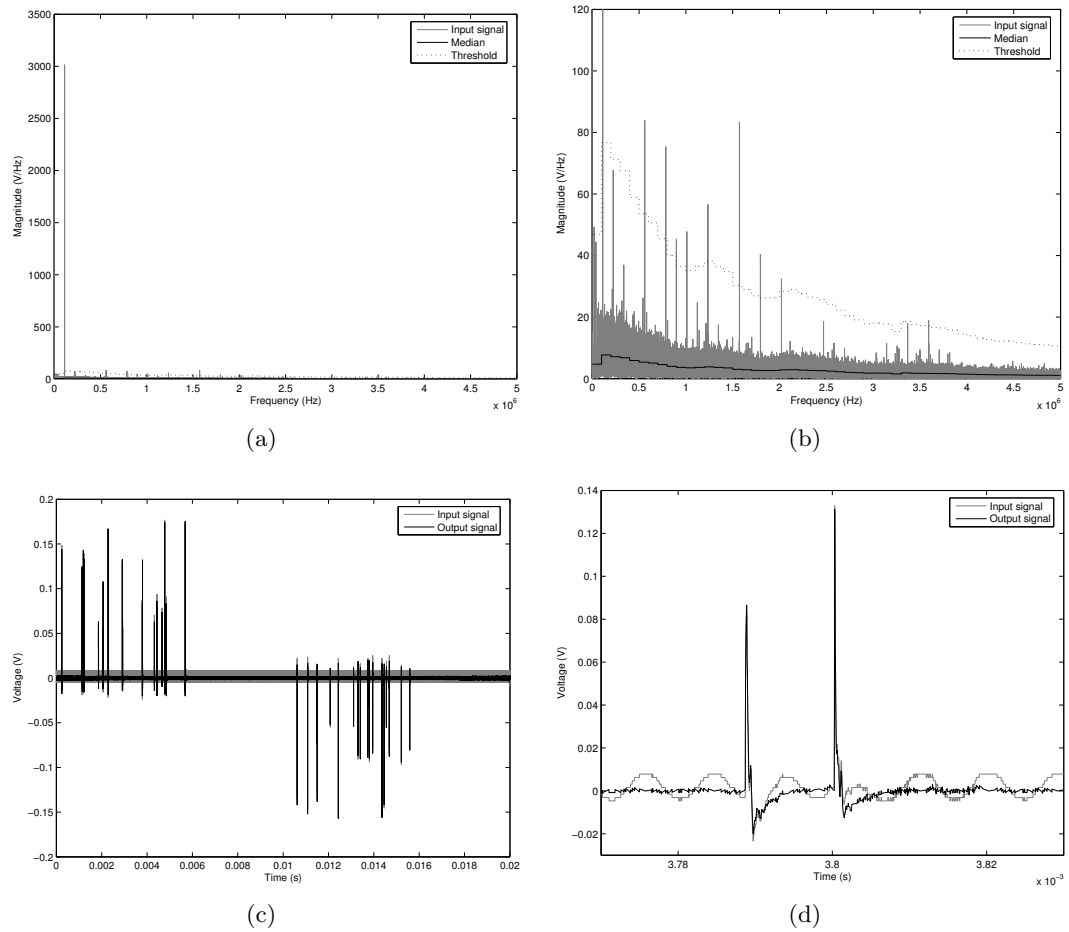


Figure 5.13 Test 1 - Effect of the FDTF for Ch1-V-HF: (a) Frequency spectrum with bin medians and bin thresholds, (b) selective zoom of (a), (c) time domain input and output signals, and (d) selective zoom of (c).

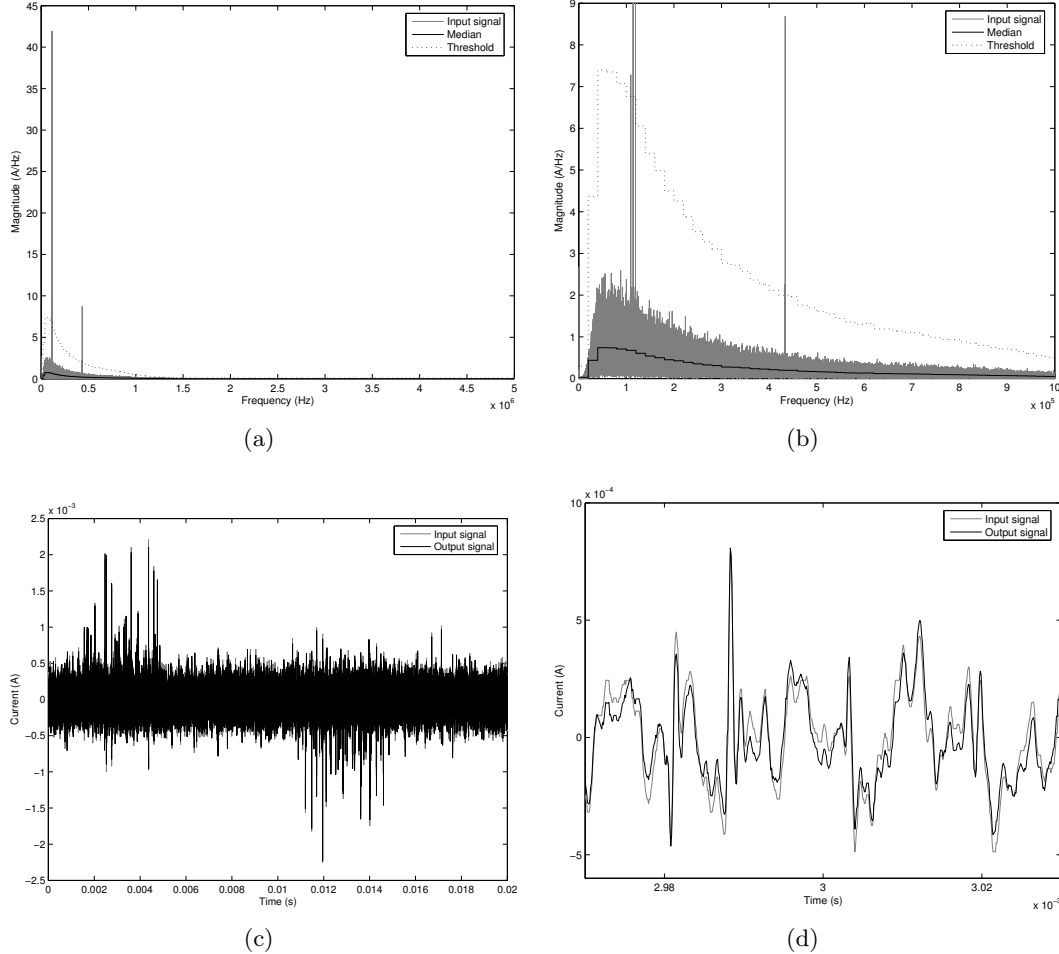


Figure 5.14 Test 2 - Effect of the FDTF for Ch1-I: (a) Frequency spectrum with bin medians and bin thresholds, (b) selective zoom of (a), (c) time domain input and output signals, and (d) selective zoom of (c).

113kHz and 430kHz narrowband signals are dominant in each frequency spectrum. Overall, the PDDS was again able to remove narrowband interference from the test signals satisfactorily, and the voltage signals show a higher signal power reduction, as in test 1.

In Figure 5.17(b), the lower part of the frequency spectrum consists of a large number of closely spaced narrowband peaks, approximately 1600Hz apart. This was expected from the artificial interference pulse source Ext-Pulse2, where the injected pulses are regularly spaced in the time domain. However, the majority of samples in the Fourier domain are within the noise floor, and therefore the threshold attenuates many of these peaks. This is an advantage, as the goal of applying the FDTF was to remove such interference peaks.

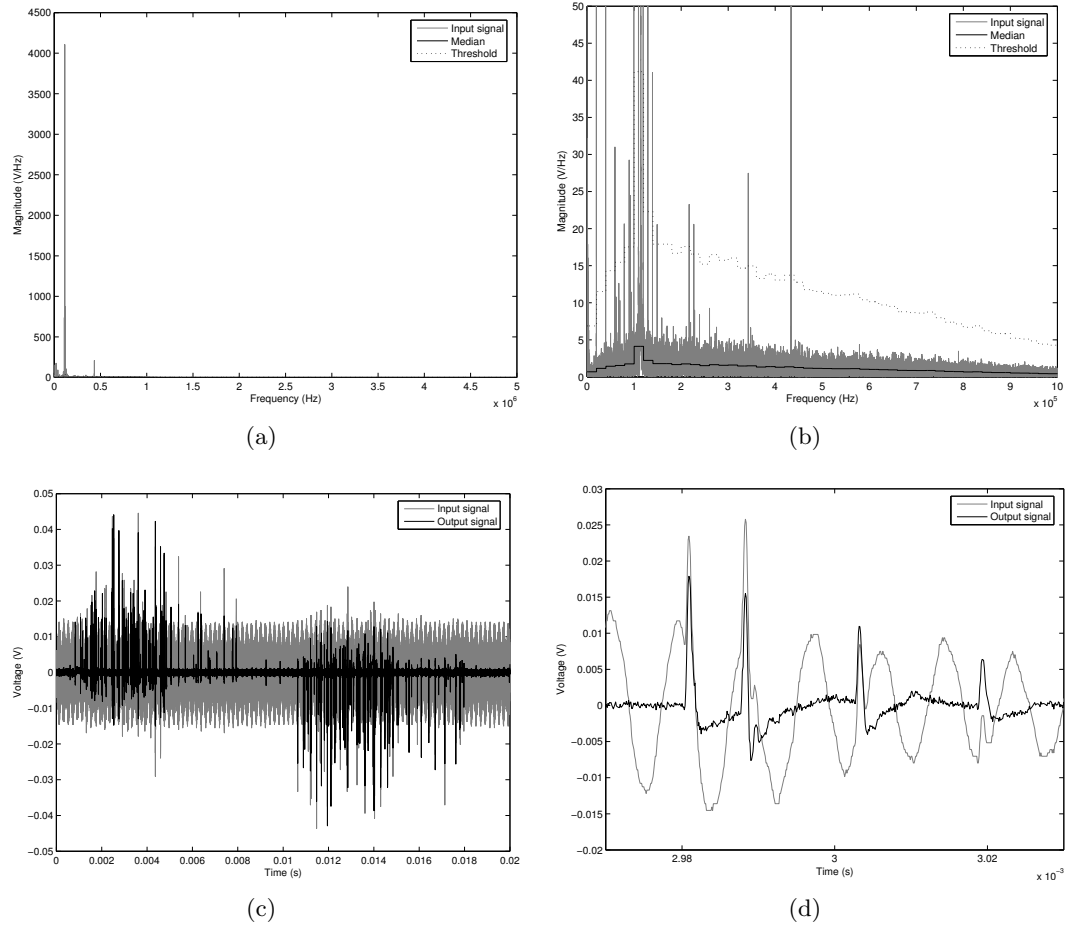


Figure 5.15 Test 2 - Effect of the FDTF for Ch1-V: (a) Frequency spectrum with bin medians and bin thresholds, (b) selective zoom of (a), (c) time domain input and output signals, and (d) selective zoom of (c).

Table 5.6 Test 2 - FDTF output to input signal power ratios (OIRs).

Signal	OIR (dB)
Ch1-I	-0.632
Ch1-V	-16.7
Ch2-I	-5.09
Ch2-V	-12.4
Ch1-V-HF	-11.2

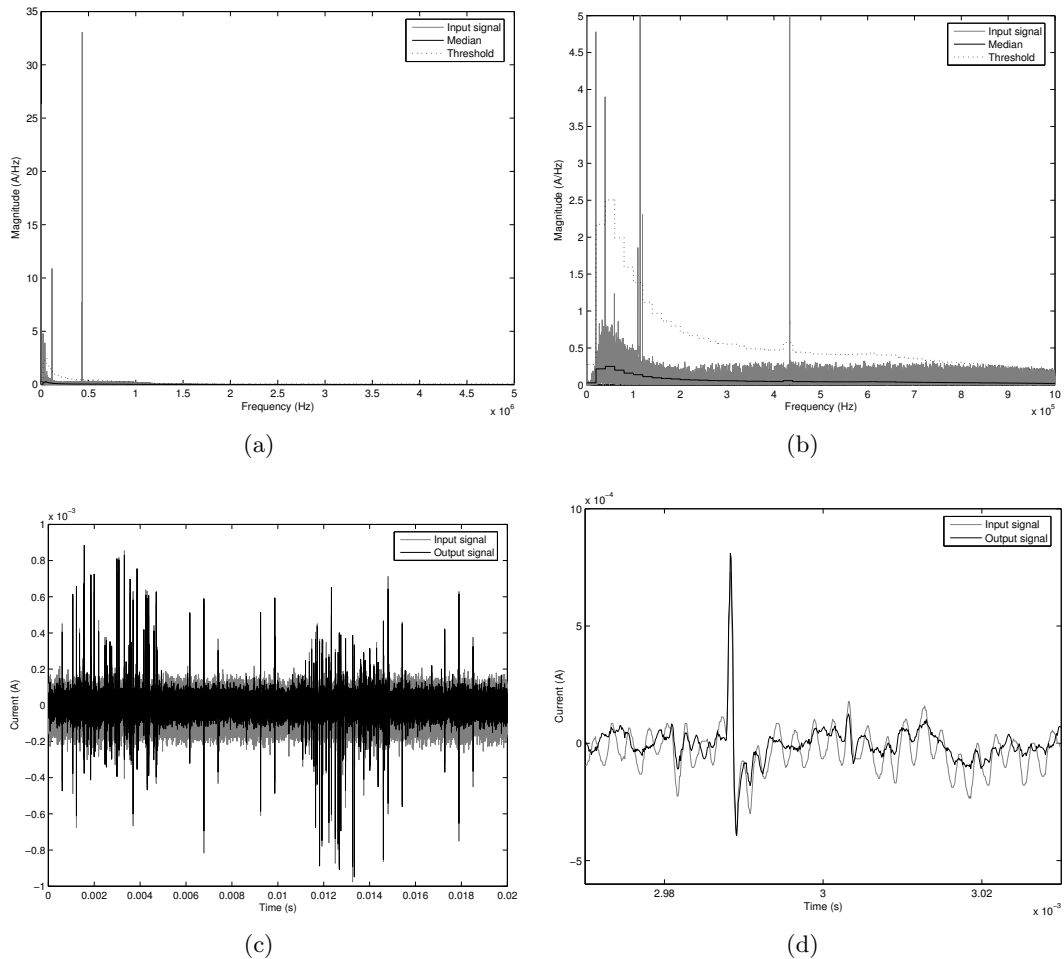


Figure 5.16 Test 2 - Effect of the FDTF for Ch2-I: (a) Frequency spectrum with bin medians and bin thresholds, (b) selective zoom of (a), (c) time domain input and output signals, and (d) selective zoom of (c).

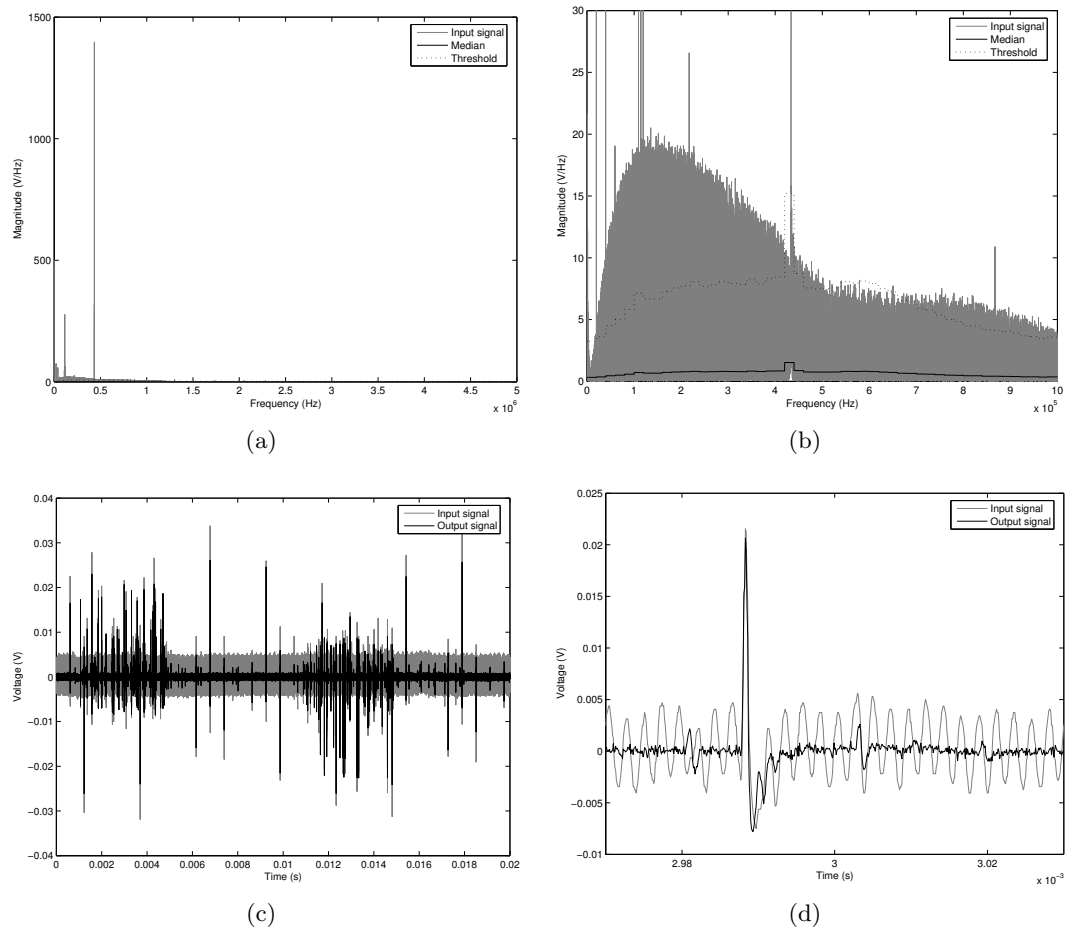


Figure 5.17 Test 2 - Effect of the FDTF for Ch2-V: (a) Frequency spectrum with bin medians and bin thresholds, (b) selective zoom of (a), (c) time domain input and output signals, and (d) selective zoom of (c).

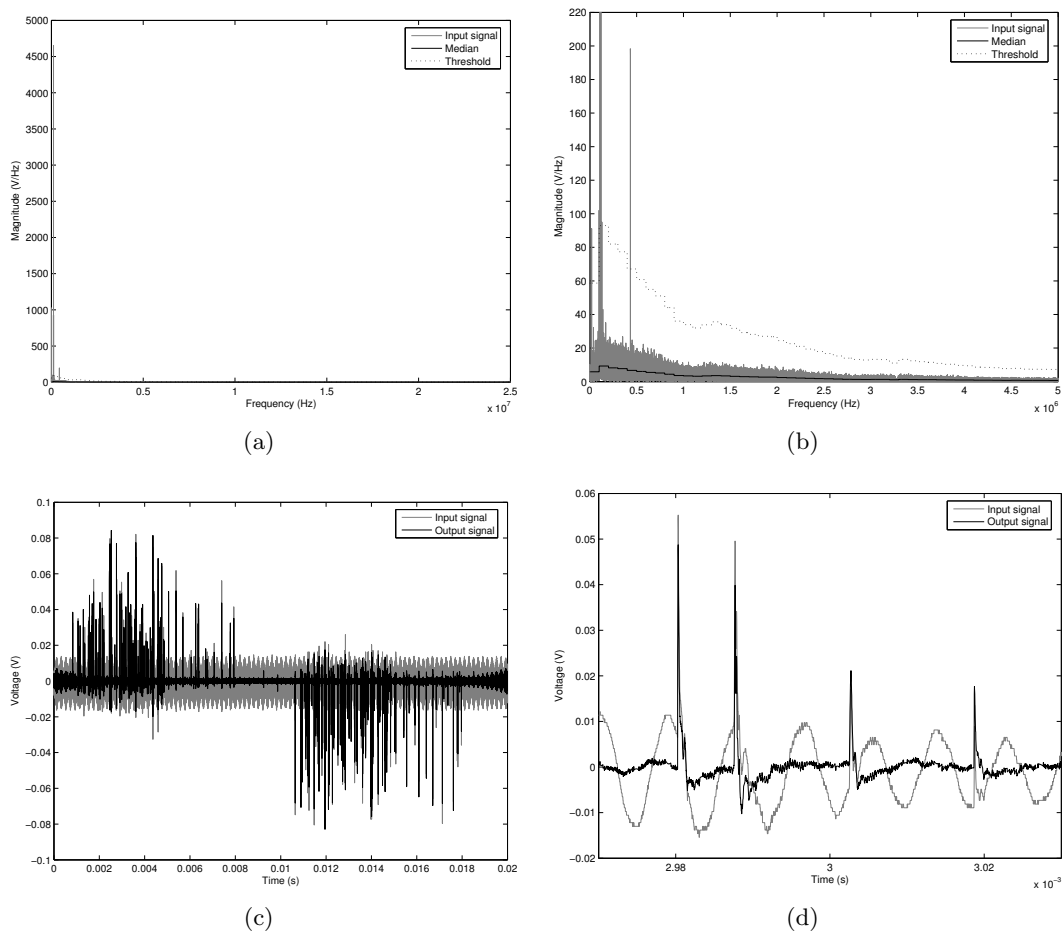


Figure 5.18 Test 2 - Effect of the FDTF for Ch1-V-HF: (a) Frequency spectrum with bin medians and bin thresholds, (b) selective zoom of (a), (c) time domain input and output signals, and (d) selective zoom of (c).

5.2.3 PD identification using the CWDCF

Figure 5.19 shows the Ch1-V signal from test 1 while varying CWDCF threshold k_{int} for data from one power cycle (20ms). This was used to determine at what level the threshold should be set when processing signals for tests 1 and 2. The threshold determines whether a pulse is considered as being internal or external to the transformer. The same threshold levels applied to the calibration pulse set are also shown in Figure 5.19. As the calibration pulses are the only internal pulse signals expected, this provided a good indication for a suitable value of k_{int} . Where k_{int} was set too low, random samples from the noise floor were classified as being an internal signal along with the calibration pulses. However, when k_{int} is too large, even the calibration pulses are not considered to be internal signals. From this, slightly different thresholds were chosen for the two tests.

Figure 5.20 shows the current and voltage signal outputs from the CWDCF for test 1, where $k_{\text{int}} = 4 \times 10^{-7}$, covering one power cycle (20ms). With knowledge from the pulse waveforms injected into transformer Tx1, it has been confirmed that each of the internal pulses has been correctly identified and their waveforms preserved with minimal distortion.

The ability of Matlab to generate random pulse patterns and upload them to the arbitrary waveform generators allowed multiple power cycles of data to be collected. Analysis from 100 power cycles of data using the conditions specified for test 1 in Table 5.3 provides the following statistics:

- 1861 artificial PD pulses were injected into the transformer by Int-Pulse1 and Int-Pulse2 over 100 power cycles. All of these pulses were detected in the output of the CWDCF stage. This is a 100% success rate.
- 2 other pulses that did not represent internal artificial PDs were present in the output of the CWDCF in two different power cycles. Both were relatively small in amplitude. Closer analysis of each of them showed a situation where apparently random noise had formed what appeared to be an internal pulse of low magnitude. This is a 0.107% error rate of incorrect pulses over all internal detected pulses.

Figure 5.21 shows the current and voltage signal outputs from the CWDCF for the more difficult test 2, where $k_{\text{int}} = 8 \times 10^{-7}$. In this test, a slightly larger k_{int} value was found more suitable to prevent false positives. Separation of internal and external pulses is excellent, even when these pulses are very close together. Also, the waveshapes of the internal pulses detected are still preserved, allowing pulse peak value collection and making further analysis possible.

Analysis from 100 power cycles of data using conditions specified for test 2 in Table 5.3 provides the following statistics:

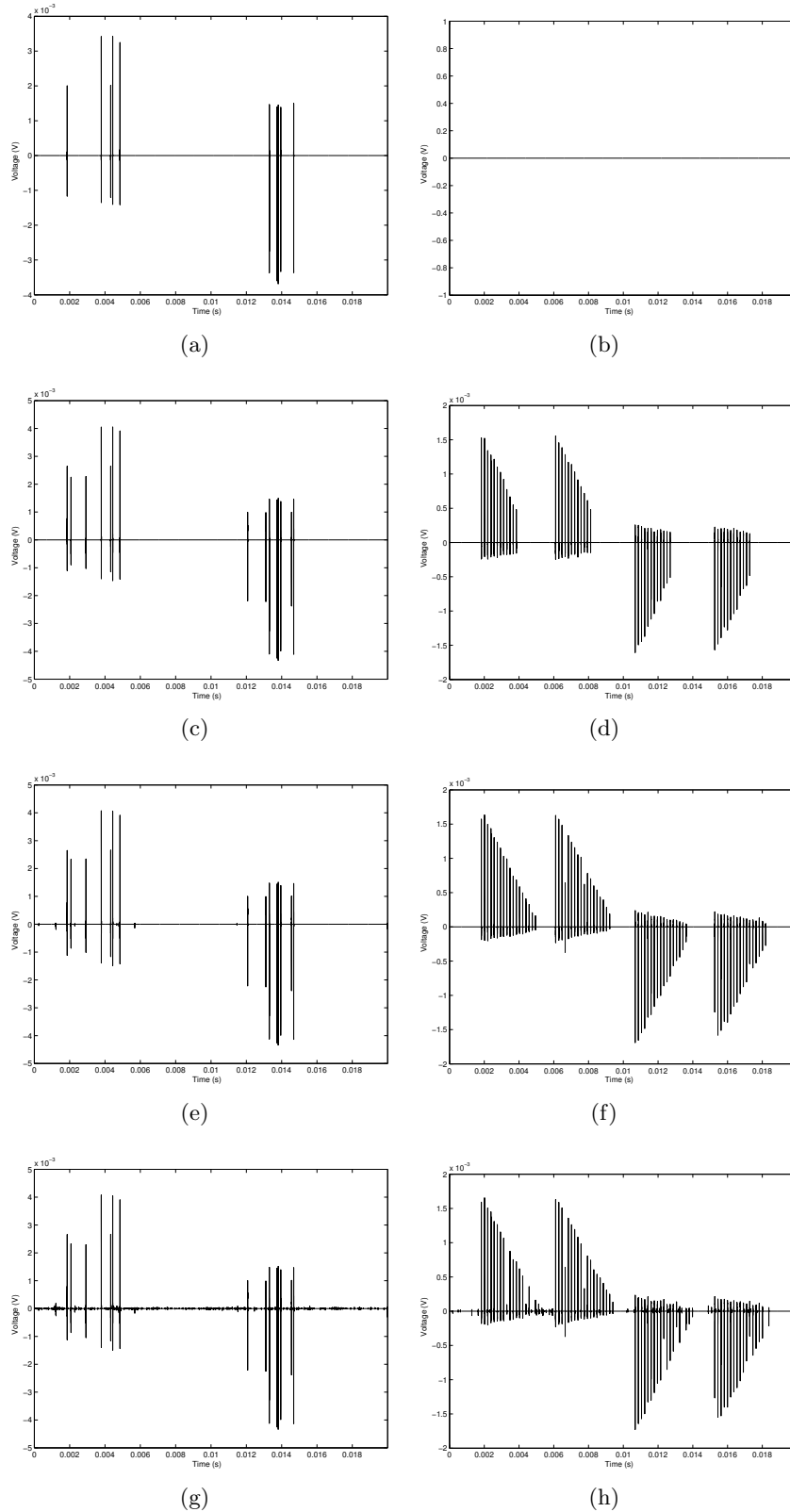


Figure 5.19 Tests 1 and 2 - Effect of varying the CWDCF threshold k_{int} : (a,c,e,g) test 1 Ch1-V signal and (b,d,f,h) Ch1-V calibration pulses, where $k_{int} = (a,b) 1 \times 10^{-5}$, (c,d) 4×10^{-7} , (e,f) 5×10^{-8} and (g,h) 1×10^{-8} .

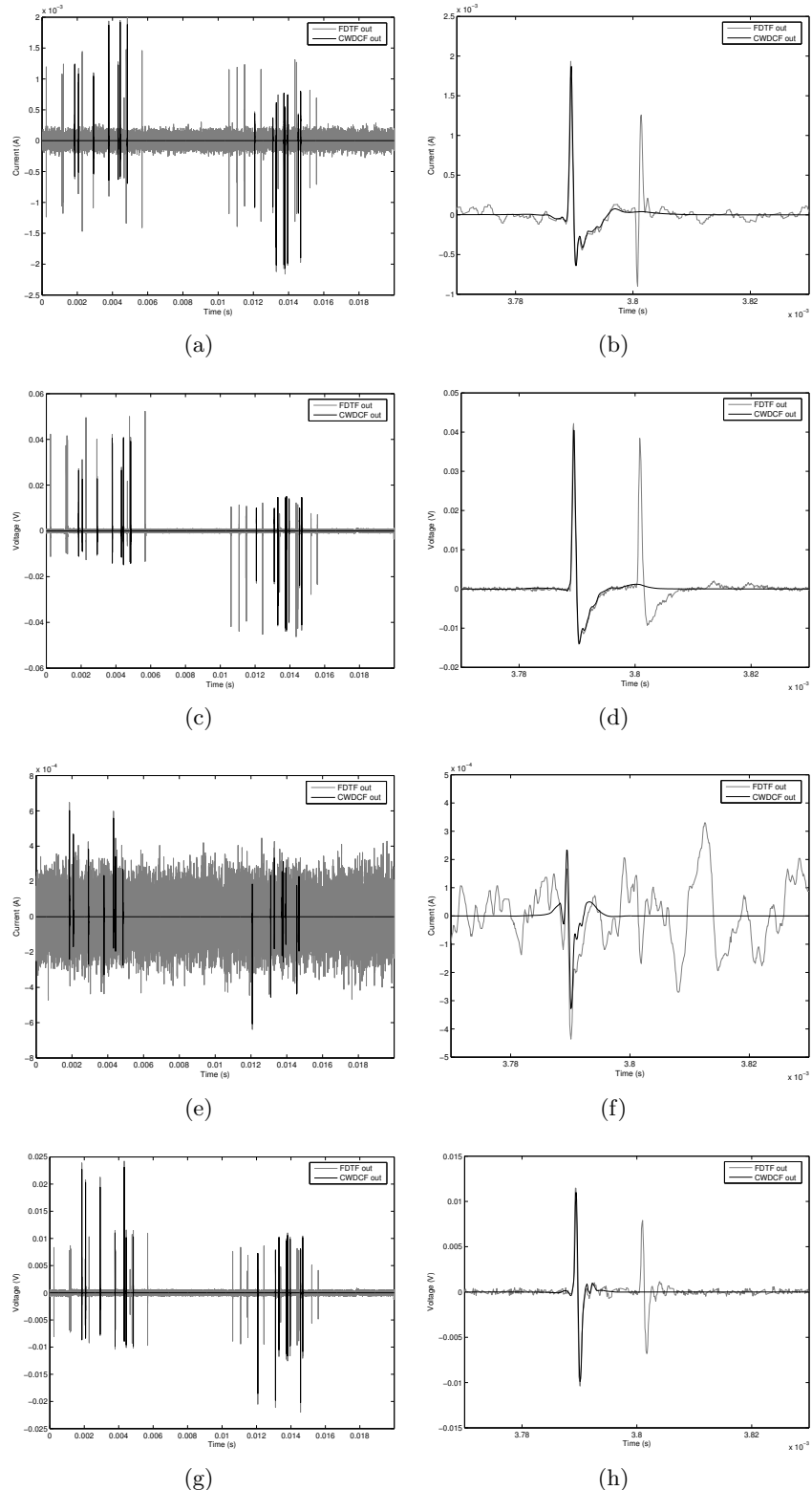


Figure 5.20 Test 1 - Output from the CWDCF where $k_{int} = 4 \times 10^{-7}$: (a) Ch1-I, (c) Ch1-V, (e) Ch2-I and (g) Ch2-V. (b,d,f,h) are corresponding selective zooms that show a known internal pulse followed by a known external pulse.

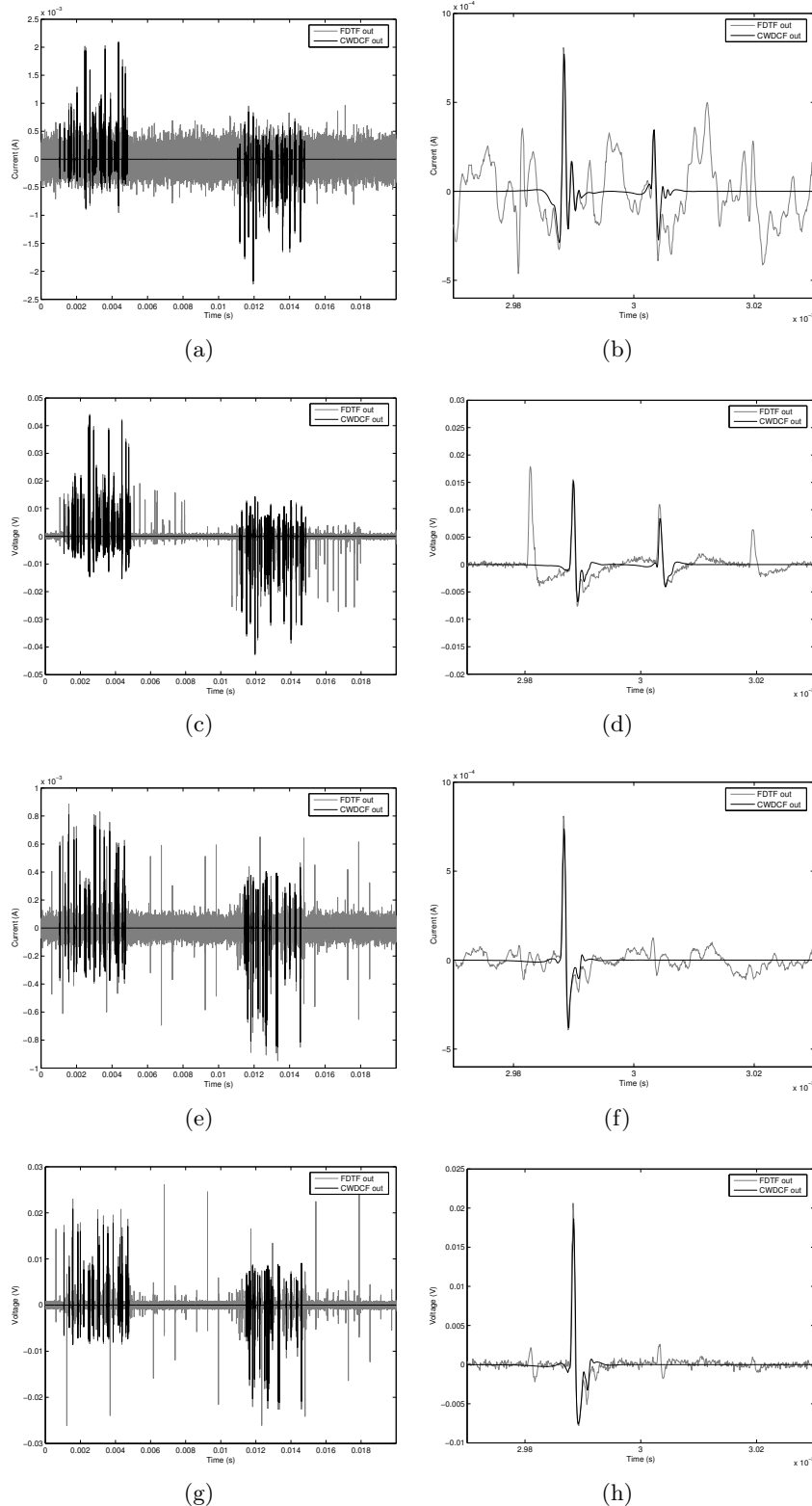


Figure 5.21 Test 2 - Output from the CWDCF where $k_{\text{int}} = 8 \times 10^{-7}$: (a) Ch1-I, (c) Ch1-V, (e) Ch2-I and (g) Ch2-V. (b,d,f,h) are corresponding selective zooms that show two known internal pulses centred between two known external pulses.

- 11679 artificial PD pulses were injected into the transformer by Int-Pulse1, Int-Pulse2 and Int-Pulse3 over 100 power cycles. 10543 of these pulses were detected in the output of the CWDCF stage. This is a 90.3% success rate. Missed pulses came mostly from Int-Pulse2 and were typically small when injected. The threshold k_{int} was not low enough to detect these pulses. However, it is considered more important to lower false positives than to collect all internal PD pulses, which is the reason that a higher threshold was selected. In addition, very small internal PD pulses may be buried in the noise and not able to be detected.
- 145 other pulses that did not represent internal artificial PDs were present in the output of the CWDCF stage. These are false positives. This is a 1.36% error rate of incorrect pulses over all internal detected pulses. These were mostly small in amplitude, and the majority of them occurred where random noise had formed what appeared to be an internal pulse of low magnitude. These pulses would be filtered out if the threshold k_{int} was even higher, but at the same time, less PD pulses would be detected.

5.2.4 Identification of separate PD sources

To determine the number of internal PD sources without prior knowledge, an excessive number of neurons have to be used for CNN training. Multiple neurons will cluster and identify the same waveshape, and the resulting difference in the weights of these neurons will be small, so that the number of different sources can be identified, as described in Section 4.6.

As an indication of how many neurons to use in test 1, a trial training run with 5 neurons was performed with the pulses collected over the first 3 of the 100 power cycles. The change in neuron weights during training, as described in Section 4.6, is shown in Figure 5.22, which shows that all neurons have settled to a local cluster at the end of training. The sum of the absolute differences in weight values between neurons after training was complete, as described in Section 4.6, is shown in Table 5.7. Neurons 1 and 5 are similar and neurons 2, 3 and 4 are similar. This would suggest that 2 internal PD sources were active in test 1, which is known to be correct.

The ability of the PDDS to accurately group pulses not used for training is important. All pulses identified in the output of the CWDCF stage could be used for training the CNN to ensure that the neural network is ‘familiar’ with all potential possibilities. However, training is computer processing intensive and slow, while identification performed by the trained network is fast. The ability of the PDDS to correctly group pulses submitted for CNN training was tested, as well as its ability to group pulses that were not submitted in training. Since the number of PD sources had already been identified as two, only two neurons were used to minimise processing time.

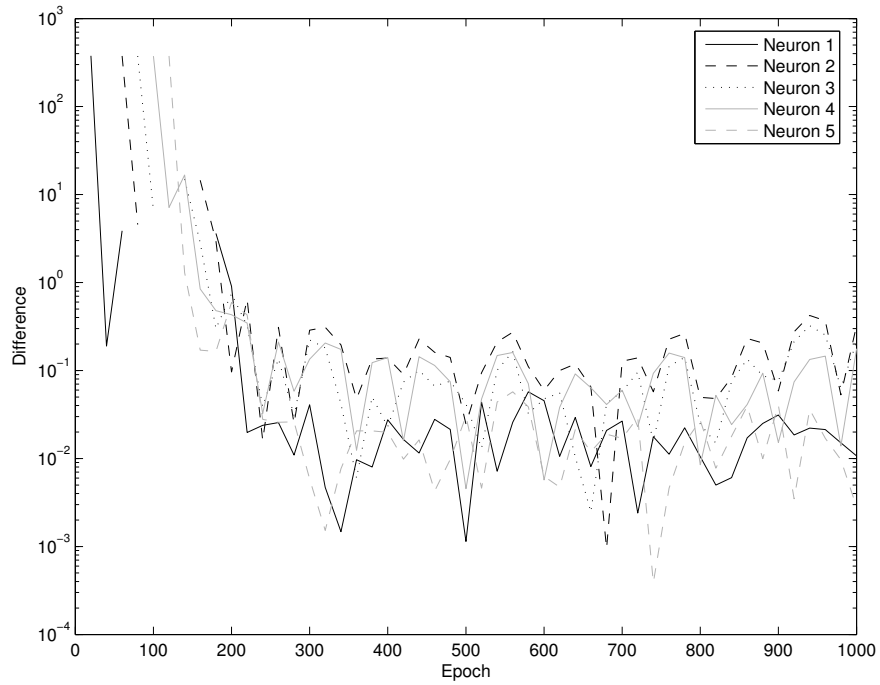


Figure 5.22 Test 1 - Change in neuron weights while training with 5 neurons.

Table 5.7 Test 1 - Sum of absolute differences in weight values in a trial run with 5 neurons.

Neurons	Difference
1 and 2	141
1 and 3	149
1 and 4	160
1 and 5	26.7
2 and 3	20.8
2 and 4	37.4
2 and 5	154
3 and 4	22.6
3 and 5	161
4 and 5	172

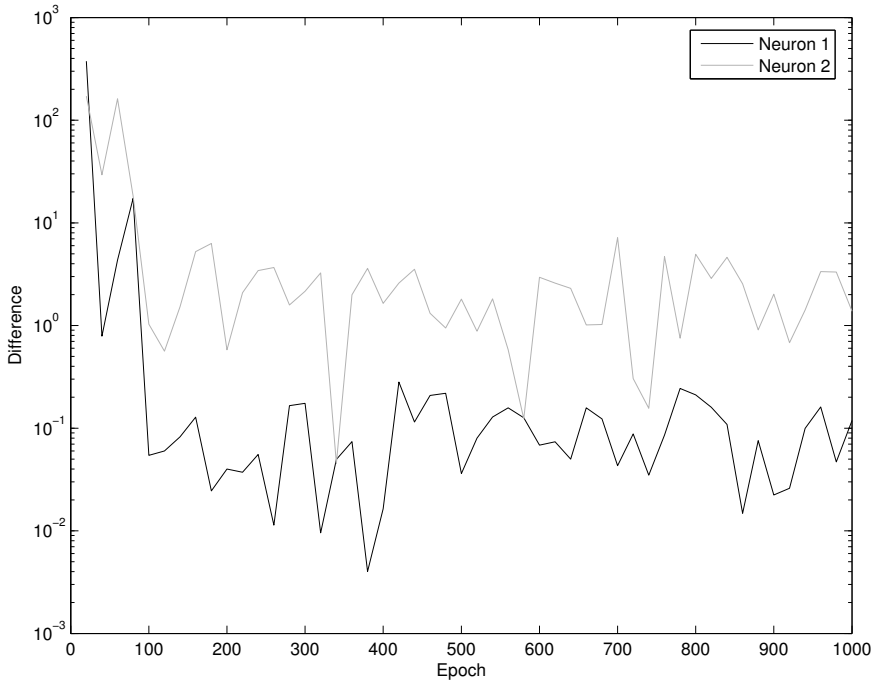


Figure 5.23 Test 1 - Change in neuron weights while training with 2 neurons.

Using 2 neurons for test 1, the internal PD pulses detected in the first 10 power cycles were used for CNN training. A total of 188 pulses were collected as inputs from these 10 power cycles. The pulses from the last 90 power cycles were submitted for grouping once the CNN was trained. These pulses had not previously been seen by the trained CNN. Figure 5.23 shows the progressive change of neuron weights while training. From this, the variation in pulse shapes that neuron 1 is classifying is tighter, as the change in neuron weights after the first 100 epochs is small over epochs. Figure 5.24 shows the neuron weights of each trained neuron. The shape of the weight values closely matches the two types of pulses submitted as inputs for training, as seen in the CWT coefficients in Ch1-V-HF.

Analysis from 100 power cycles of data in test 1, using 2 neurons, provides the statistics in Table 5.8, according to an arbitrary source number (SN). Two neurons were used. Recognition rates were very similar for the first 10 power cycles and the last 90 unfamiliar power cycles. 99.7% of pulses were allocated into the correct groups, allowing accurate PRPDA plots to be displayed. In some situations, a pulse was not allocated to a group because it was too close to a previous pulse to be considered a separate pulse for classifying. Several of these pulses actually occurred at the same time, making separation impossible. It is expected that as pulse counts increase per power cycle, this situation would occur more often. Some single pulses were incorrectly recognised as two separate pulses and each allocated a SN. These pulses were oscillatory in nature where the third or fourth oscillation was identified as a separate pulse.

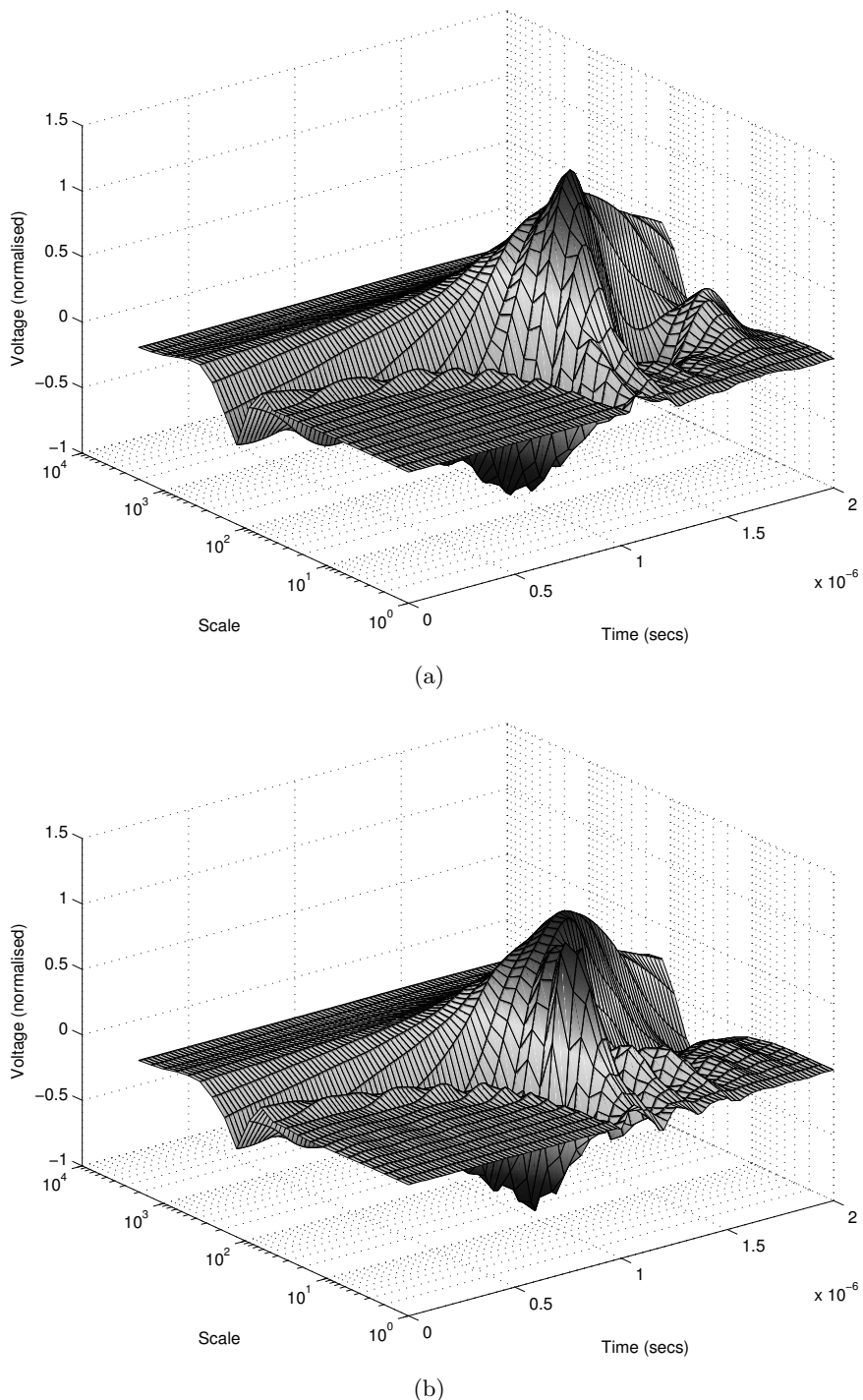


Figure 5.24 Test 1 - Weights of (a) neuron 1 and (b) neuron 2 after the training of the neural network with pulses collected from 10 power cycles.

Table 5.8 Test 1 - Internal PD recognition rates according to SN.

Actual PD source	SN1	SN2	No group
Int-Pulse1	926	0	20
Int-Pulse2	6	947	0
Other pulses	6	0	0

Table 5.9 Test 2 - Sum of absolute differences in weight values in a trial run with 5 neurons.

Neurons	Difference
1 and 2	160
1 and 3	27.1
1 and 4	201
1 and 5	183
2 and 3	170
2 and 4	271
2 and 5	262
3 and 4	213
3 and 5	195
4 and 5	51.9

Figures 5.25 to 5.28 show the artificial PD patterns over 100 power cycles in a PRPDA format for test 1. The calibration scaling constants z_i and z_v , calculated from Section 5.2.1, are used for conversion of pulse peak amplitude to pC. In test 1, identification of two sources is relatively easy, as the two pulse groups are distinct and, hence, obvious. The CNN confirms this observation.

To gauge the number of pulse sources in test 2, and therefore the minimum number of neurons required for classifying, a CNN was trained using 5 neurons with pulses from the first 3 power cycles of data. The change in neuron weights during training is shown in Figure 5.29. All neurons seem to have settled to local clusters at the end of training. The sum of the absolute differences in weight values between neurons after training is completed is shown in Table 5.9.

Neurons 1 and 3 appear to be in the same group, as do neurons 4 and 5, while neuron 2 represents its own group. This suggests that there are 3 groups, which is known to be correct. However, when training the network again with only 3 neurons and pulses from 3 power cycles, the situation presented in Table 5.10 occurred. The sums of the absolute differences in weight values suggest now that neurons 1 and 2 might be representing the same group, which therefore leaves a group of injected pulses without a neuron representing them. However, from Section 4.5, it is known that the Conscience Bias learning rule forces each neuron to classify a similar number of input vectors, and also that regions with higher input vector densities attract more neurons. Therefore, where one pulse source is creating significantly more pulses per power cycle

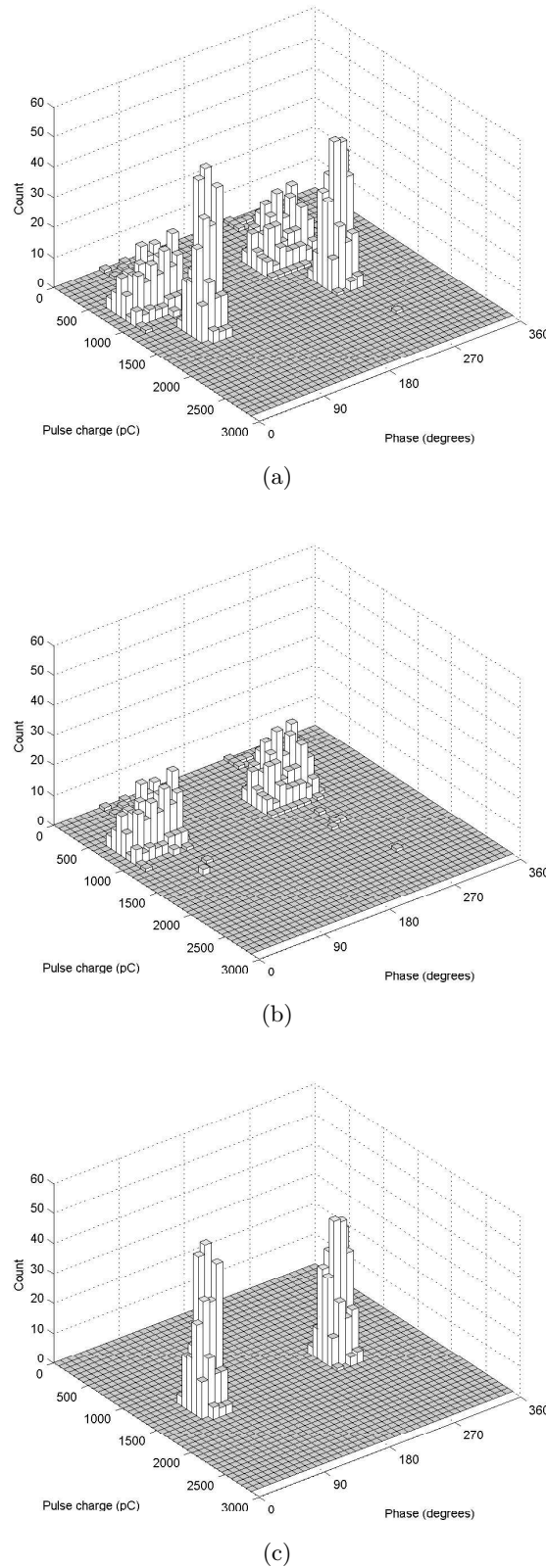


Figure 5.25 Test 1 - Internal PD pulse counts and apparent charges from Ch1-I relative to the phase of the power cycle: (a) all pulses, (b) SN1 and (c) SN2.

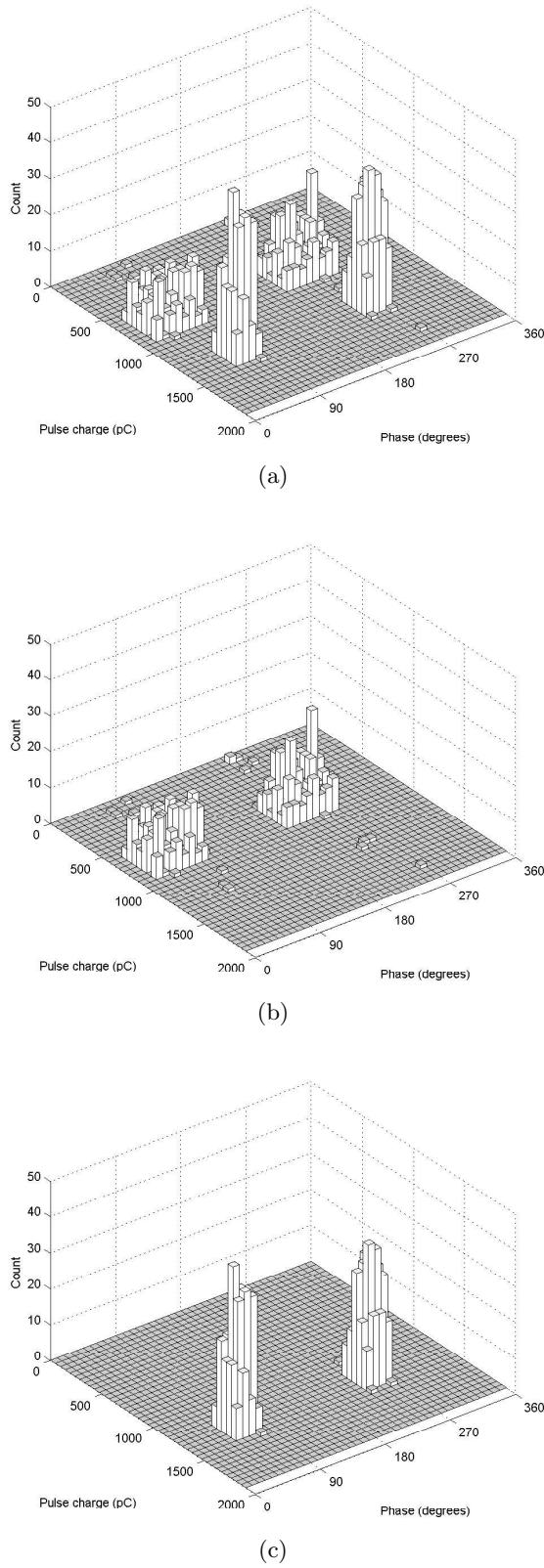


Figure 5.26 Test 1 - Internal PD pulse counts and apparent charges from Ch1-V relative to the phase of the power cycle: (a) all pulses, (b) SN1 and (c) SN2.

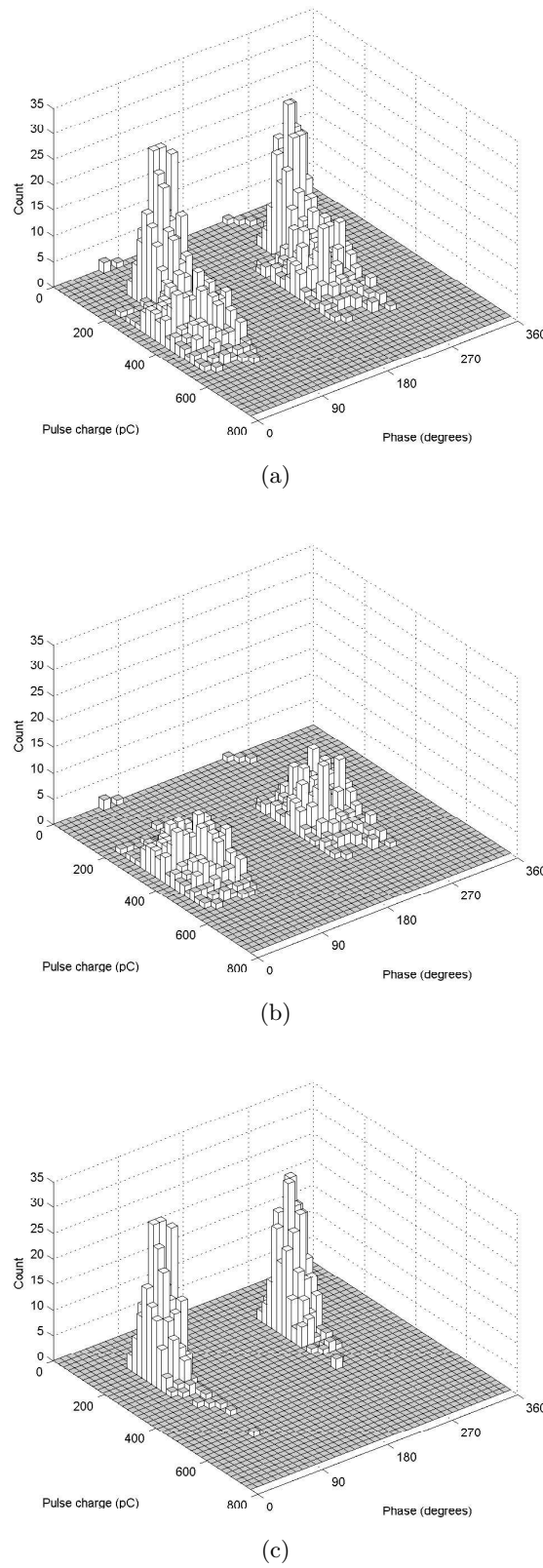


Figure 5.27 Test 1 - Internal PD pulse counts and apparent charges from Ch2-I relative to the phase of the power cycle: (a) all pulses, (b) SN1 and (c) SN2.

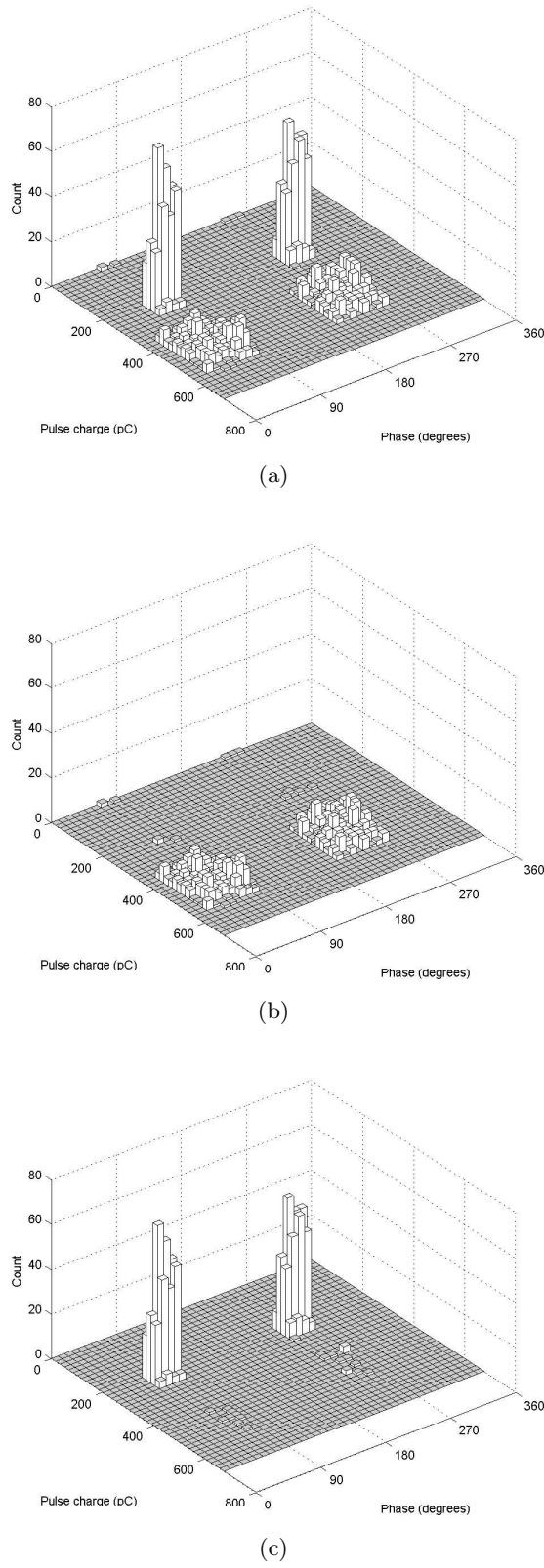


Figure 5.28 Test 1 - Internal PD pulse counts and apparent charges from Ch2-V relative to the phase of the power cycle: (a) all pulses, (b) SN1 and (c) SN2.

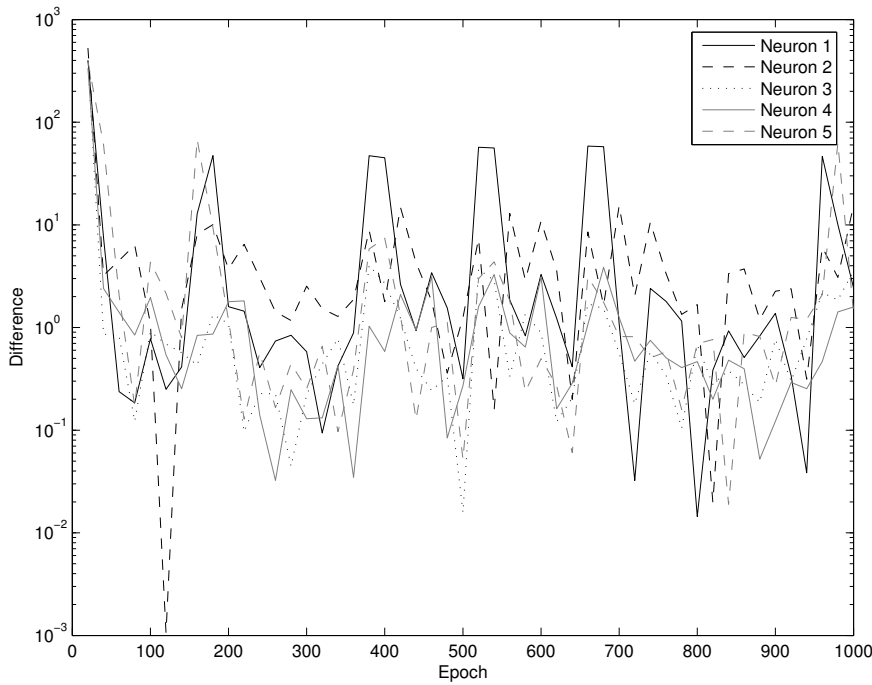


Figure 5.29 Test 2 - Change in neuron weights while training with 5 neurons.

Table 5.10 Test 2 - Sum of absolute differences in weight values in a trial run with 3 neurons.

Neurons	Difference
1 and 2	84.8
1 and 3	196
2 and 3	222

than another source, there is a strong chance that, if there are only a limited number of neurons available, they will all be attracted to the former source and therefore only represent the source with the higher pulse count. From the parameters for test 2 in Table 5.3, it is known that Int-Pulse3 generated fewer pulses per power cycle than the other sources, and it is therefore possible that this source is not being represented by a neuron when only 3 neurons are used.

To prevent this situation, more neurons can be used than required, so that, while potentially more than one neuron represents a high pulse count source, every low pulse count source will be represented by at least 1 neuron. This is particularly advisable if sources with different pulse activity are suspected to be present. Therefore, if more neurons than sources are used, the number of neurons that appear to be allocated to the same source also provides a coarse estimate of the relative pulse counts for each source. Information from apparently similar pulse sources can then be merged.

For test 2, 1020 pulses from the first 10 power cycles of data were collected, and the CNN was trained with 5 neurons. Each neuron settled on a final set of weights in a

Table 5.11 Test 2 - Internal PD source number (SN) recognition rates.

Actual PD source	SN1	SN2	SN3	No group
Int-Pulse1	4567	69	137	163
Int-Pulse2	0	3666	1	1285
Int-Pulse3	1	31	1572	288
Other pulses	0	145	0	0

similar fashion to that shown in Figure 5.29 and Table 5.9 for 3 power cycles. However, in this particular training run, neurons 1 and 5 were found to be similar, neurons 3 and 4 were similar, and neuron 2 represented its own group of pulses. Hence, SN1 includes the combined results from neurons 1 and 5, while SN2 includes the combined results from neurons 3 and 4. SN3 represents results from neuron 2. The weights of each of the 5 neurons are shown in Figure 5.30, and the above mentioned similarities are apparent in the pulse shapes of the weights.

Analysis from 100 power cycles of data in test 2, using 5 neurons, provides the statistics in Table 5.11. Recognition rates were very similar for the first 10 power cycles and the last 90 unfamiliar power cycles. From the correctly identified internal PD pulses, 97.6% were allocated to the correct SN. An additional 145 pulses (1.4%) were incorrectly identified by the CWDCF as internal, which were allocated to SN2. Pulses listed in the ‘No group’ column include those that were not detected by the CWDCF and therefore not presented to the CNN. Many of these were small pulses generated by Int-Pulse2 which were consequently not detected by the CWDCF. The timing of the rest of the pulses in the ‘No group’ column occurred very close to another pulse, and the pulses were therefore obscured or not recognised as a separate pulse.

An example of three pulses close together is shown in Figure 5.31. Even though the CWDCF correctly recognised all pulses as being internal PDs, only the second and third pulses were submitted to the CNN. The first small leading pulse was considered to be part of the second pulse. This situation also leads to incorrect SN recognition as two randomly combined pulses submitted as one input to the CNN is likely to look dissimilar to all other submitted pulses.

The success rate of correct internal PD pulse grouping in test 2 allows reasonably accurate PRPDA plots to be displayed. Incorrectly grouped pulses will show in the wrong plot and often appear as ‘outliers’. Figures 5.32 to 5.35 show the internal transformer PD patterns over 100 power cycles in PRPDA format. The same calibration scaling constants z_i and z_v , as used for test 1 were applied, as the electrical circuit for test 2 is identical to test 1. The three separate groups of PD pulses are merged beyond recognition when all the pulses are combined. The PDDS provides the excellent ability to accurately present the 3 groups individually.

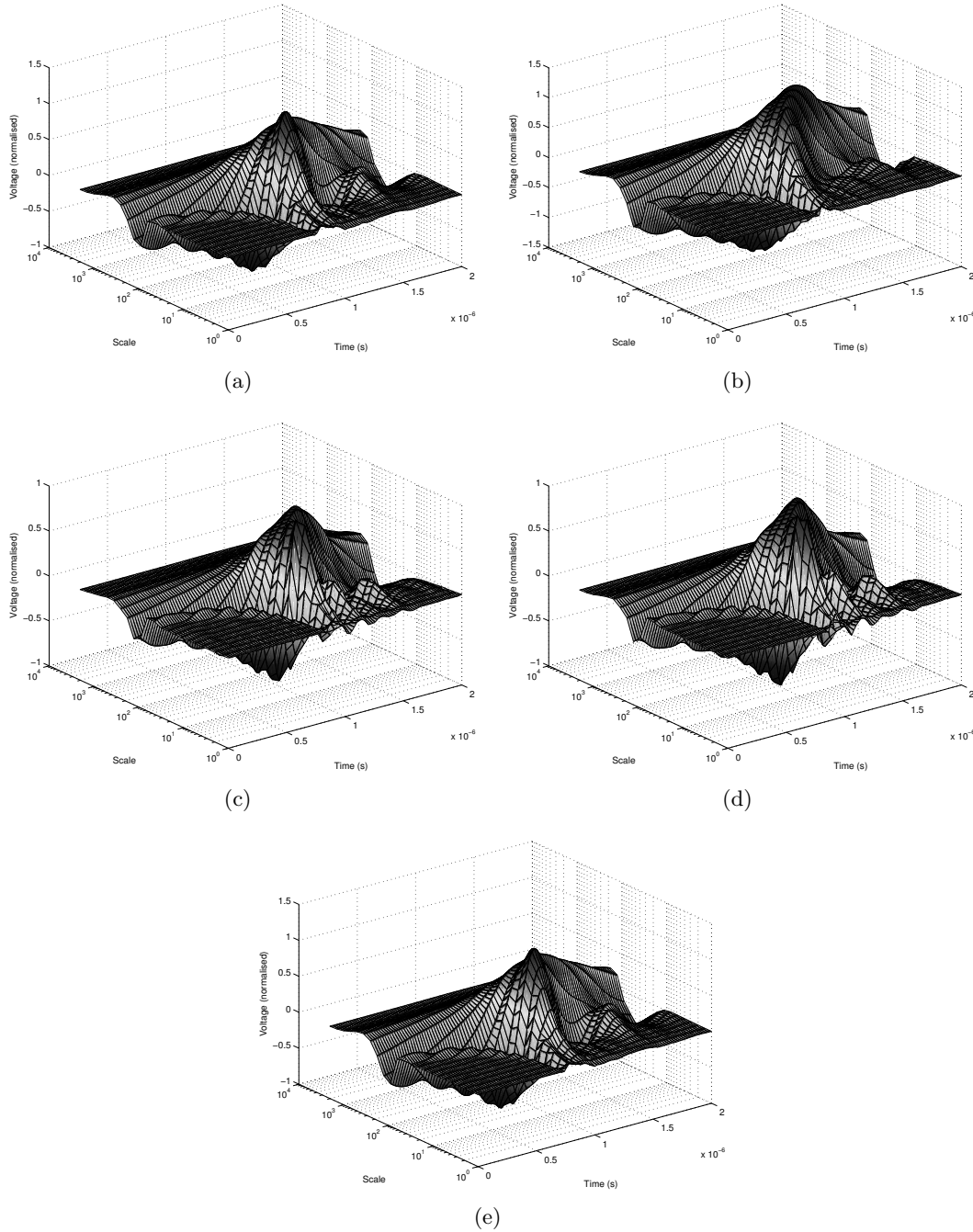


Figure 5.30 Test 2 - Weights of (a) neuron 1, (b) neuron 2, (c) neuron 3, (d) neuron 4 and (e) neuron 5 after the training of the neural network with pulses collected from 10 power cycles.

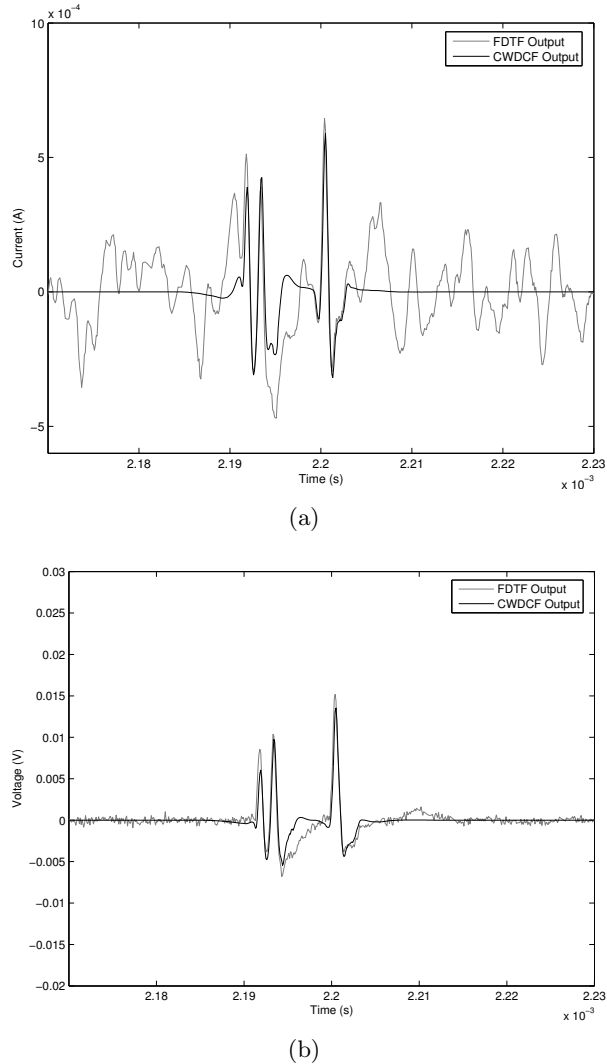


Figure 5.31 Test 2 - Output from the CWDCF where three internal PD pulses are very close together: (a) Ch1-I and (b) Ch1-V. The first two pulses were considered to be one pulse and were submitted as a single input to the CNN.

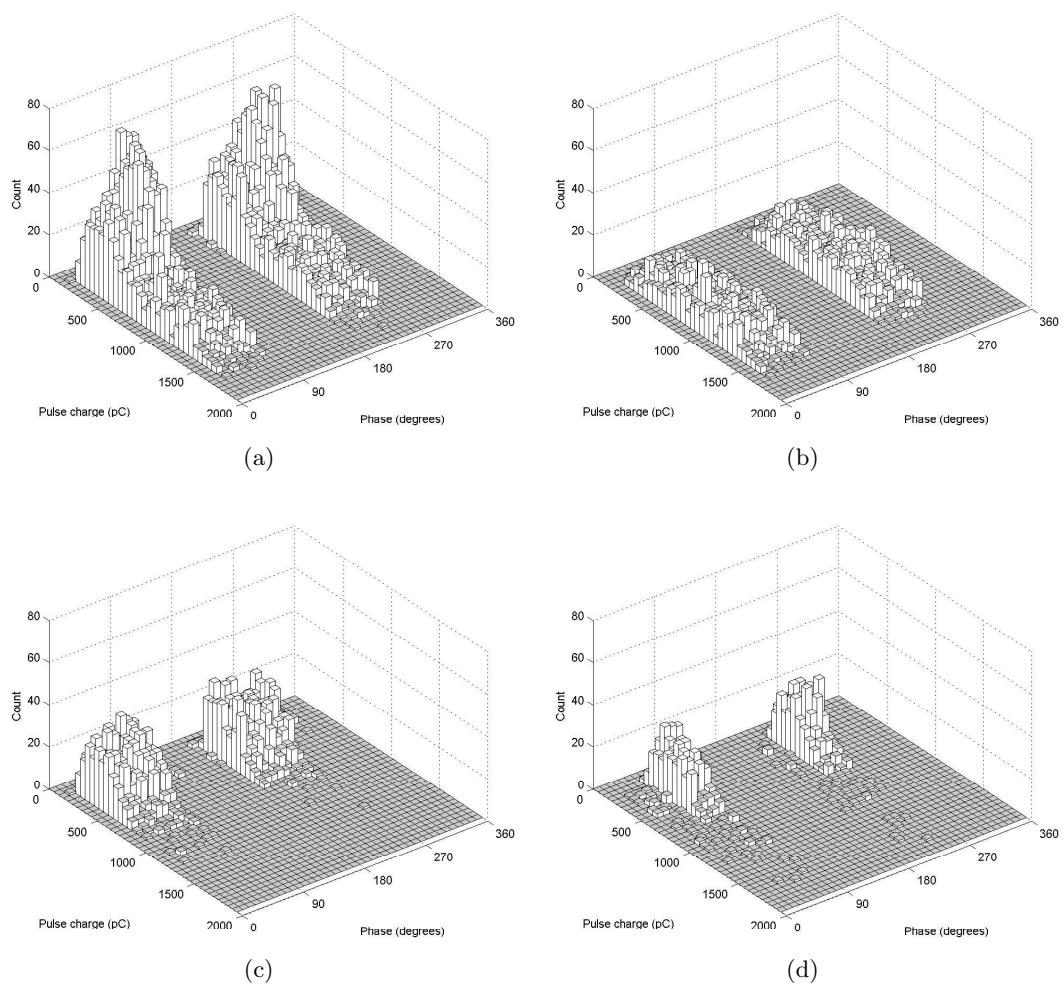


Figure 5.32 Test 2 - Internal PD pulse counts and apparent charges from Ch1-I relative to the phase of the power cycle: (a) all pulses, (b) SN1, (c) SN2 and (d) SN3.

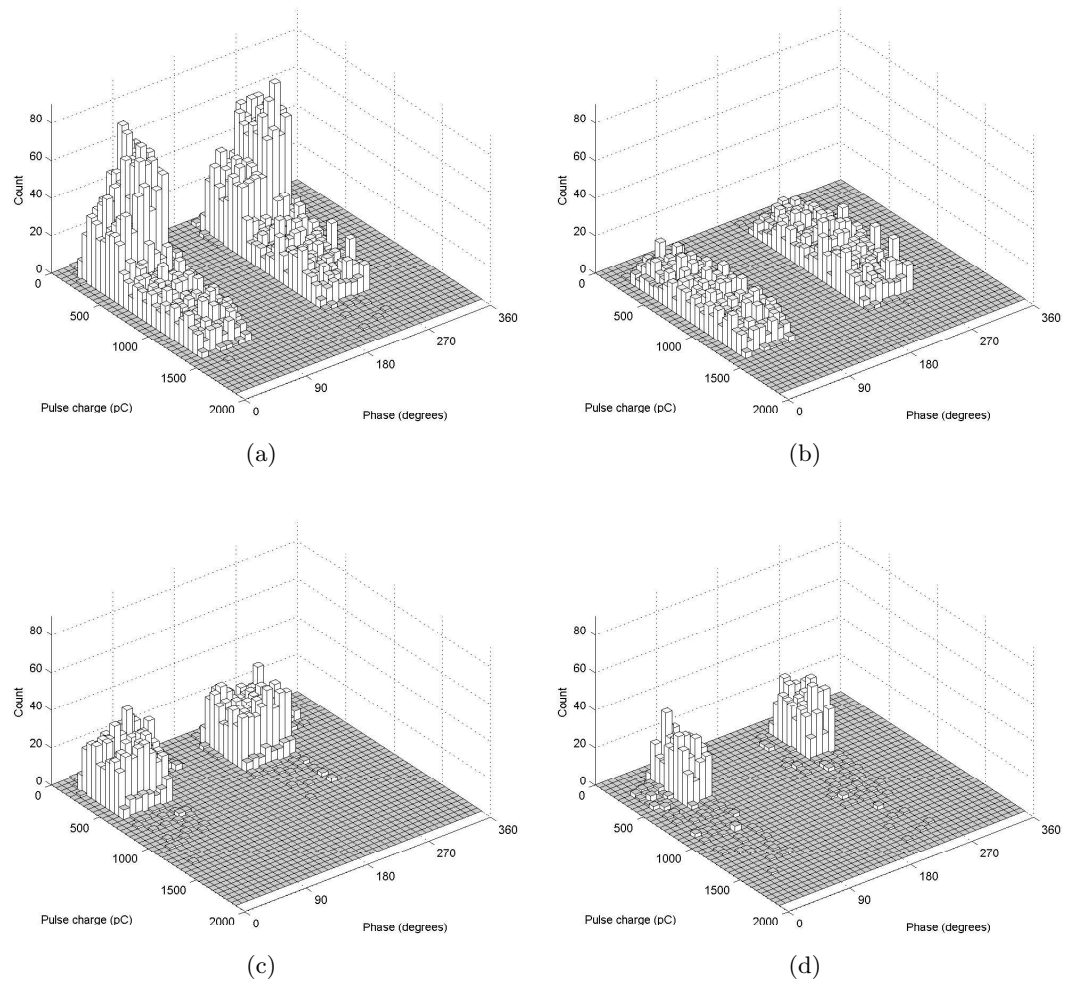


Figure 5.33 Test 2 - Internal PD pulse counts and apparent charges from Ch1-V relative to the phase of the power cycle: (a) all pulses, (b) SN1, (c) SN2 and (d) SN3.

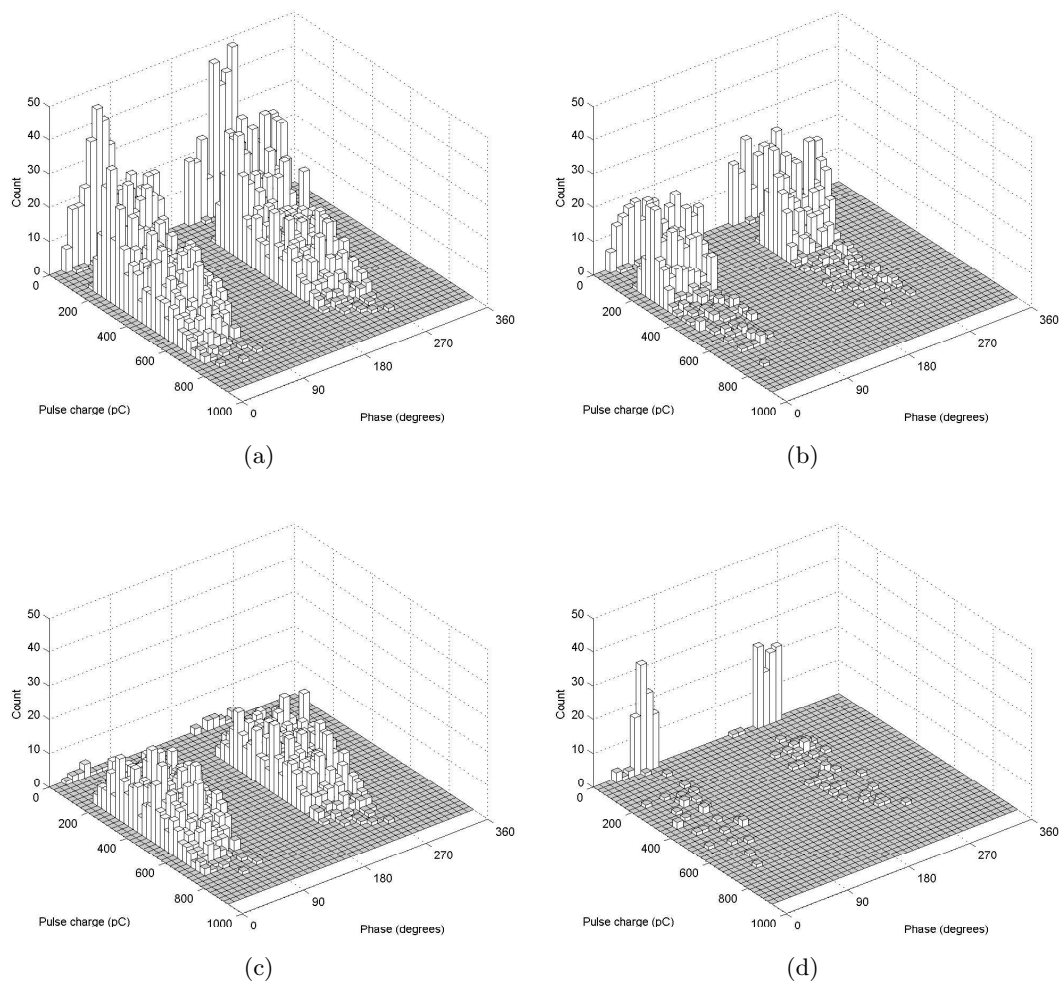


Figure 5.34 Test 2 - Internal PD pulse counts and apparent charges from Ch2-I relative to the phase of the power cycle: (a) all pulses, (b) SN1, (c) SN2 and (d) SN3.

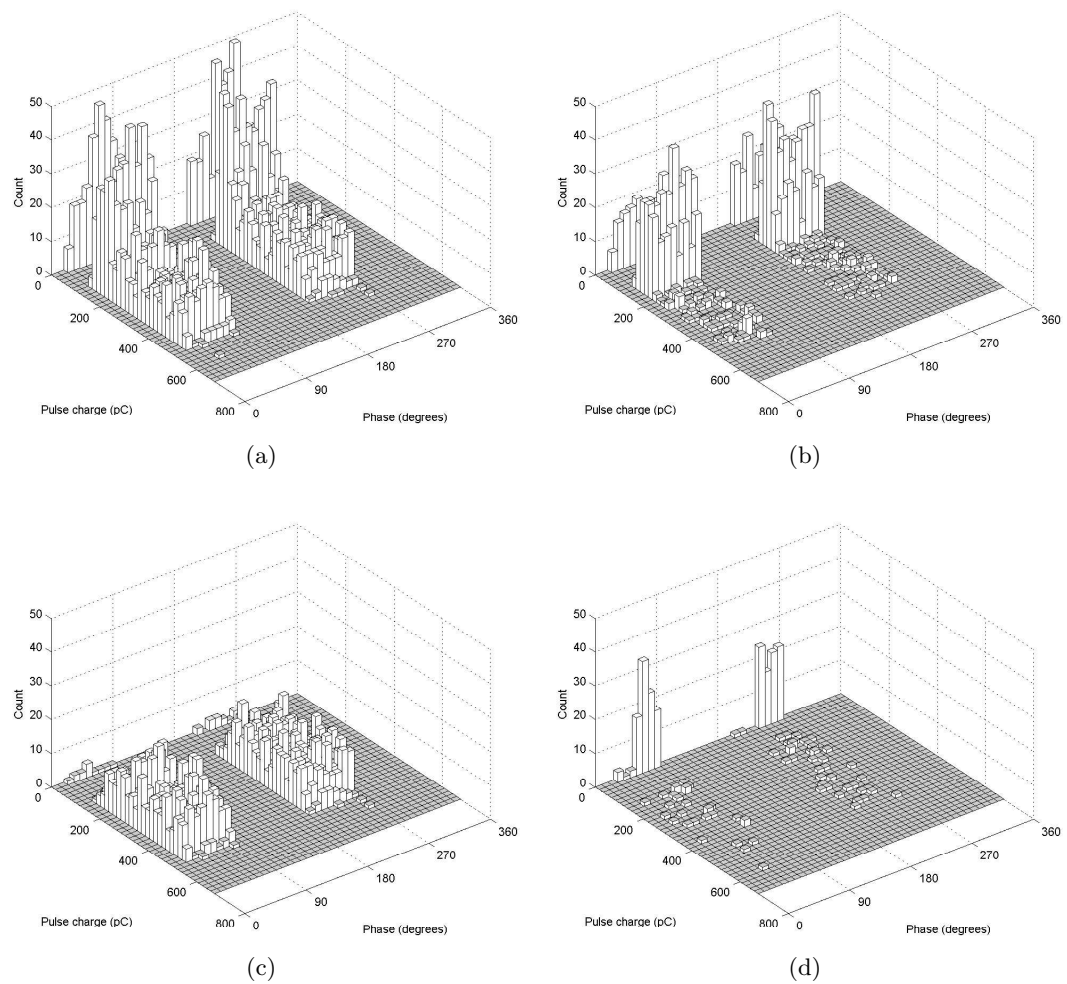


Figure 5.35 Test 2 - Internal PD pulse counts and apparent charges from Ch2-V relative to the phase of the power cycle: (a) all pulses, (b) SN1, (c) SN2 and (d) SN3.

5.3 ON-LINE PD DETECTION RESULTS

In order to apply the PDDS to an energised transformer in test 3, the same current and voltage transducers were mounted on transformer Tx2, as shown in Figure 5.36. It was unknown whether the transformer Tx2 had an actual PD problem. The transformer was not opened and analysed. However, the good performance of the PDDS in tests 1 and 2 provides justification and confidence for the results in test 3. Therefore, test 3 can be regarded as simulating an actual diagnosis situation.

The Tektronix A6302 current probes were not capable of withstanding high voltages in wires passed through their apertures. Instead, they had to be mounted on the HV wires with Tektronix CT-5 High Current Transformers. The larger aperture of these intermediary current probes allowed sufficient air gaps to withstand air breakdown. However, while the CT-5 probes have suitable frequency bandwidth, their current sensitivity is lower. To counteract that effect, each HV wire was passed through the CT-5 probe ten times, in the form of a small coil.

To provide a source of external pulse interference, a spark gap generator referenced to earth was connected to each of the HV terminals. They were adjusted so that multiple corona pulses per power cycle were generated. To simulate power transmission lines, a length of wire was connected to each HV terminal, each approximately 15m in length. This allowed high frequency pulses to radiate or capacitively couple with the surrounding earthed building environment. Narrowband interference from local radio stations was also increased in magnitude. An untraced corona source was also present on one of the HV wires, detected by hearing a distinct crackling sound. Oscilloscope settings were identical to tests 1 and 2 as detailed in Table 5.3. Photos of the test setup are provided in Appendix A.

5.3.1 Calibration

Calibration pulses were injected in a similar fashion to tests 1 and 2 while the transformer was not energised. Figures 5.37 and 5.38 show the current and voltage signals from each monitored transformer bushing, after the FDTF and the CWDCF were applied. The CWDCF threshold k_{int} was set to a low relative level to ensure that most of the calibration pulses were passed through.

5.3.2 Narrowband interference rejection using the FDTF

Results from signals covering a single power cycle (20ms) are presented for the live test in this section. Key parameters in the application of the FDTF to the signals were the same as the artificial tests, and are described in Table 5.4.

Figures 5.39 to 5.43 show the frequency domain with bin medians and bin thresholds, and time domain input and output signals of test 3 for each of the current and

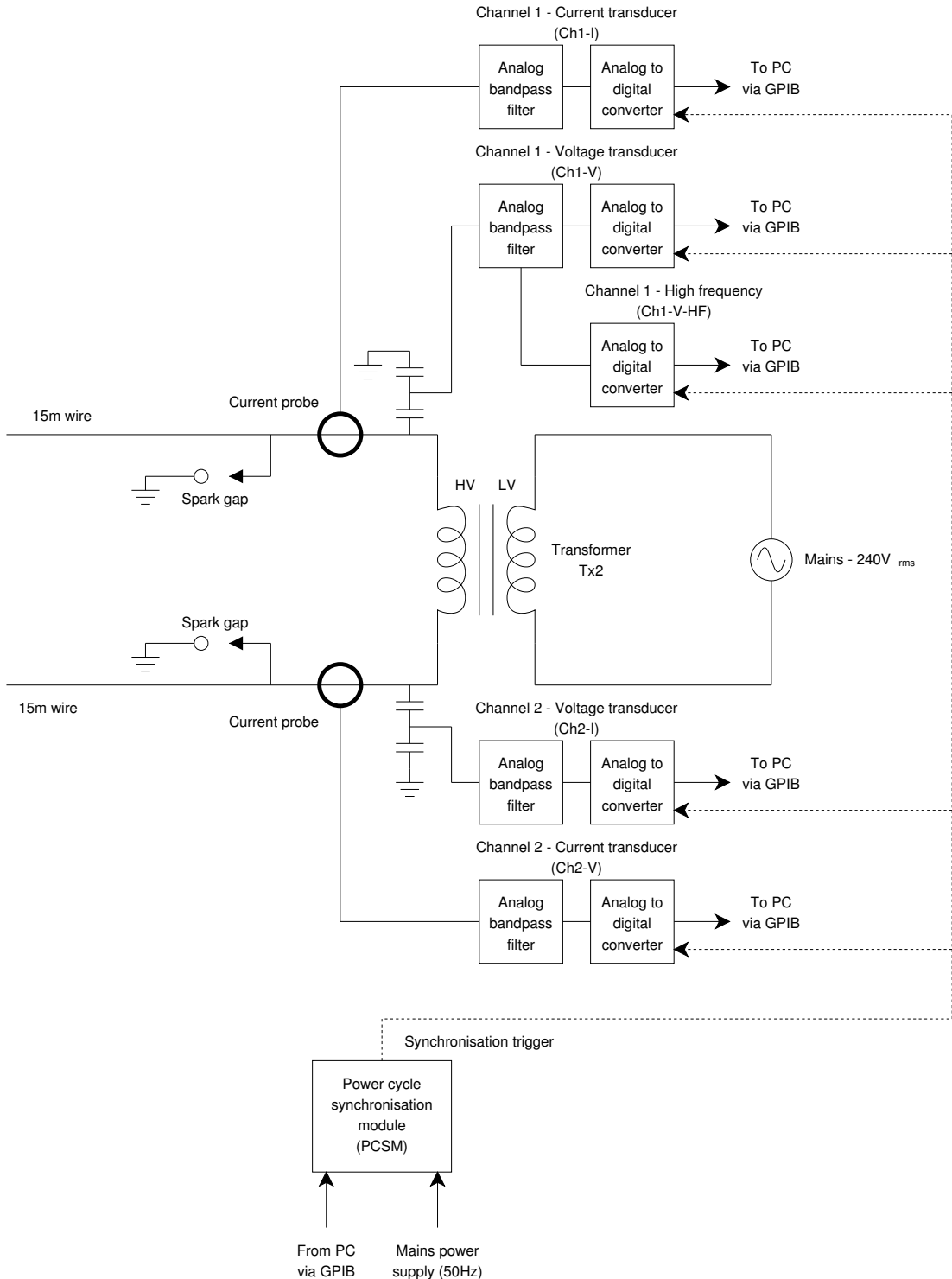


Figure 5.36 Test 3 - Test setup with corona interference for energised transformer Tx2.

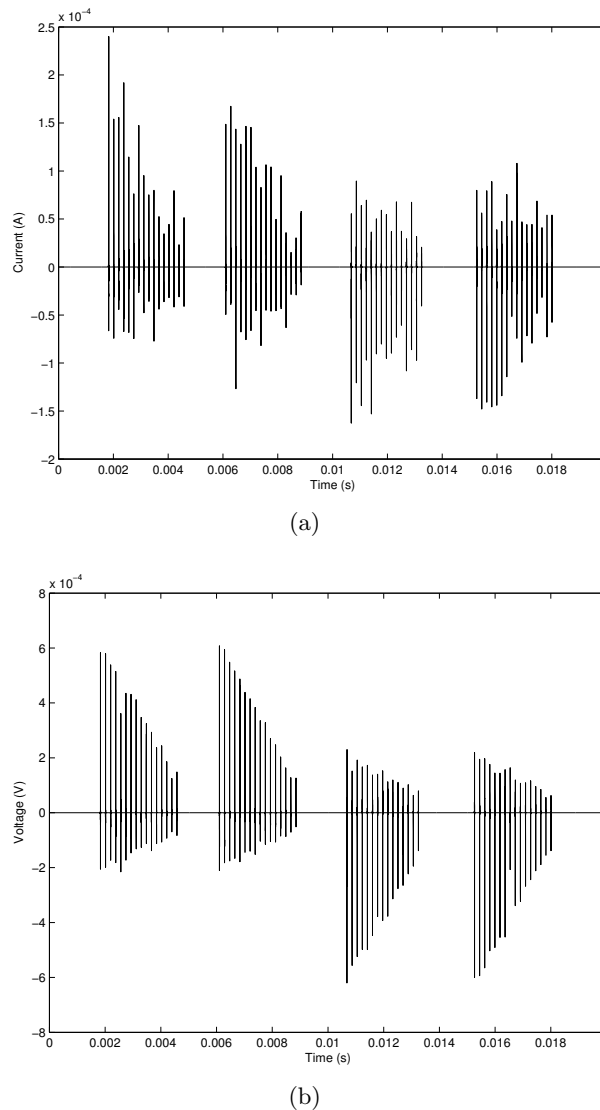


Figure 5.37 Calibration pulses for (a) Ch1-I and (b) Ch1-V after processing through the FDTF and CWDCF stages ($k_{\text{int}} = 2 \times 10^{-8}$). Calibration pulses were applied at the Channel 1 transformer bushing of Tx2.

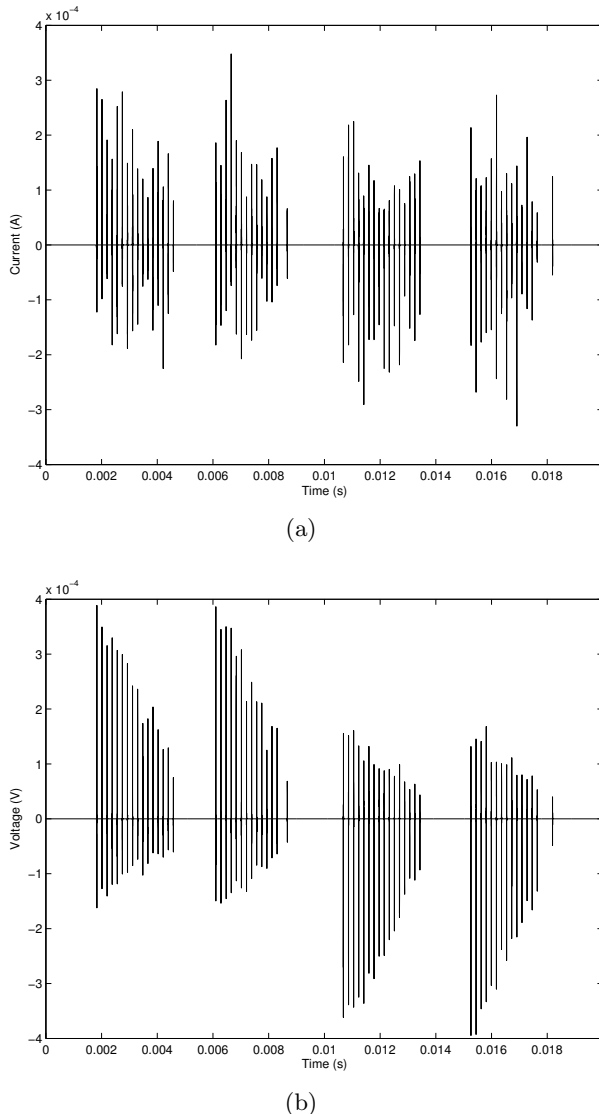


Figure 5.38 Calibration pulses for (a) Ch2-I and (b) Ch2-V after processing through the FDTF and CWDCF stages ($k_{\text{int}} = 2 \times 10^{-8}$). Calibration pulses were applied at the Channel 2 transformer bushing of Tx2.

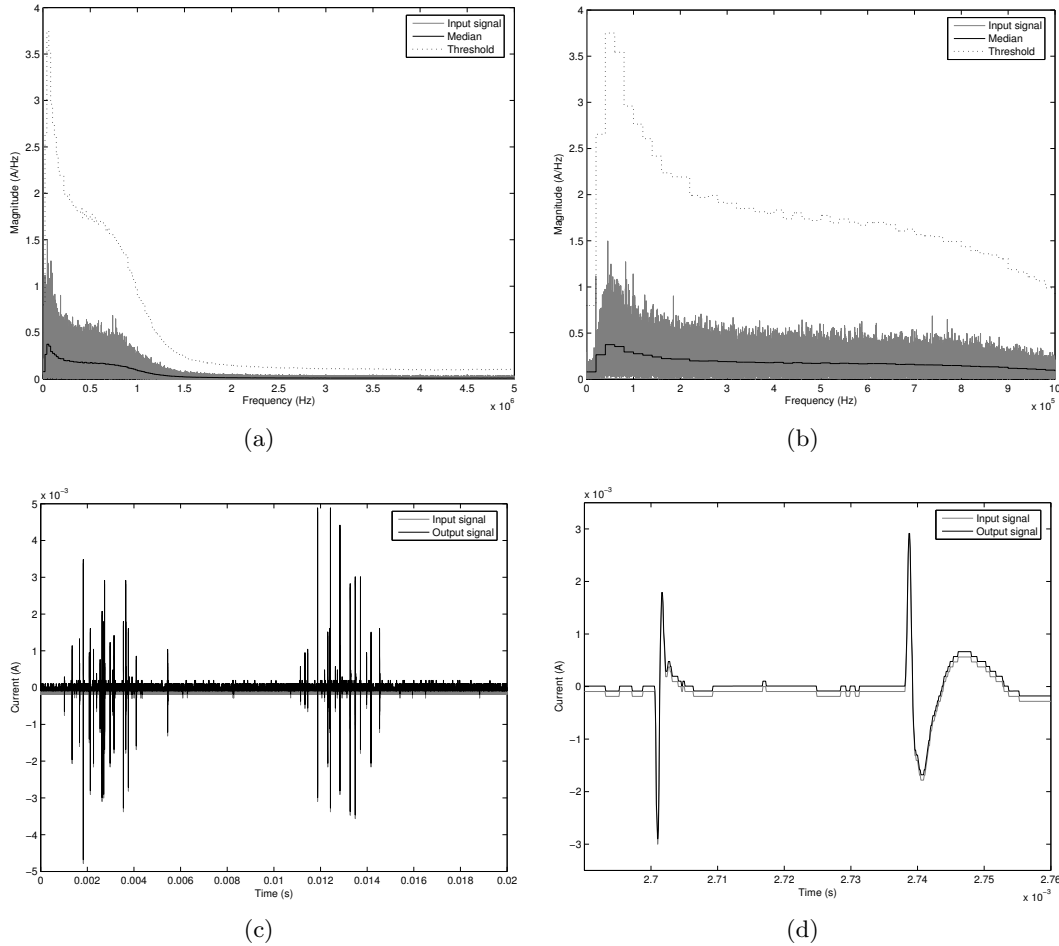


Figure 5.39 Test 3 - Effect of the FDTF for Ch1-I: (a) Frequency spectrum with bin medians and bin thresholds, (b) selective zoom of (a), (c) time domain input and output signals, and (d) selective zoom of (c).

voltage signals. Table 5.12 presents the OIR for each signal. A number of narrowband signals are shown in the Fourier domain similar to tests 1 and 2, particularly in the low frequency range. These appear to be known local radio stations. The narrowband signals were stronger in the voltage signals and therefore show greater reduction in the respective OIR values. In some cases, the FDTF also removed a DC component in the recorded signal. This was an oscilloscope setting rather than an actual DC signal being present in the circuit. In general, the FDTF successfully removed narrowband interference signals.

5.3.3 PD identification using the CWDCE

Figure 5.44 shows the Ch1-V CWDCE output at various values of the k_{int} threshold for one power cycle of data. As for tests 1 and 2, this was used to determine at what level the threshold should be set when processing further signals. The same threshold

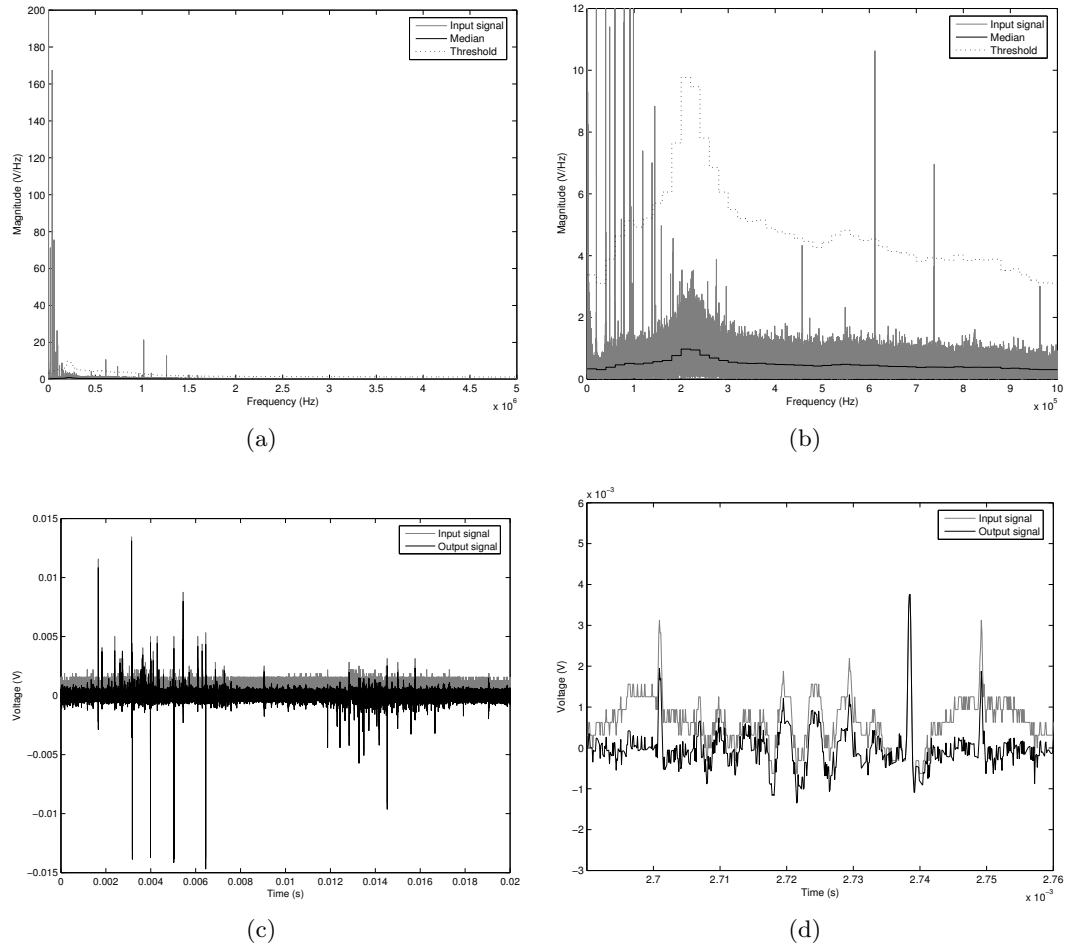


Figure 5.40 Test 3 - Effect of the FDTF for Ch1-V: (a) Frequency spectrum with bin medians and bin thresholds, (b) selective zoom of (a), (c) time domain input and output signals, and (d) selective zoom of (c).

Table 5.12 Test 3 - FDTF output to input signal power ratios (OIRs).

Signal	OIR (dB)
Ch1-I	-2.93
Ch1-V	-7.84
Ch2-I	-6.51
Ch2-V	-13.4
Ch1-V-HF	-30.8

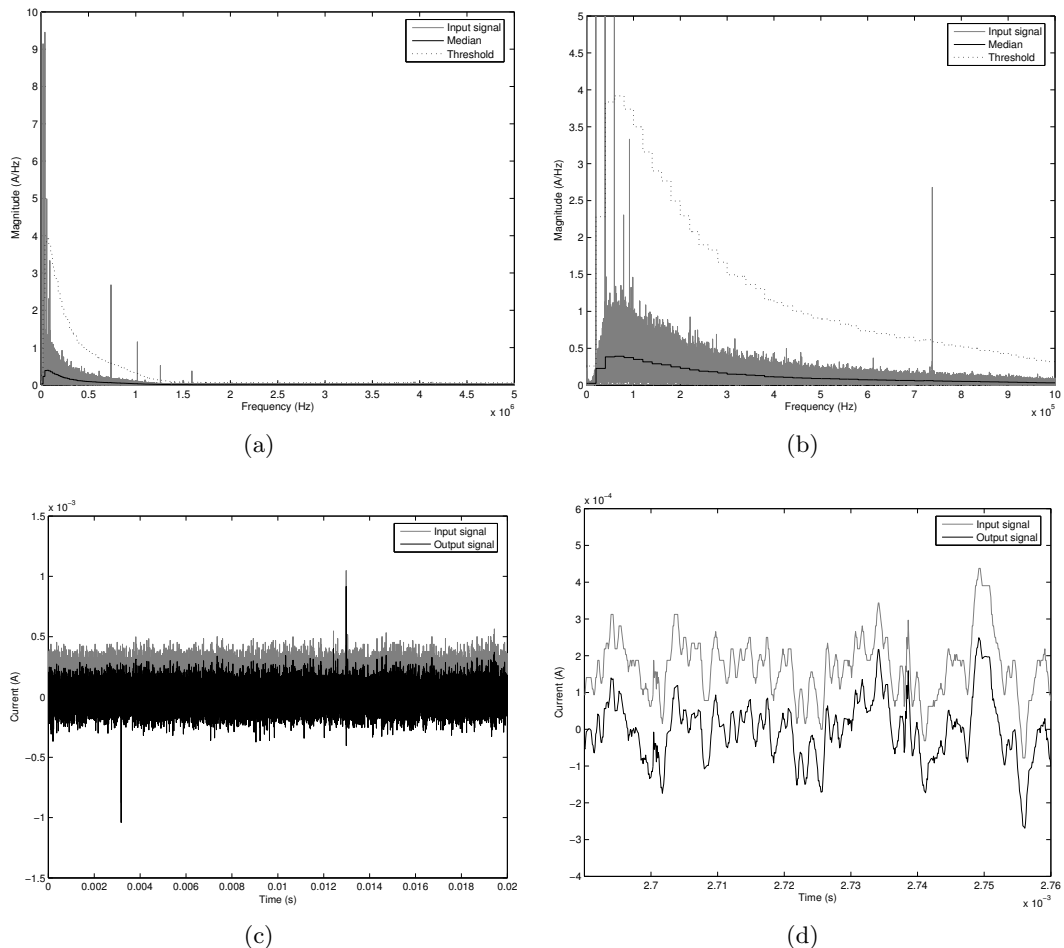


Figure 5.41 Test 3 - Effect of the FDTF for Ch2-I: (a) Frequency spectrum with bin medians and bin thresholds, (b) selective zoom of (a), (c) time domain input and output signals, and (d) selective zoom of (c).

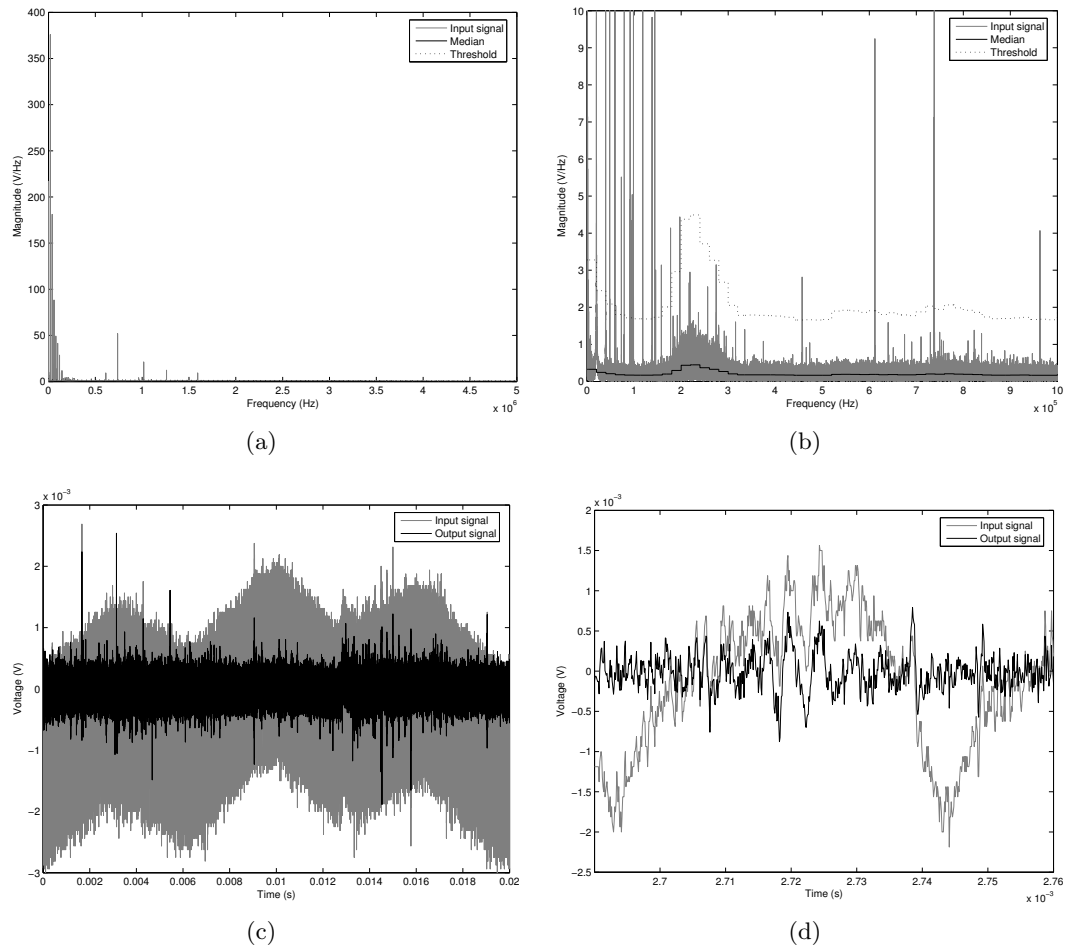


Figure 5.42 Test 3 - Effect of the FDTF for Ch2-V: (a) Frequency spectrum with bin medians and bin thresholds, (b) selective zoom of (a), (c) time domain input and output signals, and (d) selective zoom of (c).

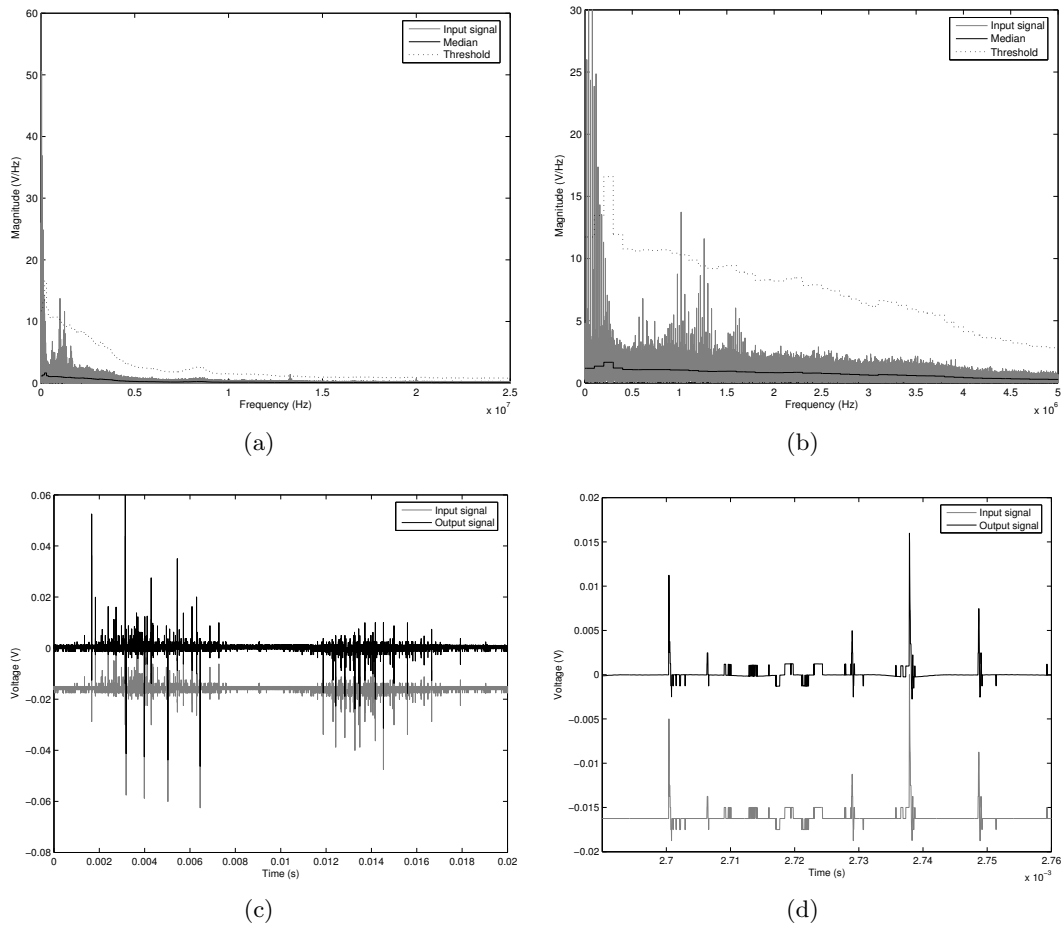


Figure 5.43 Test 3 - Effect of the FDTF for Ch1-V-HF: (a) Frequency spectrum with bin medians and bin thresholds, (b) selective zoom of (a), (c) time domain input and output signals, and (d) selective zoom of (c).

Table 5.13 Test 3 - Sum of absolute differences in weight values in a trial run with 5 neurons.

Neurons	Difference
1 and 2	65.9
1 and 3	462
1 and 4	59.2
1 and 5	147
2 and 3	412
2 and 4	52.6
2 and 5	155
3 and 4	424
3 and 5	449
4 and 5	133

levels applied to the calibration pulse set are also shown.

Figure 5.45 shows the CWDCF output of test 3 for the current and voltage signals where $k_{\text{int}} = 1 \times 10^{-7}$. These signals have a duration of one power cycle. Several pulses that have been classified as internal are clearly visible in the current and voltage waveforms from channel 1. They are significantly above the noise floor, and therefore strongly suggest that transformer Tx2 has a PD problem. As the pulses do not show in channel 2 signals, this suggests that the sources are closer to the channel 1 bushing and are being attenuated as they pass through the winding to the channel 2 bushing. Also, studying the channel 2 waveforms confirms that the pulses have not passed into the transformer from external sources connected to the channel 2 bushing. Spot monitoring of the bushings connected to the low voltage (LV) winding showed no pulse activity from any external connected source.

5.3.4 Identification of separate PD sources

As an indication of how many neurons to use in the CNN, a trial training run with 5 neurons was performed with 94 pulses collected over the first 10 power cycles. The extra cycles, compared to the 3 cycles used in tests 1 and 2 each, ensured that enough pulses were collected, as the number of PD pulses per cycle was lower than in test 2 but was a similar number to test 1. The change in neuron weights during this training is shown in Figure 5.46, which shows that all neurons have settled to a local input cluster at the end of the training. The sum of the absolute differences between neuron weight values after training is shown in Table 5.13. The neuron weights of each neuron are shown in Figure 5.47.

From Table 5.13, neurons 1, 2 and 4 were similar and thus suggest that this source produced the majority of pulses. Neurons 3 and 5 appeared to represent their own separate groups, although neuron 5 was close to being similar to neurons 1, 2 and 4. Following the same method as in test 2, SN1 includes the combined results from

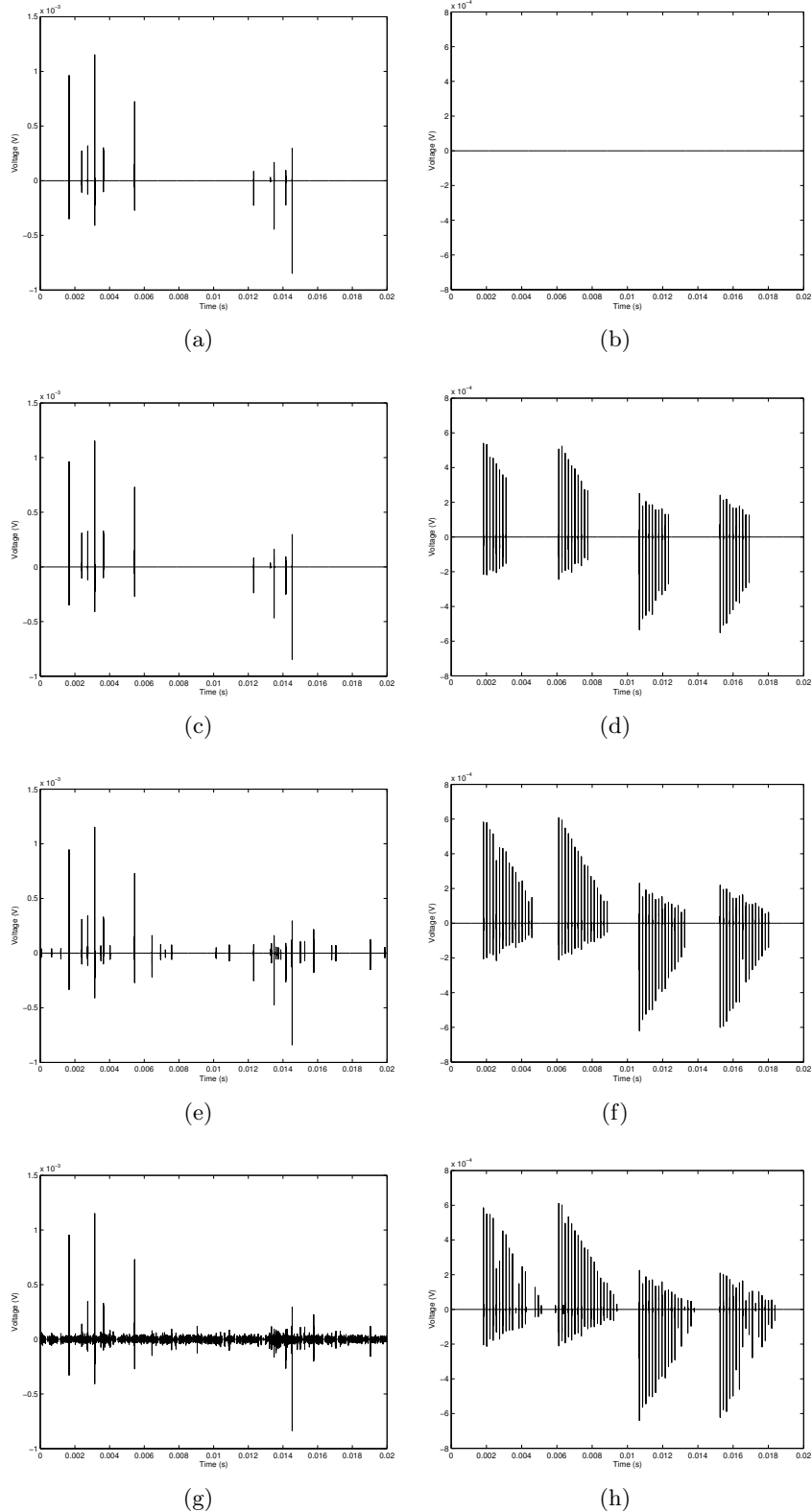


Figure 5.44 Test 3 - Effect of varying the CWDCF threshold k_{int} : (a,c,e,g) test 3 Ch1-V signal and (b,d,f,h) Ch1-V calibration pulses, where $k_{int} = (a,b) 4 \times 10^{-7}$, (c,d) 1×10^{-7} , (e,f) 2×10^{-8} and (g,h) 5×10^{-9} .

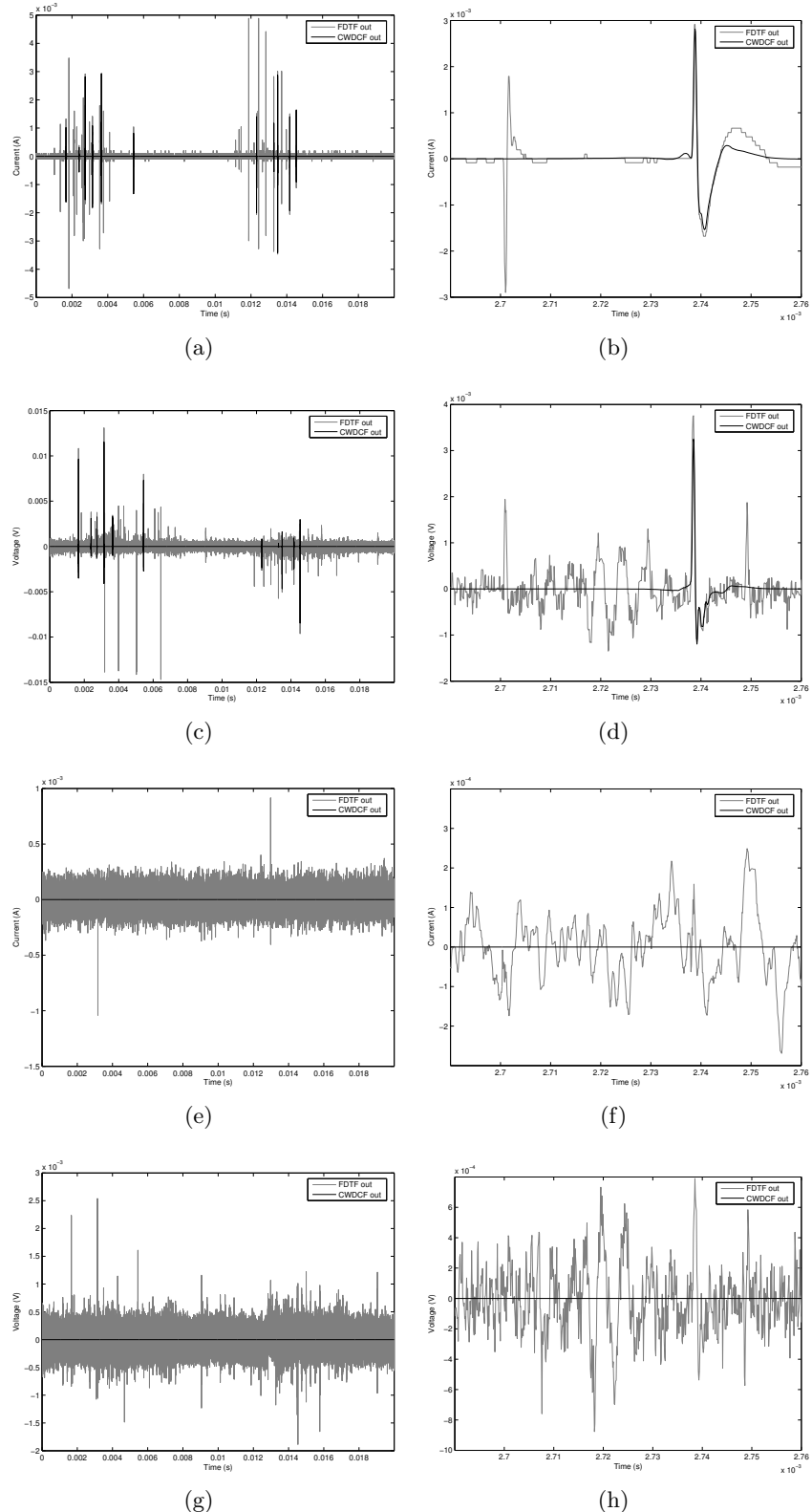


Figure 5.45 Test 3 - Output from the CWDCF where $k_{int} = 1 \times 10^{-7}$: (a) Ch1-I, (c) Ch1-V, (e) Ch2-I and (g) Ch2-V. (b,d,f,h) are corresponding selective zooms that show an apparent external pulse followed by an apparent internal pulse.

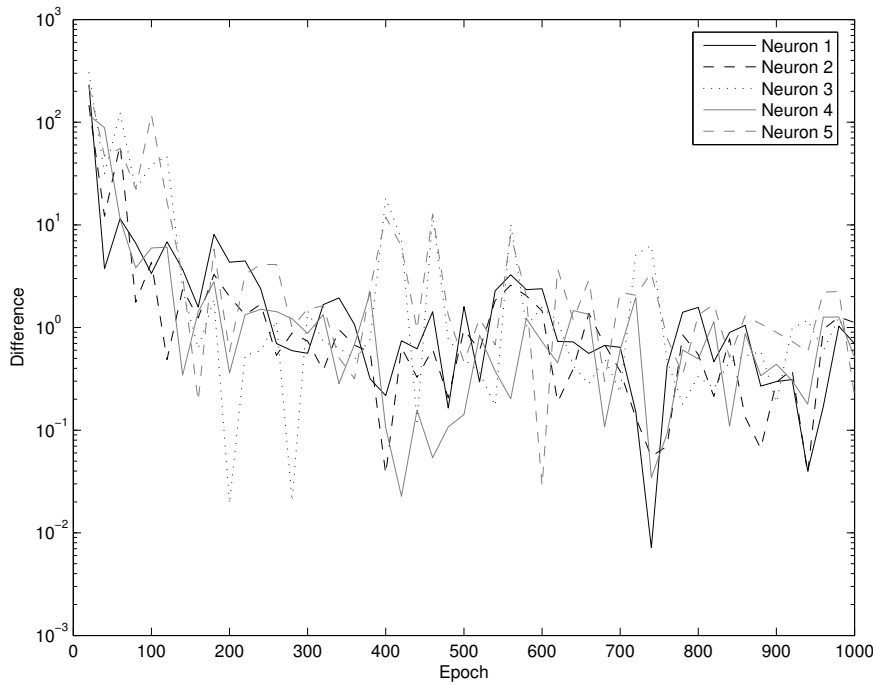


Figure 5.46 Test 3 - Change in neuron weights while training with 5 neurons.

neurons 1, 2 and 4, SN2 is the result from neuron 3 and SN3 is the result from neuron 5. The pulses from the first 10 cycles as well as pulses from an additional 90 previously unfamiliar power cycles of data were classified.

Figures 5.48 to 5.51 show the internal transformer PD patterns from 100 power cycles in PRPDA format. The calibration scaling factors z_i and z_v , calculated from Section 5.3.1, were used for unit conversion. Pulses from SN2 are mostly low magnitude and may consist of some false positives in the output of the CWDCF. Pulses from SN1 and SN3 show the typical phase distribution of internal transformer PD sources. As the pulses in SN1 and SN3 are similar in waveshape, there is a reasonable chance that the pulses are from the same source. If two separate sources are active, it is highly likely that the two sources are physically close to each other. Training the CNN with less neurons might not provide additional information since most neurons were already attracted to SN1 due to its high pulse count rate.

5.4 CONCLUSIONS

Three tests have been carried out to evaluate the effectiveness of the PDDS. The first two tests, designed to quantitatively measure the accuracy of the PDDS in identifying PD pulses and separating PD sources, showed high success rates. The identification rates of PD pulses were very high, with 0.1% false positives in test 1 and 1.4% in the more complex test 2. Unidentified PD pulses were either very small, obscured by a

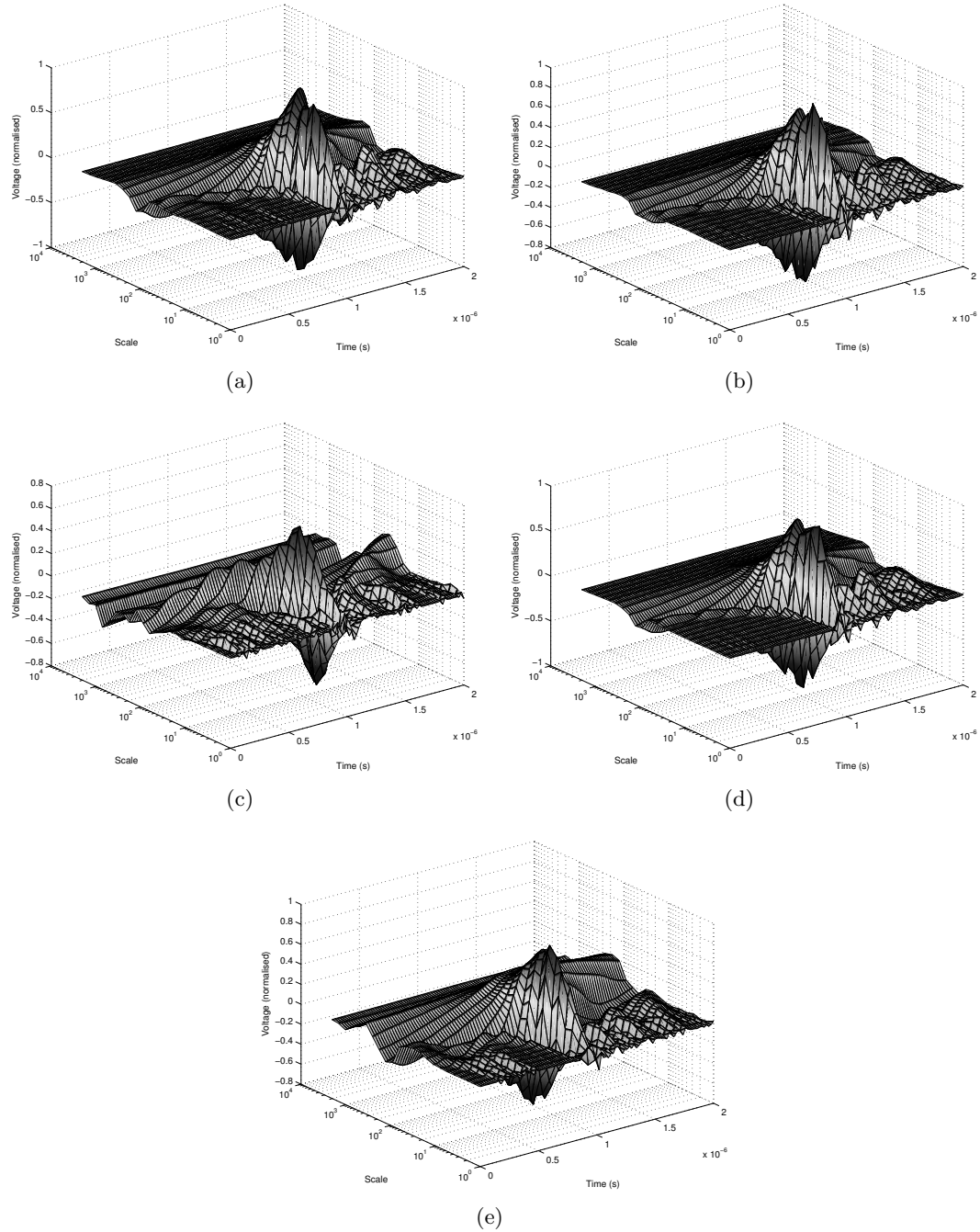


Figure 5.47 Test 3 - Weights of (a) neuron 1, (b) neuron 2, (c) neuron 3, (d) neuron 4 and (e) neuron 5 after the training of the neural network with pulses collected from 10 power cycles.

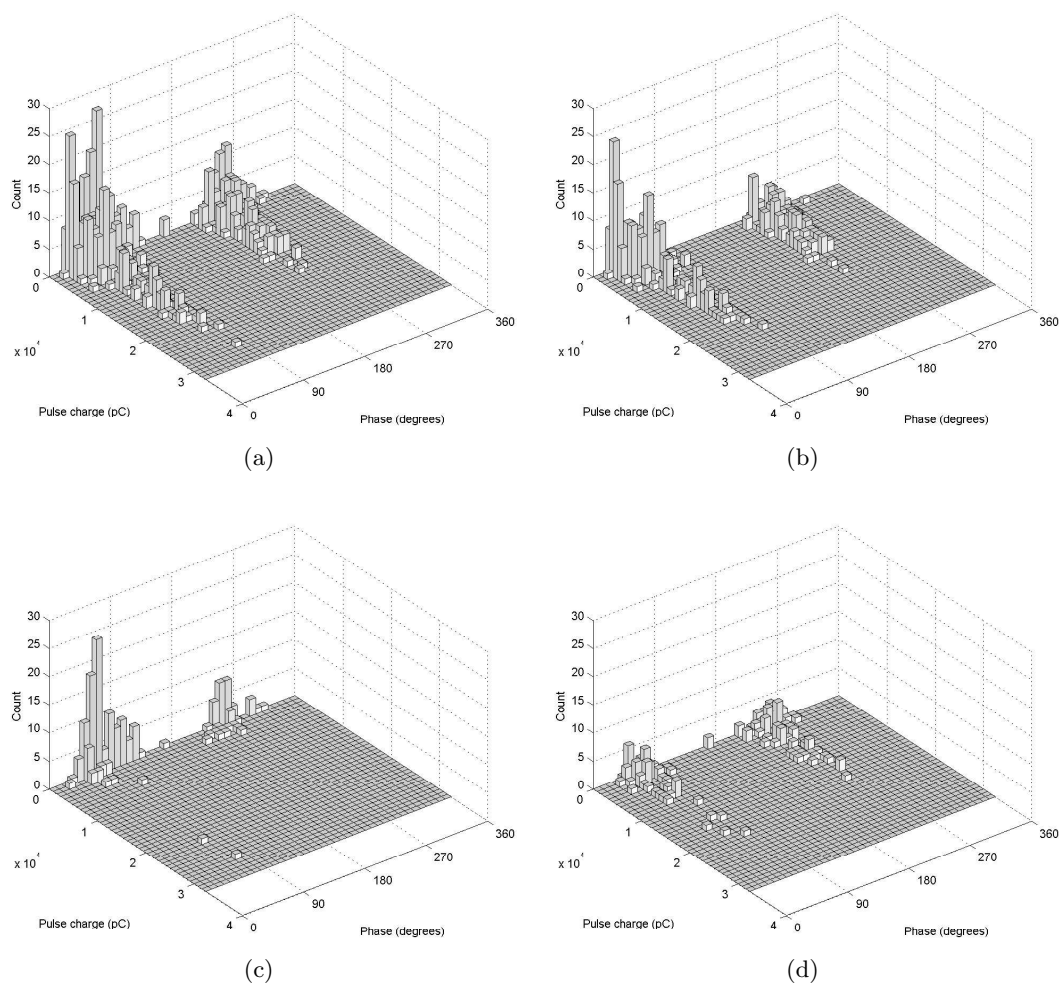


Figure 5.48 Test 3 - Internal PD pulse counts from Ch1-I relative to the phase of the power cycle:
(a) all pulses, (b) SN1, (c) SN2 and (d) SN3.

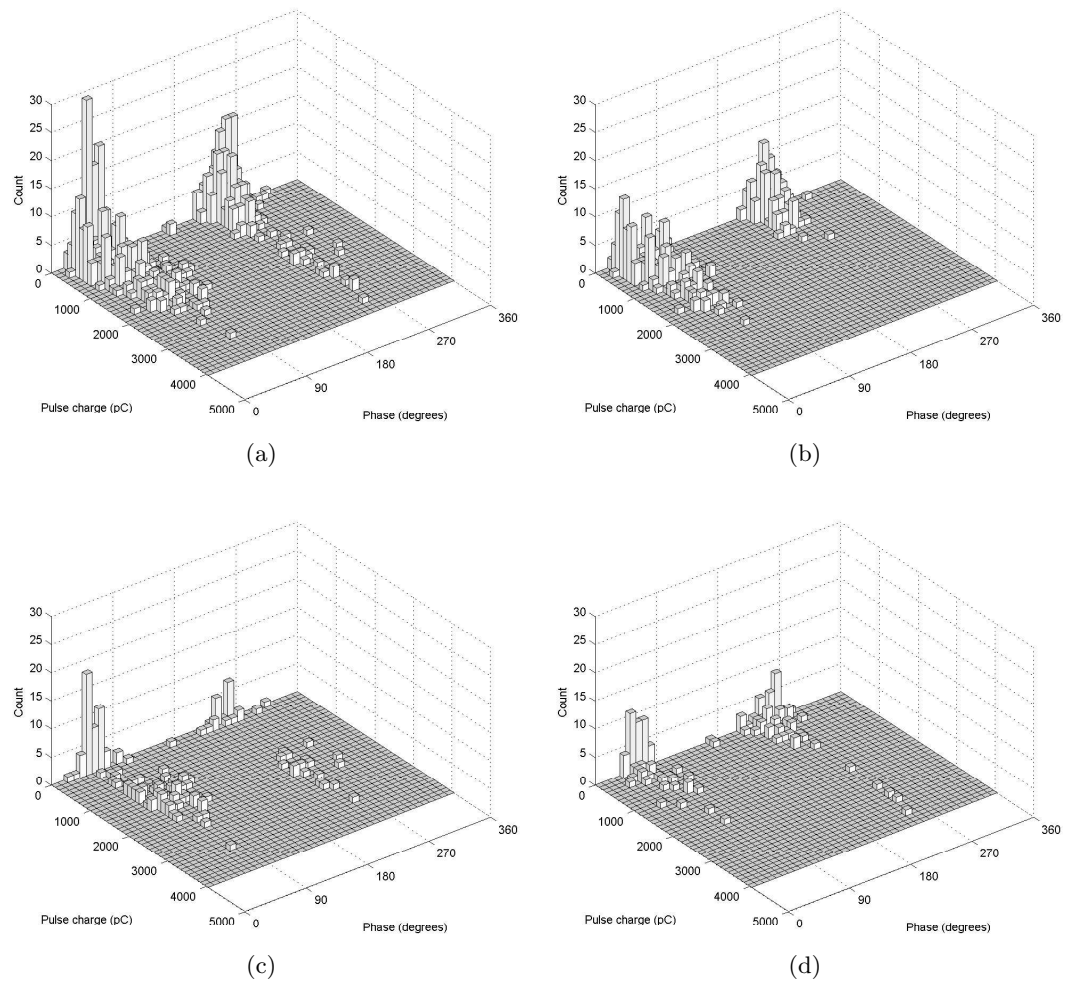


Figure 5.49 Test 3 - Internal PD pulse counts from Ch1-V relative to the phase of the power cycle: (a) all pulses, (b) SN1, (c) SN2 and (d) SN3.

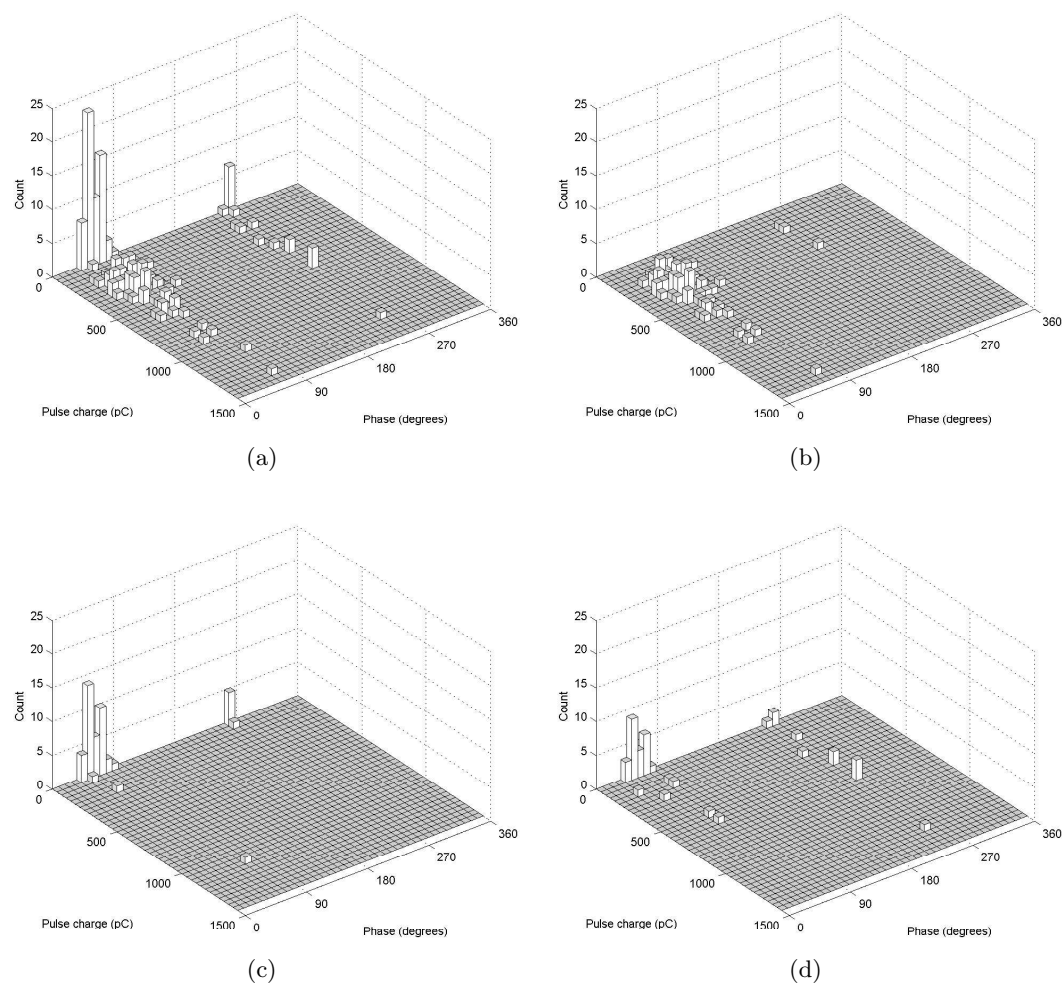


Figure 5.50 Test 3 - Internal PD pulse counts from Ch2-I relative to the phase of the power cycle:
(a) all pulses, (b) SN1, (c) SN2 and (d) SN3.

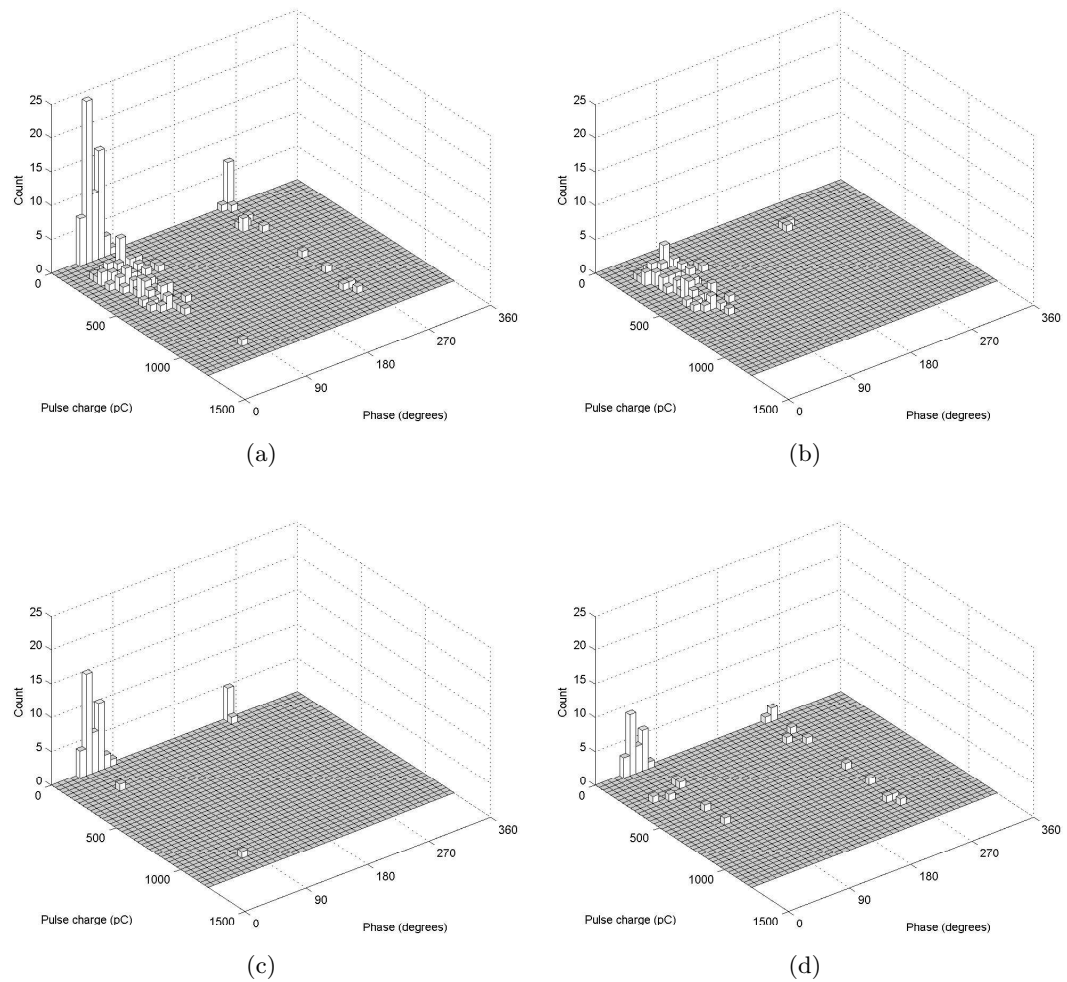


Figure 5.51 Test 3 - Internal PD pulse counts from Ch2-V relative to the phase of the power cycle: (a) all pulses, (b) SN1, (c) SN2 and (d) SN3.

large external interference pulse or too close to other pulses to be recognised as separate events. Correct separation of pulses according to the physical source was 99.7% correct in test 1 and 97.6% correct in test 2, which allows further analysis of PD phase patterns not covered in this thesis. The results from these two tests show that confidence in the PDDS is strong because it can correctly identify internal PD pulses and the number of PD sources in a transformer while interfering signals are present.

A trait of the CNN to place more neurons in areas that have high numbers of input vectors was observed. This sometimes resulted in other groups of input vectors not having a neuron to represent them. It was suggested and shown that using more neurons than PD sources ensures that all groups of input vectors have at least one representative neuron. Results from neurons with similar features, that is, that appear to represent the same group of input vectors, can then be combined.

A third test was performed where the PDDS was applied to an identically constructed transformer that was energised and whose PD state was not known. External corona and narrowband interference sources were present. The pulse count was approximately 10 pulses per power cycle with pulse magnitudes up to 2000pC being recorded. The PDDS clearly identified at least one PD source within the transformer, and manual observation of the captured signals suggests that the PDDS is correct. Two sources may be active in this transformer, although the similarity in pulse waveshapes does support the assessment that they are either from the same source or physically very close sources.

Chapter 6

CONCLUSIONS

A system that can detect PDs in a power transformer while it is on-line and subject to external interference has been developed. In addition, the PDDS can identify and separate multiple physical sources of PD generation, providing useful information for diagnosis. In the PDDS, signals from the transformer to be investigated are filtered and digitised. Narrowband interference is removed by applying a FDTF, and internal PD pulses are identified by using a CWDCF. The output of these steps serves as an input for a CNN which determines the number of PD sources in the transformer. Two off-line tests have shown that the PDDS performs with a confirmed high success rate when known artificial PD pulses are injected into a test transformer. A third test on an energised transformer has identified at least one significant PD source within it.

The transducers have been designed to be attached to a transformer without the need to open or modify the transformer. This allows the PDDS system to be easily retro-fitted to old transformers already in service, which is a significant cost saving. As the current and voltage transducers wrap around the bushings, disconnection of the transmission cables is also unnecessary. While multiple transducers are required to confirm that PD pulses originate from within the transformer, costs of transducer components, filters and digitisers are relatively low. A PDDS system can be relocated to another transformer without problems. A disadvantage of analysing many signal inputs is the computing power required. However, the use of a multi-gigahertz PC for signal processing requires only ‘off-the-shelf’ componentry and is also relatively cheap. This has the advantage that software algorithms can be updated and that results information can be easily accessed and transferred remotely, even through the internet.

In general, while high speed digitisers can collect a lot of information, there is a need to present small amounts of trusted, concise information to a technician responsible for the transformer. Requiring an in-depth knowledge of the transformer or the PDDS would limit the usefulness of the system as there may be limited personnel available with suitable skills. With this as a guide, the signal processing stages in the PDDS have been implemented with as much automation as possible. The FDTF does not

require any user intervention, and will remove any arbitrary narrowband interference without prior knowledge. Currently, a threshold value used in the CWDCF needs to be manually set, as does the number of neurons used in the neural network. However, even these stages could be automated in the future. This would allow simple output of PD information, such as pulse counts for each source and PRPDA plots, upon which decisions about the use of the transformer in question could be made.

The use of the CWT in the PDDS has shown that pulse signal energy can be localised in time and frequency. This allows easier recognition of pulses and their separation from interference that may occur at the same time but at different frequencies. If interference occurs at the same time and frequency, differentiation without prior knowledge may not be achievable. Independent of the PDDS, this situation constitutes a significant theoretical challenge. Also, since the pulse signal energy can be identified more readily in the continuous wavelet domain, the original pulse waveshape can be more accurately preserved when the signal is transformed back to the time domain.

Because the PDDS has isolated the PD pulses before presentation to the CNN for grouping according to pulse waveshape, external pulses do not have to be recognised or grouped. This would be complex as there are often many sources of corona around HV equipment. Even if the CNN classifies a PD pulse incorrectly, at least all of the pulses in the various PRPDA plots are considered to be internal, and thus the pulse patterns in the plots are not contaminated with external pulses from quite different sources. Lalitha et al. have attempted to separate PD sources in PRPDA plots by studying typical pulse patterns from different sources [101]. However, it became difficult when pulse patterns were merged. The PDDS is able to separate pulse patterns even when they are merged.

The results from tests 1 and 2 show a highly successful rate of detecting internal PD, even when there is heavy external interference. The pulses that are not detected have, after close individual analysis, either been obscured by another larger pulse, their SNR was too small or they were too close to another pulse for separation. The use of directional coupling provides better detection of PDs over random noise than the analysis of a single signal, as the pulse signals tend to be reinforced when their signals are multiplied and noise signals cancel on average. Sometimes, random noise can meet the criteria for a PD pulse. However, it requires both the current and voltage signals to meet these criteria at exactly the same time in order for an internal pulse to be registered.

Correct classification of recognised PD pulses according to their source in the transformer was very high in tests 1 and 2. Incorrect classification of a pulse mostly occurred when the pulse was obscured by another pulse, either on top or nearby, or when the pulse was very small. Here, there may have been too much random noise present or the ADC did not provide enough vertical resolution to resolve key minor waveshape

details. Clearly separated pulses of medium to strong magnitude were almost always correctly classified.

Transformer Tx2, which was used for the energised transformer in test 3, is considered fairly old and will not likely be used in service again. Because no standard PD tests have been carried out on it due to a lack of suitable test equipment, the results of the PDDS about its status cannot be confirmed. However, the PDDS provided clear results of several PD pulses per power cycle and pulses of up to 2000pC being generated within the transformer. Additional manual study of the pulse signals confirmed this result. While the pulses could theoretically have transferred from an external source connected to the LV winding, spot checks here observed no pulses of any significance. Coupling of pulses between the HV and LV windings appeared to be weak for the pulses in question. Also, it is unlikely the 240V_{rms} connected to the LV winding would be generating these typical pulses, such as corona. Therefore, it can be concluded that the transformer has at least one significant source of PD. The second apparent PD source has very similar pulse waveshapes to the first source, and either the sources are very close together or there may actually be only one source.

The PDDS does not give a definitive statement about the condition of a transformer, nor whether it should be disconnected, repaired or retired. In general, knowledge of PD patterns and world-wide collective experience of power transformer maintenance is required to interpret the PD results that the PDDS provides and to recommend a course of action. The PDDS contributes new key unambiguous information about PD pulses specifically which may not have been available before, in particular, for on-line transformers. It removes the need to make decisions about a transformer's condition and maintenance exclusively based on long term statistical averages or other less regular or less precise monitoring systems.

6.1 FUTURE RESEARCH AND DEVELOPMENTS

The PDDS consists of multiple modules, each of which performs a certain independent task. It is likely that alterations can be made to each of these stages individually to improve overall system performance. Additional areas for research include:

- Increasing the bandwidth of the transducers will allow better discrimination between pulses that occur very close to each other. The PDDS currently uses analog filters that have a low pass corner frequency of approximately 2MHz. This causes the response of PD and external corona pulses that consist of much higher frequencies to flatten in the time domain and possibly overlap if close to each other. The higher frequency content captured could also provide additional information for CNN training. While computer processing times will increase with the extra data, this compromise may be acceptable for more accurate PD detection. The

use of a data transport bus other than GPIB between the ADCs and the computer, possibly ethernet or Universal Serial Bus (USB), would be preferable to shorten analysis times. Lowering noise levels in the transducers and analog filters would also improve the identification of low amplitude PD pulses.

- While the db2 wavelet waveshape is similar to a PD pulse, the use of a custom wavelet that matches the typical PD pulse waveshape would probably improve recognition when the CWT is applied. However, variation in PD pulse waveshapes may limit the effectiveness of this technique.
- An ideal transformer monitoring and diagnostic system would not require any user input. Instead, it would provide a summary report of the status of the transformer. This requires automation of all of the components of the PDDS. Developments in this area could include:
 - Automatic adjustment of the ADCs to prevent ‘clipping’ while maximising dynamic range.
 - A CWDCF k_{int} threshold value automatically chosen based on detecting calibration pulses without passing interference signals.
 - Intelligent computation of the number of neurons to be used for PD pulse grouping and, when the CNN is suitably trained, of which neurons represent the same group of pulses.
- While the CNN gives information about the number of internal PD sources, the PDDS does not provide specific information about the location of the source within the transformer. An experienced technician may be able to estimate the location of a PD source by looking at its PRPDA plots, especially comparing plots of the same source at different bushings. This expert assessment would be based on general historic knowledge of transformer PD patterns. More precise source localisation is a difficult problem and may also require prior knowledge of the transformer under test. High speed timing of the arrival of a pulse at each bushing may provide an indication of the distance to the source as the pulse will take a fixed time to travel along the winding wire. Other methods, such as analysing the frequency content of a pulse, require prior knowledge of reference signals from an identical transformer that has been modified for injection of pulses into various points on its winding, such as transformer Tx1. Ultrasonic methods for localisation may provide better results.

A wide variety of techniques for monitoring and diagnosing power transformers have been presented in Chapter 2, some of which have already been well developed for many years. Useful information is gained from these techniques to help identify

transformer problems. However, there are limitations to each method which is evident in continuing failures of transformers today.

It is unlikely that the PDDS will be used in isolation. Rather, its results will be combined with the results of existing techniques and possibly other new methods currently under research. Their combined information will provide a clearer and more complete picture about the state of a transformer than one technique by itself could do.

Most of the existing techniques and those under research require some knowledge and experience to interpret and apply the results. Automation of techniques, especially for techniques that involve collection of large quantities of data, and intelligent processing of results will lower the costs of those techniques, which will allow them to be used more extensively. Research in techniques that involve artificial intelligence, neural networks, fuzzy logic and expert systems is necessary if automation of techniques is to be achieved. These same techniques will also aggregate information from multiple monitoring and diagnostic systems and provide a simple or detailed transformer state analysis. Historic information could be fed to these systems. However, a thorough understanding of transformer failure mechanisms and application of analysing techniques to those failure mechanisms is indispensable.

In summary, more research is needed on developing and integrating a broad variety of techniques for analysing the condition of a power transformer, especially while it is on-line. A clearer picture of the complete health of a transformer means that it can be pushed to the end of its life and repairs need to be scheduled only when it is convenient to take the transformer off-line. The final objective is a system that is able to provide warnings and a continual flow of information about all technical aspects of the operating health and predicted status of the transformer. A low cost system that provides this will be a powerful tool.

Appendix A

PDDS EQUIPMENT AND TEST PHOTOS

Photos are presented that show various components of the PDDS and the setup of the tests described in Chapter 5.

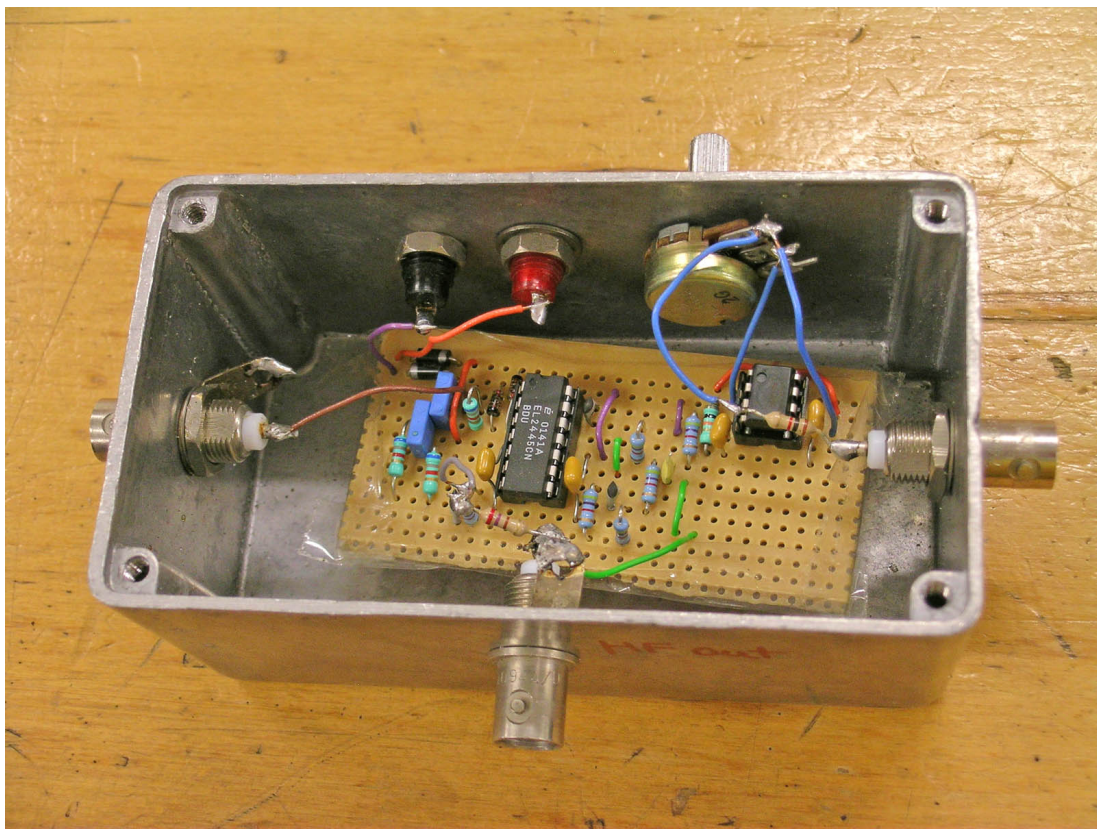


Figure A.1 Voltage signal analog filter.

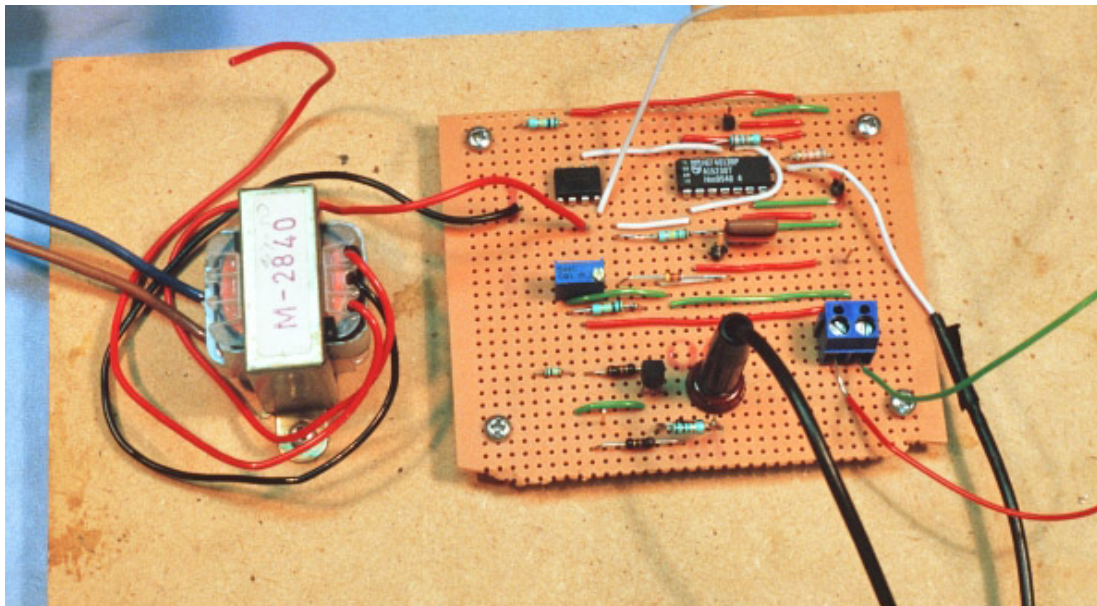


Figure A.2 Power cycle synchronisation module (PCSM).

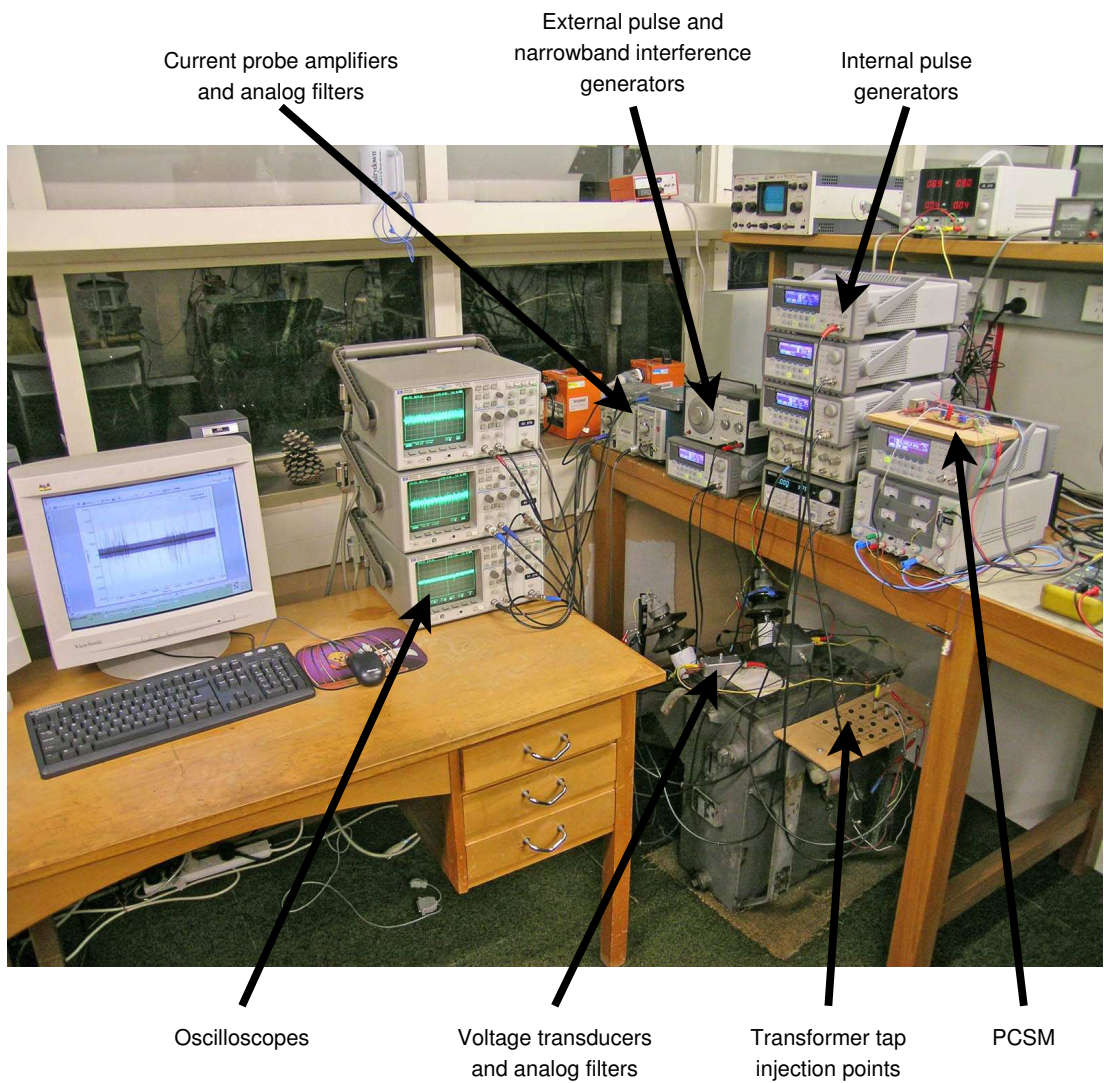


Figure A.3 Setup for tests 1 and 2 on transformer Tx1.

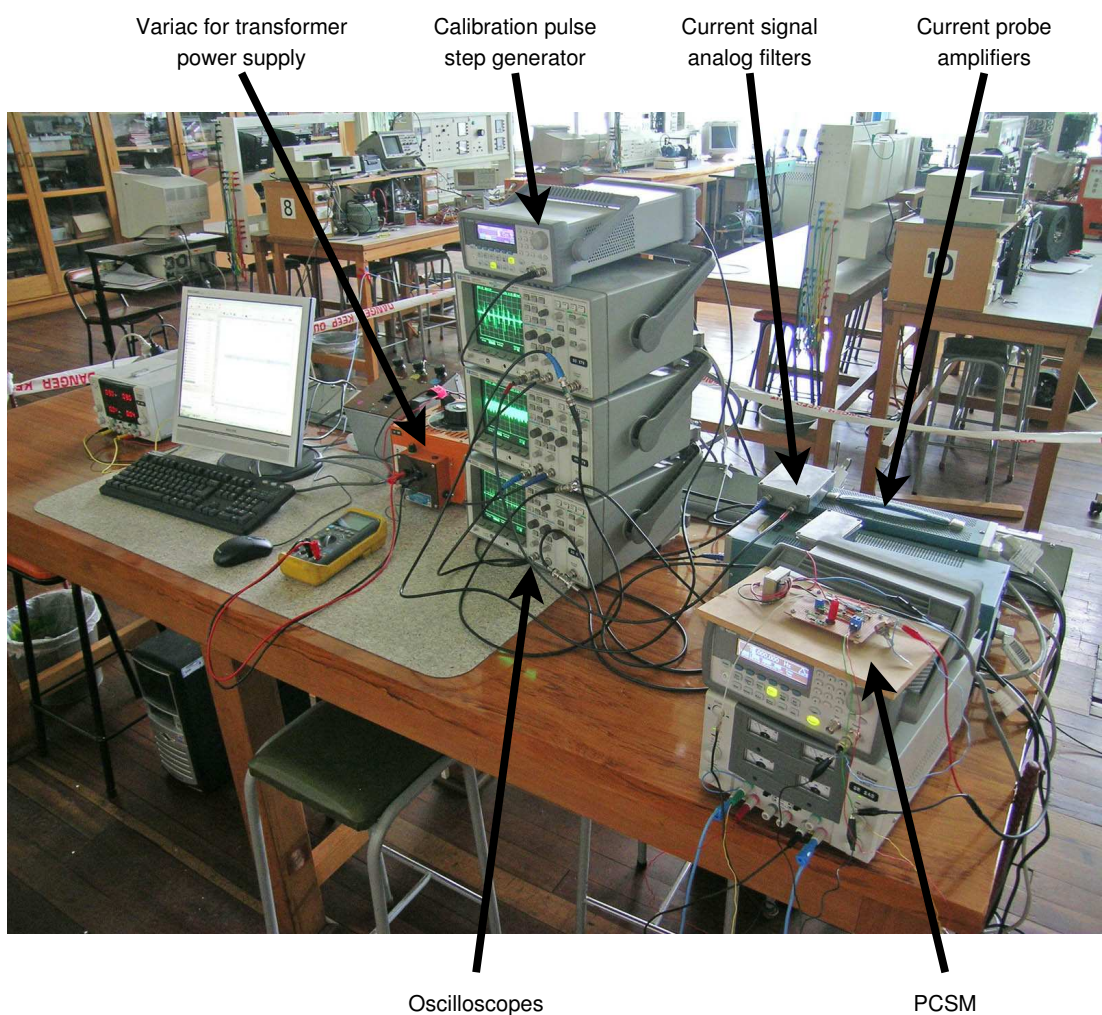


Figure A.4 On-line setup for test 3 on transformer Tx2 (front).

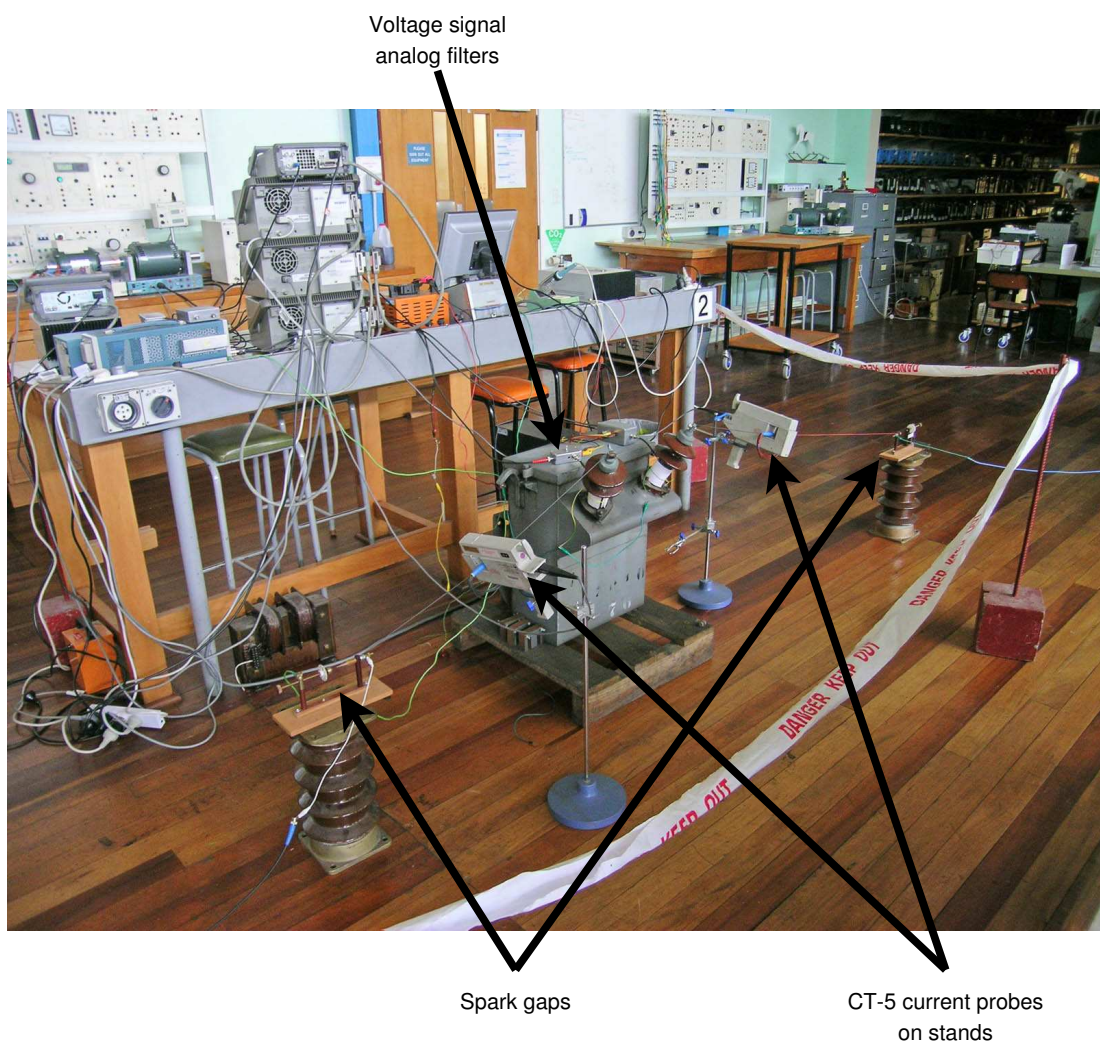


Figure A.5 On-line setup for test 3 on transformer Tx2 (back).

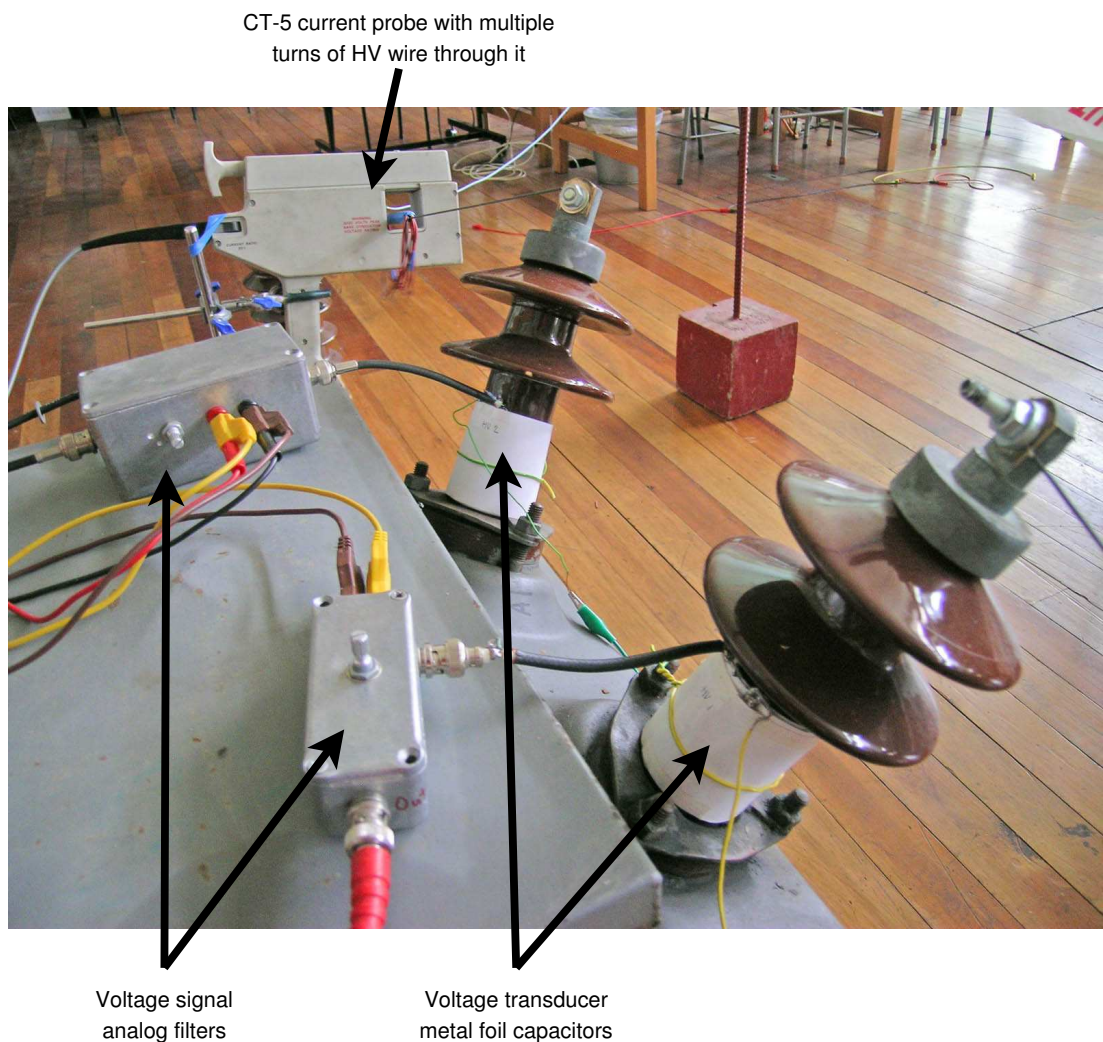


Figure A.6 On-line setup for test 3 on transformer Tx2 (detail).

REFERENCES

- [1] J.M. Wetzer, G.J. Cliteur, W.R. Rutgers, and H.F.A. Verhaart. Diagnostic- and condition assessment-techniques for condition based maintenance. In *Electrical Insulation and Dielectric Phenomena, 2000 Annual Report Conference on*, volume 1, pages 47–51, 2000.
- [2] J.C. Steed. Condition monitoring applied to power transformers-an REC experience. In *Condition Monitoring of Large Machines and Power Transformers (Digest No: 1997/086), IEE Colloquium on*, pages 4/1–410, 1997.
- [3] C. Bengtsson. Status and trends in transformer monitoring. *Power Delivery, IEEE Transactions on*, 11(3):1379–1384, 1996.
- [4] M. B. Dewe, D. W. Beatt, and A. C. Britten. Present and Future Trends in the Condition Monitoring of High Voltage Power Equipment as seen by ESKOM. In *AMEU Conference*, Cape Town S.A., 1989.
- [5] D. Chu and A. Lux. On-line monitoring of power transformers and components: a review of key parameters. In *Electrical Insulation Conference and Electrical Manufacturing and Coil Winding Conference, 1999. Proceedings*, pages 669–675, 1999.
- [6] Y. Han and Y.H. Song. Condition monitoring techniques for electrical equipment-a literature survey. *Power Delivery, IEEE Transactions on*, 18(1):4–13, 2003.
- [7] G.C. Stone. Partial discharge. VII. Practical techniques for measuring PD in operating equipment. *Electrical Insulation Magazine, IEEE*, 7(4):9–19, 1991.
- [8] M. Wang, A.J. Vandermaar, and K.D. Srivastava. Review of condition assessment of power transformers in service. *Electrical Insulation Magazine, IEEE*, 18(6):12–25, 2002.
- [9] B.H. Ward and S. Lindgren. A Survey of Developments in Insulation Monitoring of Power Transformers. In *2000 IEEE International Symposium on Electrical Insulation*, pages 141–147, Anaheim, CA, USA., 2000.

- [10] B.H. Ward. A survey of new techniques in insulation monitoring of power transformers. *Electrical Insulation Magazine, IEEE*, 17(3):16–23, 2001.
- [11] Jr. Kirtley, J.L., W.H. Hagman, B.C. Lesieutre, M.J. Boyd, E.P. Warren, H.P. Chou, and R.D. Tabors. Monitoring the health of power transformers. *Computer Applications in Power, IEEE*, 9(1):18–23, 1996.
- [12] International Electrotechnical Commission. High Voltage Test Techniques - Partial Discharge Measurements. IEC 60270:2000(3rd Edition), 2000.
- [13] T. Leibfried and K. Feser. Off-line- and on-line-monitoring of power transformers using the transfer function method. In *Electrical Insulation, 1996., Conference Record of the 1996 IEEE International Symposium on*, volume 1, pages 34–37, 1996.
- [14] W.J. McNutt. Insulation thermal life considerations for transformer loading guides. *Power Delivery, IEEE Transactions on*, 7(1):392–401, 1992. TY - JOUR.
- [15] Working Group on High Temperature Insulation for Liquid-Immersed Power Transformers. Background information on high temperature insulation for liquid-immersed power transformers. *Power Delivery, IEEE Transactions on*, 9(4):1892–1906, 1994.
- [16] V. M. Montsinger. Loading Transformers by Temperature. *AIEE Transactions*, 49:776–792, 1930.
- [17] T. W. Dakin. Electrical Insulation Deterioration Treated as a Chemical Reaction Rate Phenomenon. *AIEE Transactions*, 66:113–122, 1947.
- [18] International Electrotechnical Commission Recommendation. Loading Guide for Oil-Immersed Transformers. *International Electrotechnical Commission Recommendation*, IEC-354(1st Edition), 1972.
- [19] C. A. Bozzini. Transformer Aging Diagnosis by Means of Measurement of the Degree of Polymerisation. Results in New Experiments. *CIGRE*, Section 12-08, 1968.
- [20] D. Allan, C. Jones, and B. Sharp. Studies of the condition of insulation in aged power transformers. 1. Insulation condition and remnant life assessments for in-service units. In *Properties and Applications of Dielectric Materials, 1991., Proceedings of the 3rd International Conference on*, volume 2, pages 1116–1119, 1991.
- [21] D.M. Allan. Practical life-assessment technique for aged transformer insulation. *Science, Measurement and Technology, IEE Proceedings A*, 140(5):404–408, 1993.

- [22] W. Lampe, L. Pettersson, C. Ovren, and B. Wahlstrom. Hot-Spot Measurements in Power Transformers. *CIGRE*, 12-02, 1986.
- [23] G. McDowell. Condition Monitoring of Power Transformers to Assess Residual Life and Fault Damage. *ERA Technology*, ERA Report(88-0566R), 1989.
- [24] M. Schafer and K. Feser. Thermal monitoring of large power transformers. In *Electric Power Engineering, 1999. PowerTech Budapest 99. International Conference on*, page 98, 1999.
- [25] B. F. Hampton, M. E. Woppard, and C. C. Stinton. The Measurement of Transformer Winding Temperature. *CIGRE*, Paper No. 12-02, 1982.
- [26] P. Boss and H. Brandle. Measurement of the Temperature Profile in Transformer Windings. In *Trafotech*, volume Paper V2, Bangalore, 1994.
- [27] M. S. Hwang, W. M. Grady, and H. W. Sanders. Distribution Transformer Winding Losses Due to Nonsinusoidal Currents. *IEEE Transactions on Power Delivery*, PWRD-2(1), 1987.
- [28] M.T. Bishop, J.F. Baranowski, D. Heath, and S.J. Benna. Evaluating harmonic-induced transformer heating. *Power Delivery, IEEE Transactions on*, 11(1):305–311, 1996.
- [29] E. E. Alexander and W. Xiaoming. Estimation of Loss of Life of Power Transformers Supplying Nonlinear Loads. *IEEE Transactions on Power Apparatus and Systems*, PAS-104(3), 1985.
- [30] M. J. Heathcote. *The J and P Transformer Book*. Newnes Ltd., 12th edition, 1998.
- [31] IEEE Guide for Acceptance and Maintenance of Insulating Oil in Equipment. *IEEE Std C57.106-2002*, 2002.
- [32] D. Bossetto, P. Ciolli, and G. Zafferani. Development of measuring techniques used in evaluating the insulation condition of large power transformers. In *Dielectric Materials, Measurements and Applications, 1992., Sixth International Conference on*, pages 217–220, 1992.
- [33] An Internal Survey on Failures in Large Power Transformers in Service. *Electra* 88, 21 May 1983.
- [34] International Electrotechnical Commission. Insulating liquids - Determination of the breakdown voltage at power frequency - Test method. IEC 156:1995(2nd Edition), 1995.

- [35] J. J. Kelly. Transformer Fault Diagnosis by Dissolved-Gas Analysis. *IEEE Transactions on Industrial Applications*, IA-16(6):777–782, 1980.
- [36] G. R. Cardwell. Oil Testing and Dissolved Gas Analysis for Identifying Faults in Power Transformers, Feb 1989.
- [37] IEEE guide for the interpretation of gases generated in oil-immersed transformers. *IEEE Std C57.104-1991*, 1991.
- [38] R. R. Rogers. IEEE and IEC Codes to Interpret Incipient Faults in Transformers using Gas-In-Oil Analysis. *IEEE Transactions on Electrical Insulation*, EI-13(5):348–354, 1978.
- [39] F. W. Heinrichs. The Impact of Fault Detection Methods and Analysis on the Transformer Operating Decision. *IEEE Transactions on Power Delivery*, PWRD-2(3), 1987.
- [40] B. Pahlavanpour. Characterisation of insulating oils. In *Characterisation of Dielectric Materials: a Review*, IEE Colloquium on, pages 8/1–8/5, 1994.
- [41] R. Blue, D. Uttamchandani, and O. Farish. The determination of FFA concentration in transformer oil by fluorescence measurements. *Dielectrics and Electrical Insulation, IEEE Transactions on*, 5(6):892–895, 1998.
- [42] R. Blue, D.G. Uttamchandani, and O. Farish. A novel optical sensor for the measurement of furfuraldehyde in transformer oil. *Instrumentation and Measurement, IEEE Transactions on*, 47(4):964–966, 1998.
- [43] Hong-Tzer Yang and Chiung-Chou Liao. Adaptive fuzzy diagnosis system for dissolved gas analysis of power transformers. *Power Delivery, IEEE Transactions on*, 14(4):1342–1350, 1999.
- [44] W. Xu, D. Wang, Z. Zhou, and H. Chen. Fault diagnosis of power transformers: application of fuzzy set theory, expert systems and artificial neural networks. *Science, Measurement and Technology, IEE Proceedings-*, 144(1):39–44, 1997.
- [45] International Electrotechnical Commission. Measurement of the Average Viscometric Degree of Polymerisation of New and Aged Cellulosic Electrically Insulating Materials. *International Electrotechnical Commission Recommendation*, IEC-60450(2nd Edition), 2002.
- [46] H.B. Cummings, J.R. Boyle, and B.W. Arp. Continuous, online monitoring of freestanding, oil-filled current transformers to predict imminent failure. *Power Delivery, IEEE Transactions on*, 3(4):1776–1783, 1988.

- [47] E. Ildstad, U. Gafvert, and P. Tharning. Relation between return voltage and other methods for measurements of dielectric response. In *Electrical Insulation, 1994., Conference Record of the 1994 IEEE International Symposium on*, pages 25–28, 1994.
- [48] IEEE guide for transformer impulse tests. *IEEE Std C57.98-1993*, 1993.
- [49] A. C. Hall and P. G. Parrott. Experience with the Low Voltage Impulse Testing of Power Transformers. In *IEE/IEEE Conference*, volume 94, pages 107–113, 1973.
- [50] M. Wang, A.J. Vandermaar, and K.D. Srivastava. Condition monitoring of transformers in service by the low voltage impulse test method. In *High Voltage Engineering, 1999. Eleventh International Symposium on (Conf. Publ. No. 467)*, volume 1, pages 45–48 vol.1, 1999.
- [51] G.W.A. McDowell and M.L. Lockwood. Real time monitoring of movement of transformer winding. In *Condition Monitoring and Remanent Life Assessment in Power Transformers, IEE Colloquium on*, pages 6/1–614, 1994.
- [52] British Standards Institution. Specification for Insulation Levels and Dielectric Tests. BS171(3), 1987.
- [53] L. Boldic and J. Aubin. Detection of Transformer Winding Displacement by the FRSL Diagnosis Method. *Canadian Electrical Association, CEA RP 77-47*, 1981.
- [54] E. P. Dick and C. C. Erven. Transformer Diagnostic Testing by Frequency Response Analysis. *IEEE Transactions on Power Apparatus and Systems*, PAS-97(6):2144–2153, 1978.
- [55] S.D. Mikkelsen, J. Bak-Jensen, B. Bak-Jensen, and J.T. Sorensen. Sensitivity of identified transfer functions in transformer diagnosis. In *Electrical Electronics Insulation Conference and Electrical Manufacturing and Coil Winding Conference, 1993. Proceedings., Chicago '93 EEIC/ICWA Exposition*, pages 533–537, 1993.
- [56] R. Malewski and B. Poulin. Impulse testing of power transformers using the transfer function method. *Power Delivery, IEEE Transactions on*, 3(2):476–489, 1988.
- [57] J. Unsworth, J. Kurusingal, and R.E. James. On-line partial discharge monitor for high voltage power transformers. In *Properties and Applications of Dielectric Materials, 1994., Proceedings of the 4th International Conference on*, volume 2, pages 729–732 vol.2, 1994.
- [58] British Standards Institution. Specification of Ability to Withstand Short Circuit. BS171(5), 1987.

- [59] F. C. Pratt. Diagnostic Methods for Transformers in Service. In *International Conference on Large High Voltage Electric Systems, CIGRE*, volume 12-06, 1986.
- [60] V. Sokolov, V. Bulgakova, and Z. Berler. Assessment of power transformer insulation condition. In *Electrical Insulation Conference and Electrical Manufacturing and Coil Winding Conference, 2001. Proceedings*, pages 605–613, 2001.
- [61] M. Thibault-Carballera, D. Allaire, J. Delhaye, P. Moro, and J. Samat. Fault Detection and Location in Transformers. *CIGRE*, 12-01, 1982.
- [62] T. Bengtsson, H. Kols Li Ming, and M. Leijon. Identification of PD sources in solids. In *Dielectric Materials, Measurements and Applications, 1992., Sixth International Conference on*, pages 29–32, 1992.
- [63] K. Tomsovic, M. Tapper, and T. Ingvarsson. A fuzzy information approach to integrating different transformer diagnostic methods. *Power Delivery, IEEE Transactions on*, 8(3):1638–1646, 1993.
- [64] Zhenyuan Wang, Y. Liu, and P.J. Griffin. A combined ANN and expert system tool for transformer fault diagnosis. In *Power Engineering Society Winter Meeting, 2000. IEEE*, volume 2, pages 1261–1269 vol.2, 2000.
- [65] Zhenyuan Wang, Yilu Liu, Nien-Chung Wang, Tzong-Yih Guo, F.T.C. Huang, and P.J. Griffin. Artificial intelligence in power equipment fault diagnosis. In *Power System Technology, 2000. Proceedings. PowerCon 2000. International Conference on*, volume 1, pages 247–252 vol.1, 2000.
- [66] Qian Zheng, Yang Minzhong, and Yan Zhang. Synthetic diagnostic method for insulation fault of oil-immersed power transformer. In *Properties and Applications of Dielectric Materials, 2000. Proceedings of the 6th International Conference on*, volume 2, pages 872–875 vol.2, 2000.
- [67] S.R. Kolla and D.V. Gedeon. Microprocessor-based protection scheme for power transformers. In *Electrical Electronics Insulation Conference, 1995, and Electrical Manufacturing & Coil Winding Conference. Proceedings*, pages 195–198, 1995.
- [68] A. Wiszniewski and B. Kasztenny. A multi-criteria differential transformer relay based on fuzzy logic. *Power Delivery, IEEE Transactions on*, 10(4):1786–1792, 1995.
- [69] L.G. Perez, A.J. Flehsig, J.L. Meador, and Z. Obradovic. Training an artificial neural network to discriminate between magnetizing inrush and internal faults. *Power Delivery, IEEE Transactions on*, 9(1):434–441, 1994.
- [70] M. Gomez-Morante and D.W. Nicoletti. A wavelet-based differential transformer protection. *Power Delivery, IEEE Transactions on*, 14(4):1351–1358, 1999.

- [71] F. Jiang, Z.Q. Bo, P.S.M. Chin, M.A. Redfern, and Z. Chen. Power transformer protection based on transient detection using discrete wavelet transform (DWT). In *Power Engineering Society Winter Meeting, 2000. IEEE*, volume 3, pages 1856–1861 vol.3, 2000.
- [72] S. Tenbohlen and F. Figel. On-line condition monitoring of power transformers. In *Power Engineering Society Winter Meeting, 2000. IEEE*, volume 3, pages 2211–2216 vol.3, 2000.
- [73] T. W. Gouldsborough and J. F. Millward. On-Line Hydrogen-in-Oil Monitoring. In *Fiftieth Annual International Conference of Doble Clients*, volume 6-601, 1983.
- [74] Y. Inoue, K. Suganuma, M. Kamba, and M. Kikkawa. Development of oil-dissolved hydrogen gas detector for diagnosis of transformers. *Power Delivery, IEEE Transactions on*, 5(1):226–232, 1990.
- [75] J.-P. Gibeault and J.K. Kirkup. Early detection and continuous monitoring of dissolved key fault gases in transformers and shunt reactors. In *Electrical Electronics Insulation Conference, 1995, and Electrical Manufacturing & Coil Winding Conference. Proceedings*, pages 285–293, 1995.
- [76] D. Harris and M.P. Saravolac. Condition monitoring in power transformers. In *Condition Monitoring of Large Machines and Power Transformers (Digest No: 1997/086), IEE Colloquium on*, pages 7/1–7/3, 1997.
- [77] T. Leibfried and K. Feser. Monitoring of power transformers using the transfer function method. *Power Delivery, IEEE Transactions on*, 14(4):1333–1341, 1999.
- [78] Changchang Wang, Xianhe Jin, T.C. Cheng, Shibo Zhang, Zongdong Wang, Xuzhu Dong, and Deheng Zhu. Analysis and suppression of continuous periodic interference for on-line PD monitoring of power transformers. In *High Voltage Engineering, 1999. Eleventh International Symposium on (Conf. Publ. No. 467)*, volume 5, pages 212–215 vol.5, 1999.
- [79] A. Zargari and T.R. Blackburn. Acoustic detection of partial discharges using non-intrusive optical fibre sensors [current transformers]. In *Conduction and Breakdown in Solid Dielectrics, 1998. ICSD '98. Proceedings of the 1998 IEEE 6th International Conference on*, pages 573–576, 1998.
- [80] H. Borsi. A PD measuring and evaluation system based on digital signal processing. *Dielectrics and Electrical Insulation, IEEE Transactions on [see also Electrical Insulation, IEEE Transactions on]*, 7(1):21–29, 2000.
- [81] M. Ekberg, A. Gustafsson, M. Leijon, T. Bengtsson, T. Eriksson, C. Tornkvist, K. Johansson, and Li Ming. Recent results in HV measurement techniques.

- Dielectrics and Electrical Insulation, IEEE Transactions on [see also Electrical Insulation, IEEE Transactions on]*, 2(5):906–914, 1995.
- [82] K. Feser, E. Grossmann, M. Lauersdorf, and Th. Grun. Improvement of sensitivity in online PD-measurements on transformers by digital filtering. In *High Voltage Engineering, 1999. Eleventh International Symposium on (Conf. Publ. No. 467)*, volume 5, pages 156–159 vol.5, 1999.
 - [83] Changchang Wang, Zhongdong Wang, Fuqi Li, and Xianhe Jin. Anti-interference techniques used for on-line partial discharge monitoring. In *Properties and Applications of Dielectric Materials, 1994., Proceedings of the 4th International Conference on*, volume 2, pages 582–585 vol.2, 1994.
 - [84] Changchang Wang, Xianhe Jin, Weihong Jing, T.C. Cheng, Shibo Zhang, Xuzhu Dong, Zhongdong Wang, Du Lin, and Deheng Zhu. Interference rejection for on-line PD monitoring of power transformers. In *Electrical Insulation, 1998. Conference Record of the 1998 IEEE International Symposium on*, volume 1, pages 24–27 vol.1, 1998.
 - [85] Xiaoning Wang, Deheng Zhu, and Fuqi Li. Interference analysis and rejection of partial discharge (PD) monitoring signal on-site. In *Electrical Insulating Materials, 2001. (ISEIM 2001). Proceedings of 2001 International Symposium on*, pages 111–114, 2001.
 - [86] D. Wenzel, U. Schichler, H. Borsi, and E. Gockenbach. Recognition of Partial Discharges on Power Units by Directional Coupling. In *Ninth International Symposium on High Voltage Engineering*, Austria, 1995.
 - [87] D. Wenzel, H. Borsi, and E. Gockenbach. Partial discharge measurement and gas monitoring of a power transformer on-site. In *Dielectric Materials, Measurements and Applications, Seventh International Conference on (Conf. Publ. No. 430)*, pages 255–258, 1996.
 - [88] P. Werle, A. Akbari, H. Borsi, and E. Gockenbach. Enhanced online PD evaluation on power transformers using wavelet techniques and frequency rejection filter for noise suppression. In *Electrical Insulation, 2002. Conference Record of the 2002 IEEE International Symposium on*, pages 195–198, 2002.
 - [89] IEEE guide for partial discharge measurement in liquid-filled power transformers and shunt reactors. *IEEE Std C57.113-1991*, 1991.
 - [90] G.J. Paoletti and A. Golubev. Partial discharge theory and technologies related to medium-voltage electrical equipment. *Industry Applications, IEEE Transactions on*, 37(1):90–103, 2001.

- [91] L. Satish and W.S. Zaengl. Artificial neural networks for recognition of 3-d partial discharge patterns. *Dielectrics and Electrical Insulation, IEEE Transactions on [see also Electrical Insulation, IEEE Transactions on]*, 1(2):265–275, 1994.
- [92] D. Wenzel, H. Borsi, and E. Gockenbach. A measuring system based on modern signal processing methods for partial discharge recognition and localization on-site. In *Electrical Insulation, 1998. Conference Record of the 1998 IEEE International Symposium on*, volume 1, pages 20–23 vol.1, 1998.
- [93] H. Borsi, E. Gockenbach, and D. Wenzel. Separation of partial discharges from pulse-shaped noise signals with the help of neural networks. *Science, Measurement and Technology, IEE Proceedings-*, 142(1):69–74, 1995.
- [94] P. Werle, H. Borsi, and E. Gockenbach. Hierarchical cluster analysis of broadband measured partial discharges as part of a modular structured monitoring system for transformers. In *High Voltage Engineering, 1999. Eleventh International Symposium on (Conf. Publ. No. 467)*, volume 5, pages 29–32 vol.5, 1999.
- [95] X. Ma, C. Zhou, and I.J. Kemp. Automated wavelet selection and thresholding for PD detection. *Electrical Insulation Magazine, IEEE*, 18(2):37–45, 2002.
- [96] X. Ma, C. Zhou, and I.J. Kemp. Interpretation of wavelet analysis and its application in partial discharge detection. *Dielectrics and Electrical Insulation, IEEE Transactions on [see also Electrical Insulation, IEEE Transactions on]*, 9(3):446–457, 2002.
- [97] L. Satish and B. Nazneen. Wavelet-based denoising of partial discharge signals buried in excessive noise and interference. *Dielectrics and Electrical Insulation, IEEE Transactions on [see also Electrical Insulation, IEEE Transactions on]*, 10(2):354–367, 2003.
- [98] I. Shim, J.J. Soraghan, and W.H. Siew. Detection of PD utilizing digital signal processing methods. Part 3: Open-loop noise reduction. *Electrical Insulation Magazine, IEEE*, 17(1):6–13, 2001.
- [99] Shuzhen Xu, R. Middleton, Xiaodong liu, and Chenchen. A new method based on wavelet packet transformation to reduce narrow band noise in on-site PD measurement. In *Power Engineering Society Summer Meeting, 2002 IEEE*, volume 2, pages 898–903 vol.2, 2002.
- [100] M.S. Naderi, M. Vakilian, T.R. Blackburn, B.T. Phung, and H.O. Nam. An optimal wavelet filtering method for noise suppression of PD measured signal and its location in power transformer winding. In *Dielectric Liquids, 2005. ICDL 2005. 2005 IEEE International Conference on*, pages 269–272, 2005.

- [101] E.M. Lalitha and L. Satish. Wavelet analysis for classification of multi-source PD patterns. *Dielectrics and Electrical Insulation, IEEE Transactions on [see also Electrical Insulation, IEEE Transactions on]*, 7(1):40–47, 2000.
- [102] W. Lampe and E. Spicar. The Oxygen-Free Transformer Reduces Aging by Continuous Degassing. *CIGRE*, 12-05, 1976.
- [103] A. L. Rickley and S.H. Osborn Jr. Variation of Power Factor with Temperature. In *Fifty-First Annual International Conference of Doble Clients*, volume 2-301, 1984.
- [104] C. K. Mechefske. Correlating Power Transformer Tank Vibration Characteristics to Winding Looseness. *Insight*, 37:599–605, 1995.
- [105] C. Booth and J. R. McDonald. The Use of Artificial Neural Networks for Condition Monitoring of Electrical Power Transformers. *Neurocomput*, 23(1-3):97–109, 1998.
- [106] Agilent Technologies, Inc. *Agilent 33250A 80MHz Function/Arbitrary Waveform Generator, User's Guide*. 1st edition, 2000.
- [107] G. Lavery. A Prototype Transformer Insulation Condition Monitoring System. PhD thesis submitted at the University of Canterbury, New Zealand, 1999.
- [108] S. Haykin. *Communication Systems*. John Wiley and Sons, Inc., 3rd edition, 1994.
- [109] Rocoil Rogowski Coils Limited. Harrogate, England.
- [110] Tektronix, Inc. *Instructions, A6302 Current Probe*. 1st edition, 1981.
- [111] Tektronix, Inc. *AM503 Current Probe Amplifier, Instruction Manual*. 1st edition, 1976.
- [112] Philip R. Geffe. *Simplified Modern Filter Design*. John F. Rider Publisher, Inc., New York, 1963.
- [113] Hewlett-Packard Co. *HP 54645A Oscilloscope and HP 54645D Mixed-Signal Oscilloscope, User and Service Guide*. 1st edition, 1997.
- [114] Y. Sheng. Wavelet Transform. In *The Transforms and Applications Handbook*, pages 747–827. CRC Press, 1996.
- [115] I. Daubechies. *Ten Lectures on Wavelets*. SIAM, 2nd edition, 1992.
- [116] T. Kahonen. *Self-Organization and Associative Memory*. Springer-Verlag, Berlin, 2nd edition, 1987.